Remote Sensing for Precision Agriculture: Yield mapping and delineation of management zones with multispectral satellite imagery and GIS data

vorgelegt von

Dipl. Geologin
Claudia Vallentin

- née Claudia Georgi -

ORCID: 0000-0003-2587-556X

an der Fakultät VI – Planen Bauen Umwelt
der Technischen Universität Berlin
zur Erlangung des akademischen Grades

Doktor der Naturwissenschaften
- Dr. rer. nat. -

genehmigte Dissertation

Promotionsausschuss:

Vorsitzende: Prof. Dr. Irina Engelhardt
Gutachterin: Prof. Dr. Birgit Kleinschmit
Gutachter: Prof. Dr. Hermann Kaufmann
Gutachter: Prof. Dr. Christopher Conrad

Tag der wissenschaftlichen Aussprache: 17. November 2020

Berlin 2021

Acknowledgement

I would like to take this opportunity to thank all those who have made this thesis possible. I would like to thank Prof. Dr. Birgit Kleinschmit from the Technical University of Berlin for supervising and reviewing this thesis, as well as for the insightful comments on the research manuscripts. I would like to thank Prof. Dr. Hermann Kaufmann, long-term head of the remote sensing section at the Helmholtz Centre Potsdam - GFZ German Research Centre for Geosciences for the review of this thesis. I would also like to thank Prof. Dr. Christopher Conrad of the Martin Luther University in Halle for his review of this thesis and his sharp comments on the research manuscript. I would like to thank my supervisors at the GFZ Potsdam, Dr. Sibylle Itzerott and Dr. Daniel Spengler for their years of support, the many constructive discussions and suggestions for improvement for all the parts of this thesis. I would like to thank Prof. Dr. Eike Stefan Dobers for his hospitality in Neubrandenburg and for the many intensive discussions and ideas for this work. My thanks also go to the anonymous reviewers of the manuscripts and the developers of the open source software, who do a great service to science and society. I would like to thank the very cooperative farm, without whose data this work would not have been possible.

I would like to thank my colleagues in the Remote Sensing and Geoinformation Section for the discussions, the entertaining coffee breaks, the exciting field campaigns and many enjoyable hours while crafting. In particular, I would like to thank Katharina Harfenmeister, Kathrin Ward and Dr. Julia Neelmeijer for the personal talks and Dr. Carsten Neumann and Katharina Harfenmeister for their regular support in programming.

My greatest thanks is dedicated to my husband Dr. Daniel Vallentin. For your love and your endless support and patience during this time. For the many conversations, the motivation and your unbeatable ability to structure. Thanks for our wonderful daughter, without both of you this work and I would not be complete.

Abstract

Background: Agriculture is a large and dynamic sector, essential for the supply of the population and thus in a complex area of tension. The growing population and the resulting need for optimization, greater efficiency and intensification are in direct conflict with the demand for sustainability, environmental compatibility and, above all, mitigation of climate change and its consequences. Precision agriculture can make a decisive contribution to increasing efficiency in particular. Because through the targeted and demand-oriented application of fertilizers and pesticides, but also spatially variable sowing, resources can be used better and in the best case even increase yields. Above all, if fertilizers are applied in the way that the plants need and can absorb them, in contrast to uniform application across the entire field, a surplus that can be washed into the groundwater can be avoided. A basis is therefore needed on which this variable application of resources can be determined. In practice, maps of current condition in the form of zones in the field or on-the-go measurements from sensors on the tractor are often used here. However, for comprehensive planning and holistic cultivation of crop, current and past spatial information maps, such as zone maps, are necessary. Satellite data are a data basis for such zones, as they are available in various types, current and retrospective and cover large areas spatially.

Objective: This work explores possibilities to derive this zoning from satellite data and developes different approaches. The interrelations between satellite data, geoinformation data and agricultural data such as yield will be investigated and combined. The focus of the method development is the applicability in practice and the associated requirements of the farmer.

Data: For method development and analysis 179 RapidEye scenes, 512 Landsat scenes, 43 Sentinel-2 scenes and 21 Planetscope scenes were used. Furthermore, the soil map „Bodenschätzung“, which not only transmits the information about the respective soil type, but also a quantification of the fertility respectively the yield potential in the form of „Bodenzahl“ and „Ackerzahl“. Digital terrain models in different spatial resolutions were used as well as in-situ measurements of nutrients, electrical conductivity and phenology.

Methods and Results: In this thesis two methods and a data analysis are presented. The first method uses only optical satellite data (RapidEye) and processes these automatically into five relative yield zones, which reflect the expected relative yield averaged over several years. The method independently selects the appropriate data sets for a prescribed field, using different thresholds resulting from the reflectance values of individual bands. The zones are then separated on the basis of quantile values using an synthetic, averaged raster of the near infrared bands. The method is validated with actual yield data using the characteristics of box plots. The yield zones generated can then be used as management zones in precision farming. The second method also generates relative yield zones, suitable for use as a management zone, using RapidEye satellite data as well as soil map and relief information. This data fusion for yield zone modeling is based on belief structures and uses

the Transferable Belief Model. Thus, individual expert knowledge from practical agriculture can be integrated into the fusion process. The knowledge generated in the course of method development about the relationship between remote sensing and GIS data and the actual yield on the field will be extended and consolidated in a large-scale data analysis with a time series of 13 years and 755 satellite scenes. It shows that there is a strong correlation between satellite data and yield data (up to a correlation value of r = 0.75, some values even higher). However, this correlation depends strongly on the phenological timing of - in this case - cereals and canola. In addition, the spectral and spatial resolution, as well as the growing conditions and the soil available water.

Conclusion: Satellite data are very well suited for agricultural applications and for the derivation of management zones for precision crop cultivation. However, a lot of expert knowledge has to be applied in the selection of the appropriate remote sensing data as well as in the processing and methodology. The scientific and practical use of remote sensing data should be adapted to the specific problem and external conditions.

Zusammenfassung

Hintergrund: Die Landwirtschaft ist ein großer und dynamischer Sektor, essentiell für die Versorgung der Bevölkerung und dadurch in einem komplexen Spannungsfeld. Die steigende Bevölkerung und der dadurch bestehende Bedarf an Optimierung, mehr Effizienz und Intensivierung steht im direkten Konflikt mit dem Anspruch nach Nachhaltigkeit, Umweltverträglichkeit aber vor allem der Eindämmung des Klimawandels und seiner Folgen. Gerade bei Fragen der Effizienzsteigerung kann der Bereich der Präzisionslandwirtschaft einen entscheidenden Beitrag leisten. Denn durch die gezielte und bedarfsorientierte Anwendung von Dünger und Pflanzenschutzmitteln, aber auch die gezielte und räumlich variable angepasste Aussaat, können Ressource besser genutzt werden und im besten Falle den Ertrag sogar steigern. Vor allem wenn Düngemittel so ausgebracht werden, wie die Pflanzen ihn benötigen und aufnehmen können, im Gegensatz zu einer uniformen Ausbringung über das ganze Feld hinweg, kann ein Überschuss, welcher in das Grundwasser ausgewaschen werden kann, vermieden werden. Es braucht also eine Grundlage, auf welcher diese variable Ausbringung von Ressourcen bestimmt wird. Hier werden in der Praxis oft Zustandskarten in Form von Zonen im Feld verwendet oder „on-the-go"-Messungen von Sensoren auf dem Traktor. Für die umfassende Planung und eine holistische Bearbeitung der Bestände sind aber aktuelle und zurückliegende, wie zusammenfassende Zustandskarten, beziehungsweise Zonenkarten nötig. Eine Datengrundlage für solche Zonen sind Satellitendaten, da sie in verschiedenster Art, aktuell und retroperspektiv vorliegen und große Flächen räumlich erfassen.

Ziel: Diese Arbeit erforscht Möglichkeiten aus Satellitendaten eben diese Zonierung abzuleiten und sucht dabei verschiedene Herangehensweisen. Es sollen die Zusammenhänge zwischen Satellitendaten, Daten der Geoinformation und landwirtschaftlicher Daten wie Ertrag untersucht und miteinander kombiniert werden. Im Fokus der Methodenentwicklung steht die Anwendbarkeit in der Praxis und die somit einhergehenden Anforderungen des Landwirtes.

Daten: Für die Methodenentwicklung und die Analyse wurden 179 RapidEye Szenen, 512 Landsat-Szenen, 43 Sentinel-2 Szenen und 21 Planetscope-Szenen verwendet. Weiterhin die Bodenkarte Bodenschätzung, welche nicht nur die Informationen über die jeweilige Bodenart übermittelt, aber auch eine Quantifizierung der Fruchtbarkeit beziehungsweise des Ertragspotentials in Form von „Bodenzahl" und „Ackerzahl". Digitale Geländemodell in unterschiedlichen räumlichen Auflösungen wurden verwendet, ebenso wie in-situ-Messungen von Nährstoffen, elektrischer Leitfähigkeit und Phänologie.

Methoden und Ergebnisse: In dieser Doktorarbeit werden zwei Methoden und eine Datenanalyse vorgestellt. Die erste Methode verwendet einzig optische Satellitendaten (RapidEye) und verarbeitet diese automatisiert zu fünf relativen Ertragszonen, welche den zu erwartenden relativen Ertrag gemittelt über mehrere Jahre spiegelt. Die Methode wählt dabei eigenständig die passenden Datensätze für ein vorgeschriebenes Feld aus, unter Verwendung verschiedener Schwellwerte, die sich aus den Rückstrahlwerten einzelner Bänder ergeben. Auf Basis eines gemittelten Rasters

der Bänder des nahen Infrarots werden dann auf Basis von Quartilswerten die Zonen separiert. Die Methode wird mit tatsächlichen Ertragsdaten mithilfe der Charakteristika von Boxplots validiert Die erzeugten Ertragszonen können dann als Bearbeitungszonen in der Präzisionslandwirtschaft verwendet werden. Die zweite Methode erzeugt ebenfalls relative Ertragszonen, geeignet für die Verwendung als Management Zone, verwendet neben RapidEye Satellitendaten auch die Informationen der Bodenkarte und des Reliefs. Diese Datenfusion zur Modellierung von Ertragszonen basiert auf Überzeugungsstrukturen und verwendet das Transferable Belief Model. Somit kann individuelles Expertenwissen aus der praktischen Landwirtschaft in den Fusionsprozess integrieren werden. Die Erkenntnisse, die im Laufe der Methodenentwicklung über die Zusammenhänge von Fernerkundungs- und GIS Daten und dem tatsächlichen Ertrag auf dem Feld generiert wurden, werden in einer großangelegten Datenanalyse mit einer Zeitreihe von 13 Jahren und 755 Satellitenszenen erweitert und gefestigt. Sie zeigt, dass es einen starken Zusammenhang zwischen Satellitendaten und Ertragsdaten gibt (bis zu einem Korrelationswert von r = 0.75, einzelne Werte höher). Diese Korrelation hängt aber stark ab vom phänologischen Zeitpunkt von – in diesem Falle – Getreide und Raps. Außerdem von der spektralen und räumlichen Auflösung, sowie den Wachstumsbedingungen und dem bodenverfügbaren Wasser.

Fazit: Satellitendaten eignen sich sehr gut für die Anwendung in der Landwirtschaft und für die Ableitung von Bearbeitungszonen für den Präzisionspflanzenbau. Allerdings muss in der Auswahl der passenden Fernerkundungsdaten und auch der Verarbeitung und Methodik viel Expertenwissen angewandt werden. Die wissenschaftliche und praktische Verwendung von Fernerkundungsdaten sollte an die spezifische Fragestellung und die äußeren Bedingungen angepasst werden.

Table of Contents

List of figures

List of tables

1 Introduction

1.1 Motivation and Structure

1.1.1 Motivation

Modern agriculture finds itself in a global field of tension in which very different interests and challenges meet. A growing world population, including a growing middle class with increased nutritional demands, is driving up the demand for agricultural products. At the same time, agricultural land and soil as a resource are limited. A changing climate aggravates the situation of farmers, as the probability of extreme weather events - whether droughts or floods - increases with climate change (IPCC 2019; Semenov and Shewry 2010; Zhang et al. 2019).

Agriculture must therefore manage its resources more efficiently and use them sustainably. Politics and society are additionally strengthening the demand for nature conservation and sustainable agriculture. It is not easy for agricultural companies to find their way in this area of tension, especially since price pressure on the national and international agricultural market is very high. Many stakeholders, including the German Federal Government, are relying on the digitization of agriculture (BMEL 2018) to make it more efficient and sustainable. The agricultural industry has long recognized the potential of digitization and precision farming as a large market, which is why new machines and software solutions are constantly being developed and distributed. However, the area of satellite data evaluation for precision farming applications is still relatively small and very little represented among end users, at least in Germany.

Satellite data provide frequent information about large areas with little or no cloud cover. Meanwhile, there are a number of satellites relevant for agriculture, including the freely available data from the European COPERNICUS mission and the American LANDSAT series. However, the path from data acquisition in space to the user in the field is very long and can currently hardly be taken without expert knowledge about data processing and interpretation. For use in precision farming applications, raster data based on pixels is currently still very poorly suited and zoning for further processing is often necessary.

This work therefore deals with the investigation of the potential of satellite data in precision farming and methods for zoning an agricultural field. Two methods are presented which have been developed and validated in this thesis. In addition, the question under which conditions satellite data correlate with yield data on the field and for what reason is investigated.

1.1.2 Structure of thesis

At the beginning of the work in Chapter 1, the scientific background on precision farming, remote sensing in agriculture and zoning methods is presented. Chapter 1 also includes the research objectives and a brief summary of the three consecutive stand-alone manuscripts presented in chapters 2-4. These were written as stand-alone manuscripts for international peer-reviewed journals. Two manuscripts were published (Georgi et al. 2017; Vallentin et al. 2019) in „Precision Agriculture“. The third article was recently submitted to “Agronomy” (10th of February 2020).

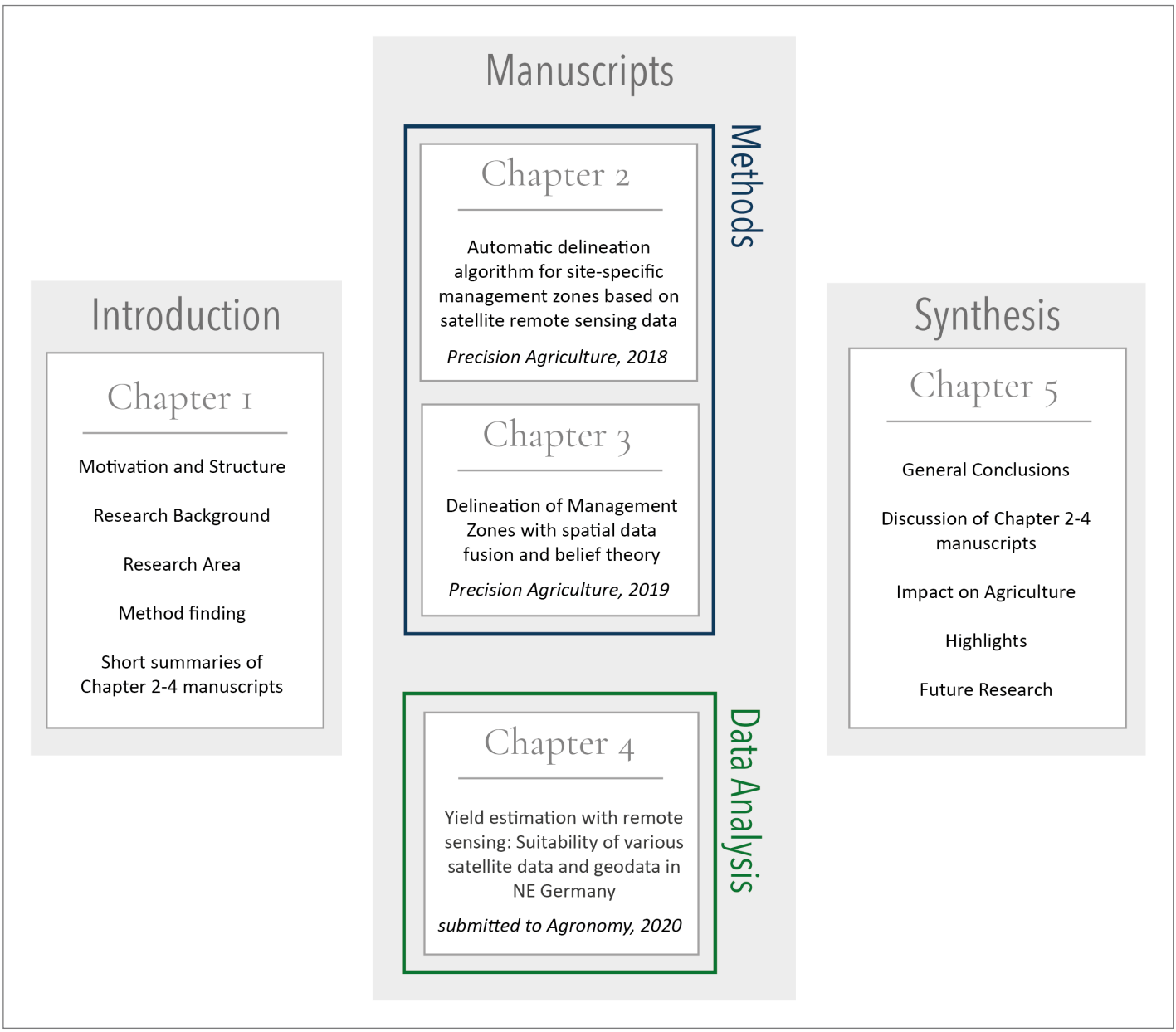

Fig. 1.1 Structure of this cumulative dissertation.

1. Georgi, C., Spengler, D., Itzerott, S., Kleinschmit.B (2018). **Automatic delineation algorithm for site-specific management zones based on satellite remote sensing data**. *Precision Agriculture*, 19, 4, pp. 684-707. DOI: 10.1007/s11119-017-9549-y (***Chapter 2***)

2. Vallentin, C., Dobers, E.S., Itzerott, S., Kleinschmit, B., Spengler, D. (2019). **Delineation of Management Zones with spatial data fusion and belief theory. Precision Agriculture**. DOI: 10.1007/s11119-019-09696-0 (***Chapter 3***)

3. Vallentin, C., Itzerott, S., Kleinschmit., B., Conrad, C., Spengler, D. (2020). **Yield estimation with remote sensing: Suitability of various satellite data and geodata in NE Germany**. Submitted to *Precision Agriculture* on 22nd of March 2020, *author's preprint version* (***Chapter 4***)

The first manuscript introduces an automatic delineation method for agricultural fields in which suitable multispectral satellite images are automatically selected over several years and five relative yield zones are identified. The second manuscript presents a data fusion method that not only takes into account multispectral satellite data, but also combines it with GIS data to delineate relative yield zones within a field. The third manuscript analyses the relationship between different multispectral satellite data and thresher yield data in a time series of 13 years.

The Synthesis in Chapter 5 discusses the research findings of Chapter 2-4 and suggests future research on the topics.

1.2 Research Background

1.2.1 Precision agriculture

The basis for precision agriculture (PA) is the spatial and temporal variability and heterogeneity of soil and crop characteristics within a field (Zhang,Wang and Wang 2002). PA practice in crop farming includes better management of resources such as fertilizers, herbicides, seeds, but also fuel consumed in field cultivation. Better management means using these resources in the right place at the right time (Mulla 2012).

The widespread practice - at least in Germany - in agriculture is the uniform spreading of these resources onto a field. The PA approach means to divide a field into management zones (MZ), where each zone gets customized inputs of the resources. This customization depends, for example, on soil differences or the heterogeneity of plant vitality. PA offers a more efficient use of the resources used and, in the case of precisely applied fertilizers or herbicides, can protect the environment (Robert et al. 1993; Mulla,Perillo and Cogger 1996; Mulla et al. 2002; Tian 2002).

However, the profitability of PA is discussed controversially (Swinton and Lowenberg-DeBoer 1998; Robert et al. 1999; Griffin et al. 2018). On the one hand, the acquisition costs of corresponding machines working with PA are very high. It is debatable though, if the precise output saves costs. More efficient use can, however, have the aim of homogenizing yields in the field and facilitating harvesting or push the high-potential yield zones and neglect low-potential yield zones to save resources. Ultimately, PA does not usually save on resources, but distributes them around the field according to the needs of the plant, thus preventing fertilizer from being released into the groundwater, for example. The profitability seems to depend on the type of PA measure taken (Griffin et al. 2018) and is less for example for variable rate application of fertilizer and quite higher for the implementation of GPS controlled vehicles, which is quite common in modern agriculture anyway. However, it is conceivable that PA could be applied to the application of pesticides and thus preserve biodiversity to a greater extent than application without PA. Furthermore, the analysis of the data on which PA is based could also lead to new management strategies that promote nature conservation and biodiversity. These include, for example, the designation of flower strips or renaturation zones, for example on the basis of yield zones with low profitability.

The basis of PA is the aggregation and evaluation of data and the associated information management (Mulla 2013). The central component of PA - the GPS positioning of agricultural vehicles - is already well established in practice. In order to make decisions in the PA, however, spatial and temporal data must inevitably be evaluated. Relevant data here are yield data, satellite and other remote sensing data, soil maps, records of ground-level sensors, measurements of electrical conductivity and nutrient content, as well as topographic maps and their products.

Most PA-optimized machines work on the basis of zones, they need vector data or polygons as input. Very few applications rely on continuous data, raster data, when adjusting fertilizer or spreading rates.

1.2.2 Spatial variability and management zones

The spatial variability of a field is therefore currently represented by zones. Management zones are subdivisions of a field, each characterized by relative homogeneity of crops and/or environmental parameters (Doerge 1999). The more general term „management unit“ was introduced by Lark and Stafford in 1997. Since then, many methods have been developed to divide a field into zones. A very obvious possibility to divide a field into zones and at the same time to establish a relation to the yield potential of a field is to use yield data (Lark 1998; Pedroso et al. 2010). However, this presupposes that yield data is also available and can be trusted. A standard yield measurement is, however, not given at harvest time and, above all, not common for many cropss. The data recorded by a thresher during harvesting can involve many sources of error (Blackmore and Marshall 1996; Doerge 1999; Dobers 2002), such as when several threshers are harvesting in the field and not calibrated, as well as uncertain recordings at the boundaries of the field. However, if a farmer has reliable yield data, this is a valuable data basis and is very suitable for delineation of MZ.

Information on soil and topography can also be used to spatially divide a field into zones (MacMillan et al. 1999; van Alphen and Stoorvogel 1999). The quality of the soil has a very large influence on the yield potential of a field as well as on the topography, especially in regions with high altitude differences. Erosion of topsoil on steep slopes can have just as unfavorable an effect on the cultivation of crops as sandy hilltops. However, depressions in which fine, loamy material accumulates can be good conditions for cultivation - unless they are too wet. MZ on the basis of soil characteristics is common in practice to derive seed maps, since the agricultural expert has experience with the emergence potential of his seed depending on the soil type. However, as for soil inventory maps, a sufficient scale is needed for precision farming applications (Franzen et al. 2002). Additionally, the question of relevance arises, when for example the standard soil map – such as the “Bodenschätzung” in Germany – dates back to the 1930s. Intensive soil grid mapping for status-quo maps is often not cost-effective and does not necessarily reflect the total spatial variability of crop growth (Hornung et al. 2006). The derivation of MZ from soil and topography information as a basis for a management decision on the crop during the season, as well as the application of nitrogen fertilizer during the growth phase, rather harbors risks concerning this data source. Although there is a strong relationship between soil and yield, soil patterns do not necessarily reflect crop patterns in a field (Chapter 4).

The zoning of a field is sometimes derived from data from near-soil sensors, such as maps of electrical conductivity (EC) (Kitchen et al. 2005; Cambouris et al. 2006). One standard instrument to measure electrical conductivity in the field is “EM38”. The interpretation of these data refers to soil

parameters, such as the grain size of the soil. The electrical conductivity of the soil depends on it as well as on the water content, texture and salinity. In addition, EC of soil is influenced by a number of complex and mostly inter-related parameters (Lück et al. 2009), therefore interpretation is not necessarily straightforward.

Since spatial patterns in EC measurements are affected by seasonal effects (e.g. weather conditions; Lück et al. 2009), single EC maps cannot be compared to EC maps for other fields in every case. The suitability as a basis for the derivation of MZ is therefore not ideal if the interesting variable is related to the plant growth itself, the vitality and the yield. Information on the condition of the crop during the vegetation phase, as well as retrospectively, is obtained by looking at the crop itself. It is common practice for a farmer to regularly check the condition of his crops. However, especially with large farms, not all areas and all spatial heterogeneity can be recorded manually on the ground. Remote sensing data promise to provide comprehensive information about the fields, plant covered or uncovered. In theory, the farmer has a lot of remote sensing data at his disposal, from images of various satellite sensors, as well as drone and aircraft mount sensors. The derivation of MZ from remote sensing data is becoming more and more important both in science and in the advisory agricultural sector (e.g. Song et al. 2009; Hank,Bach and Mauser 2015; Georgi et al. 2017).

In addition to the briefly mentioned methods for delineating MZ, which usually focus on one data type, there are also approaches to combine and merge several data types and data sources and to increase the information content (Fridgen et al. 2003; De Benedetto et al. 2013; Yao et al. 2014; Vallentin et al. 2019). These approaches are primarily an attempt to address the complexity of vegetation growth and to compensate for uncertainties in individual data sources. A detailed treatment of the topic of data fusion and MZ is given in Chapter 3.

Fig. 1.2 Spectra of vegetation and soil.

1.2.3 Remote sensing in agriculture

Remote sensing in agriculture is based on the interaction of electromagnetic radiation emitted from the sun with soil and plant material. Optical remote sensing measures the proportion of electromagnetic radiation reflected by the earth's surface materials rather than the transmitted and absorbed radiation. The degree of reflection, transmission and absorption depends on the chemical and physical composition of the material to which the solar radiation is incident. This results in characteristic reflection curves, so-called reflection spectra. With the help of these spectra, which plot the reflection against the wavelength of the electromagnetic radiation, materials and partly their condition can be detected. Thus, the spectra of vital vegetation differ from dry vegetation and from soil (*Fig. 1.2*).

Reflection can be measured on different platforms. These include satellites, aircraft, drones (UAV - Unmanned Aerial Vehicle), tractors and hand-held sensors. Optical remote and near sensing covers the spectral range from ultraviolet up to infrared, including the visible fraction of light. In this work the reflection from the visible to the near infrared was evaluated. The most common sensors of mentioned platforms, especially the satellites, are operating on the multispectral principle. A multispectral sensor therefore only records in certain wavelength ranges, the channels or bands of the sensor. The respective channels form an average value over a certain bandwidth of the electromagnetic spectrum. The satellite sensors, whose data are the basis of this work, often have very different positions and numbers of their bands (*Fig. 1.3*).

The analysis of vegetation makes use of the high contrasts in the vegetation spectrum (*Fig. 1.2*). By forming ratios from the different bands, vegetation indices (VI) can be calculated, which can indirectly measure the condition of the vegetation cover. The most common VI is the Normalized Difference Vegetation Index (NDVI)(Rouse et al. 1974; Tucker 1979). The NDVI calculates a ratio by using the red and the near infrared (NIR) band. A high, positive NDVI indicates a high vegetation coverage or a high vitality, while a low, positive NDVI indicates vegetation-free areas. NDVI has also been widely used since the early 1980s because of its strong correlation with the Leaf Area Index (LAI) and fAPAR (fraction of Absorbed Photosyntetically Active Radiation)(Prince 1991).

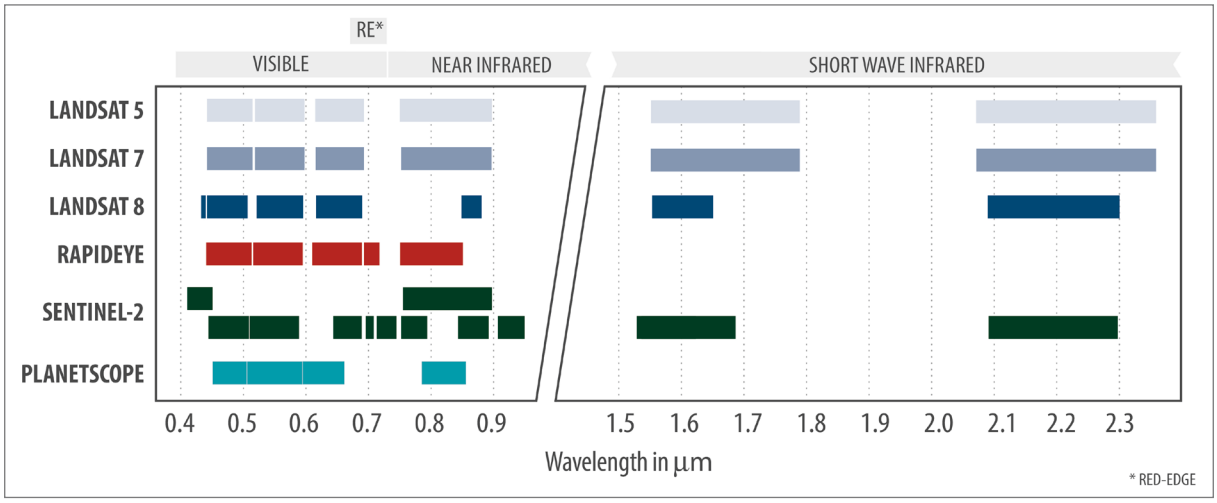

Fig 1.3 Band postions of optical satellite sensors used in this thesis.

In addition to multispectral sensors, there is a whole range of other sensors which are certainly relevant for agricultural applications. These include the hyperspectral sensors, which contain even more spectral information and can therefore offer new possibilities in the field of agriculture (Mauser et al. 2012). They draw a nearly continuous spectrum in very many and very narrow bands. This property is important in the agricultural context in soil science for the mapping of organic carbon and nutrients (Zheng 2008). Furthermore, hyperspectral data are used in the determination of water stress in plants (Tilling et al. 2006; Cao,Wang and Zheng 2015), determination of pigments and plant nutrients (Blackburn 2007; Zhang et al. 2008; Clevers and Kooistra 2012), as well as biomass (Hansen and Schjoerring 2003) and numerous others.

Temperature sensitive remote sensing sensors such as thermal systems can provide valuable informa-tion on crop temperature and detect stress situations. Similarly, the analysis of soil moisture with thermal data is conceivable (Qui 2006; Elsayed et al. 2017; Khanal,Fulton and Shearer 2017). How-ever, thermal and hyperspectral sensors on satellite basis have a rather low spatial resolution (> 30m). For PA applications in Germany such Ground Sampling Distances (GSD) are often too coarse resolved.

Radar data can be used to make different statements in agricultural remote sensing. These systems actively transmit a signal which they receive again after various scattering. In contrast to optical systems, radar systems are independent of cloud cover. In agriculture, radar data are used for example in phenology determination (Nasrallah et al. 2019), soil moisture determination (Paloscia et al. 2013) and biomass estimation (Harfenmeister,Spengler and Weltzien 2019).

1.2.4 Remote sensing for precision agriculture

The use of satellite data in PA focuses on the detection and analysis of spatial variability of field parameters. This variability may concern plant vitality, biomass, LAI, chlorophyll content, weed dispersal or soil differences. The principle of PA is the active management of spatial variability, which is best captured by spatial data.

Remote sensing should derive the condition of the plant or the soil in order to make appropriate decisions in farming. Soil moisture (Ahmad,Kalra and Stephen 2010; Rahimzadeh-Bajgiran et al. 2013) or organic carbon (Zheng 2008; Blasch et al. 2015) derived from remote sensing can serve the farmer to create spatially variable seed maps or to evaluate the yield potential of the field differently. Such soil characteristics can also be used as an aid in designing soil sampling schemes. In this procedure, a soil sample is taken selectively at different positions in the field. This procedure is obligatory and cost-intensive for farmers in Germany, which is why targeted sampling, depending on the heterogeneity of the field, is desirable.

Remote sensing in precision agriculture can also derive parameters of the condition of the crop, the most relevant for the farmer being the nitrogen status, which can also be conditionally derived from remote sensing, especially hyperspectral sensors (Zheng 2008; Mahajan et al. 2014). The retrieval of canopy chlorophyll is more established and also possible with multispectral sensors (Delloye, Weiss and Defourny 2018) and linked with nitrogen uptake. On the basis of this information, fertilization can then be adjusted during the growing season. Such a variable and precise adjustment then supplies the crop with the amount of fertilizer they need and saves the scrap of unneeded fertilizer

which could otherwise be washed into the groundwater. Precision farmers often use an agricultural machine equipped with a sensor to measure the nitrogen status during fertilization. In this case the remote sensing data can make a contribution by feeding and improving the „online“ measured data of the near plant sensor in the „Map Overlay“ procedure.

Remote sensing of plant ripeness (Herwitz et al. 2004) can give the farmer the opportunity to make decisions about the optimal harvest time, especially when meteorological low pressure areas and storms are expected. The estimation of yield (Benedetti and Rossini 1993; Drummond et al. 2002; Kowalik et al. 2014) and yield potential (Raun et al. 2001; Andarzian et al. 2008; Van Wart et al. 2013) are also useful applications in precision farming. The estimation of the yield, for example, contributes to economic planning and precise fertilizer application. The yield potential can be used to optimize crop rotation or to divide entire fields into sub-fields in order to make sustainable use of variability. The derivation of absolute yield data is, however, extremely difficult, since a remote sensing sensor does not directly measure the grain yield. Absolute modelling may be possible if past yield data from the same field are used to calibrate the model parameters and if the quality of such yield data is sufficient. The use of growth models and the integration of meteo-data (Hank,Bach and Mauser 2015) is also promising here.

The derivation of yield from satellite data is an interpretation, but the correlation between the reflectance and the cereal yield and with limitations canola is definitely given (Chapter 4, Kyratzis et al. 2015; Sulik and Long 2016). The yield - especially for cereals - is a function of a rate of biomass or seed dry matter accumulation expressed over a finite time (Egli 2017). The number and density of plants is also related to the final yield, at least at certain phenological stages (Geisler 1983). Yield cannot be assessed by remote sensing directly, but grain growth is based on cell multiplication and the assimilation rate in the plant. Grain-growth important assimilation is driven by the photosynthetic activity of the top most plant parts (Geisler 1988), which is visible to the remote sensing sensors.

If it were possible to determine the absolute yield on a field and subfield basis on the basis of remote sensing data only, this would certainly be valuable for farmers, authorities and scientists alike. But also, the relative yields, which are the focus of this paper, contribute a valuable part to precision farming applications. Since most agricultural machines used for PA management work with zoned maps anyway, the methods presented here have been developed towards zoning and not with the aim of maps with continuous pixel values.

Numerous scientific publications deal with the topic of yield modelling from satellite data with varying success (e.g. Shanahan et al. 2001; Doraiswamy et al. 2003; Gontia and Tiwari 2011; Pantazi et al. 2016). Investigated are the most frequently cultivated crops in Germany, cereals (Labus et al. 2002; Laurila et al. 2010), canola (Cowley et al. 2014; Gong et al. 2018), maize (Sakamoto,Gitelson and Arkebauer 2013; Torino et al. 2014) and grassland (Jianlong,Tiangang and Quangong 1998), as well as numerous other arable crops such as soya (Ma et al. 2001) and wine (Cunha,Marçal and Silva 2010) are also investigated. However, the questions and the data basis of many publications cannot be applied to the data basis of this work and are therefore only comparable to a limited extent in the development of methods. The yield modelling is often focused on regional (Ren et al. 2007, 2008) scales. In some cases on global scale through the modelling of net primary production (Field,Randerson and Malmström 1995), country-wide scale (Laurila et al. 2010; Bolton and Friedl 2013), whereby the heterogeneity of yields within a field is very rarely investigated with satellite

data. Studies on within-field variability mostly deal with the creation of management zones. The availability of high-resolution yield data as dense point measurements on fields with an average size of more than 100 hectares is rather rare. Especially the fourth chapter of this thesis exploits the immense time series of remote sensing and agricultural yield data scientifically.

1.3 Research Objectives

The advancing digitization in agriculture continues to require solutions especially for precision farming in order to make agriculture sustainable, efficient and adapted. With „Big Data“ as the data basis, the information is available, but the methods for data processing must be constantly developed. The objectives of this dissertation are the analysis of optical satellite data and their usability in PA as well as the development of methods to automate and partially automate the analysis of these data in order to generate added value for farmers in practice. Data from 6 satellite sensors from the years 2006-2018 were used as a basis for this analysis and the development of methods and were linked to agricultural data such as yield maps, soil information and nutrient content. The concrete research objectives (R) are:

R-01: ***Development of a fully automated method based on optical satellite data, which divides an agricultural field into long-term relative yield zones, which can be used as MZ.***

R-02 a: ***Development of a method which, in addition to satellite data, also considers other map material, such as soil information, to generate relative yield zones using a data fusion model.***

R-02 b: ***Evaluation of a statistical model which is able to integrate the expert knowledge of a farmer into the data fusion in order to open the algorithm for human knowledge and thus improve the method.***

R-03: ***Analysis of the relations between optical satellite data of different sensors at different times and the yield data of the corresponding years. Which satellite data are best suited for yield-relevant questions and at which point in time?***

The scientific questions are of high relevance for both science and practice. An accompanying goal is to develop applications that can be transferred into practice, which is why applicability has a high priority in development. However, the transferability of the developed methods to other scientific areas and questions in dealing with spatial data also has potential. Above all, the analysis of the purely statistical relationships between satellite data and yield as well as GIS data is a valuable contribution for research and practice.

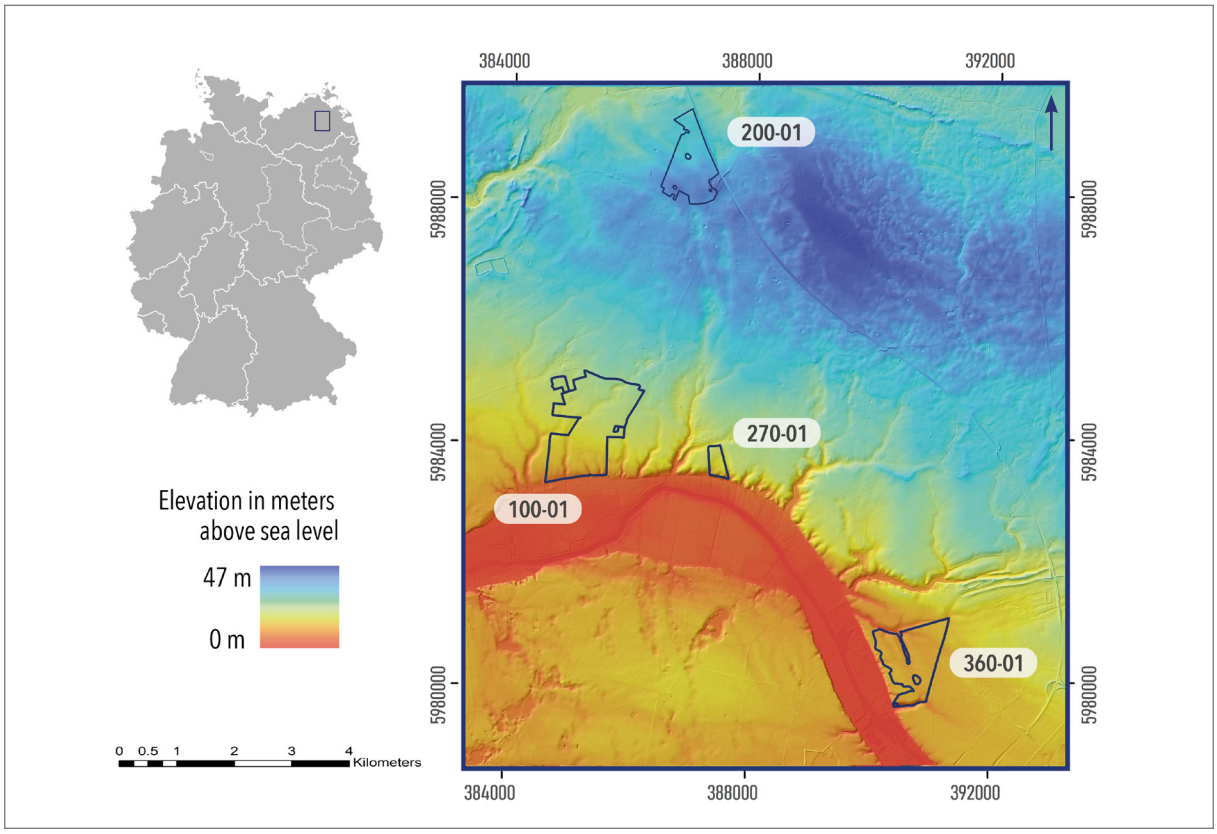

Fig. 1.4 Research area, located in the NE of Germany. Below: Topography of main research area with agricultural fields investigated.

1.4 Research Area

The research area is located in the federal state Mecklenburg-Vorpommern, in the north-eastern lowlands of Germany (*Fig. 1.4*). The federal state is sparsely populated (≤67 inhabitants per km²) and is used intensively for agriculture (approx. 58% cultivated area). Half of the cultivated crops are cereals (51.9 %). Also widespread is the cultivation of canola as part of the oil crops (18.5%) and crops for green harvest (18.7%), which includes maize (Statistisches Amt Mecklenburg-Vorpommern 2019).

The soils of the research area belong to the young moraine soil-covered areas of northern Germany. They have typical glacial morphological features, such as extensive ground moraine areas, push (end) moraines, glacial valleys, lake basins, eskers, kettle holes and sandars, formed by recurrent glacial processes during the Weichselian Glaciation of the last Pleistocene. Characteristic soil types in the research area are Luvisole, Stagnosole, Cambisole and Albeluvisole. In the floodplains there are peaty soils (Bundesanstalt für Geowissenschaften und Rohstoffe 2006). The research area is part of the observatory TERENO-NE (Heinrich et al. 2018).

The method development of this work was primarily carried out on fields of an agricultural company, 15 kilometers southwest (53°99'N,13°27'E) of Greifswald. The farm cultivates about 2000 hectares of cereal, canola, maize, sugar beet and grassland. During the data recording period on which this dissertation is based, the farm operated precision agriculture, especially in the area of fertilization. The topography on this area is not very pronounced, with the southern fields descending towards the Peene River, where the greatest topographical differences can be seen, e.g. in the pronounced drainage channels. For the analytical part of this work, fields of a second farm were also used, which extend over a large area between Greifswald and Demmin (53°54'N, 13°3'E).

1.5 Data

The primary data basis for this work are optical satellite data of the following sensors: RapidEye, Landsat-5, Landsat-7, Landsat-8, Sentinel-2 and Planetscope (*Table 1.1*). Each of these satellite data has different spectral and spatial characteristics and therefore addresses different questions. The method development was carried out on the basis of RapidEye satellite data. As additional information in the background, optical ortho photos of the state of Mecklenburg were used as a WMS service, as well as UAV photos and data from hyperspectral flight campaigns. For the analysis, a map of organic carbon generated from satellite data by Blasch et al. 2015 was also used.

The GIS data used included field boundaries, soil maps, yield data, nutrient sampling and electrical conductivity measurements. A detailed description of these data can be found in the publications summarized here.

Table 1.1 Data sets used in this thesis for method development and analysis

Data source or type	Years	No. of data sets	Spatial resolution [1]	Spectral resolution used in study [2]	Used in chapter [3]
Satellite Data					
RapidEye from RESA Archive	2009-2018	179	6.5 / 5 m	5 bands: blue, green, red, red edge, nir	Chapter 2-4
Landsat 5	2006, 2007, 2009-2011	105	30 m	4 bands: blue, green, red, nir	Chapter 4
Landsat 7	2006-2017	280	30 m		
Landsat 8	2013-2018	127	30 m		
Planetscope	2017-2018	21	3 m		
Sentinel-2	2017-2018	43	10 m/ 20 m	8 bands: blue, green, red, 3 red edge bands, nir	
Other Raster Data					
Digital elevation model	2011	1	5 m	-	Chapter 3, 4
Corg Map	2009-2014	1	5 m		Chapter 4
Vector Data					
Soil map	1930s	1	Polygon	-	Chapter 3, 4
EM38	2009	1	Point		Chapter 4
Yield Data	2006-2018	947	Point		Chapter 2-4

1 *of used bands*
2 *Sensors offer more band choices*
3 *For methods, calculations and analysis*

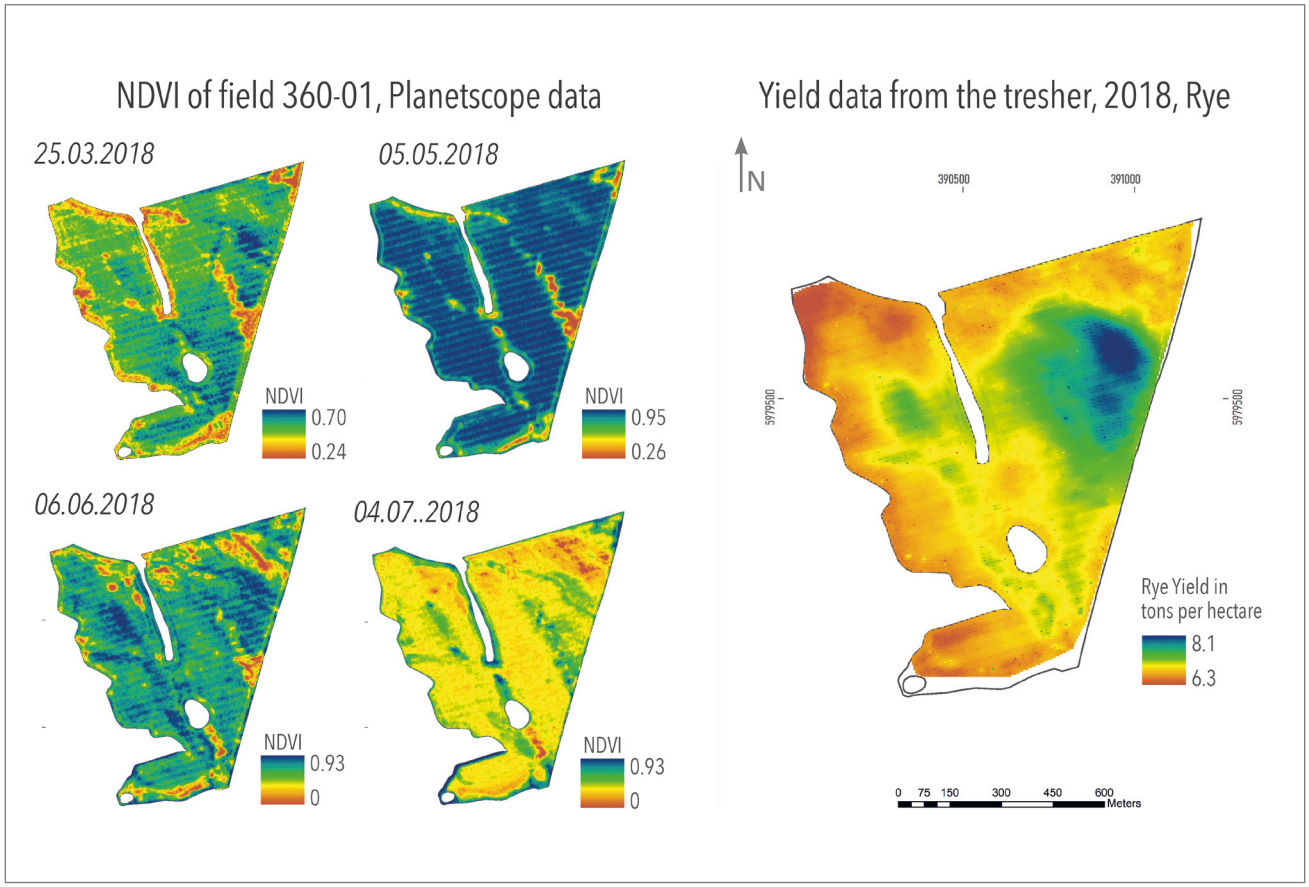

Fig. 1.5 Time series of NDVI rasters, calculated from Planetscope data for four dates in 2018 on field 360-01.

1.6 Method Finding

For the processing of research objectives and the development of practical methods, techniques of image processing, segmentation and data fusion had to be explored. In this section the steps to find these methods are explained.

Selection of the appropriate remote sensing data

The RapidEye satellite system was used for the method development of Chapter 2 and Chapter 3. It consists of five equivalent satellites and has a high spatial resolution of 6.5 meters, which are resampled to 5 meters by the provider as standard. The repetition rate of the recording is 5.5 days at Nadir and the spatial coverage is sufficiently large with a 77 km long swath width. The primary suitability, however, for the analysis of crop patterns lies in the spectral resolution of the system. RapidEye has five spectral bands, the channels blue, green, red, red edge and near infrared (NIR). Since vegetation reflects particularly strongly in the NIR range, this channel is a crucial component and is of great importance in the method of Chapter 2.

The extensive data available from the RapidEye Science Archive (Grant Number 617 FKZ) (Borg, Daedelow and Johnson 2012), free of charge for research, therefore provides a valuable basis for questions in the field of agriculture.

For the analysis of Chapter 4, the data set has been extended to test other optical satellites suitable for yield modelling. The systems Landsat, Sentinel-2 and Planetscope (*Table 1.1*) were considered, which are either completely freely available or, like the latter, free for research purposes and students. All these systems have spectral properties relevant for the research of crops and crop parameters.

Choosing the right GIS data

For the method development of Chapter 3 and the analysis of Chapter 4, the GIS data already mentioned were used. Especially the soil information as soil map with several information layers and the digital elevation model are of relevance, because they offer area-wide and relevant information. In order to analyse, understand and model crop patterns and related parameters, the combination of elevation model and soil type provides more information on the pattern distribution.

Evaluation of the appropriate segmentation method for plant patterns

Segmentation approaches are widely used in the field of remote sensing and even companies like Trimble have specialized in pattern mapping with software like eCognition (Trimble). Segmentation algorithms differ from image classification in that they are object-oriented. This results in discrete zones rather than classes with certain properties (such as landscape classification of forest, field, soil, water, etc.). Segmentation algorithms aim at homogeneous zones with respect to the selected parameter (e.g. soil color, plant vitality). Most segmentation methods follow two basic principles: the contour-based and the region-based ones (Bolon et al. 1995; Pedroso et al. 2010). The contour-based family is particularly suitable for object recognition, while the region-based family is more suitable when no clear lines are present. This is the case with within-field variations of soil or plant parameters and is therefore very well suited for agricultural data zoning. Object-oriented questions can be solved with commercial software (Liu et al. 2017), the claim of method development from Chapter 2 and Chapter 3 of this dissertation was primarily a non-commercial solution, which is applicable and transferable into practice. Commercial software as part of the workflow therefore had to be excluded. In the agrar-specific remote sensing disciplines, plant and soil patterns are segmented with k-means (Johann et al.; Cheng, Peng and Liu 2013) or fuzzy kmeans (Song et al. 2009) after exclusion of these criteria.

The k-means approach forms clusters of similar attributes in a collection of values but can lead to marginalization of certain classes in a raster data set. If there are a few pixels whose values are extremely different from all others, they form their own class, which is mathematically correct, but does not naturally fit with the visual analysis of a satellite image of a field. If plants were destroyed on a densely overgrown field, for example by damage caused by boars or other wild animals, and the soil signal dominated, then this local place in the field would receive its own class. Especially yield data can contain a number of outliers that occur locally. At the edge of a field or around a sink hole. If these outliers have a critical number of points, they themselves are identified as the center of a cluster. A further hurdle when using k-means is that it is not clear which class stands for which value range. So, it is not clear which class represents low and which high vitality.

As explained in Chapter 1.2.3 (*Remote sensing for precision agriculture*), there are strong correlations between yield and reflectance, especially in the NIR range. In order to perform a simple segmen-

tation, the segmentation method in Chapter 2 uses exactly this band and divides it into five zones. The thresholds are four evenly distributed quantiles of each data set. If fixed NIR values were to be used for all data sets, the data range of each individual data set would not be respected and classes with an unequal number of values could also result. The use of quantile values guarantees that there are enough pixels in each class, while the result is verifiable.

This method allows data sets of different ranges to be segmented, while the classification of zones into the interpretation „very low yield", „low yield", „medium yield", „high yield" and „very high yield" follows the assumed and proven dependence on remote sensing data and yield in Chapter 4.

Evaluation of the suitable data fusion method

The use of satellite data for spatial questions, which document the actual state, is increasing in value, since the availability of data is also constantly increasing. Not only current problems can be dealt with, but also change analyses and comparisons can be carried out, which can draw on an ever-increasing data archive. As already explained, under the right conditions there is a high correlation between satellite data and yield, especially for cereals, which is related to the intensity of the back radiation and the associated degree of vitality. However, it is quite possible that other plants, such as weeds, also produce a high level of reflection and that modelling with - only the satellite image - in these areas is wrong. Of course, yield modelling with satellite images also entails the uncertainty that not only the connection between yield and vitality, but also the connection between reflection and vitality is an interpretation. The question therefore arises as to whether this more up-to-date data can be upgraded by combining it with existing GIS data. Especially if these other data also allow conclusions to be drawn about the yield and are also used and better understood by a farmer than satellite data. The second method of this work (Chapter 3) therefore deals with the question of whether and how satellite data, a soil map and relief information can be combined to achieve the best possible yield zoning.

The use of fusion methods in remote sensing is not new, but highly complex. This is due to the fact that different data have different formats (raster, polygons, points), different spatial and spectral resolution or are recorded and interpreted in a completely different way (e.g. radar). There are many ways to combine different data sources into the same parameter, such as Bayesian techniques (Xue, Leung and Fung 2017), Neural Networks (Teimouri, Mokhtarzade and Valadan Zoej 2016), Support Vector Machines (Park and Im 2016), Random Forest (Crnojevic et al. 2014) and Dempster-Shafer Theory (DST) (Le Hegarat-Mascle, Richard and Ottle 2002; Ran et al. 2008).

The challenge of method finding in this thesis was that most fusion approaches in the field of remote sensing aim at classification. For example, the classification of a scene into forest, meadow, field, water, urban development. The division of a field into yield zones, whose boundaries are naturally fluid, is a topic that can hardly be found in the current publication landscape. Another claim of the method is to work simply and transparently. Even a user - the farmer or a consulting firm - must be able to understand the fusion method. The use of a „black box" algorithm in this industry is more likely to lead to mistrust and resentment. Machine-learning algorithms such as Support Vector Machine or Random Forest were therefore out of the question. The method should support the farmer and at the same time be able to incorporate the expert knowledge and experience of the farmer into its calculation.

For the method from Chapter 3, an interpretation of the Dempster-Shafer theory was used, the Transferable Belief Model (TBM), developed by Smets and Kennes in 1994. The suitability for agricultural questions has already been tested by co-author Dobers in 2008. In its functionality and structure, the TBM is very similar to the Bayesian model, but is based on quantified beliefs and not on probabilities. It is able to integrate expert knowledge based on experience and knowledge.

The use of the Bayes method has been intensively studied, precisely because there is much more experience with this approach in the literature. However, the calculation in the fusion process does not allow a conviction for the occurrence of several classes to be possible. For example, if the farmer in a sink of the field expects both a high yield (because it is constantly humid) and a low yield (because it could be too wet or flooded by heavy rain).

The TBM allows the assignment of a combined quantified belief for the assumption of both events, whereas in the Bayesian model one belief or probability has to be assigned for each event. This in turn affects the practicability for the farmer in practice and could realistically only be supported by a machine learning algorithm.

The TBM, on the other hand, is also very flexible in this respect. The default settings and interpretations of the individual data sources and classes of data sources can be carried out completely manually by the expert. Optionally an automatically generated input based on machine learning is possible as well as the correction of these suggestions by the expert himself. A detailed explanation of the TBM as well as the terminology and mathematics of the model are described in Chapter 3.

1.7 Summary of Chapters 2 – 4: Research Manuscripts

Chapter 2: **Automatic delineation algorithm for site-specific management zones based on satellite remote sensing data**

The aim of this study was to develop a method to divide an agricultural field into five relative yield zones based on satellite data. The algorithm works automatically and requires only the field boundaries as a vector file and a collection of multispectral satellite data recorded in the years relevant to the user. Relative yield zones averaged over these selected years are modelled. The mapping of these yield zones is based on the growth and vitality patterns of the field crops wheat, rye, barley and canola and deals with research objective R-01. The method is transparent and simple and was successfully transferred to other fields as part of the method development. As with the other manuscripts, the test area for the development corresponds to the research area described in Chapter 1.4 (*Research Area*). The working steps of the manuscript are:

- Select RapidEye satellite images of a field to investigate and define appropriate images which show plant patterns (and are not free of vegetation or too dense vegetation)

- Recognize plant patterns on a field with RapidEye satellite data and define the spectral bands that are most sensitive to these patterns.
- Establish the relationship between plant patterns, reflection values of satellite imagery and yield data.
- Design an automated workflow with selection criteria and thresholds that automatically selects the appropriate RapidEye scenes for the field
- Choose a method that divides the selected acquisitions into five relative yield zones
- Validate the result with actual yield data
- Test the transferability of the method on three other different fields

***Chapter 3*: Delineation of Management Zones with spatial data fusion and belief theory**

The aim of this study was to find a way to combine satellite data, soil map and relief information in order to derive relative yield zones within a field within the framework of research objective R-02 a. With this method, the integration of expert knowledge (R-02 b) is possible, since the delineation of the management zones is carried out on the basis of belief structures. The study presents the possibilities of this data fusion with beliefs, describes their possibilities and limitations and gives several examples of the combination and the respective results. In comparison to the manuscript from Chapter 2, only three relative yield zones are formed, which is due to the complexity of the method. The study tries to test the data fusion algorithm at the simplest level in order to test the feasibility and explain the principles. The steps include:

- Analysis of the input data: RapidEye satellite images, soil map, relief information and their correlation with the thresher yield data.
- Analysis of relations between input data and yield data for evaluation of the input data as data source for the Transferable Belief Model (Hypotheses, Belief, Reliability)
- Set-up of the TBM: Formatting / classifying the input data, assigning variables relevant for the TBM and programming the workflow.
- Validation of combination results with actual yield data
- Testing of all possible combinations of the eleven input data sets and ranking of the best results in a combination matrix
- Selection of the most relevant and correlating results

***Chapter 4*: Yield estimation with remote sensing: Suitability of various satellite data and geodata in NE Germany**

The study analyses the correlation between a series of multispectral satellite data and selected GIS data with actual yield data from two farms in the study area. The aim is to investigate which data sets correlate best with the yield data and which parameters characterize these well correlated data sets (R-03). One additional goal is to provide assistance for those who want to model yields using satellite data and seek the appropriate data for the appropriate time periods. In the flood of satellite data - often freely available - it is often not trivial to find the most suitable and reliable data to model the yield. The study investigates the significance of the factors spectral and spatial resolution, time of recording and phenology of the crop and examines the suitability of a number of vegetation indices. The work steps include:

- Collection and processing of satellite data from the Landsat (5,7,8), RapidEye, Sentinel-2 and Planetscope sensors from 2006 onwards for the study area
- Establish a correlation table that takes into account the above factors and allows identification of the best correlating data sets
- Identification of the best correlating data sets and analysis of the parameters which describe the respective datasets
- Derivation of new knowledge about which data at which phenological stage are most suitable for which crop to model yield

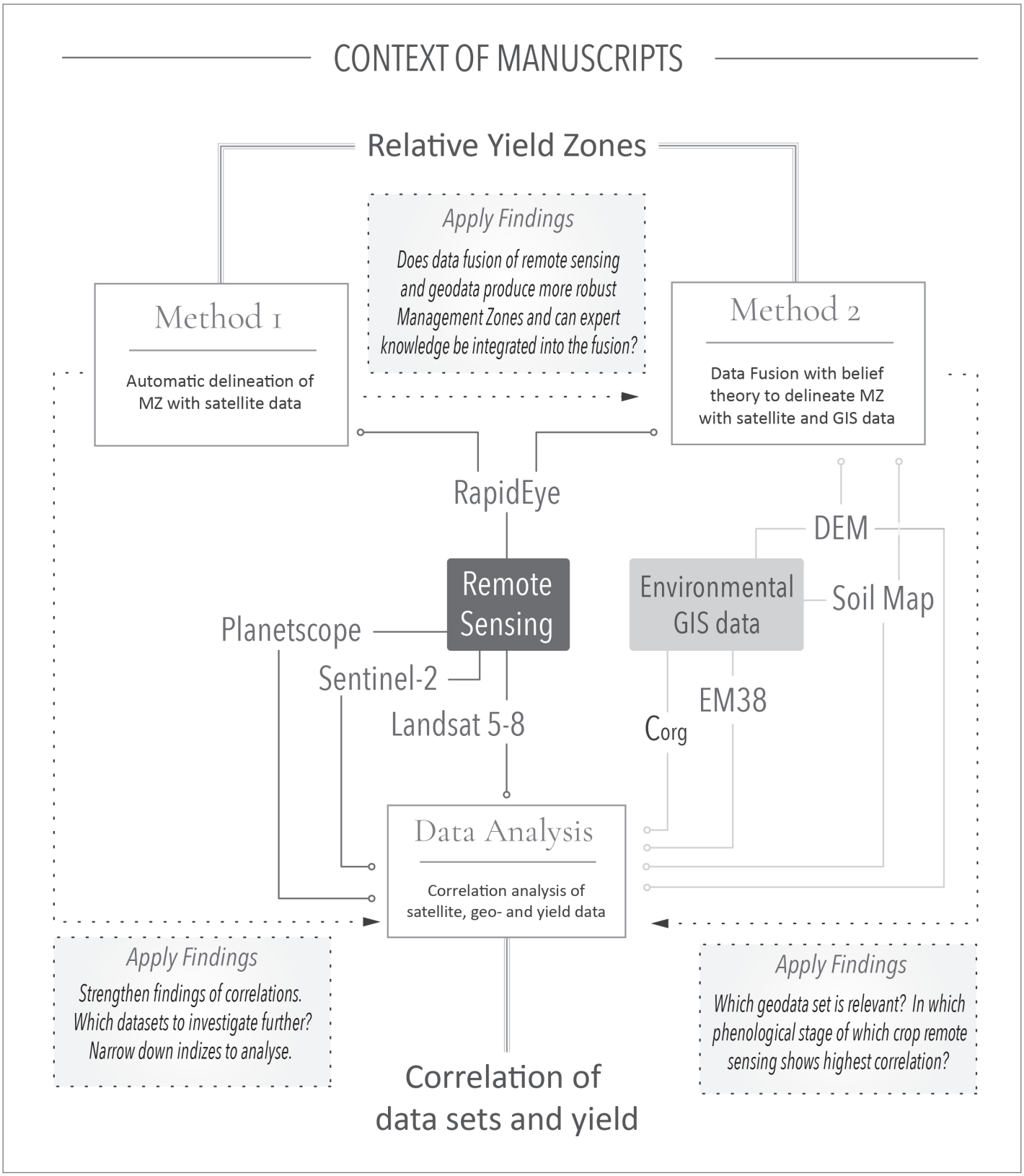

Fig. 1.6 Context and relations of research manuscripts in this thesis.

2 Automatic Delineation of Management Zones

Georgi, C., Spengler, D., Itzerott, S. and Kleinschmit, B. (2017).
Automatic delineation algorithm for site-specific management zones based on satellite remote sensing data. *Precision Agriculture*. Springer US, 19(4), 684–707.

Accepted manuscript

Published online: 15 November 2017 (doi: 10.1007/s11119-017-9549-y.)

Abstract

In light of the increasing demand for food production, climate change challenges for agriculture, and economic pressure, precision farming is an ever-growing market. The development and distribution of remote sensing applications is also growing. The availability of extensive spatial and temporal data – enhanced by satellite remote sensing and open-source policies – provides an attractive opportunity to collect, analyze and use agricultural data at the farm scale and beyond. The division of individual fields into zones of differing yield potential (management zones (MZ)) is the basis of most offline and map-overlay precision farming applications. In the process of delineation, manual labor is often required for the acquisition of suitable images and additional information on crop type. The authors therefore developed an automatic segmentation algorithm using multispectral satellite data, which is able to map stable crop growing patterns, reflecting areas of relative yield expectations within a field. The algorithm, using RapidEye data, is a quick and probably low-cost opportunity to divide agricultural fields into MZ, especially when yield data is insufficient or nonexistent. With the increasing availability of satellite images, this method can address numerous users in agriculture and lower the threshold of implementing precision farming practices by providing a preliminary spatial field assessment.

2.1 Introduction

The major aim of precision agriculture is to optimize crop management by addressing spatial variability, and thus optimize the use of farm inputs such as fertilizers and herbicides (Mulla 2013). In general, vast information is accumulated and used for the analysis of field inventory, crop growth and yield patterns. With this information, customized inputs can be applied to management zones (MZ), i.e. the units into which large farm fields are divided (Mulla 2013).

The delineation of MZ is the basis of most precision agriculture (PA) practices, addressing the within-field variability of crop and crop yield. MZ are subdivisions of a field, each characterized by relative homogeneity of crops and/or environmental parameters (Doerge 1999), which therefore differ in the need for specific input rates of treatment. The more generic term 'management unit' was introduced by Lark & Stafford (1997), and numerous delineation methods have emerged since then. They are usually either based on yield maps (Pedroso et al. 2010; Lark 1998), soil and topographic properties (MacMillan et al. 1999; van Alphen and Stoorvogel 1999), electrical conductivity data (Kitchen et al. 2005; Cambouris et al. 2006), remote sensing and vegetation indices (Ahn et al. 1999; Song et al. 2009), or a combination of these methods (Fridgen et al. 2003; De Benedetto et al. 2013; Yao et al. 2014).

Every automatic method to determine MZ has several disadvantages in terms of accuracy and applicability. Commonly, segmentation applications rely on yield maps, which are acquired neither by every farmer nor for every field, even if the company is in possession of the required technology. Yield data have significant error sources, such as via sensor, georeferencing, operator or data processing errors (Simbahan et al. 2004), and are also complicated to prepare (Blackmore and Marshall 1996). Moreover, the irregular distribution of data points in regard to the spatial variation in yield can impede accurate interpolation, which is a necessity for most spatial analyses.

The use of soil sampling data and soil maps for delineation of MZ is also a common approach, especially if yield maps are not available. However, as for soil inventory maps, a sufficient scale is needed for precision farming applications (Franzen et al. 2002). Additionally, the question of relevance arises, when for example the standard soil map – such as the "Bodenschätzung" in Germany – dates back to the 1930s. Intensive soil grid mapping for status quo maps is often not cost-effective and does not necessarily reflect the total spatial variability of crop growth (Hornung et al. 2006).

Electrical conductivity (EC) maps acquired with instruments like the standard "EM38" can also be used for successful MZ delineation (Cambouris et al. 2006). They reflect soil differences due to such factors as moisture content, salinity and texture. However, even if these characteristics influence crop growth significantly, EC maps may not always give a direct picture of in-season vegetation patterns. In addition, EC of soil is influenced by a number of complex and mostly interrelated parameters (Lück et al. 2009), therefore interpretation is not necessarily straightforward. Since spatial patterns in EC measurements are affected by seasonal effects (e.g. weather conditions; Lück et al. 2009), single EC maps cannot be compared to EC maps for other fields in every case.

Promising point-based measurement approaches are fusion and (fuzzy) clustering techniques (Fridgen et al. 2003; Fu et al. 2010; Shaddad et al. 2016), though they have only been tested on small and medium fields (≤ 40ha) according to the literature. Point measurements, whether from soil sampling, EC or, in some cases, topographic information, are expensive and time consuming to acquire and may be unsuitable for large commercial fields, since they do not completely represent spatial variability (Cohen and Levi 2013).

Satellite remote sensing provides added value mainly with its spatial continuity and extent, spectral crop information and low cost – depending on satellite type. When analyzing time series, satellite remote sensing is often more cost-effective and offers an archive of already acquired data by operating sensors. When it comes to determining MZ on the basis of actual crop growth patterns, satellite imagery applications are valuable tools in precision farming (Basnyat et al. 2005).

Compared to drone and aircraft-based images, as well as data from crop and soil sensors, most open-source and commercial multispectral remote sensing data has a coarser spatial resolution (centimeters versus meters). The major disadvantage of optical satellite imagery however is the dependence on a clear, cloud-free view of the object of interest, which is especially challenging in temperate and rainy regions.

Still, remote sensing has a long tradition in agriculture, Seelan et al. (2003) reported the early beneficial use of aerial photography dating back to 1929. However, by the launch of the Landsat series of satellites in the 1970s and the subsequent availability of recurring landscape imagery and spectral reflectance characteristics, remote sensing for agriculture has truly emerged. It has been used for a wide variety of agricultural applications, such as crop yield estimation (Idso et al. 1980; Hank et al. 2015; Lobell et al. 2015), biomass monitoring (Lu 2006; Ahamed et al. 2011), soil parameter derivation (Barnes et al. 2003; Ge et al. 2011) and many others (Moran et al. 1997; Atzberger 2013; Mulla 2013). A considerable number of studies related to crop growth and yield are based on satellite images within one growing season (Ren et al. 2007; Song et al. 2009).

However, Thenkabail (2003) pointed out the potential of multi-temporal analysis of archived remote sensing data in combination with real time data. The time series approach is especially important for the identification of stable recurring crop patterns, which consequently define general MZ. Yield zones, which are comparable to MZ, are characterized by temporal variability and need to be addressed by a multi-temporal approach, which considers yield data and landscape attributes (Schepers et al. 2004).

A variety of approaches for delineating MZ with multispectral satellite images have been developed. Song et al. (2009) generated and compared delineation methods based on soil, nutrient and yield maps, a vegetation index (VI) distribution of one multispectral satellite scene, and combinations thereof. De Benedetto et al. (2013) used a data fusion method of proximal and remote sensing information, while Boydell & McBratney (1999) based their delineation on modelled yield data from Landsat imagery.

However, methods in the literature have so far mostly relied on additional information besides satellite images. Additionally, manual selection of imagery is required to avoid cloud-covered scenes, as well as to determine specific dates representing specific phenological stages (emerging and ripening). These are preferred (Idso et al. 1980; Boydell and McBratney 1999; Sakamoto et al. 2013) because they are assumed to reflect yield and yield potential.

While these approaches address the complexity of crop cultivation, they do not also imply an easy, cost-effective and practical usage for farmers. This leads to the question as to whether the delineation of a field into MZ is possible based only on satellite data. If so, this would make basic precision farming information available for every farmer, especially in the light of the open data development of earth observation data. To answer this question, the authors propose an automatic segmentation algorithm for within-field crop patterns by using only multi-temporal multi-spectral satellite images.

The following study showed that this algorithm works well on fields with stable spatial and distinguishable patterns and fairly on more complex fields, which either change their appearance over time and/or are very homogenous in crop vigor. While the algorithm addresses the requirements of simplicity and efficiency, the use of satellite images narrows the accurate and competitive outcome mainly because of the disadvantages of frequency/acquisition date (no or not enough cloud-free images available in certain time frames) and unilateral information (e.g. no crop type information).

2.2 Materials and Methods

The algorithm presented automatically selects suitable images for crop pattern delineation and works independently of additional information regarding crop type, growth stage and soil type. The subdivision of the field is performed on the near-infrared (NIR) spectral band of RapidEye (Tyc et al. 2005) satellite images. The result is a division into five classes, each resembling different productivity or yield expectancy zones (YEZ). These relative yield zones are suggested as being functionally equivalent to MZ.

2.2.1 Study area

The segmentation algorithm was developed and predominately tested on a 120 ha tilled field ("field 100-01"; Upper Left Corner (ULC): 13°14'E, 53°59'N; Lower Right Corner (LRC): 13°16'E, 53°58'N), part of a 2000 ha farm near the village of Görmin, located 15 km SW of Greifswald in the North-Eastern Lowlands of Germany. All other test and validation fields belong to the same farm and vary in area, crop rotation and soil type distribution. Geologically, the region was shaped by recurring glacial processes during the Weichselian Glaciation, and evolved into a hilly ground moraine landscape with representative glacial features. Flat, hilly and undulating ground moraines alternate with hilly terminal moraines, glacial valleys, lake basins, kettle holes, eskers and outwash plains (Bundesanstalt für Geowissenschaften und Rohstoffe 2006). Lakes and river systems, including the nearby river Peene, are closely associated with the near-surface ground water table.

The altitude of field 100-01 ranges from 9 m to 25 m above sea level (mean 19 m , standard deviation 3 m) and slope angle varies between 0° and 5.5° (mean 0.8°, standard deviation 0.5°; Amt für Geoinformation Vermessungs- und Katasterwesen, 2011). This results in relatively flat topography at the field scale, which is traversed by natural drainage towards the River Peene (*Fig. 2.1*) as it lowers in elevation towards the southern boundary. Field 100-01, similarly to the region, is characterized by a young morainic soil inventory, dominated by Stagnosols (northern part) and Luvisols. These glacial tills are clayey and loamy sands, with increasing loam content towards the southern end of field 100-01.

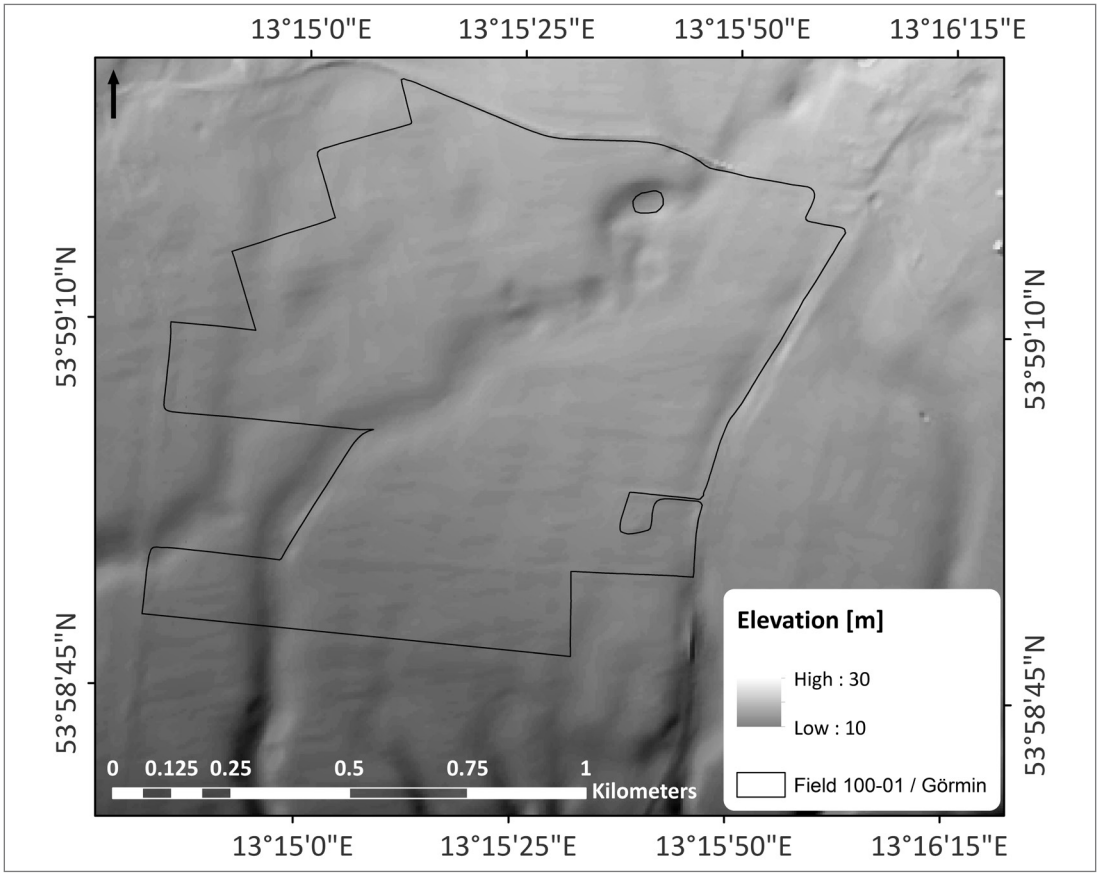

Fig. 2.1 Digital elevation model of field 100-01 with a decrease of elevation towards the southbound river Peene. Cavities in the fields shape represent a kettle hole (North-East) and housing (East).

Weather recordings from the Greifswald weather station (1985-2014) indicate a mean temperature of 8.94 °C and a mean precipitation of 607 mm/year. On field 100-01, the crop rotation is dominated by winter wheat, canola and, rarely, beetroot.

2.2.2 Remote sensing data

The method was developed using a RapidEye time series from April 2009 until August 2015. The RapidEye satellite system works with five spectral bands (blue, green, red, red edge, near infrared), where the near infrared (NIR) is, in general, especially sensitive to the vigor of vegetation (Rees 2001; Basnyat et al. 2005). The return frequency at nadir is 5.5 days and the spatial resolution is 6.5 m, resampled to 5 m. The images were made available through the RapidEye science Archive (RESA), where 74 radiometric calibrated and georeferenced scenes (Level 1B, Level 3A) could be found for field 100-01 (*Table 2.1*). Atmospheric correction was performed using ATCOR (Richter 2010) for ERDAS Imagine 2014 (Leica Geosystems, Atlanta, Georgia, USA) and the images were geometrically aligned using an image to image coregistration algorithm developed in-house (Behling et al. 2014). Further preparations for the development and testing of the segmentation algorithm included coordinate transformation, cartographic projection, and clipping the scenes to the area of interest, which is at the farm-scale in this case.

Table 2.1 Number of RapidEye images available for the Görmin area, per year and month

month / year	Jan	Feb	Mar	Apr	May	June	July	Aug	Sep	Oct	Nov	Dec
2009				2	1	2	1	1	2			
2010						3	2	1	1	1		
2011			1	4	4	4	1	2	3	3		1
2012		1			3	1	1	2	1	2		
2013				1	1							
2014			2	2	1	1	2		2	1		
2015			2	3	1	1	1	2				

number of images: 0, 1, 2, 3, 4

2.2.3 Farm data

For this study, field boundary, crop cultivation and yield data for the test field were provided by an agricultural company. Additional available data, not used by the algorithm, but by the authors for understanding the field, were: soil map, nutrient supply from 2009 (phosphorus, pH, magnesium and potassium), map of electrical conductivity.

Yield data were available as point measurements for the years 2006, 2007 and 2009 – 2015 (well above 60,000 point measurements per harvest), although 2012 was an exception, since the field was divided into two areas of different crop. Yield data from 2015 was also insufficient, due to technical problems during harvesting and consequential data gaps. For visualization, kriging was performed

on yield data with the software VESPER (Haas 1990; Whelan et al. 1996) with a local kriging and local variogram method, especially designed for yield map kriging with respect to local, rather than global prediction models. Field 100-01 has been managed with precision farming practices (mostly variable fertilization rates) for at least ten years, which is why the field appears very dynamic over time. The appearance and separability of the predominant crop patterns fade over time, since the PA measures are somewhat successful and compensate low yield zones – leading to more spatial homogeneity in vigor and yield. Field 100-01 was chosen despite this development, because of its size, number of patterns with differing origins and density of available farm and field data. Additionally, the analysis of all data show which patterns are stable over time (e.g. soil), which patterns can be homogenized (e.g. lack of nutrients) and how long this process takes. Bearing in mind that field 100-01 changes its appearance, the algorithm was tested on three other fields with – according to yield and remote sensing data – less dynamic patterns.

2.2.4 Segmentation algorithm

For the automatic delineation of MZ, a segmentation algorithm was developed on the basis of RapidEye satellite images. The workflow (*Fig. 2.2*) was divided into three steps: a) automatic selection of suitable satellite images which reflect crop patterns, b) combining the NIR bands of all selected images to one averaged raster and dividing the result into five classes, c) conversion into vector data and assignment to areas of relative yield expectation (corresponding to MZ). Detailed information on these steps are described below.

Before the selection process, every image was clipped to the extent of the field 100-01, including a negative buffer of 18 m to exclude margin artefacts, especially in the area of headland.

The algorithm was programmed in R (R Core Team 2012) with the use of the packages ‚raster', ‚maptools', ‚stringr', , rgeos', ‚diptest' and ‚moments'.

2.2.5 Selection of suitable images

The principal idea behind the selection process was automation. A selection of suitable images is necessary, since not every scene offers the contrast of reflectance values caused by crop patterns. Images disturbed by clouds, or other spatial objects overlapping crop patterns, must be left out. However, the potential user of this algorithm should not have to manually select appropriate images. Therefore, the algorithm makes its own selection, using standard deviation (SD) thresholds of the blue and the NIR band, as well as thresholds of bimodality of the normalized differenced vegetation index (NDVI) histogram, NDVI mean value and NDVI SD (*Fig. 2.2*). The SD was chosen instead of the variation coefficient (CV), since the SD does not vary along with the mean value. Consequently, an increase of SD values throughout a selection of subsets does not have to coincide with an increase in CV values. The thresholds were generated empirically by expert knowledge, after analyzing all available field subsets and their statistics. The chosen thresholds have been successfully tested on other test fields of the company, though not with different sensor data or in a completely different region/ environmental setting.

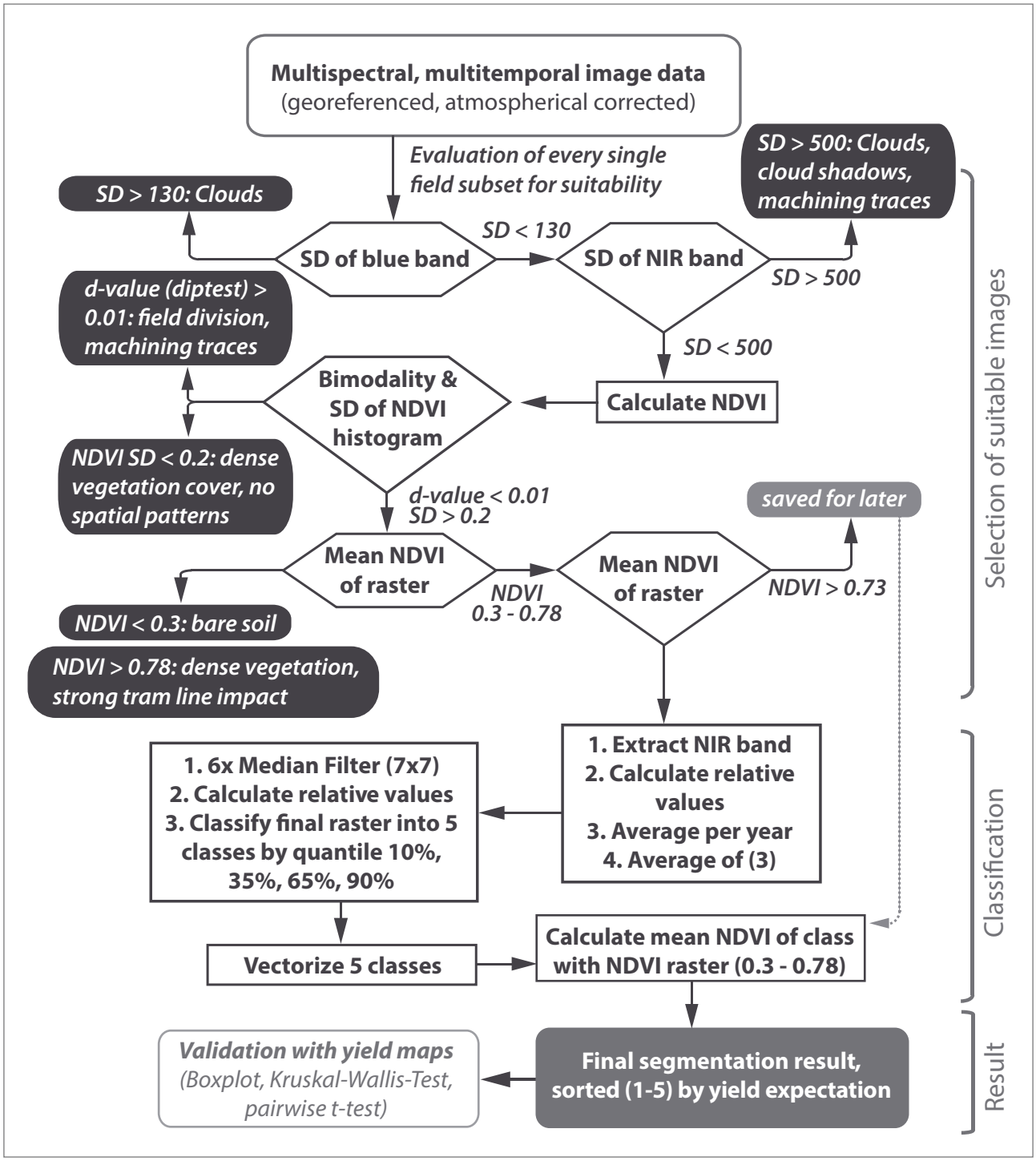

Fig. 2.2 Workflow of segmentation algorithm.
NDVI = Normalized Difference; Vegetation Index, SD = Standard deviation

In total, the algorithm used three spectral bands of the RapidEye sensor: blue, red and NIR.

a) Blue band: Clouds

For elimination of cloud-covered scenes, the blue band proved to be the most suitable, even though cloud reflection is high in all optical wavelengths (Jensen 2007). In the blue band, the reflection signal of vegetation and soil is rather low in comparison, leading to a high contrast between cloud and non-cloud. For every field subset, the standard deviation (SD) of the blue band reflectance values was calculated. If the SD exceeded a threshold of 120, the subset image was removed from further steps in the algorithm.

b) NIR: Cloud Shadow, small clouds and machining artefacts

The blue band threshold did not detect subsets with marginal cloud coverage or cloud shadows. Here, the SD of the near-infrared band was used as a limit for selection. If the subset exceeded a SD value of 500, the entire image was removed. This approach removed not only cloud-disturbed subsets but also processes like harvest or the complete division of the field into subfields with different crop (and therefore growth cycles). These disturbances showed a high contrast in the near-infrared reflection, which superimposed the native growth patterns.

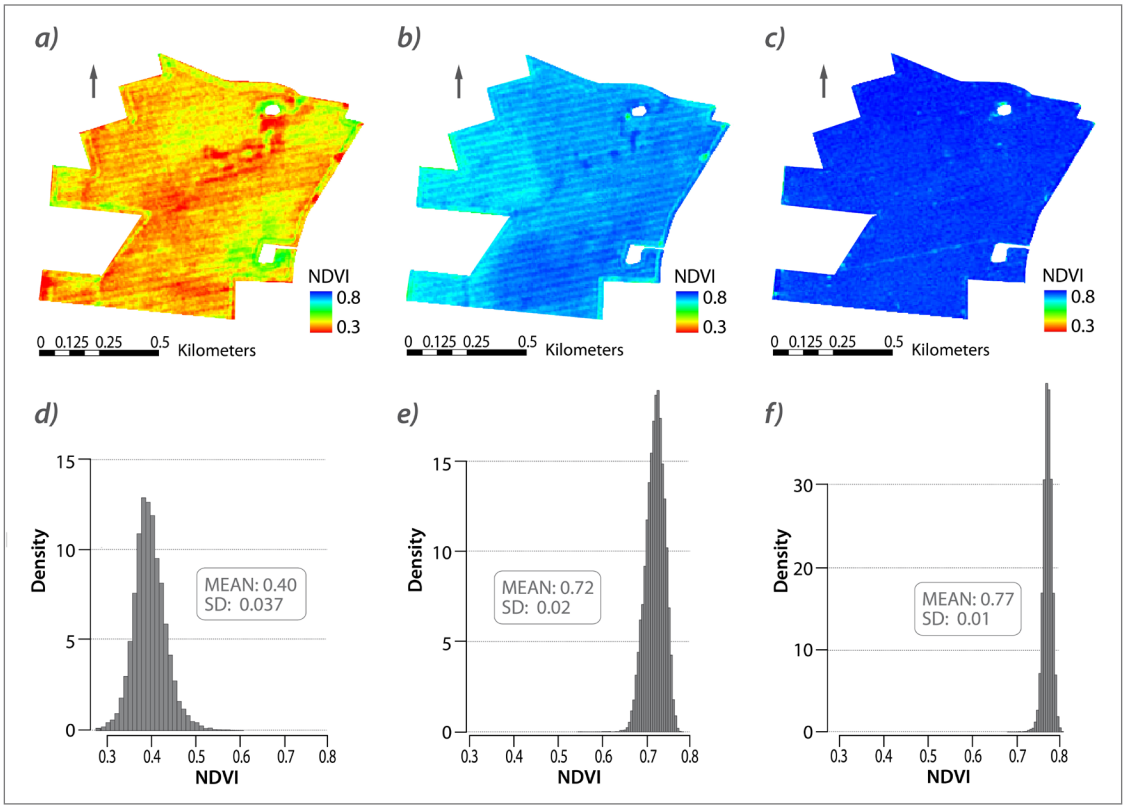

Fig. 2.3 a-c RapidEye false-color subsets of field 100-01 (NIR-G-B); a 09-04-2011, wheat at tillering; b 28-06-2011, wheat at ripening; c 17-6-2010, canola at fruit development; d-f Histograms of NDVI of each subset raster, y-axes not graphical-ly normalized due to value range of f to d and e.

c) NDVI: Field partitioning, growth stage

For the next selection step, the NDVI was calculated for each pixel, as well as the mean per subset. The NDVI histogram was tested for bimodality by applying the dip test, revealing images of field partitioning (*Fig. 2.10, Chapter Appendix*) or similar disturbances which were possibly not filtered by the prior step. The histogram of regular subsets covered by vegetation and their (natural) patterns appeared unimodal.
During this step of the selection process, decisions were made on the basis of vegetation growth and vegetation vitality. Thus the NDVI, as a normalized value, was sufficient for the estimation and comparison of crop activity (Ustin 2004). The mean NDVI of each subset was used to remove all images of bare soil (< 0.3) and very dense vegetation (> 0.73) (*Fig. 2.3 c*). While this mean was not a direct indicator for crop coverage, spectrally distinguishable crop patterns were still apparent during early and very late crop phenological stages (*Fig. 2.3*). In contrast, vegetation that was too dense – especially on high potential plots like field 100-01 – led to a high mean or even saturated NDVI (*as shown in Fig. 2.3 c*). This was additionally characterized by a small SD of the histogram. This was especially true for cereal crops, which developed a high spatial density within the planting rows while leaving the tramlines free of biomass (in contrast to canola, sugar beet or other crops). Hence, if the cereal biomass was high overall, reflecting a high NDVI value, the only apparent patterns were the tramlines.

2.2.6 Classification of the averaged image

The NIR band of all remaining images was used to determine the final vegetation patterns, for the following two reasons:

1) NIR reflectance and yield relationship

Relative reflectance values in the NIR have been shown to quite adequately reveal patterns seen in yield maps. Reflectance in the NIR is an indicator of health for leaf tissue, cell structure and, therefore, the vitality of the plant (Gausman 1973, 1977; Jones and Vaughan 2010). Consequently, it is a major indicator for final yield. On a macroscale, crops under advantageous growing conditions are more likely to grow taller and denser. They develop more biomass and leaves, which leads to increased NIR reflectance relative to the entire field. Leaf area index (LAI) is expected to be closely related to yield for certain crops, since grain yield is closely linked to crop growth (Serrano et al. 2000; Song et al. 2009). On the other hand, a reduction in LAI, similar to reduced chlorophyll content or surface temperature, is an expression of stress symptoms in plants (Baret et al. 2007). Reasons for stress symptoms are often water shortage, insufficient nutrient supply, and diseases like fungi or pests. Crops under stress often show decreased leaf area production and an increased senescence rate. On a microscale, the cell structure of the leaf is heavily altered, since the plant mobilizes all protein and minerals for the development of seeds. Senescence, either natural or stress-induced, is also accompanied by a decrease in leaf water content (Hurd-Karrer and Taylor 1929). This overall collapse of the leaf structure leads to decreased reflection in the NIR region, since the electromagnetic waves strongly scatter within healthy mesophyll tissue. In conclusion, reflectance in the NIR is a very suitable indicator for field growing conditions and prospective yield. Naturally, the red-edge band as a chlorophyll indicator (Barnes et al. 2000) was also considered. However, empirical analysis

of the data sets in this study did not show a strong correlation between reflection and yield as in the NIR band. Additionally, yield prediction on the basis of red-edge reflectance seems to be highly dependent on the phenological stage (He Ke-xun et al. 2013). In this study, the NIR reflectance values were converted into relative values, enhancing crop type and possibly regional independence.

2) Difficulties using vegetation indices for segmentation

The classification was not conducted using ratio images, such as NDVI, due to increased noise patterns and artefacts which are a common disadvantage of band ratios (Lillesand and Kiefer 1987). This effect is less desirable when a high degree of internal homogeneity is required for segmentation. The algorithm was nevertheless also tested by using NDVI images instead of NIR images. The results here were characterized by described noise patterns and numerous artefacts and did not lead to the same homogenous spatial patterns as when NIR is used.

Although precautions (single band basis, median filter) are taken to avoid small polygons in the end result, small features will still occur (< 3%). In agricultural practice, the user must decide how much detail is necessary and which features should be neglected.

Every NIR raster was normalized to a percentage, where 100 % is equal to the average NIR value of each raster. To balance years with differing amounts of available satellite raster images, all rasters for each year were averaged (e.g. three rasters of 2009 become one average NIR raster). The resulting yearly average raster were also normalized. The subsequent raster was processed using a 7x7 median filter for six times to smooth boundaries and eliminate small fragments. Of course, the use of such intense smoothing filters had a strong impact on the level of detail and information in the image. However, the focus here was on the delineation of geometric zones. In precision agriculture applications, spatial zones do not necessarily benefit from small-scale details, since farming machinery has practical limits when it comes to fine-tuned control and implementation of highl detailed GIS data.

The post-filter raster was classified into five value ranges, using quantiles of 10%, 35%, 65% and 90%. Due to the fact that every averaged NIR subset may have different value ranges, predefined values for separate classes are not feasible. The quantile values were chosen empirically on field 100-01 and others. The goal was to achieve class boundaries that generate well-balanced (amount of pixel) and clearly visual spatial classes. A change of the quantile values may lead e.g. to a dominant 'middle' class and very marginal classes of very low and very high NIR values.

A cluster method (e.g. k-means) was not used at this point, because the generated clusters a) were not guaranteed to entail an "average" class with values around 100% NIR reflectance, b) lack of information about their relative sorting ("very low" to "very high" and c) therefore lack of a stable, reoccurring control factor like the preset quantile thresholds.

In the process of (visually) analyzing the yield maps and satellite images of field 100-01 and neighboring fields, the class number of five was found to be suitable to map and reflect the heterogeneity of especially large fields. The odd number ensures a resulting "average" middle class. In theory, every desirable class number can be accomplished by the algorithm. Less classes (3) could be considered for a broader overview or in the case of low-contrast patterns. More classes (7) would lead to a more fragmented result, which would be less feasible for technical implementation into current machine systems for fertilizer or seed distribution. These systems mostly work in increments (e.g.

+/- 20% grain), rather than with continuous rates, which justifies the decision on discrete classes. An odd number of classes is required to generate an average class. Every class was exported into a polygon (not necessarily continuous), with which further analysis could be done. The resulting classes resembled zones of increasing vitality, relative to one another, which is why the five classes were named “very low” (1), “low” (2), “average” (3), “high” (4), “very high” (5) yield expectation.

2.2.7 Attributes of classes

To better assess the vitality status and yield expectancy of each class, and because the value range of the reflection within the NIR band seemed quite narrow, every class was additionally assigned a relative NDVI value and stored in a protocol. This value was generated by averaging all disturbance-free NDVI rasters with a NDVI between 0.3 and 0.78. For every class, the mean NDVI value within the class polygon was extracted, resulting in five relative NDVI values in percent. In this study, these NDVI values were highly linear (R2 > 0.9) to the relative yield values extracted from an interpolated yield map (average of multiple years, corresponding to satellite data selection). Since no universal, field-independent conversion equation from relative NDVI to relative yield could be determined, the results shown in this paper will refrain from focusing on these NDVI values.

2.2.8 Validation with yield data

The segmentation algorithm aims to give insights into yield distribution, especially for farmers lacking sufficient or total yield maps of their fields. In order to test the segmentation result in regard to yield expectancy zones, actual yield data were used for this validation (described in 2.3).

Stratified sampling

For validation, the concept of stratified sampling was preferred. As described in Webster & Oliver (1990), the sample points for validation were randomly distributed within regular grid cells, dividing the target raster area. Sample points within a 10 m buffer of the segmentation boundaries were eliminated. The sample size ranged around roughly 6%. Yield values are based on point measurements, converted into relative values in % and averaged over the selected years. For each sample point, the relative yield value and the corresponding class id (1-5) were extracted.

The result was plotted as a boxplot, depicting relation and separability between each class. In addition, two statistical tests were applied: a) the Kruskal-Wallis-Test and b) the Pairwise T-Test (class ID versus relative yield value). The result with a p-value < 2.2e-16 confirmed the general separability of the five classes, even if run based on different sample points.

The Pairwise T-Test applied compares each test series with one another and tests if there are statistically significant differences. This test normally requires normally distributed data, which is not necessarily given in this case. However, this condition may be violated if the number of sample points is high (Bartlett 1935) and the variance of the test series is comparable. With both of these being the case, the test was run a second time with logarithmic transformed values, to assure normality and test the validity. Additionally, the Pairwise Wilcox-Test for data without a normal distribution was run.

2.3 Results and Discussion

After the automatic selection process, 14 out of 74 rasters for field 100-01 remained for segmentation (*Table 2.2*). Data from the years 2012 and 2013 were neglected by the algorithm, which will be examined later on. Therefore, the method is discussed based on a result from five non-continuous years (*Table 2.2*).

Table 2.2 Final raster (acquisition dates) for segmentation and crop type

year	date	crop
2009: 3	21-04-2009 25-04-2009 24-06-2009	wheat
2010: 1	16-07-2010	canola
2011: 6	08-04-2011 09-04-2011 20-04-2011 21-04-2011 28-06-2011 16-07-2011	wheat
2014: 3	10-03-2014 20-03-2014 09-07-2014	canola
2015: 1	17-03-2015	wheat

Figure. 2.4 shows a final result of the segmentation process, compared to the averaged relative yield map of the corresponding years (2009, 2010, 2011, 2014, 2015). On first examination, the five classes resembling yield expectation zones (YEZ) moderately resemble the actual yield zones of high-, low- and medium yield.

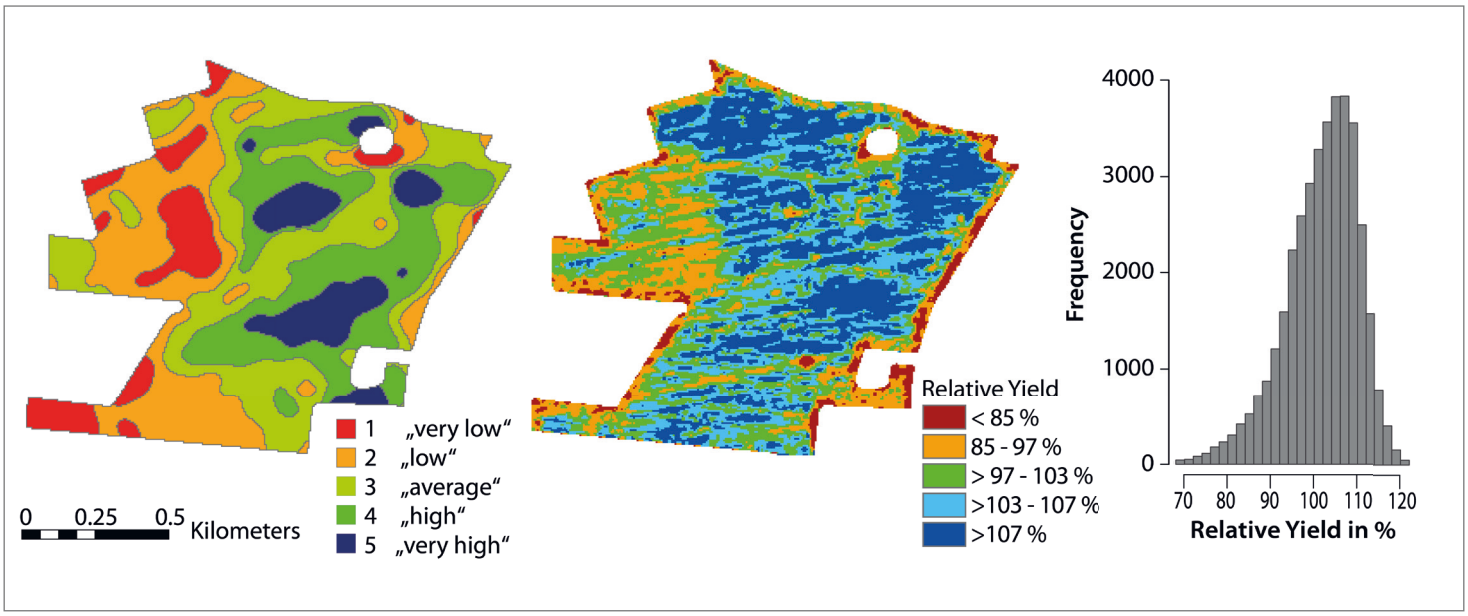

Fig. 2.4 Left Segmentation result; Middle relative yield map; Right Histogram of yield raster, Average of years: 2009, 2010, 2011, 2014, 2015

2.3.1 Validation

All three statistical tests had p-values lower than the significance level (0.05), indicating a good separability of the five determined classes (*Table 2.3*).

Despite that, the boxplot (*Fig. 2.5*) still shows overlapping sampling values for every segment, whereas only segment 1, "very low yield expectancy", appears to have slightly more discrete values than the other segments. Statistically, the Pairwise T-Test indicates independence between the classes.

This overlapping of classes and left-skewed outliers is apparent in all segmentation test runs, even if the criteria (quantiles of class boundary; number of classes; NDVI thresholds as described above) for segment building are adjusted. Due to the overall high yield potential of field 100-01 (and therefore lack of strong contrast), the segmentation process has difficulties in distinguishing five apparently separated classes.

An average yield map of the years 2009, 2010, 2011, 2014, 2015 does not present drastic yield variance over the field (*Fig. 2.4*), compared to fields in more vulnerable regions of Germany (Dobers 2005). The relative yield ranged from 25.0 % to 141.9 % (mean: 102.2 %, SD: 8.5 %), whereas field 100-01 yields were above average and could be assumed to be relatively homogenous with a small yield variance.

Table 2.3 Statistical significance tests on segmentation result. The separability of each seg-ment by extraction of actual yield values is tested and expressed as the significance value „p-value" (< 0.05 supports separability hypothesis)

Test	Result (p-value / significance value)				
Kruskal-Wallis-Test	< 2.2e-16				
Pairwise T-Test		1	2	3	4
	2	3.1e-14	-	-	-
	3	< 2e-16	3.8e-12	-	-
	4	< 2e-16	< 2e-16	3.9e-13	-
	5	< 2e-16	< 2e-16	< 2e-16	1.2e-06
Pairwise T-Test (log of data)		1	2	3	4
	2	3.0e-13	-	-	-
	3	< 2e-16	2.5e-12	-	-
	4	< 2e-16	< 2e-16	5.1e-12	-
	5	< 2e-16	< 2e-16	< 2e-16	7.2e-06
Pairwise Wicox-Test		1	2	3	4
	2	< 2e-16	-	-	-
	3	< 2e-16	1.7e-13	-	-
	4	< 2e-16	< 2e-16	< 2e-16	-
	5	< 2e-16	< 2e-16	< 2e-16	3.2e-06

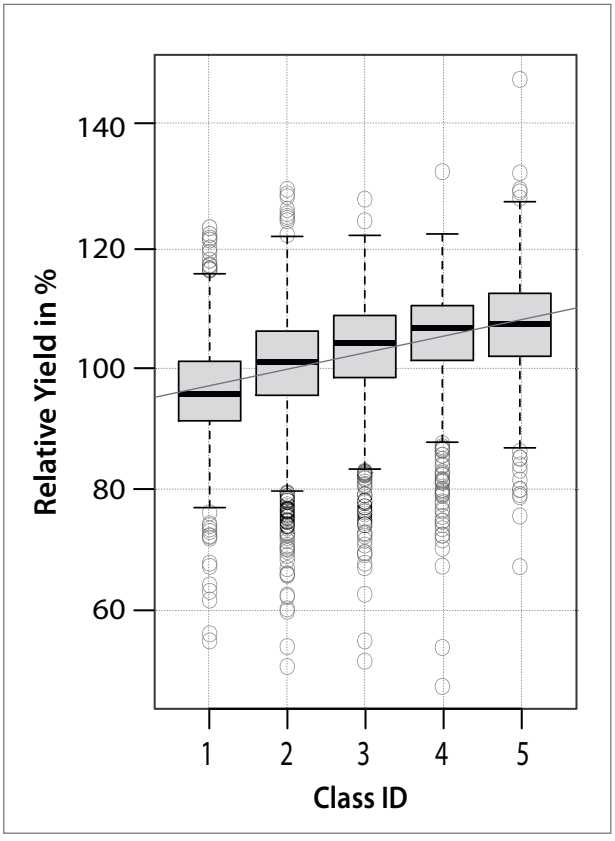

Fig. 2.5 Boxplot of sampling result, yield per segment

2.3.2 Interpretation of results

1) NDVI and yield expectation relationship

The result shows the capacity of the method to form zones of different growth and yield levels for one field. However, it is problematic to reliably link these zones to percent-based relative yield values, and even more difficult to determine absolute yield values. A comparison of the five NDVI mean values with the actual yield values (mean value per class) reveals a highly linear relationship (R2 = 0.97), as well as NDVI values that are slightly lower (1-2 %) than the mean relative yield values per class. Unfortunately, any empirical relationship determined for this field cannot be applied elsewhere, since a universal conversion from vegetation indices to yield values does not exist.

Numerous efforts have been made to determine this relationship (Shanahan et al. 2001; Doraiswamy et al. 2003; Dalla Marta et al. 2013), with results indicating that replicability is mostly limited by crop type and climate zone. In this study, however, the focus is on identifying field zones of similar crop growth and vitality, regardless of the crop type cultivated. Therefore, the resulting crop patterns resemble a mixed signal of vitality patterns indicated by more than one crop type or even crop group. For absolute yield estimation, crop type knowledge as well as date and duration of critical phenological stages (Idso et al. 1980) are required in order to use the given satellite data and spectrally sensitive parameters impacting yield (Dalla Marta et al. 2013). This algorithm, however, seeks simplicity and functionality based on multispectral satellite images alone.

2) Disregard of crop type

The individual demands and phenological characteristics of crop types has not yet been considered by the algorithm. It can be argued that each crop type responds differently to field inventory and development prerequisites, and should therefore not be compared to other crop types. However, the analysis of satellite images, yield maps, soil and nutrient data of field 100-01 and the rest of the farm shows that the main drivers for reoccurring crop patterns are soil type and nutrient supply (*Fig. 2.10, Chapter Appendix*). This observation is relevant for the crop types grown in the area: cereal, canola, maize and sugar beet. Vitality patterns are stronger in more sensitive crop types such as cereal, and more prominent under unfavorable weather conditions.

Still, for the image segmentation, the crop cultivated is of no importance. The thresholds only select subsets with a certain amount of spectral heterogeneity. In most cases – at least during early phenological stages or at the transition between green and dry biomass – the plants reveal spatial patterns regardless of the type.

The algorithm currently yields good results even without the crop information, and can be validated even if the result shows a mixed crop signal. With an increasing number of satellite images and recorded years, the impact of specific phenological events, crop type specifications, or outstanding weather conditions would be alleviated However, it is equally true that the algorithm could be even better with knowledge of the crop type. Hence, future research could focus on adapting the algorithm to crop families (e.g. cereal; discussed further in the section “Outlook and Possibilities”).

2.3.3 Stability of the results

1) Variation of input years

Figure 2.6 shows the segmentation and validation results of three trial runs with different input years. *Figure 2.6a* is the result of the fully automated selection, which includes data from years 2009-2011 and 2014-2015. The result is similar to that of 2009-2011 (*Fig. 2.6 c*). *Figure 2.6 b* lacks year 2009, and appears to produce a much more homogenous result. The classes appear to be the most separable in *Figure 2.6 c*, the only test run without the year 2015. For this year, the yield data were only moderately reliable due to technical difficulties during harvest.

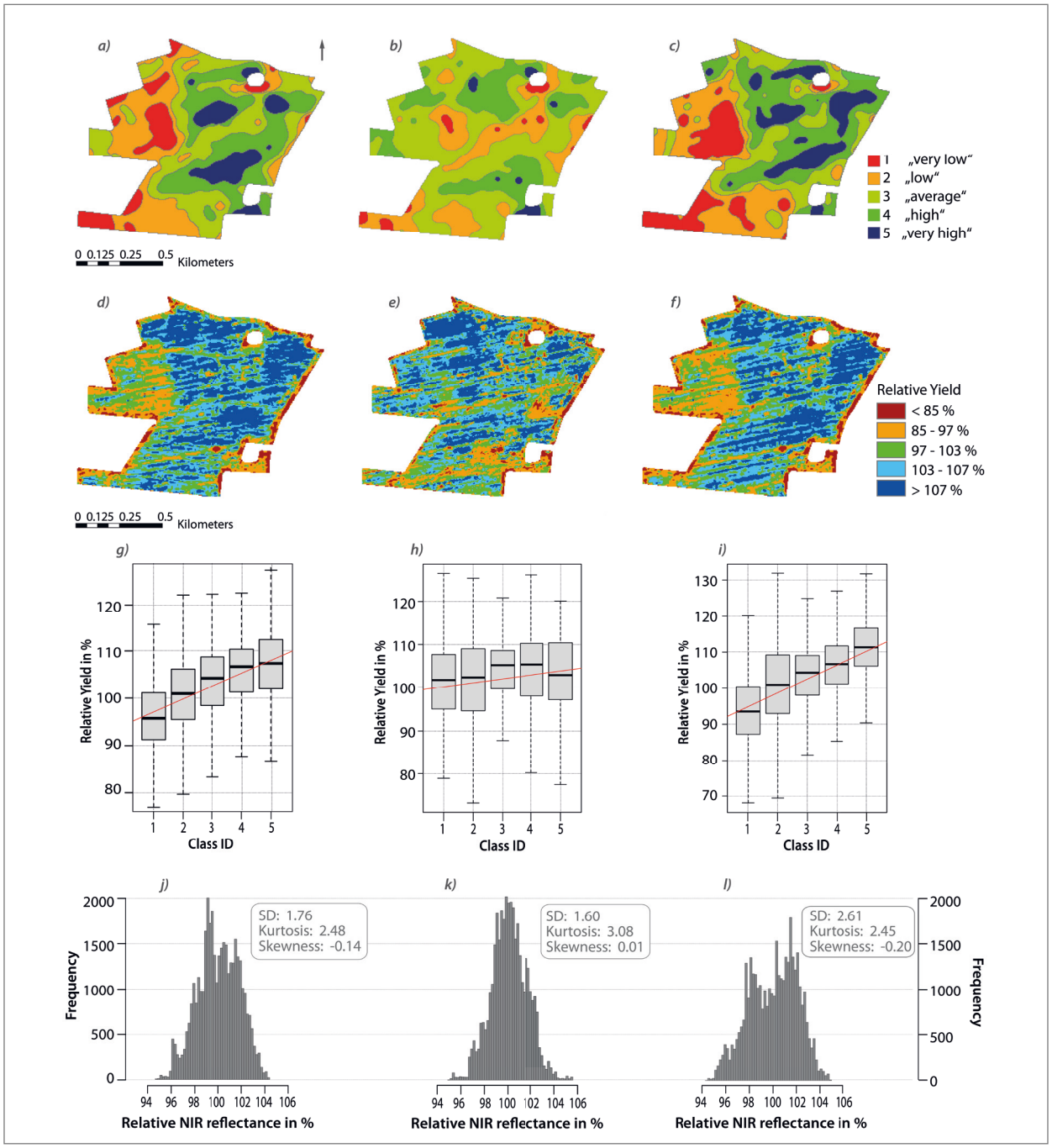

Fig. 2.6 Segmentation results of different test runs; a automatic selection (years 2009, 2010, 2011, 2014, 2015); b years 2010, 2011, 2014, 2015; c Period of 2009-2011; d-f Corresponding average yield maps; g-i Boxplots of sampling, yield per class; j-l Histograms of average NIR raster, on which basis classification is done

It is clear that the segmentation results can differ depending on the selected satellite imagery. This is why the target parameter is yield expectancy and not yield potential. Additionally, the result has to be interpreted as average yield expectancy for the n number of years (which are selected for segmentation) under the conditions x (weather and growing conditions), which were present in the selected years. Consequently, the segmentation result is a reflection of spatial growth and vitality variability over plot 100-01.

Data from the year 2012 was not selected due to field partitioning in this year (wheat/ sugar beet). For 2013 (wheat), an insufficient number of cloud-free images were available and the remaining images did not match the thresholds.

The year 2009 had an obvious impact on segment building, which is explained by the combination of crop type and nutrient supply. The rectangular patch of low yield expectancy in the NW corner of field 100-01 is lacking in several nutrients (*Fig. 2.10, Chapter Appendix*), primarily indicated by wheat, as is the case in 2009 and in 2011 (*Fig. 2.7, Fig. 2.10, Chapter Appendix*). If 2009 is not taken into account, the image changed (*Fig. 2.6 b*) to a more homogenous result, showing less high-contrast nutrient patterns and more closely resembling soil type and relief patterns (*Fig. 2.10, Chapter Appendix*). This change is explained by the dynamics of field 100-01. For one, the farmer was able to compensate the nutrient deficiencies from 2009 onwards (*Fig. 2.10, Chapter Appendix)* .Additionally, his precision farming management led to an increasing equalization of yields, represented in *Figure 2.8* by the decreasing value ranges in boxplots of 2009, 2011 and 2013 (all wheat).

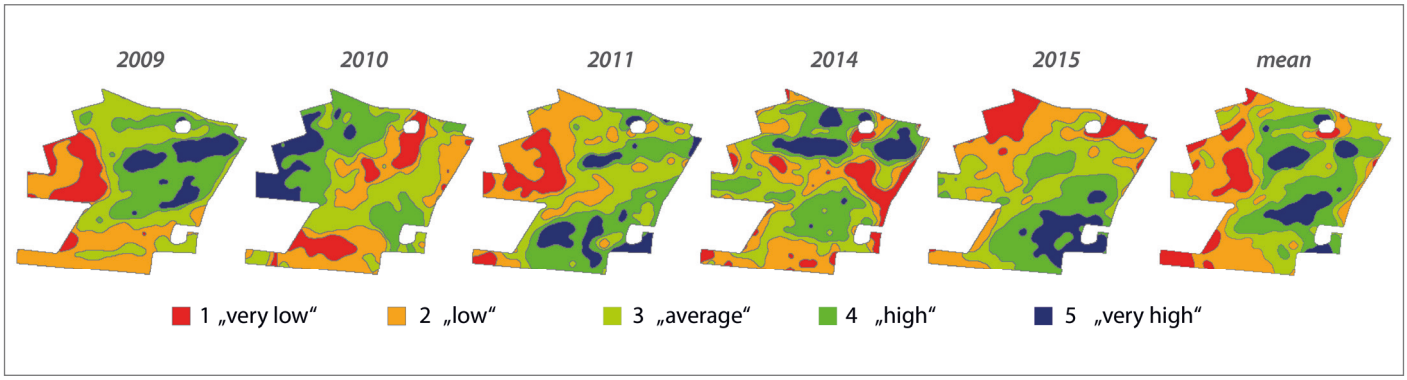

Fig. 2.7 Segmentation run on satellite data for each year, 2010 and 2015 are only based on one input image. The „mean“ result is – as the automatic segmentation – based on all the displayed years.

This successful development in farming practice has the disadvantage of affecting the stability and reliability of this segmentation algorithm, when there are simply no high-contrast plant patterns on a field. The NIR image can still be classified by quantiles, but the resulting classes can no longer be successfully validated for their separability (*Fig. 2.8*). The value ranges of each class are very similar, and small segments with a low pixel count (e.g. class number 5) do not fit yield maps. This phenomenon is reflected in the histogram of the averaged NIR band subset (*Fig. 2.6 k*), which is slightly less stretched than the other histograms. It can be concluded that the segmentation results following averaged NIR subset histograms with low scatter of values and high uni-modality are not trustworthy. Classes with a very low number of pixels should also be evaluated with caution since they mostly do not coincide with the yield data. For dynamic fields like 100-01, five or more growing seasons are required to depict average patterns and to compensate strong changes or high impacts of crop types and overall conditions. For other fields, a time frame of three years is enough to map out crop pattern.

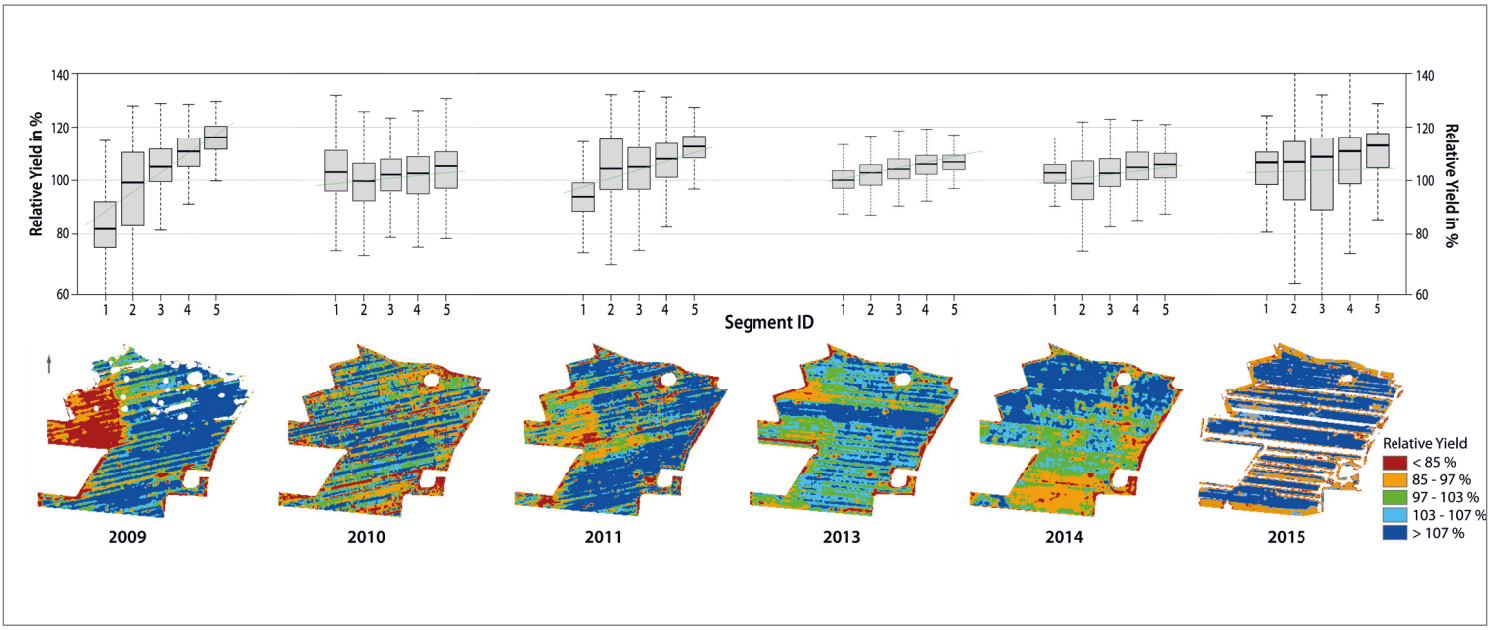

Fig. 2.8 Upper row Validation boxplots; segments (2009-2011) vs. average yield in % of single year yield maps; Lower row Yield maps of years 2009-2015 (wheat,canola, wheat, wheat, canola, wheat); Map 2009 includes data gaps; map 2015 is a little unreliable, due to technical problems during harvest, resulting in gaps in yield

2) Validation with single yield maps

In precision farming practice, the question arises as to the reliability of computed MZ, and whether they can be utilized for adapting management in future cultivation seasons. In principle, the presented segmentation algorithm can fulfil these requirements, if the crop patterns are more or less stable and high in contrast over multiple years. In the case study of field 100-01, this demand can only be met to a certain extent. *Figure 2.8* shows the validation boxplots of the five segments (result of 2009-2011, *Fig. 2.6c*) versus the relative yield of single yield maps. Ideally, the order of the mean relative value continuously increases from segments 1 to 5. This is the case for the yield maps of 2009, 2011, 2013 and 2015 – all of which were years of wheat cultivation. However, the range of yield values and the position of the boxes change. Despite yearly individual weather regimes, the strong crop patterns of 2009 and (partially) of 2011 decreased over time. This was due to the sustainable management of field 100-01 by the farmer, who constantly equalized nutrient deficiencies and optimized fertilization during the growing season. This explains why, in this case, the segmentation result is not always applicable for every year.

The greatest potential of the algorithm lies within fields where there is no comparable positive change, and crop patterns are more or less stable. Otherwise, the result has to be interpreted strictly as what it is: an averaged reflection of plant growth over multiple years. As *Figure 2.8* shows, the segmentation does not validate well with canola yield maps (2010, 2014). For a detailed analysis from a farmer's perspective and the linked crop-type-specific measures, crop cycle information is needed. However, the multi-year approach is still feasible because it does not favor crop specifications, but rather growth patterns with sufficient impact.

2.3.4 Method transferability to other fields

The automatic segmentation method was tested on three other farm fields, with varying areas and crop rotations (*Table 2.4*). Validation was likewise carried out with yield data (for the one season of sugar beet, yield data was not recorded).

Table 2.4 Crop rotation and area of the three additional fields, 2009 - 2015

	ha	2009	2010	2011	2012	2013	2014	2015
200-01	11.6	barley	canola	wheat	canola	wheat	barley	canola
360-01	74.5	rye	canola	wheat	rye	rye	canola	wheat
270-01	89.3	canola	wheat	sugar beet	wheat	canola	wheat	wheat

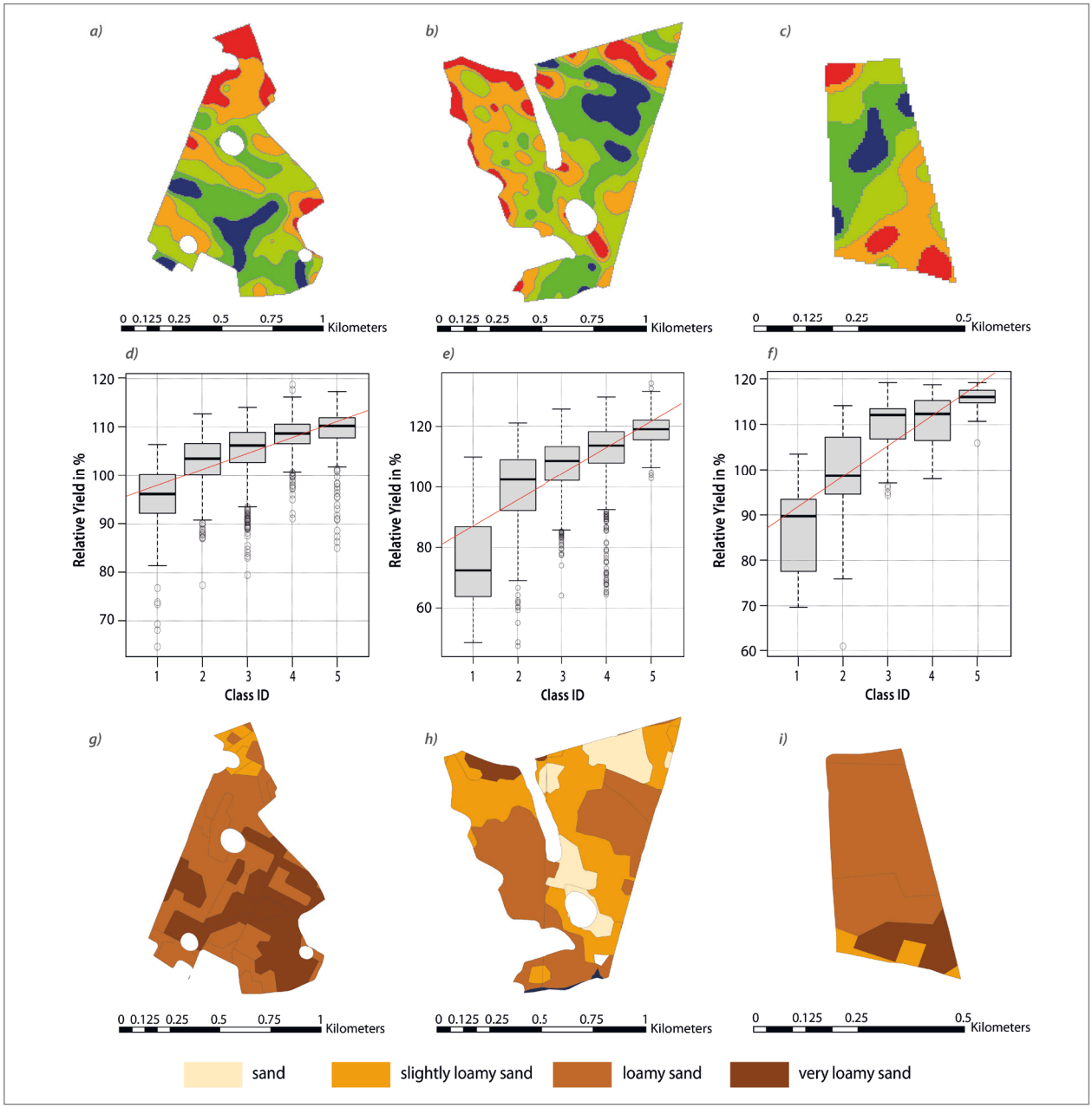

Fig. 9 a-c Segmentation result of field 200-01, 360-01, 270-01: 2009-2015; d-f validation boxplots; g-i soil map for each field

The result (*Fig. 2.9*) shows the successful transferability of the method to other fields, which is attributable to the fact that all three plots show heterogeneous crop patterns for all years and are less dynamic than field 100-01. Test runs comparing the number of input years (three versus six years) resulted in similar results. The authors can therefore conclude that the algorithm performs well with a small amount of multi-temporal images (from three years) – if high contrast crop patterns predominate and if these are roughly spatially stable. This is mostly the case when crop patterns are mainly inherited by soil patterns, which is generally the case for these three fields (*Fig. 2.9 i*). However, a large number of satellite images is still preferred, since the result is increasingly independent of crop type impact on patterns and temporal changes due to weather events. The size of a field does not matter. It can be up to the farmer in practice, as to whether five classes of yield expectancy are suitable for small fields like 270-01, or if three are sufficient.

2.3.5 Outlook and possibilities

Therefore, suggested future improvements include the implementation of a cloud mask and further testing of vegetation indices and existing studies for the derivation of yield values. This testing would require knowledge of the crop type and could be addressed by either a crop classification method (Itzerott and Kaden 2006; Foerster et al. 2012) or better yet by manual input of the potential user. These users are assumed to be farmers and agricultural consultants, interested in cultivating their crop with precision farming methods.The method offers a quick delineation of the desired field, especially if yield maps are not or are insufficiently available. The segmentation could then be used for management decisions in fertilization, seeding or crop protection. An upcoming milestone will be the coupling of the segmentation results with additional geospatial data, such as soil, relief and nutrient maps. This would allow for further optimization of the results and enable a transition from yield expectancy zones to yield potential zones. Additionally, the fusion of different multispectral sensor systems such as RapidEye, Sentinel-2 and Landsat could be an attractive method for further exploiting the big data pool and increasing the density of information for image segmentation. With a vast data base and additional crop information from the user, the segmentation could also be computed for crop types or families, adding more stability and knowledge for crop-specific strategies.

2.4 Conclusion

This study presented a straightforward algorithm for the delineation of crop patterns on agricultural fields based solely on optical multispectral satellite data, but with certain limitations. The crop patterns can be interpreted as relative yield expectancy zones, and are influenced by prior growing conditions on a field. The result can be utilized as potential MZ, in order to implement and enhance precision farming practices. The algorithm operates with atmospherically corrected remote sensing reflectance data, and does not need any further information besides the field outlines. Consequently, the method enables an effortless and quick overview of past averaged growing conditions, without manual work. As such, this algorithm addresses upcoming important developments of big data, open source satellite data access and digital / smart farming. As a disadvantage, the method is unable to use partly cloud-covered images and suffers slightly from images with a strong tramline

imprint, leading to noisy images which require smoothing filters. The result is also unreliable for fields lacking crop patterns and homogenous growing conditions, which is indicated by the output variables of the algorithm. As with numerous agricultural remote sensing methods, parameters and values are derived from image interpretation. Although the segmentation result could be validated with yield maps, it is also an interpretation of crop spectral characteristics. The gross division of crop patterns can be assumed to reflect overall growing conditions. However, small adjustments of the algorithm's parameters are reflected in changes on a pixel scale, confirming the belief that actual crop can seldom be addressed by image interpretation on a detailed scale. Generally, algorithms based on optical remote sensing are always dependent on the availability of sensor data for the desired time frame and the quality of the data.

2.5 Acknowledgements

The authors would like to thank Climate-KIC for project funding, Edgar Zabel and the cooperating farm for data and support. Further, we would like to thank Katharina Heupel (GFZ) for programming support and Eike Stefan Dobers (Applied University of Neubrandenburg) for support on content and agricultural knowledge. We thank the German Aerospace Centre (DLR) for providing the data from the RapidEye Science Archive (RESA 617 FKZ).

2.6 Author Contributions

Claudia Vallentin, Daniel Spengler and Sibylle Itzerott designed to overall approach. Claudia Vallentin did the methological development and programming, as well as the analysis and the manuscript. Birgit Kleinschmit contributed to the discussion and general paper review.

2.7 Conflict of Interest

The authors declare no conflict of interest.

2.8 Chapter 2 Appendix

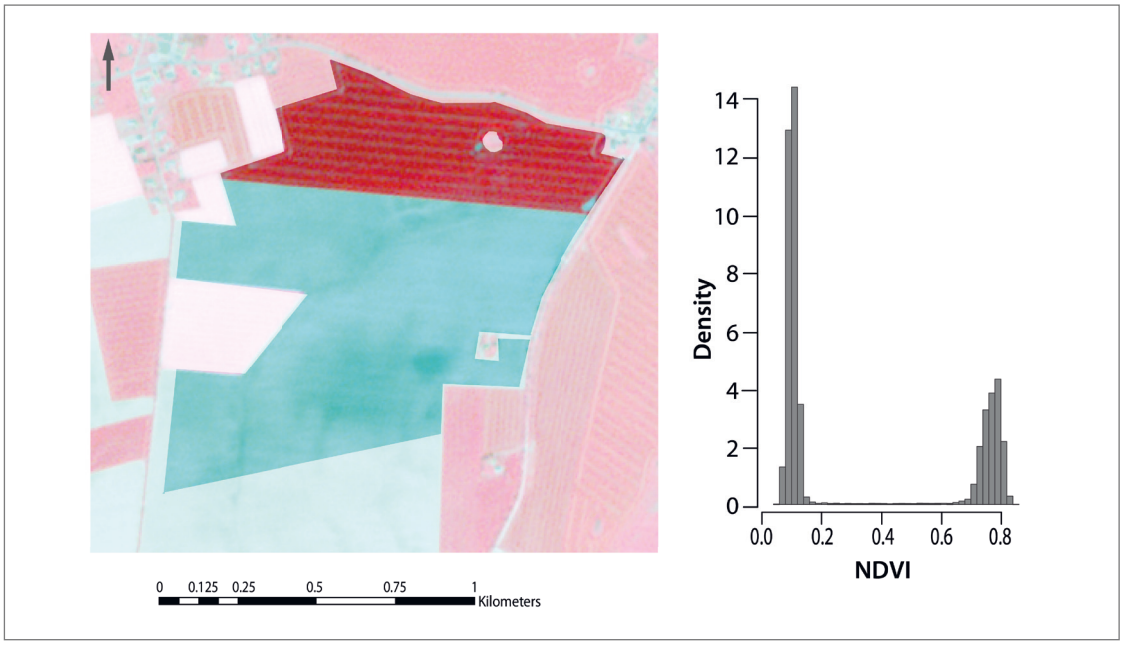

Fig 2.10 (Left) RapidEye subset, false-color (NIR-G-B), 14-05-2012 wheat and bare soil; (Right) NDVI histogram of field raster with strong bimodality, which would not pass the selection process of the algorithm

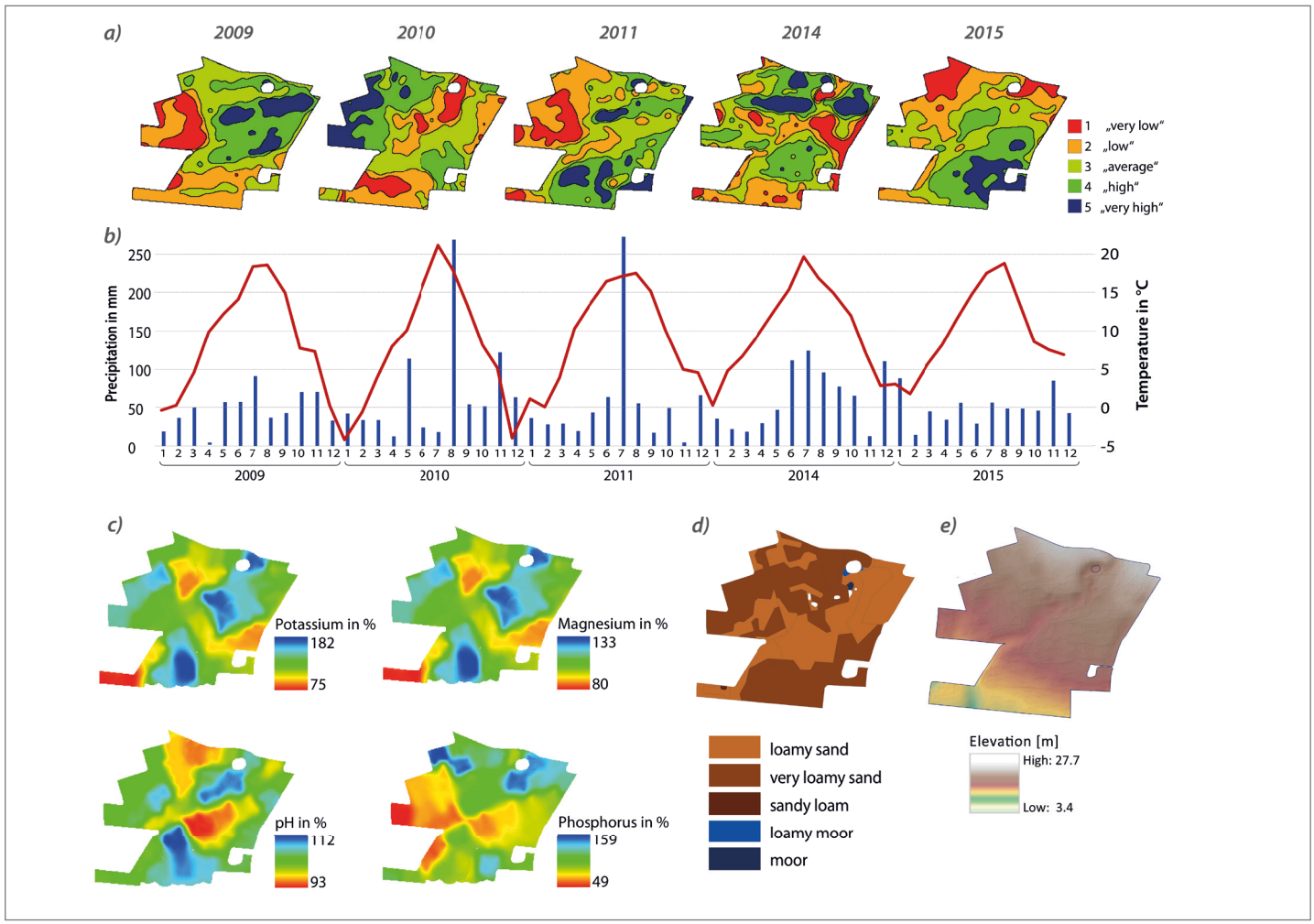

Fig. 2.11 a) segmentation for single years, no suitable images in 2012-2013; b) precipitation and temperature 2009-2015, weather station Greifswald by Deutscher Wetterdienst "German Weather Service"; c) interpolated nutrient data of field 100-01(potassium, magnesium, pH and phosphorus), August 2010; d) soil map of field 100-01 e) relief of field 100-01

3 Delineation with spatial data fusion and belief theory

Vallentin, C., Dobers, E. S., Itzerott, S., Kleinschmit, B. and Spengler, D. (2019).
Delineation of management zones with spatial data fusion and belief theory.
Precision Agriculture. Springer US, 21, 802-830.

Accepted manuscript

Published online: 22 November 2019 (doi: 10.1007/s11119-019-09696-0.)

Abstract

Precision agriculture, as part of modern agriculture, thrives on an enormously growing amount of information and data for processing and application. The spatial data used for yield forecasting or the delimitation of management zones are very diverse, often of different quality and in different units to each other. For various reasons, approaches to combining geodata are complex, but necessary if all relevant information is to be taken into account. Data fusion with belief structures offers the possibility to link geodata with expert knowledge, to include experiences and beliefs in the process and to maintain the comprehensibility of the framework in contrast to other „black box" models. This study shows the possibility of dividing agricultural land into management zones by combining soil information, relief structures and multi-temporal satellite data using the Transferable Belief Model (TBM). It is able to bring in the knowledge and experience of farmers with their fields and can thus offer practical assistance in management measures without taking decisions out of hand. At the same time, the method provides a solution to combine all the valuable spatial data that correlate with crop vitality and yield. For the development of the method, eleven data sets in each possible combination and different model parameters were fused. The most relevant results for the practice and the comprehensibility of the model are presented in this study. The aim of the method is a zoned field map with three classes: „low yield", „medium yield" and „high yield". It is shown that not all data are equally relevant for the modelling of yield classes and that the phenology of the plant is of particular importance for the selection of satellite images. The results were validated with yield data and show promising potential for use in precision agriculture.

3.1 Introduction

The dissemination of Precision Agriculture (PA) as an essential component of crop production has become increasingly important in recent years. New and intelligent solutions are constantly being developed and sought with a view to sustainable agriculture, which must nevertheless increase its efficiency. PA is not a new development (Mulla 2013), but it is an important component for modern agriculture and its problems (IPCC 2014; DLG e.V. 2017). Data-based PA applications rely on data from a variety of sources, such as proximal sensor techniques (Adamchuk 2011; Colaço and Bramley 2018), remote sensing (RS) and Geographic Information Systems (GIS) (Goswami 2012; Mauser et al. 2012; Mulla 2013). With the help of these data and the PA applications, the application of fertilizers (Sharma and Bali 2017; Colaço and Bramley 2018), plant protection (Mahlein et al. 2012; Šedina,Pavelka and Raeva 2017) or irrigation (Navarro-Hellín et al. 2016), for example, can be adapted to the needs of plants and soil.

In the spatial analysis of field data the partitioning of a field in Management Zones (MZ) is of great importance in many publications (Flowers,Weisz and White 2005; Pedroso et al. 2010; Gili et al. 2017) and applications. Within ideally stable zones homogeneity is expected and represented by similar level of plant vitality, yield potential and / or soil quality. MZs have been successfully delineated on the basis of spatial data such as yield maps (Brock et al. 2005), soil attributes (Yao et al. 2014), electrical conductivity (EC) measurements (Cambouris et al. 2006; Moral,Terrón and Silva 2010) and remotely sensed images (Song et al. 2009; Georgi et al. 2017).

However, the use of one type of data source poses risks. The data currently available may be unreliable or the information density needed for safe interpretation may be low. Therefore, data fusion methods are a valuable addition to the breadth of MZ delineation methods.

The most common scientific motivation for the development of data fusion methods is the classification of spatial data, such as RS imagery, elevation data or soil maps into surface units, such as cities, water bodies or forest. Successfully applied models for this type of data fusion are for example Bayesian techniques (Xue,Leung and Fung 2017), Neural Networks (Teimouri,Mokhtarzade and Valadan Zoej 2016), Support Vector Machines (Park and Im 2016), Random Forest (Crnojevic et al. 2014) and Dempster-Shafer Theory (DST) (Le Hegarat-Mascle,Richard and Ottle 2002; Ran et al. 2008). DST belongs to the group of evidential reasoning, a generic evidence-based multi-criteria decision analysis approach.

For this study, the authors applied an interpretation of the DST, namely the Transferable Belief Model (TBM), developed by Smets and Kennes, 1994. In its functionality and structure, the TBM is similar to the Bayes Model. However, it does not work with quantified probabilities, but with quantified beliefs. The specific rules and variables address the needs of agricultural issues much better. Wu et al. 2002 find the DST (consequently also the interpretation TBM) much more suitable than the Bayesian interference for mapping human thought processes and argumentations. The concept of evidence-based models is therefore very well suited for integrating expert knowledge into the process of geodata fusion. In agricultural practice, it is rarely an algorithm that interprets data and maps and makes decisions, but the farmer or his advisor. Each data source is evaluated with background knowledge and often many years of experience with a field. Different types of data are related to each other and their information content is enhanced. To illustrate and automate this way of decision making in a model, the authors present a fusion method for delineation of MZ using the TBM.

The subject of this study is therefore the question of how remote sensing data can be combined with other GIS data to make a common statement about the yields of a field. However, this fusion also focuses on the question of how the knowledge and experience of the farmer himself can theoretically be integrated into this mathematical fusion process. Another objective is to find an alternative fusion method to the less comprehensible fusion methods in the field of machine learning.
The visual and numerical evaluation of satellite data and GIS data from many fields studied suggests that there are connections between the data mentioned and the yield maps. This leads to the scientific hypothesis that a mathematical approached data fusion with incorporation of the human estimation must be possible. The delineation method presented was developed in order to achieve the general goals of this study and to confirm this research hypothesis, but also to create an application for practical agriculture. The validation of the functionality of this method by the comparison of modelled yield zones and actual yield zones, derived from the yield data of the farmer, is at the same time the validation of the scientific hypotheses.

Since the possibility to put the application into practice as well should be given, the focus during development was on the requirements of the farmer. Since MZ represent the field-internal variability, the method presented was developed on one field and not across fields on the whole farm. The application models yield classes with relative values that can be used as MZ. A classified map is not only more understandable than continuous data, most agricultural machines with variable rate applications work on the basis of classes. Modeling classes involves the risk of information loss

through generalization. However, they are better suited for setting up the model and for the usability of the end product.

The preparation of the data fusion with the TBM is so far very labour intensive. Both in terms of data formatting and the integration of expert knowledge. However, the method is transparent and the fusion logic understandable, in contrast to algorithms that work according to the black box principle. The presented method can be individually adapted to individual agricultural fields and their yield-relevant characteristics. The data used in the model can be weighted according to relevance, reliability, up-to-date status or completeness. After each individual fusion with an additional data set, the model output displays where the data sources contradict each other with regard to the parameter yield to be modelled and where they suggest the same interpretation. These conflict maps are another important advantage of the method for evaluating the result, but also the individual data sources. This study gives some examples how the combination of soil, relief and satellite data is possible for modelling three yield zones of a wheat field for PA application.

3.2 Study Area and Data

3.2.1 Study area

The presented method for delineation of yield zones on the basis of evidential reasoning has been developed on field "200-01", part of a 2000 ha farm near the village of Görmin, located 15 km SW of Greifswald in the North-Eastern Lowlands of Germany. Geologically, the region was shaped by repeated glacial processes during the Weichselian Glaciation and transformed into a hilly ground moraine landscape with representative glacial features. Flat, hilly and undulating ground moraines alternate with hilly terminal moraines, glacial valleys, lake basins, kettle holes, eskers and outwash plains (Bundesanstalt für Geowissenschaften und Rohstoffe 2006). The differences in topography on a field basis are quite modest and represent relative flat terrain in the region (*Fig. 3.1*). Natural and artificial drainage systems impact the

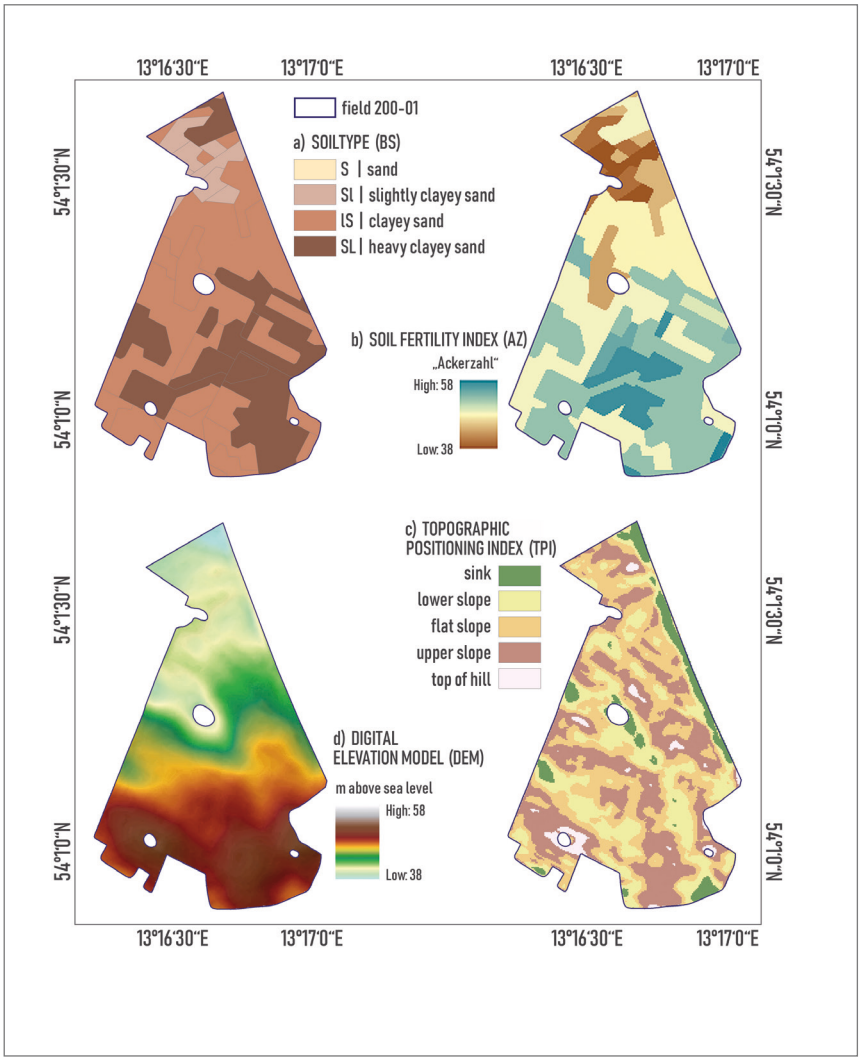

Fig. 3.1 Field 200-01, central coordinate: 54°1'13.10"N, 13°16'39.25"E; mean elevation: 36.22 m above sea level; mean slope: 2.43°; field has three kettle holes, which are not cultivated. Soil type (a), fertility index „Ackerzahl" (b), topographic positioning index (c), digital elevation model (d)

topography and consequently the soil inventory of the fields. All fields are characterized by a young morainic soil type.

3.2.2 Data

In the process of delineation MZ with data fusion, 11 data source raster are processed and combined. These data sets entail soil and relief data, as well as satellite derived crop information.

Soil map

Soil information is based on the German "Bodenschätzung" (1:10.000) (BS) (Arbeitsgruppe Boden 2005), a soil map edited in the 1930s, which is kept updated, though not at the same spatial grid as the original data acquisition (50 x 50 m). The soil map contains soil polygons with information about parent material, integrated soil texture to a depth of 1 m and the soil development stage. Dobers, Ahl and Stuczyński (2010) elaborate on the development and characteristics of the BS. The parameters "Bodenzahl" (BZ) and "Ackerzahl" (AZ) are quantitative assessments of soil fertility and an indicator for potential agricultural productivity. They are given in integers in a range from 0 to 100, where 100 is the reference for the most fertile soil in Germany. The BZ is based on soil type and therefore productivity only, while the AZ takes other factors such as morphology and climatic characteristics into account. *Figure 3.1* shows the BS of field 200-01 with soil type and AZ, which is the index used further in this study.

Digital elevation model

The digital elevation model (DEM) has a resolution of 5 m and is based on airborne LIDAR measurements (Amt für Geoinformation Vermessungs- und Katasterwesen 2011). The elevation data was used to calculate the Topographic Positioning Index (TPI) (Jenness 2006) with the GIS software SAGA (Conrad et al. 2015). The TPI has generally six classes describing lands forms such as hilltop, upper slope, etc. and is dependent on the scales used in the calculation and classification process. *Figure 3.1* shows the calculated TPI for field 200-01.

Satellite data

The method was developed using a RapidEye images from April 2011 until July 2011. The RapidEye satellite system works with five spectral bands (blue, green, red, red edge, near infrared), where the near-infrared (NIR) is, in general, especially sensitive to the vitality of vegetation (Rees 2001; Basnyat et al. 2005). The return frequency at nadir is 5.5 days and the spatial resolution is 5 m. The radiometric calibrated and georeferenced scenes (Level 1B, Level 3A) were made available through the RapidEye science Archive (RESA). Atmospheric correction was performed using ATCOR (Richter 2010) for ERDAS Imagine 2014 (Leica Geosystems) and the images were geometrically aligned using an image to image co-registration algorithm developed in-house (Behling et al. 2014). Further preparations for the development and testing of the segmentation algorithm included coordinate transformation, cartographic projection, and clipping the scenes to the area of interest, which is at the farm-scale in this case.

The Normalized Difference Vegetation Index (NDVI) was calculated and used for the method development. Numerous studies have shown a close connection between NDVI at a certain phenological stage of the grain and the biomass of the plants, which can be an indicator of the final yield (Benedetti and Rossini 1993; Ren et al. 2007; Knoblauch et al. 2017).

The satellite images available were selected according to their acquisition date. In the test region, suitable images for the method were acquired in spring approximately at the "Stem Elongation" phase of cereal, end of May/ beginning of June during and after "Heading" and end of June during the (BBCH) development of fruit phase.

The NDVI raster have been divided into three classes to simplify the necessary interpretation within the model. The two class boundaries are defined by the quantile value of the lower third (33% quantile) and the quantile value of the upper third (66% quantile). This results in three classes that have a stable number of pixels per class, regardless of the value range. If, on the other hand, a k-means approach is used, a few extreme values can lead to a spatially very small class that is difficult to interpret and makes little sense in terms of suitability for agricultural machinery.

Phenological data

Phenological data was provided by The German Meteorological Service (DWD) according to the BBCH-Codes (Hack et al. 1992), which is a decimal code system to identify phenological develop-

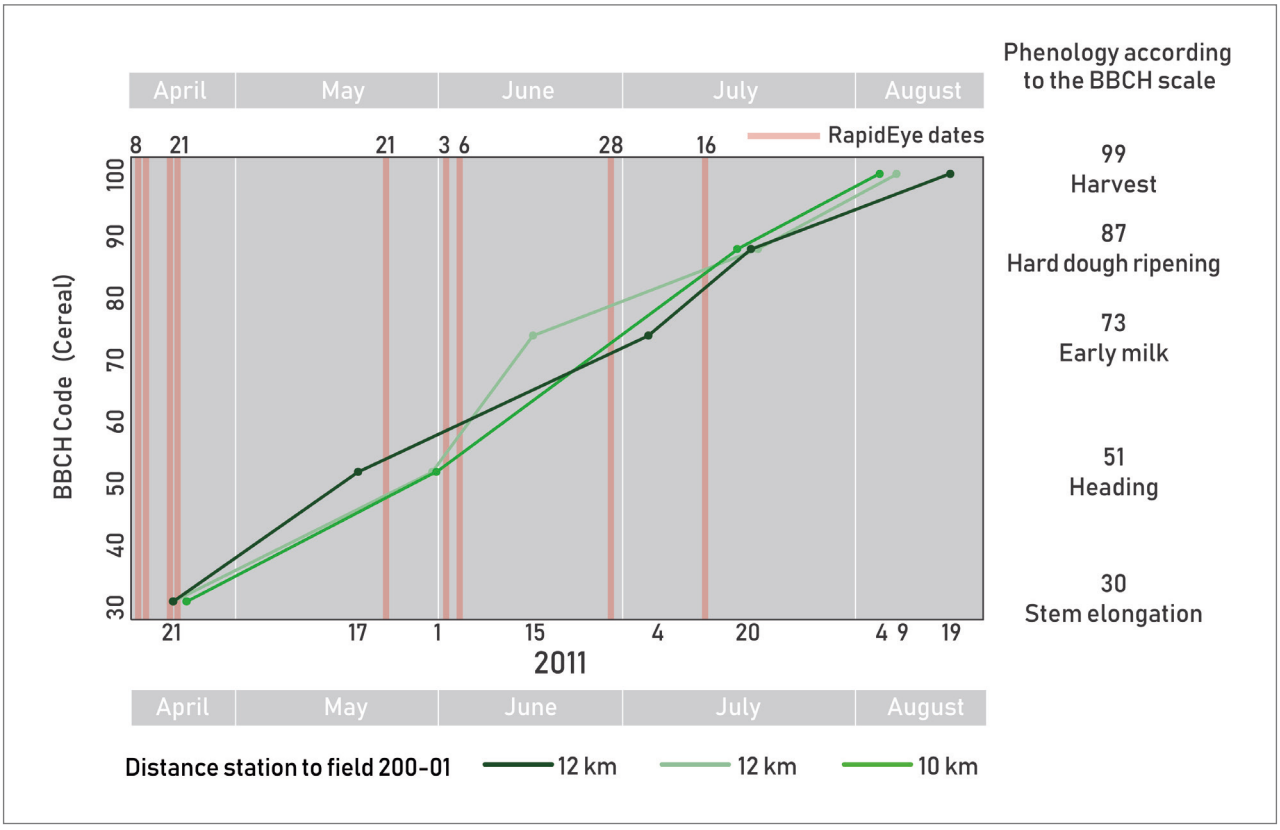

Fig. 3.2 Phenology data (BBCH Scale) acquired at three DWD stations near Görmin from April to August (green lines). The phenology at different stations is not always the same but shows slight differences in the development of plants at similar times. The stages of wheat phenology are numbered and described according to the BBCH scale (right side); Acquisition dates of RapidEye images (red lines)

ment stages of a plant and the standard phenology-scale in Germany. *Figure 3.2* draws data from three stations in 10-12 kilometers distance from the test site. Phenology was not measured directly on the test field, but in regular, though not weekly, DWD stations in the surrounding area. Coming from this official institution, these data are considered to be very reliable.

Farm and yield data

For this study, field boundary, crop cultivation and yield data for the test field were provided by an agricultural company. The yield data was taken during harvest by a GPS controlled harvester. Yield measure was taken approximately every 1 meter within a tram line, if the sensor operated flawless, which is not always the case. After acquisition, questionable yield measurements were removed for the most part, by applying filters on tresher speed (discarding of values < 2% and > 99%), swath width (discarding of values < 4 m and > 9 m) and statistical outliers (e.g. grouping of point values and discarding of yield values with a difference of more than 2.5 times the standard deviation of the group). Kriging was performed on yield data with the software VESPER (Haas 1990; Whelan et al. 1996) with a local kriging and local variogram method, especially designed for yield map kriging with respect to local, rather than global prediction models. Kriged pixels with a high kriging variance, hence a large distance between interpolated pixel and original yield value, were deleted.

3.3 Method

3.3.1 Evidential reasoning

The Dempster-Shafer Theory (DST) of evidence is probably the best-known and most widely used theory in evidential reasoning fusion models. The DST is a mathematical theory from the field of probability theory. It is used to assemble information from different sources with the so-called Dempster rule of combination to an overall statement, whereby the credibility of these sources is taken into account in the calculation. Evidence theory is used above all where uncertain statements from different sources have to be combined to form an overall statement. DST can quantify uncertainties and incompleteness of data. When modelling a parameter or classifying spatial objects, data fusion with a DST model can also be achieved with data sources that are not fully trusted individually or that have data gaps. The principle of evidential reasoning is therefore very relevant for agricultural problems. There is no doubt that each image or map is subject to a certain uncertainty compared to the actual state of, for example, soil, crop and yield. This may be due to interpolation, acquisition errors, coarse spatial or spectral resolution, and much more. Evidential reasoning is particularly useful when merging data sources of different spatial resolutions and units. It can also integrate information from older maps and current spatial data such as satellite images within a vegetation period. The processes in belief theory are understandable and comprehensible for the user, in contrast to black box methods from machine learning such as neural networks or support vector machines.

Fusion methods based on evidential reasoning should reduce uncertainties in the overall model and improve the classification result. Successful examples of the fusion of geodata with the DST

have been achieved by Al Momani, McClean and Morrow 2007; Mora, Wulder and White 2013; Okaingni et al. 2017. All used satellite data, products thereof, digital elevation data and other geo-data. The difference between these studies lies in the way a belief (the equivalent of probability in Bayes' model) is assigned to a pixel of a grid. In the DST, this transfer of belief to an expected class (e.g. „wheat", „grassland", „forest") is called a mass function. In these studies, this mass function is derived differently using the methods of the Maximum Likelihood and Classification Tree Method and the pixel occurrence statistics.

The common element of these studies is the structure of the mass functions and the combination of these by Dempster's rule of combination. Nevertheless, the mass function in the DST is associated with a kind of probability assessment or measurement (as in the Maximum Likelihood Method) and this is a disadvantage of the DST argue Smets and Kennes 1994. Their interpretation of the DST is called the Transferable Belief Model (TBM), which does not require underlying probability distribution, even though they may exist. It is a model for representing quantified beliefs based on belief functions and therefore a very suitable fusion method to work on agricultural problems, while supporting the expert knowledge of the user (e.g. farmer, farming consultants). This knowledge and experience are a major key factor for success in agriculture as well as precision agriculture and cannot be replaced by algorithms and software applications. The latter may aid the farmer little or tremendously, but only in combination with expert knowledge

Compared to other multi-source methods such as neural networks, probabilities and reliability of data sources within the TBM do not need to be calculated in advance. In addition, the data sources do not need to be classified into end parameters beforehand, which would be difficult for the farmer as end user to achieve. For example, it would be difficult to divide a satellite image without experience into yield classes (the final parameter). As a solution, a pre-defined set of rules, as one example described in this study, can be used to support the farmer.

Table 3.1 Terminologies of the TBM

Terminology	***Description***	***Scale***
Source of evidence (SOE)	A data source that delivers information and is part of the fusion process	Raster
Reliability (r)	The degree of how much the interpreter / expert trusts the SOE on a scale from 0 to 1	Raster
Hypothesis { }	Resemble the classes of the end parameter (here: yield class 1, 2, 3). Hypotheses are assigned pixelwise, based on what the expert would expect in accordance with the SOE value of that raster cell. The assumption of more than one hypothesis is also possible.	Pixel
Frame of discernment Ω	The range of all hypotheses, the whole hypotheses set.	Pixel
Masses of belief (MOB)	A weighing assigned to the hypothesis, depending on how much the expert believes in this assignment on a scale from 0 to 1.	Pixel

3.3.2 The Transferable Belief Model

Hypotheses and masses of belief

The TBM is a model for representing quantified beliefs based on belief functions (Smets and Kennes 1994). In other words, it can represent an idea of reality with a number of hypotheses (Dobers 2008). As listed in *Table 3.1*, the term „hypothesis" is part of the fixed terminology in the TBM. In the following, the term „hypothesis" is used as part of this terminology and differs from and should not be confused with the research hypothesis. The hypotheses of the TBM are weighted by quantified beliefs, called masses of belief (MOB), by means of an interval between 0 and 1:

$$m : 2^{\Theta} \rightarrow [0, 1] \tag{1}$$

with

$$\sum_{A \in 2^{\Theta}} m(A) = 1 \tag{2}$$

The whole set of hypotheses is called the *frame of discernment* Ω and the sum of all MOB assigned to the hypotheses is 1.
In this study, the hypotheses describe and include three classes of relative yield of a field. These yield classes can be used as MZ in practice and are described as follows: {1} - „Low yield", {2} - „Average yield", {3} - „High yield".

The theory of TBM states that the number of hypotheses may increase if additional knowledge is gained or a paradigm shift occurs. For example, if the TBM is used to improve the accuracy of soil maps, where the different soil types (e.g. clay or sand) correspond to the hypotheses (Dobers 2005, 2008). However, the evaluation of the data sources consulted can provide evidence that further soil types are available that are not yet represented in the entire set of hypotheses Ω. This is the case, for example, when old soil maps are used as evidence and past soil processes, such as erosion or tillage, have uncovered unmapped soil types. In the TBM, the case described corresponds to the „open-world assumption". It is therefore assumed that there are other classes or hypotheses than those that have been defined. In this study, this „open-world assumption" does not have to be taken into account, since the three relative yield classes cover the entire range of possibilities in a field. The „low yield" class therefore also includes areas in which no return is to be expected at all, which is very rarely the case. In the TBM, this is referred to as the „closed world assumption".

Sources of evidence

The aim of this study is to use the TBM to combine various data sources in order to find the most realistic yield class per pixel and thus obtain an overall picture, a map. The data sources used are called sources of evidence (SOE). All available SOE available at time t form the evidence corpus. In this example, eleven data sources (*Table 3.2, Fig. 3.9*), SOE, are used to model the yield classes. In addition to the eleven selected SOE, it is possible to use many other SOE, which can provide information on the distribution of the yield classes.

Table 3.2 Selection of used sources of evidence to model yield zones

Data source	Description	Original Spatial Resolution	Usage	Source
Satellite image (9 scenes from 9 dates in total)	RapidEye multi-spectral data (Product Level 3A), NDVI	5 m	Used as SOE in the TBM	RapidEye Science Archive, 2011 (8, 9, 20, 21 April; 21 May; 3,6,28 June, 16 July)
Soil map	"Bodenschätzung" with quantified description of soil quality / yield potential ("Ackerzahl")	50 m		Original data from the 1930s as described in Arbeitsgruppe Boden (2005)
Digital elevation model	Converted to a Topographical Index (TPI) map	5m		(Amt für Geoinformation Vermessungs- und Katasterwesen 2011)
Yield maps	Derived from GPS-tracked harvester in tons per hectare	Irregular point data (1.5 – 10 m)	Used for validation	GPS-Tresher of farmer, 06 August 2011

Before data fusion, each SOE must be interpreted. At this point, the expert knowledge is integrated into the model. Each class or value range defined for each SOE is interpreted with respect to the hypotheses in Ω - the available hypotheses of each unit are thus assigned to the SOE. For example, when interpreting a soil map, one might expect „low yield" in the very sandy soil class due to lower fertility. The hypothesis of „high yield" could be attributed to highly fertile loess soils. However, several hypotheses can also be assigned to an SOE class. If, for example, the class of loess soils lies in a strong depression, the expert could define both „high yield" and „low yield" as hypotheses due to possible waterlogging in wet years. If a class of an SOE cannot be clearly interpreted with regard to the hypotheses, the entire set of hypotheses can also be assigned. This would be the case, for example, if a topographical map were interpreted and the „level" class could not provide any significant conclusions about the level of yield. The fact that the TBM allows this multiple assignment distinguishes it from the classical probability theory, in which the singletons of Ω must be weighted individually. In the TBM, the MOB (i.e. the quantification of belief) can also be assigned to subsets of Ω.

Reliability

Every SOE is assigned a reliability r with a value between 0 and 1. For example: the expert might find the soil map more reliable (e.g. 0.9) then the elevation data, because in his[1] experience the soil

1 *or her*

map does reflect the real yield potential distribution more likely than the elevation map. Contrary, the expert could also argue, because of the low spatial resolution or early date of acquisition of the soil map (e.g. 1930s), he assigns a lower reliability (e.g. 0.6). The reliability of the SOE alters the MOB given for every pixel by multiplication.

Fusion and Dempster's Rule of Combination

With a minimum of two SOE, both assigned with MOB and reliabilities, the MOB can be combined using Dempster's Rule of Combination (Shafer 1976, 2016), which mathematically is a cross product. Any two independent mass functions m_1 and m_2 are combined to a single function $m_{1,2}$:

$$m_{1,2}(A) = (m_1 \otimes m_2)(A) = \sum_{B \cap C = A} m_1(B) m_2(C) \tag{3}$$

where

$$A, B, C \in 2^{\Theta} \neq \emptyset \tag{4}$$

An example from this study applies Dempster's combination rule as follows:

SOE 1, the soil map, is combined with SOE 2, the topographic positioning index TPI. For one pixel x, the class of SOE 1 is class 3 and for SOE 2 is class 2 (*Table 3.3*).

Table 3.3 Example of the assignment of hypotheses, masses of belief and reliability to one pixel x

Parameter	SOE 1 (class 3)	SOE 2 (class 2)
expected hypotheses / yield zone	"average yield", „high yield" = {2,3}	"low yield" = {1}
MOB	0.8	0.6
reliability r	0.7	0.9
Ω	"low yield", "average yield", "high yield" = {1,2,3}	

The expert is 80% convinced (MOB = 0.8) that in class 3, SOE 1 „average yield" or „high yield" can be expected. However, it gives SOE 1 only 70% confidence (r = 0.7) to be the appropriate source to make a reliable statement about the yield level. Following the same pattern, the expert assigns the hypotheses, beliefs and reliability for SOE 2, class 2.

With this defined interpretation, the fusion process of SOE can now begin and Dempster's Rule of Combination applied:

Table 3.4 Example for Dempster's Rule of Combination for values set in Table 3.3

		SOE 2	
		{1} m({1})= 0.54	{Ω} m({Ω})=0.46
SOE 1	{2,3} m({2,3}) = r · mob = 0.7 · 0.8 = ***0.56***	m{Ø} = **0.30**	m{2,3} = 0.26
	{Ω} m({Ω}) = ∑mob - m({2,3}) = 1 - 0.56 = ***0.44***	m{1} = 0.24	m{Ω} = 0.20

The hypothesis that receives the highest value of MOB after cross-counting is the hypothesis (or hypotheses) that both SOEs agree with. Unless the SOE support opposing hypotheses - as in this example - and a conflict arises. The hypothesis with the highest MOB value is the empty set {∅}. From here the TBM offers two ways: the open and the closed world acceptance. As already explained, the latter is chosen in this study. In this case {∅} is ignored and all remaining MOB values are normalized to a sum of 1. From the height of the MOB of {∅} the weight of conflict (woc) is calculated. It is later a measure for the contradiction between the data sources. After the normalization there is a new distribution of the MOB and a new hypothesis, which gets the highest MOB: m{1} = 0.34, m{2,3} = 0.37, m{Ω} = 0.29. The woc is given by

$$woc = \log\left(\frac{1}{\sum m(\bar{\emptyset})}\right) \tag{5}$$

In the example, the maximum belief lies with the hypotheses set {2,3}. One can also calculate the degree of belief of a hypothesis or set of hypothesis (A). Bel(A) is defined as the sum of all masses that support A

$$Bel(A) = \sum_{\emptyset \neq X \subseteq A} m(X) \tag{6}$$

The degree of plausibility function Pl(A) quantifies the total amount of belief that might support A:

$$Pl(A) = Bel(\Omega) - Bel\left(\bar{A}\right) = \sum_{X \cap A \neq \emptyset} m(X) \tag{7}$$

Consequently, Bel({1}} = 0.24 and Pl({1}) = 0.63, because {1} is also part of Ω. Plausibility can be interpreted as "the pessimistic assumption". Total Ignorance is represented by m(Ω) = 1, hence bel(A) = 0 – In this case, one has no useful indication of a realistically modelled hypothesis and must assume that any hypothesis or combination of all is possible.

The result of this SOE combination can then further be combined with another SOE and so on, until all data sources are integrated in the model. Because the combination is multiplicative, the order in which the SOE are combined is irrelevant. The simplicity in which evidence is considered, weighed and combined is a tremendous asset of DST and TBM, because it is comprehensible not only for developers of applications, but for users (e.g. farmers) too. Contrary to other current models, it is not a black box and very transparent.

3.3.3 Application of the TBM

In this study, the TBM was used to model yield zones, or MZ by fusion of the spatial soil information, elevation and satellite-derived NDVI images. Each data source – already classified as described above – was interpreted with regard to the expected yield zone(s), which are represented by the hypotheses. Following the workflow of *Figure 3.3*, the data was prepared for and combined with the TBM.

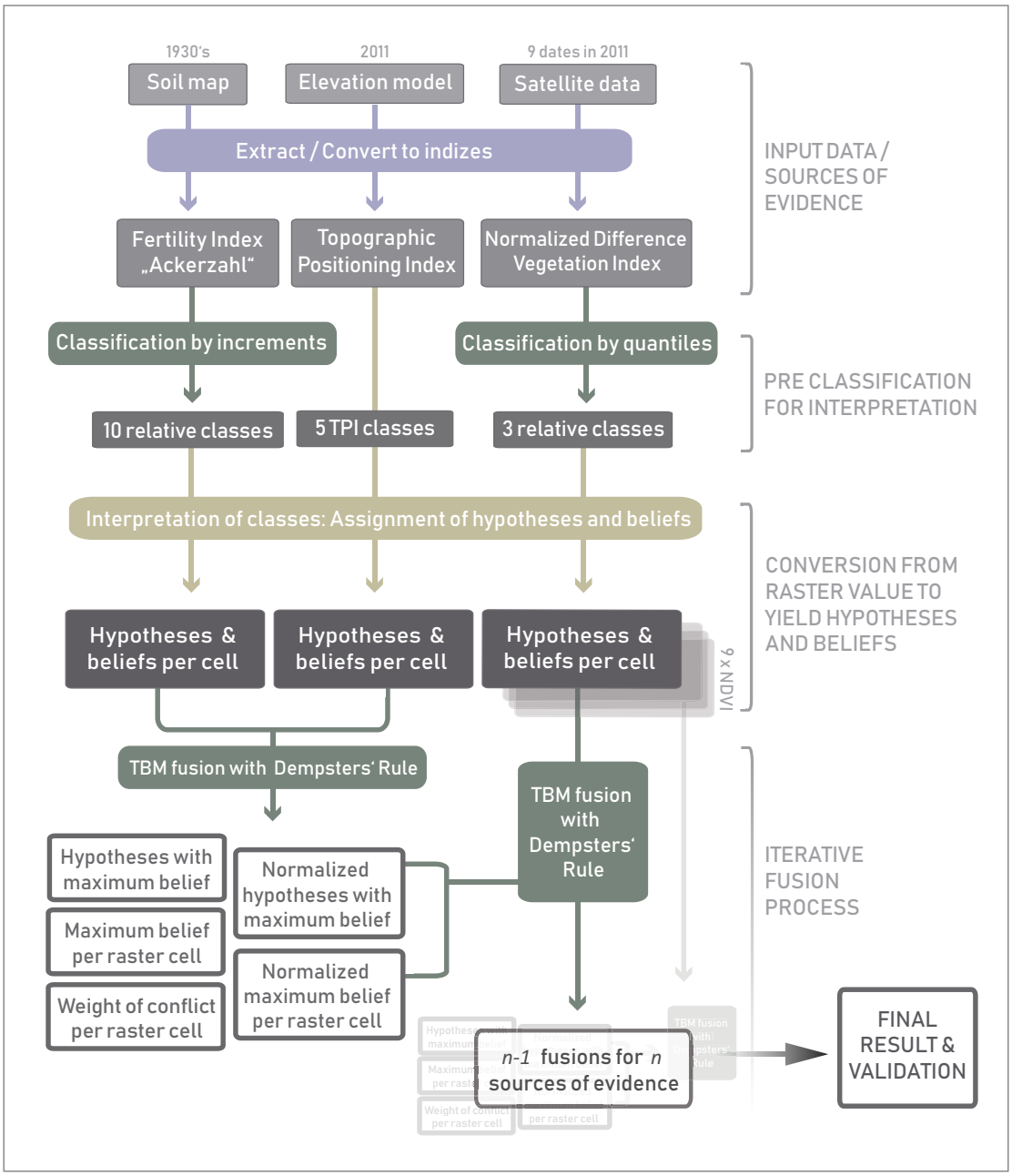

Fig. 3.3 Workflow for the fusion process

Table 3.5 Example for a lookup table for field 200-01. "SOE" describes the source of evidence, "hypo" the hypotheses, "MOB" the masses of belief and "r" the reliability. The TPI lacks a class 3, which is characterized by a steep slope, which is not given in this region.

SOE	unit	description	hypo	MOB	r	explanation
TPI (relief)	1	Ridge	{ 1 }	1	0.6	Erosion of upper layers of soil on and around hilltops is expected to produce lower yield
	2	Upper slope	{ 2 }	1		
	4	Flat terrain	{1,2,3}	1		The relationship between flat slope and yield is undefined, all yield classes can be expected
	5	Lower Slope	{ 3 }	1		Land forms favouring water supply and alluvial soils are expected to foster high yield.
	6	Dip	{ 3 }	1		
Satellite NDVI	1	low NDVI (0 – $^1/_3$ Quantile)	{ 1 }	0.8	0.55 - 0.9	Final yield is expected to be positively correlated with plant vitality at certain crop stages, indicated by the NDVI. NDVI class 1-3 is therefore interpreted in favour of yield classes 1-3. The reliability is variable, since the correlation between NDVI and yield varies in accordance to the phenological stage of crop.
	2	medium NDVI ($^1/_3$ Quantile – $^2/_3$ Quantile)	{ 2 }	0.7		
	3	high NDVI ($^2/_3$ Quantile – 1)	{ 3 }	0.6		
Soil					0.8	It is expected, that with increasing fertility index, hence with increasing relative % value, higher yield can be expected. Average fertility index regions could be also under the influence of relief or precision management, so all yield classes are expected. Relative values assure an easier transfer of the method to other fields.
	1	< 75 %	{1}	1		
	2	75 - 85 %	{1}	1		
	3	85 - 90 %	{1,2}	1		
	4	90 - 95 %	{1,2}	1		
	5	95 - 99 %	{1,2,3}	1		
	6	99 - 101 %	{1,2,3}	1		
	7	101 -105 %	{2,3}	1		
	8	105 - 110 %	{2,3}	1		
	9	110 – 120 %	{3}	1		
	10	< 75 %	{3}	1		

Pre-Processing

The TBM is applied on field basis. Therefore, SOE are clipped (with a "crop" function) to the same extent and – if needed – resampled to a resolution of 5 m (pre-classified images with the method 'nearest neighbour').

Interpretation

Each SOE and each unit / class of SOE must be interpreted prior to data fusion with respect to the yield classes expected. This interpretation is given a quantified conviction, the MOB. During

the development phase of this model, a MOB of 1 was defined for almost all classes of the SOE for reasons of simplification. However, some test runs of the data fusion also provided indications that a gradation of the MOB for the NDVI maps is reasonable, which were subsequently adjusted. The interpretations are stored in a lookup table (*Table 3.5*) and one can create each field individually or use them for all fields, but then lose individuality. For better results, individual interpretation of the data on a field basis is recommended, as in practice the farmer also evaluates each field individually.

The presented method is supposed to be driven by expert knowledge and in this case resulted from literature research, empirical comparison of SOE and yield data and many conversations within the work group, including a farmer and a farming consultant. Still, a machine learning approach to derive most likely hypotheses could be possible to generate a rule set to begin with. Existing yield records can give indications of which hypotheses are likely to occur in the units of the SOE.

Fuzzy boundaries

For the TBM, the SOE must be classified in advance so that the interpretation remains comprehensible. Geodata to which hard limits are assigned, however, do not reflect the reality of yield distribution. On the other hand, the conversion of continuous data into narrow classes and a large number of classes in order to almost map the actual continuity is difficult to handle, at least for a human interpreter.

To resolve these hard boundaries, a distance-dependent fuzzy function is applied to the class boundaries. Adapted from Dobers 2008, the overlapping class solution (OCS) assumes, that within a buffer b outside of one class boundary (e.g. polygon boundary), two classes are possibly valid. Consequently, if the SOE is transferred to a spatial polygon, every polygon feature overlaps into the neighbouring feature. Within b, the MOB would decrease form 1 (on the boundary) towards 0 (distance b into the neighbouring feature. Class boundaries are thus respected and softened through a weighting.

Output layers

The model produces several output layers, which can be converted to raster for visualisation and validation, as described in *Table 3.6*.

3.3.4 Validation

For validation, the concept of stratified sampling was applied. As described in Webster & Oliver (1990), the sample points for validation were randomly distributed within regular grid cells, dividing the target raster area. Yield values are based on point measurements. For each sample point, the relative yield value and the corresponding class labels (= hypotheses) were extracted.

The result was plotted as a box plot, depicting relation and separability between each class. In addition, two statistical tests were applied: a) the Kruskal-Wallis-Test and b) the Pairwise T-Test (class ID versus relative yield value). The result with a p-value < 2.2e-16 confirmed the general separability of the classes, even if run based on different sample points.

Table 3.6 Output layers of the TBM and their descriptions.

Name of layer	Description of value in a raster cell
Winning hypothesis	The hypothesis or hypotheses with the maximum belief
Normalized	The hypothesis or hypotheses with the normalized maximum belief (without the empty set)
Weight of Conflict	The measure of conflict between the SOE being fused
Maximum of Belief	The maximum belief as numeric value
Most Plausible Hypothesis	The hypothesis with the highest plausibility
Maximum Plausibility	Highest plausibility as numeric value

The Pairwise T-Test applied compares each test series with one another and tests if there are statistically significant differences. This test normally requires normally distributed data, which is not necessarily given in this case. However, this condition may be violated if the number of sample points is high (Bartlett 1935) and the variance of the test series is comparable.

In addition to the statistical tests, the modeled yield classes (1-3) were compared to an interpolated yield map, classified into three classes divided by the 33% (1/3) and 66% (2/3) Quantile. The sampling scheme followed a 5 x 5 m grid, coherent with the SOE raster resolution. The pixel-wise comparison provided a measure of accuracy, roughly indicating the quality of each fusion result. Roughly and best compared in relation to the range of all accuracy values (9% - 57%), because the pre-classification of the validation basis can be chosen quite randomly (e.g. rigid thresholds, k-means classification). Therefore, the final quality assessment of a fusion result was a combination of the physical properties of the box plot (indicators implying a high separability of classes 1, 2, 3), a visual analysis of the box plot and the accuracy.

During the model development, all possible 2047 combinations of fusing 11 sources of evidence (*Fig. 3.9, Chapter Appendix*) with each other and with varying number of SOE (1-11) were fused. Following this process is a combination matrix, listing an accuracy index, which is either the actual accuracy, if the statistical tests mentioned above were negative, or the actual accuracy plus 100, if the statistical tests were positive. This way, the results can be distinguished in a fast manner.

3.4 Results and Discussion

In order to explain the TBM and its application in agricultural questions, five combinations of the eleven SOE are presented. These examples can be used to show the success of the method, but also to generate information on how to work with the TBM and where it has weak points. *Table 3.7* lists the five examples presented here, together with the number of data sources considered and the corresponding figure reference.

Meaningful results are indicated by a good separability of the three modelled yield classes in the corresponding box plots. The statistical tests must support the separability. The calculation of the accuracy has a lower priority in the ranking of the results, since it can only be a guideline and not the „true" accuracy. On the one hand, the yield measurements in this study were not collected manually with absolute reliability, but the data from the thresher is trusted. Secondly, the yield map itself was classified before the 1:1 calculation of the accuracy and it is difficult to say which class boundaries would reflect a zoning on the field with absolute reliability.

If that accuracy is accepted it is first and foremost a relative measure, analyzing the evolution of the values calculated after each fusion from the respective result is very revealing. With fusion steps that bring a gain in information, the accuracy value increases. If another data source does not bring relevant or even false information into the model, the accuracy decreases after such a fusion. This is the case with result R1 (*Fig. 3.4*) and the last iterative step.

R1 shows the case when all eleven available SOE are combined, without regard to their individual relevance, but with the aim of combining as much information as possible. *Figure 3.4 b* is the normalized

Table 3.7 Overview of TBM combinations presented in this study

Result	Number of SOE	Names of SOE	Iterative step	Figure
R1	11 (all SOE)	1. Soil Quality ("Ackerzahl")	1	*Fig. 3.4* *Fig. 3.5* *Fig. 3.10*
		2. TPI (Relief Index)		
		3. NDVI 08 April 2011	2	
		4. NDVI 09 April 2011	3	
		5. NDVI 20 April 2011	4	
		6. NDVI 21 April 2011	5	
		7. NDVI 21 May 2011	6	
		8. NDVI 03 June 2011	7	
		9. NDVI 06 June 2011	8	
		10. NDVI 28 June 2011	9	
		11. NDVI 16 July 2011	10	
R2	5	1. Soil Quality ("Ackerzahl")	1	*Fig. 3.6* *Fig. 3.11*
		2. NDVI 20 April 2011		
		3. NDVI 21 May 2011	2	
		4. NDVI 03 June 2011	3	
		5. NDVI 28 June 2011	4	
R3	2	1. Soil Quality ("Ackerzahl")	1	*Fig. 3.7*
		2. NDVI 20 April 2011		
R4	2	1. Soil Quality ("Ackerzahl")	1	*Fig. 3.10 (Iteration 1)*
		2. TPI (Relief Index)		
R5	4	1. NDVI 20 April 2011	1	*Fig. 3.12*
		2. NDVI 21 May 2011		
		3. NDVI 03 June 2011	2	
		4. NDVI 28 June 2011	3	

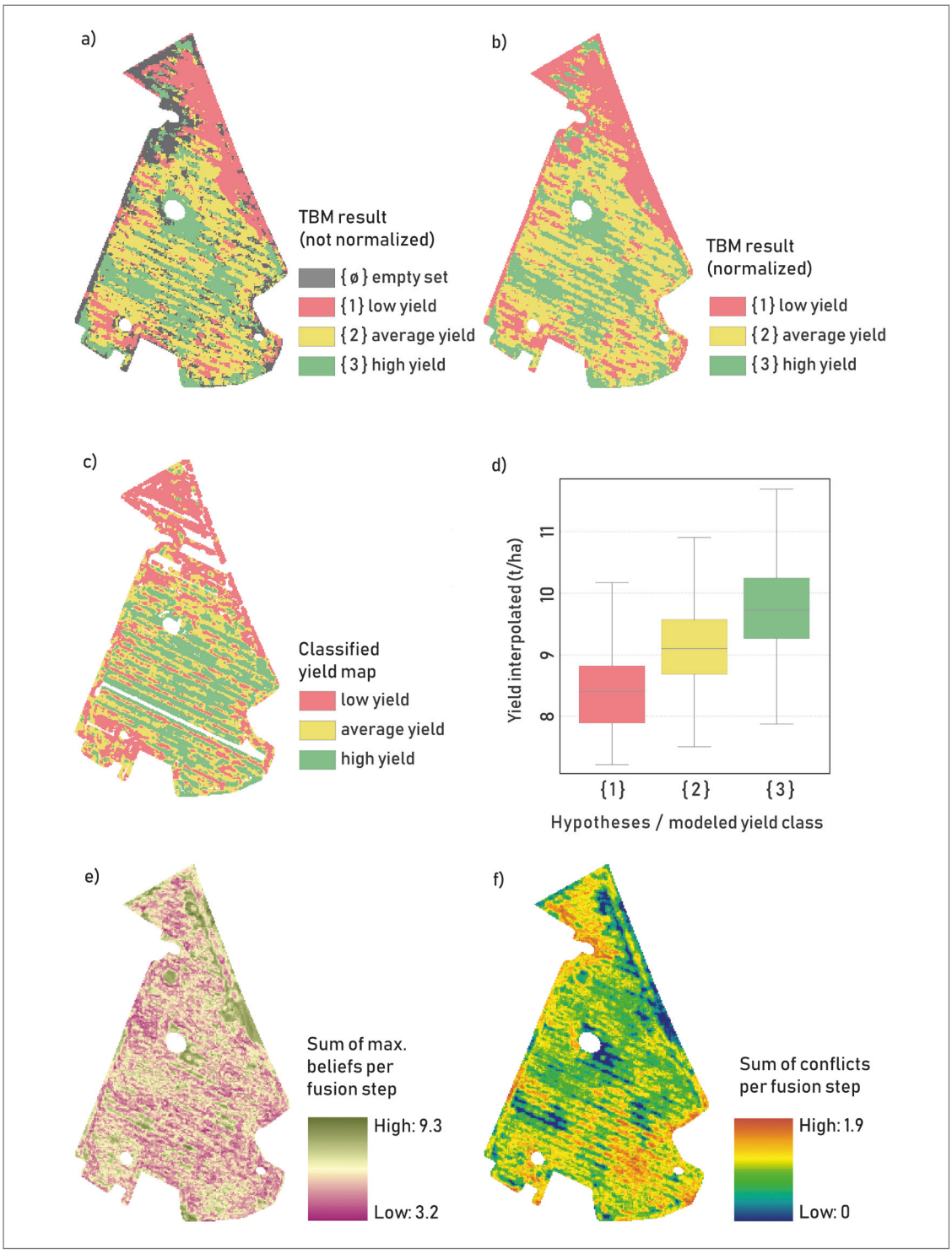

Fig. 3.4 R1 - Fusion result with all 11 SOE

result of the TBM fusion and shows a map with three yield classes. The corresponding box plot (*Fig. 3.4 d*) implies that the three yield classes can be effectively separated. The distribution of the three classes can also be seen visually in the yield map (*Fig. 3.4 c*). Looking at the non-normalized result (*Fig. 3.4 a*), the occurrence of the conflict areas that occurred during the last iteration step of the fusion can be traced. In these conflict areas the class of the empty set appears. If one adds up all weights of conflict (*Fig. 3.4 f*) that occur during the fusion steps, one can see in which areas in the field there are large uncertainties in the modelling and in which areas the data sources agree. The distribution of conflicts is slightly comparable with the modeled yield classes, where the highest sums of conflicts are mostly associated with zones of lower yield. If the soil map indicates good fertility

conditions, but the crop growth is limited by other factors, such as weather or short-term nutrient deficiency, the soil map conflicts with the satellite derived NDVI mapping the actual growth. If the soil map indicates less fertility, but the farmer takes measures to compensates the preconditions by precision agriculture actions, the growth would reflect positively in the NDVI SOE and therefore contradict with the soil SOE. Conflicts are not thus not a measure for the unfitness of the model, but an indicator for the relevance of each SOE concerning the modeled parameter.

R1 and also all other presented results are strongly fragmented and the classes are often not connected as a unit. This effect is a product of the high-resolution satellite images which, during the growing season, also record the stripped patterns through the lanes or rows of wheat. For agricultural practice, a kind of standardization of the result would have to be made at this point. This could be a multiple median filter, as applied to similar data in Georgi et al. 2017. Or a resampling of the satellite images to a coarser spatial resolution. With these methods, of course, information is lost, which is why the authors in this study have refrained from smoothing the results for purely scientific reasons.

The interim results of the data fusion provide information on how additional data sources affect the final outcome of the fusion and which data sources are particularly appropriate. *Figure 3.5* shows the box plots of the validation of the intermediate results of the fusion process of result R1, as well as the course of the accuracy. It is noticeable that after the first five fusion steps there are still pixels in the result for which the TBM does not model concrete classes but assumes several hypotheses (*Fig. 5a - 5d*). The reason for this is the preliminary interpretation of the SOE, as described in the lookup table (*Table 3.5*). In this case (R1) SOE1 (soil map) and SOE 2 (TPI) are almost exclusively represented by multiple hypotheses.
The more satellite data are added, which here are basically only assigned with the hypotheses {1}, {2} and {3}, the more the pixels with the diffuse classes disappear, which do not make a clear statement. This is of course desirable in this method, since the result is more user-friendly, especially when using yield classes or MZ in GIS systems or machine software. In contrast, the areas with multi hypotheses also offer more flexibility and room for interpretation of the result. At this point the farmer himself can decide whether in his experience a class {1,2} is to be assigned to a rather low or rather medium yield.

Figure 3.5a - 3.5i also shows that the spread of the modelled yield classes {1}, {2} and {3} increases steadily during the fusion steps 1-10 and the result is improved, especially from the 5th fusion onwards. The same trend is indicated by the trend of accuracy (*Fig 3.5 I.*). Only the last fusion with the final result (*Fig. 3.5 j*) does not provide any improvement, the separability of the classes in the box plot decreases again. The SOE added is a NDVI map from 16.7.2011, during which the wheat is already too ripe. The plant patterns on the satellite image correlate much less strongly with the yield at this time.

R1 is an example of a large data basis for the TBM, which is mostly not the case and not always necessary. It was found – on the basis of the combination matrix - that the relief information does not add significant information regarding yield on this specific field and is dispensable in this case. The result R4, which is part of R1 and the result of the first fusion of soil and relief information (*Fig. 3.5* and *Fig. 3.10*) supports this finding by a box plot with lack of separability, especially class 2 and 3, as well as a relatively low accuracy compared to other fusion results (*Fig. 3.5 I.*). For the delineation of MZ on this field, remote sensing data is clearly necessary.

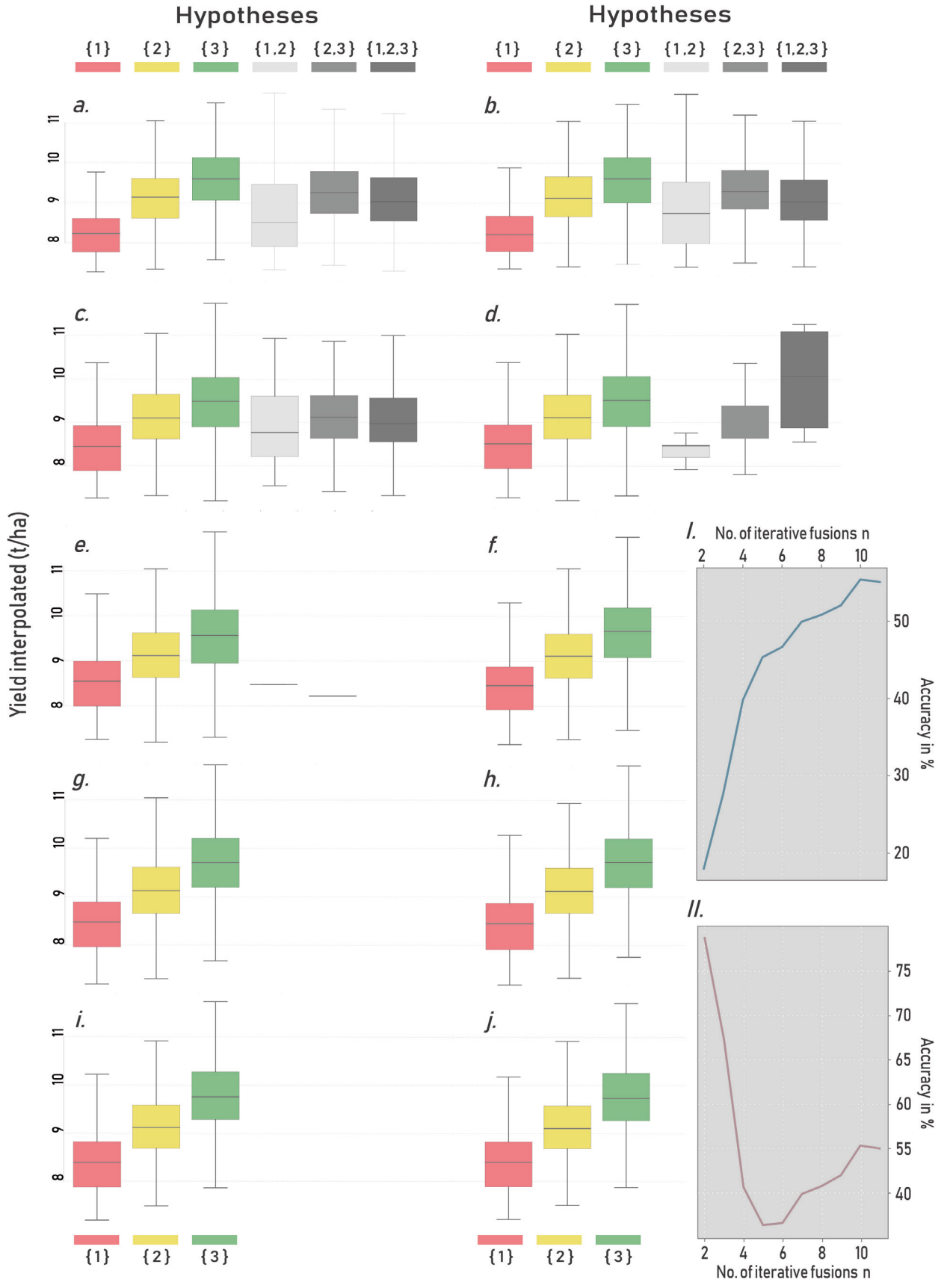

Fig. 3.5 Validation box plots for every fusion step (a-j), y-axis represents the value of the yield map taken for validation, x-axis represents the modeled hypotheses up for validation; accuracy throughout the fusion process for normalized results (I.) and for normalized result with the assumption, that pixel with multi-hypotheses count as successfully classified, if they include the yield class provided by the yield map (II.)

The acquisition of optical satellite images is highly dependent on cloud-free conditions and, while the importance of each satellite image is dependent on the acquisition date and the according phenological phase. Depending on the current phenology, the reliability of each individual satellite image can be adjusted. The values used in this example were determined in several test loops, during which results of fusions with all possible reliability combinations were validated with the yield data. The reliabilities for each NDVI data set reflect the correlation between final yield and certain phenological phases. The most relevant NDVI input layers are taken on the 28th June (development of fruit[1] / ripening[1]), 03rd and 06th June (heading) and 20th April (stem elongation[1]).

3.4.1 Suitability of multi-temporal satellite images

When modelling the yield, it therefore makes sense to use only certain satellite images of selected recording times. During the early phenological phases of cereal, the growth patterns reflect the basic spatial differences of soil, nutrients and water supply. These patterns are often very well visible in multispectral satellite data (Georgi et al. 2017).

The NDVI as an indicator of plant vitality highlights where more or less plants with more or less vitality grow in the field (e.g. because more or less seeds have developed and/or soil conditions are different). The number and density of the plants should correlate with the final yield, since the ability of the cereal crop to enter the phenological tillering phase depends on the germination capacity and the amount of plants from the seed (Geisler 1983). The latter plant distribution is exactly what NDVI can represent. A high distribution of weeds can mislead this impression, but it is not assumed that there are many weeds in field 200-01 - especially not at the beginning of the growth phase and the conventional agricultural methods applied. Thus, satellite data recorded in spring around the tillering and the stem elongation phase are very suitable for an early assessment of the plant growth of wheat. Consequently, these data are suitable for an early estimation of the yield differences (Marti et al. 2007), which also indicates the result R4, in which only the soil information and a satellite image data set from April were used for the TBM.

However, the yield of plants such as wheat does not consist of above-ground biomass, but of storage organs, which is why yield measurement with RS can only be indirect. In addition, these yields are dependent on the meteorological conditions in critical growth conditions (Knoblauch et al. 2017) and for modelling yield zones additional RS data throughout the growing season is crucial.

A very positive influence on the TBM result in this study was a satellite image taken on May 21 at the beginning of the phenological heading phase. In this phase, the leaf coverage of wheat is at its maximum (Geisler 1988).

Some studies have shown the highest correlation between NDVI and yield in this phase (Knoblauch et al. 2017), Field 200-01 correlates most strongly during the milk development stage of grain development (BBCH 71-77), which is also described by Marti et al. 2007. However, a high leaf area index (LAI) can also have a negative effect. If the crop is too homogeneous, the NDVI is saturated and the differences in vitality in the field are no longer visible. In this case, other vegetation indices would have to be used. If this is not the case, yield modelling can use the direct relationship between plant density and yield as one of many influencing factors on yield (Geisler 1988).

1 *Phase name according to the BBCH scale in English*

The most positive impact on the fusion process has the NDVI at 28 June. During milk-grain stage, where the wheat grains reached a maximum volume, whereas the grain, the spike and the top most leaves are green and synthetically active (Geisler 1988). As mentioned, wheat yield cannot be assessed by RS directly, but grain growth is based on cell multiplication and assimilation rate in the plant. Grain-growth important assimilation is driven by the photosynthetic activity of the top most plant parts, which is precisely the plant parts most visible to RS and the reason why the NDVI is sensitive to potential prospective yield differences in a field.

Finally, when the ripening process advances and the overall vitality is decreasing after milk-grain stage (Geisler 1988), remote sensing information decreases in relevance. The Mid-July image in this study does not show significant correlation with the final yield map.

3.4.2 Combination of only relevant SOE

The result R1 and the explanations on the relevance differences in satellite imagery imply that only certain relevant SOEs are preferable for the TBM. If only relevant evidence sources (*Table 3.7*, SOE as basis for R2) are used under exactly these aspects, the result R2 shows a high separability of the box plot classes as well as a relatively high accuracy (56.7 %). R2 is thus the best possible result of all combinations and would be recommended for use in practice. The accuracy increases during the fusion process and all intermediate results are statistically positively validated (*Fig. 3.11*).

It is also possible to model yield zones without GIS data and only with satellite data (*Table 3.7*, *Fig. 3.12*). The corresponding result R5 also achieves a good result with good separability of the individual classes (*Fig. 3.12*) and an accuracy of 55.4%. However, the result is not quite as accurate as R2 and the soil information adds more value to the fusion process.

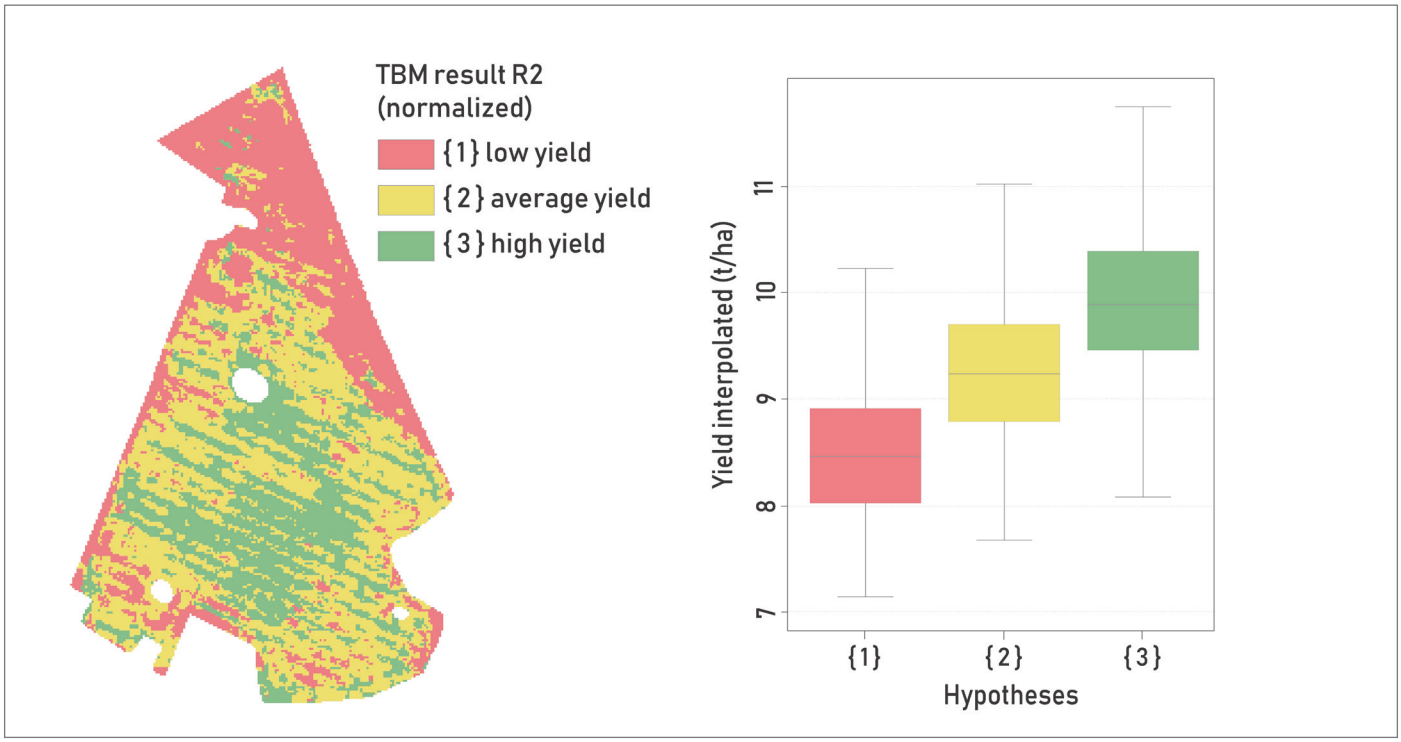

Fig. 3.6 Result R2, Normalized resulting hypotheses (left), validation box plot (right)

3.4.3 Early yield zone prediction

The most optimal result R2 integrates satellite data that are recorded late in the season. Early detection of vitality structures is also possible in spring. The fusion with an early satellite image from 20 April with the soil information can give an early estimate of the yield zones (*Fig. 3.7*). However, the TBM result is strongly dominated by zones to which the TBM has assigned multiple hypotheses. From this and resulting from the geometric structure of the soil map and the fuzzy boundary function, the result R3 is difficult to interpret (*Fig. 3.7 a*). The separability of the box plot classes is very high (*Fig. 3.7 b*), but the accuracy is only 14.37 %. If one tests whether one of the modelled multiple hypotheses corresponds to the actual yield class of the yield map per pixel (e.g. {1} [yield map] in {1,2} [TBM]), the accuracy increases to 85.4%. The sources of evidence find a result that is not wrong, but that cannot be used in practice. One solution is to use another TBM product, the most plausible hypothesis (*Table 3.6*, *Fig. 3.7 c*). Thus, the hypothesis with the highest plausibility is presented instead of the hypothesis per pixel that received the most belief during the application of Dempster's Rule of Combination. This is the hypothesis that appears most frequently in the cross calculation, whether as a single hypothesis or as part of a hypothesis set. The result (*Fig. 3.7 c*) is clearer, more comprehensible and achieves an accuracy of 51.6% in the validation with the yield map.

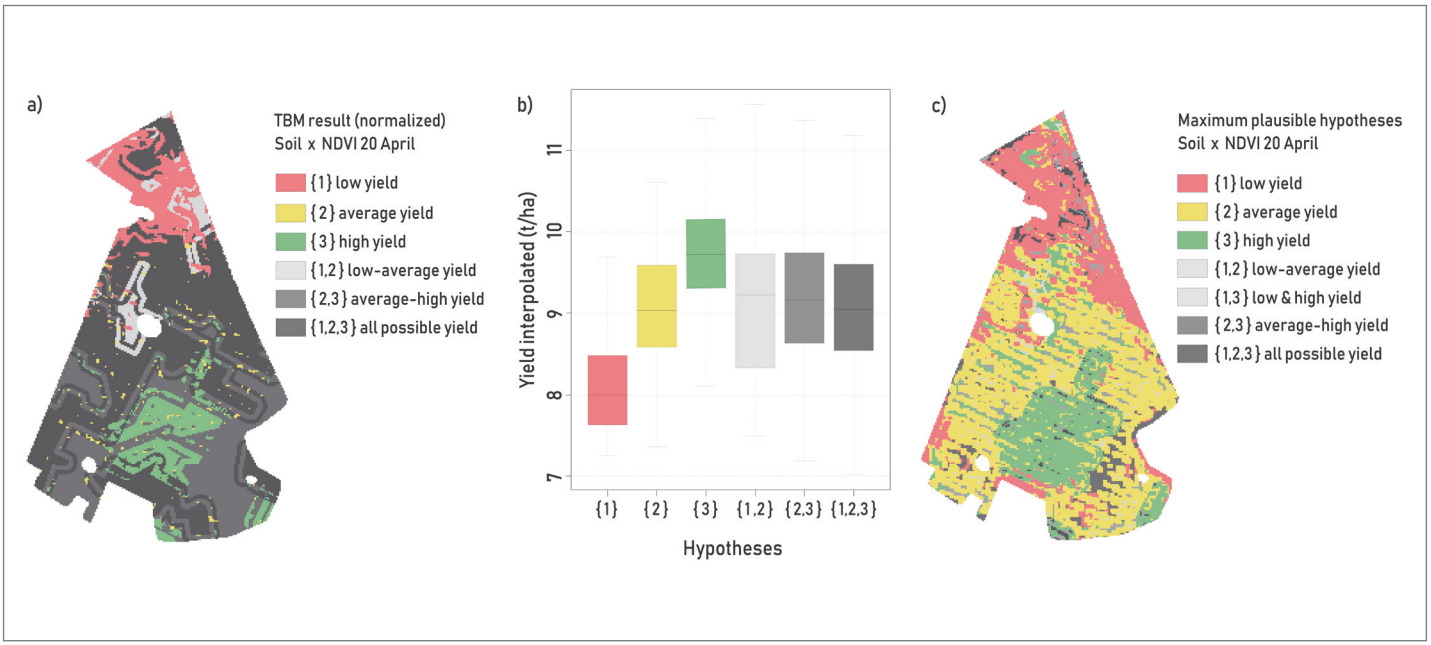

Fig. 3.7 Result R3, normalized resulting hypotheses (left), validation box plot (middle), maximum plausible hypotheses (right)

3.4.4 Comparison of selected results

The comparison between R1 and the 9th fusion result of R1, R2 and R5 shows a great visual similarity (*Fig. 3.8*). The classified NDVI map from June 28 also shows similar patterns, which is also due to the high weighting of the reliability of this data source in R1, R2 and R5 and increases the dominance of this data source. In the validation step R2 turns out to be the most optimal result, but

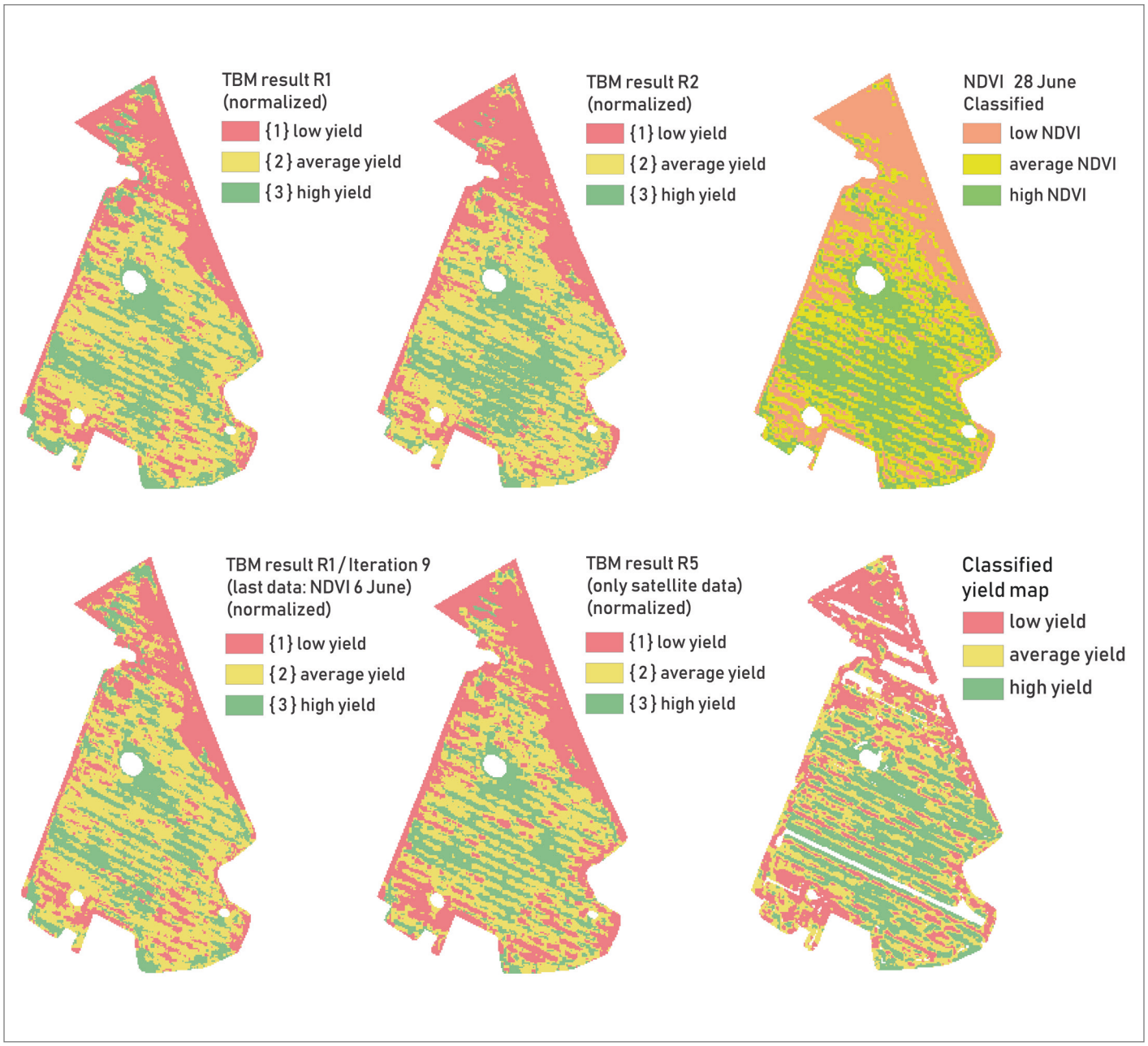

Fig. 3.8 Comparison of Results R1, R2, NDVI at 28 June, R1 at fusion iteration 9 and R5 (only satellite data), as well as the classified yield map

Figure 3.8 shows that several results of the TBM are usable in practice and it may be the case that there is not one correct result. Even if the yield structures can already be seen on the satellite image from 28 June, it is advisable to compress the information by several data sets. After all, it is not certain that a satellite data set is available at the desired time or whether it is dominated by clouds. The penultimate intermediate results of the fusion of R2 and R5 *Fig. 3.11* and *Fig. 3.12*) show that there is a well validated result even without this data set, although it is less accurate.

The comparison of all results with each other shows small and less small differences and thus also the nature of the TBM. The model is very flexible and can be fully adapted to the individual characteristics of a field and the farmer‘s experience. However, this requires a high degree of preparation and definition of several parameters by the user. The user has full control over the model and can

easily understand the values and the calculation. The parameters hypothesis, mass of beliefs and reliability can be adjusted in such a way that little or no pixels with multiple hypotheses appear in the result. This reduces the scope for interpretation and could also lead to incorrect classification if the classes of the sources of evidence are interpreted very rigidly.

3.5 Conclusion and Outlook

This study presents a method for data fusion based on evidential reasoning in the agricultural context. With the Transferable Belief Model, satellite data and GIS data can be fused independently of their unit and spatial resolution to model yield zones. These yield zones can then be used as management zones in precision farming applications, because they represent vitality differences in the field, which can be addressed by precision farming measures. The TBM calculates with quantified beliefs, not probabilities, because probabilities are very difficult to determine in an agricultural context. The beliefs allow the expert knowledge and experience of the user - e.g. a farmer or a consultant - to be integrated into the model. The calculation of the quantified beliefs is easy to understand and transparent. A wheat field in north-eastern Germany was used to show how the method works and what values the parameters influencing the TBM could have. The method leaves the farmer a lot of freedom in decision making and does not risk patronizing him with an intransparent, finished solution. In practice, however, the determination of this large number of parameters can be an obstacle to the successful implementation of the method. A further development of the method could therefore be to automatically develop a standard ruleset on the basis of past yield maps and the data used as sources of evidence. The farmer could then still adapt this standard rule set individually but would not have to work without reference. An analysis of a large amount of yield data in similar habitats and the existing GIS data as well as the large archive of remote sensing data could be a reliable data basis for such a ruleset. Especially if the farmer does not have his own yield data. Data mining algorithms would be very effective for the analysis.

The study presents only one field in one year as a development environment, but the method has to be tested on many fields, in various years and in different natural areas before being introduced into practice. The AgriFusion project (Spengler and Heupel 2017) is also further developing the TBM method, also on fields in other regions of Germany.

For practical relevance, it is important to generate an output format that can be used for agricultural machinery. The hitherto fragmented raster data dominated by pixels could be smoothed with a filter function and then converted into coherent vector polygons. This study aims to demonstrate the principle, relevance and feasibility of the method.

In the context of „big data“ development, the TBM offers endless possibilities for data fusion. Many yield-relevant data can be integrated into a TBM, such as electrical conductivity maps, nutrient distribution, water balance maps, and remote sensing data from other satellite sensors or drones. This further development is particularly important in years with heavy cloud cover to guarantee the recording of remote sensing data. In terms of yield expectations as well as in modelling yield potential, yield data from previous years can also be used as source of evidence in order to improve the accuracy of the results.

Based on this and other studies, the approach of evidential reasoning as part of Precision Farming applications is quite relevant for further development and implementation in practice. The method adapts organically to the complexity of plant growth and yield development and integrates exactly the valuable knowledge that farmers have generated over the years.

3.6 Acknowledgements

The authors would like to thank Climate-KIC for project funding, Edgar Zabel and the cooperating farm for data and support. We thank the German Aerospace Centre (DLR) for providing the data from the RapidEye Science Archive (RESA 617 FKZ).

3.7 Author Contributions

Claudia Vallentin and Eike Stefan Dobers designed to overall approach. Claudia Vallentin did the methological development and programming, as well as the analysis and the manuscript. Daniel Spengler, Sibylle Itzerott and Birgit Kleinschmit contributed to the discussion and general paper review.

3.8 Conflict of Interest

The authors declare no conflict of interest.

3.9 Chapter 3 Appendix

Fig. 3.9 All sources of evidence in this study

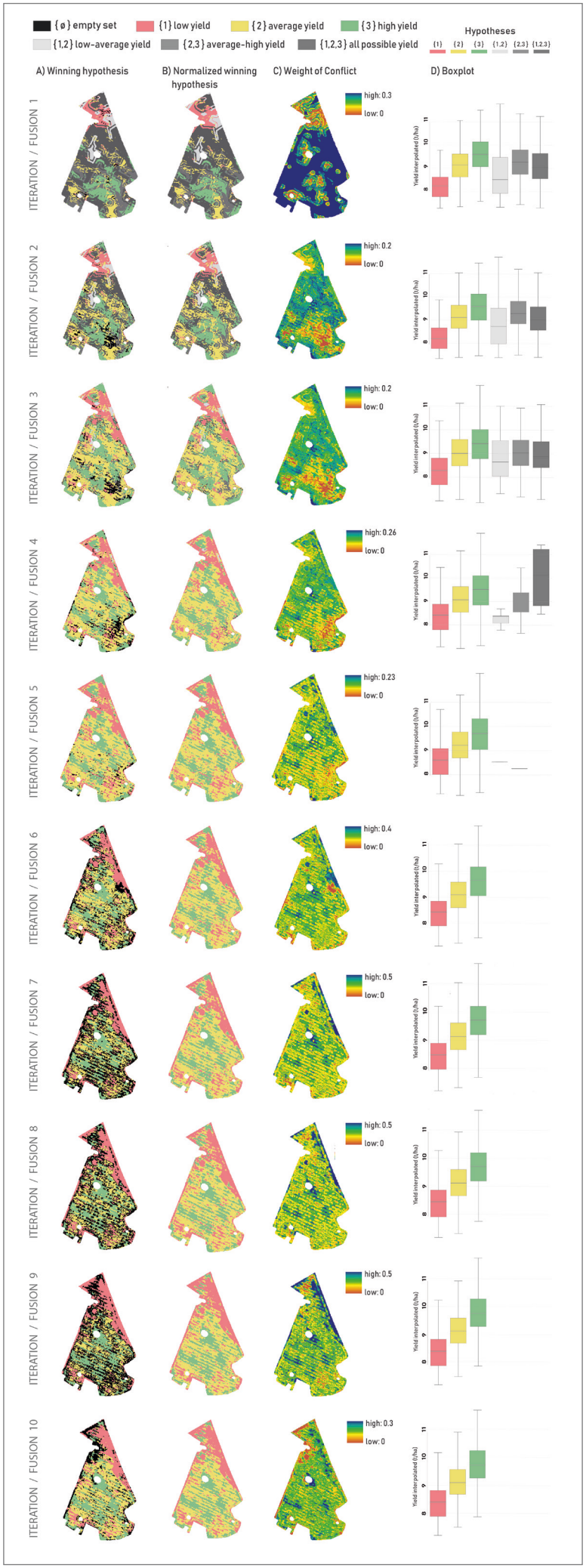

Fig. 3.10 Fusion process of result R1 with all SOE. Pictured are the hypotheses with the maximum of belief, the hypotheses based on the normalized maximum belief, the weight of conflict and the validation box plot.

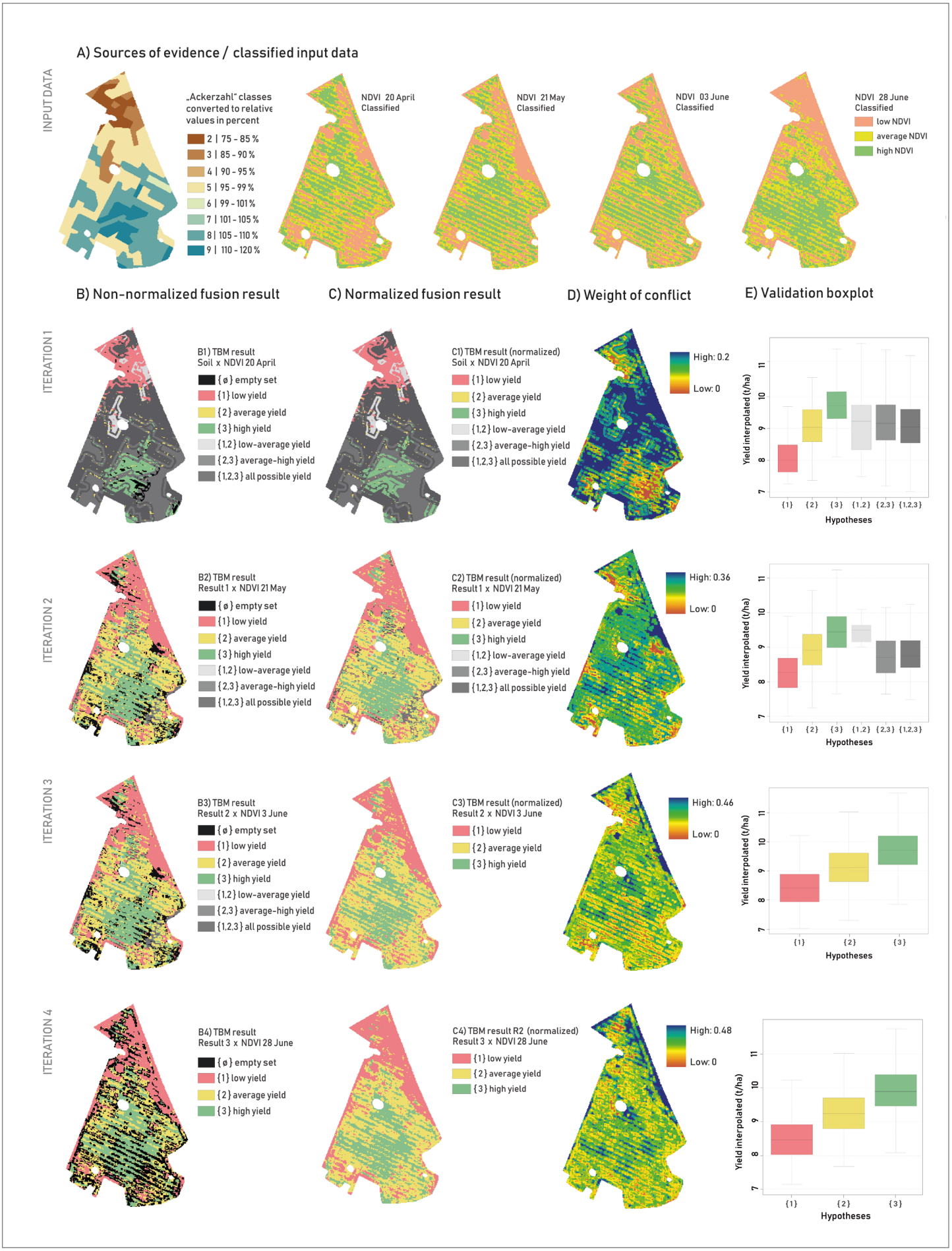

Fig. 3.11 Fusion process of result R2. Pictured are the hypotheses with the maximum of belief, the hypotheses based on the normalized maximum belief, the weight of conflict and the validation box plot.

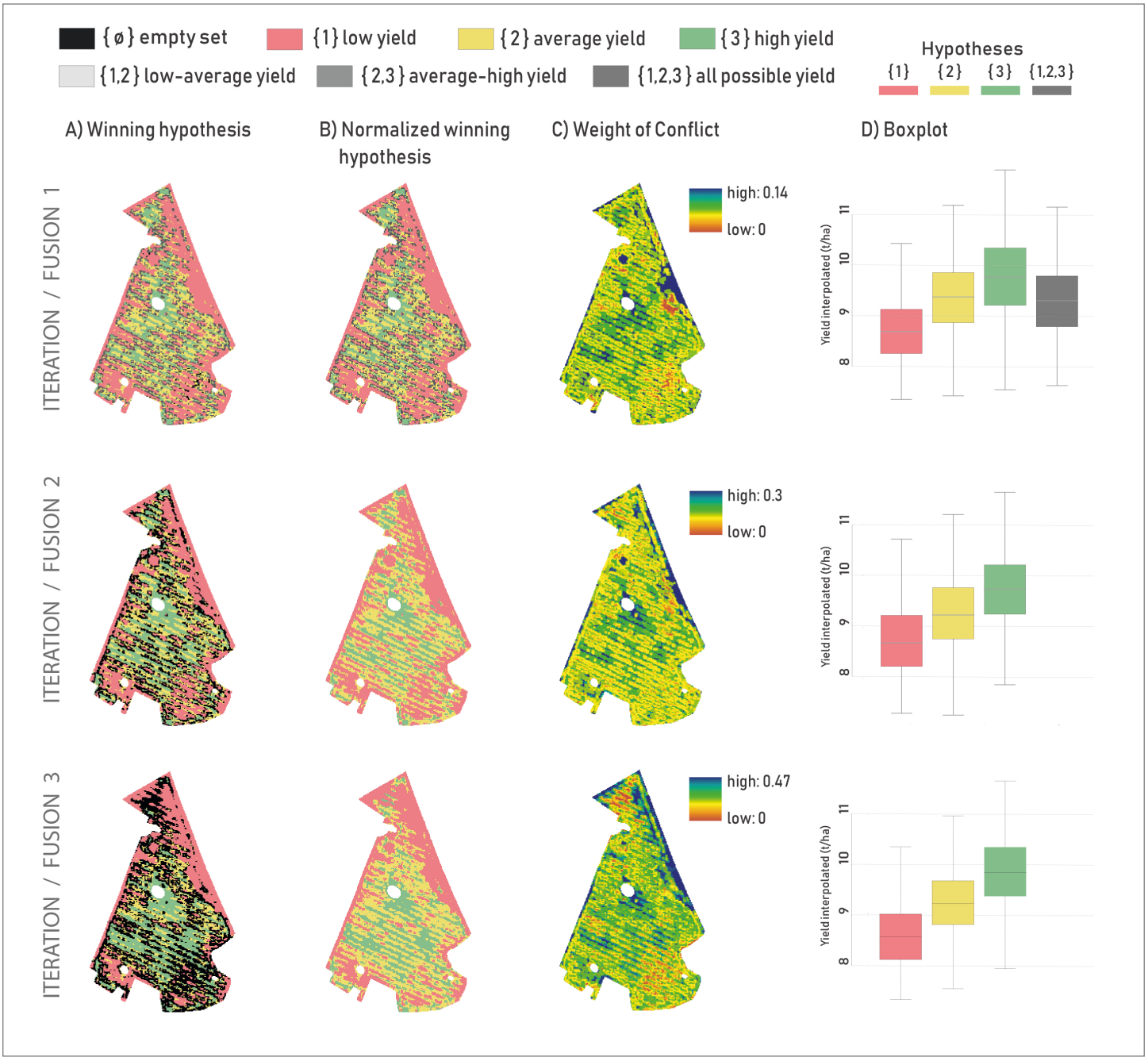

Fig. 3.12 Fusion process of result R5 (satellite data only). Pictured are the hypotheses with the maximum of belief, the hypotheses based on the normalized maximum belief, the weight of conflict and the validation box plot.

4 Yield estimation with remote sensing and geodata

Vallentin, C., Itzerott, S., Kleinschmit, B., Conrad, C. and Spengler, D.
Yield estimation with remote sensing: Suitability of various satellite data and geodata in NE Germany. Submitted to *Precision Agriculture,* Springer.

Author's preprint version

Submitted to *Precision Agriculture*: 22nd of March 2020

Abstract

Information provided by satellite and geodata in general is becoming increasingly important in the field of agriculture. Estimating biomass, nitrogen content or crop yield can improve farm management and optimize precision agriculture applications. A vast amount of data is made available both as map material and from space. However, it is up to the user to select the appropriate data for a particular problem. Without the appropriate knowledge, this may even entail an economic risk. This study therefore investigates the direct relationship between satellite data from six different optical sensors, as well as different geodata and yield data from cereal and canola recorded by the thresher in the field. A time series of 13 years is considered, with 947 yield data sets consisting of dense point data sets and 755 satellite images. In order to answer the question of how well the relationship between remote sensing data and yield is, the correlation coefficient r per field is calculated and interpreted in terms of crop type, phenology and sensor characteristics. The correlation value r is particularly high when a field and its crop are spatially heterogeneous and when the correct phenological time of the crop is reached at the time of satellite imaging. Satellite images with higher resolution, such as RapidEye and Sentinel-2 performed better in comparison with lower resolution sensors of the Landsat series. The additional Red Edge spectral band also has advantage, especially for cereal yield estimation. The study concludes that there are high correlations between yield data and satellite data, but several conditions must be met which are presented and discussed here.

4.1 Introduction

Modern agriculture is increasingly primarily a digital agriculture and the solutions to the major challenges can hardly do without data. In precision farming, Geographic information systems (GIS) and increasingly satellite data serve as a basis for the management. The flood of data from space is both a curse and a blessing. With the launch of the Sentinel satellite series, data, highly relevant for agriculture due to their spectral, spatial and temporal resolution, are now freely available. In cloud-free conditions, a data set can provide information on the growth and condition of the crop up to once a week, allowing conclusions to be drawn on parameters such as biomass, plant density and drought stress. But for the user himself, especially at farmer level, it is still difficult to interpret the data and select the appropriate satellite images. The estimation of crop yield is of great importance for the farmer, but also for the authorities – both historically and during the season.

The derivation of yield from satellite and GIS data is not trivial, since the yield formation of each plant species depends on complex factors and is different for every crop type (Geisler 1988). The final yield of a field is mainly dependent on number of seeds, soil type and therefore soil fertility, water supply, nutrient supply and duration of sunshine throughout the season (Geisler 1988; T., Evans and A. Fischer 1999). The grain yield of cereals, for example, cannot be measured directly from satellite data, which is why such methods are based on proxies such as biomass (Babar et al. 2006; Ren et al. 2008), leaf area index (LAI) (Gaso, Berger and Ciganda 2019; Peng et al. 2019) or

chlorophyll content (Guo et al. 2018; Serrano,Filella and Pen 2000). These proxies are often modelled using vegetation indices such as the Normalized Difference Vegetation Index (NDVI) (Marti et al. 2007; Bognár et al. 2017), which is considered to be very reliable. But also, less used indices like the Enhanced Vegetation Index (EVI) or the Normalized Difference Red Edge Index (NDRE) can be used successfully to estimate yield indicators.

But it is not only a question of the right index, but also of the time of acquisition. The correlation between a vegetation index and the crop yield is not congruent with every phenological stage. For wheat, the stages stem elongation (BBCH-Code 31), Heading (BBCH-Code 51) and Development of Fruit until early Ripening (BBCH-Code 75-83) of the BBCH scale (Hack et al. 1992; BBCH working group 2001) are stated to be suitable to derive the spatial yield patterns from satellite data (Knoblauch et al. 2017; Marti et al. 2007).

One limiting factor, however, is the spatial resolution of the products of many publications. This is because yield models on a (sub)national or regional basis (Ren et al. 2007, 2008; Baruth et al. 2008) with spatial resolutions of 250 meters (MODIS) to 1000 meters (SPOT VEGETATION) can only be used to a limited extent in agricultural practice. In European countries, the average field size of around 56 hectares (Statistische Ämter des Bundes und der Länder 2010) is many times smaller than, for example, in the USA with around 447 hectares (Macdonald,Korb and Hoppe 2013). If a farmer wants to integrate products from satellite data into his precision farming routine, information at field level is needed. Mainly because the main strategy of precision farming is the variable application of resources within a field.

The approach to field-based yield estimation must therefore answer the following questions: Which satellite sensor with which spatial, spectral and temporal resolution is best suited for yield estimation of the individual crop? At what point in time do these data have to be acquired to obtain a robust estimate and can geodata do the same? The current publication landscape covers only partial aspects of these questions, but cannot answer all of them, especially for grain and canola. And rarely for long periods of time.

For this reason, this study analyzes the statistical correlation of high-resolution yield data and satellite data of various spatial and spectral resolutions. 947 yield data sets from wheat, barley, rye, and canola fields collected between 2006 and 2018 are available. In addition, 755 satellite images, from which 15 different indices were calculated. Additionally, environmental GIS-data, such as soil type, soil quality, relief information and wetness index, were taken into the analysis. The correlations were compared with phenological stages, weather data and modelled plant-available soil water. The study evaluates for which crop type and which phenological stage yield estimation is mostly suited and which sensors are with which spatial and spectral resolution is necessary.

4.2 Study Area

The study area lies in the north-eastern lowlands of Germany (Figure 1), where the analyzed fields are located within the observatory TERENO-NE (Heinrich et al. 2018). The observatory is operated by Helmholtz Centre Potsdam - GFZ German Research Centre for Geosciences (GFZ) The central point of the study is roughly around 53.948 N, 13.186 E. Geologically, the region was

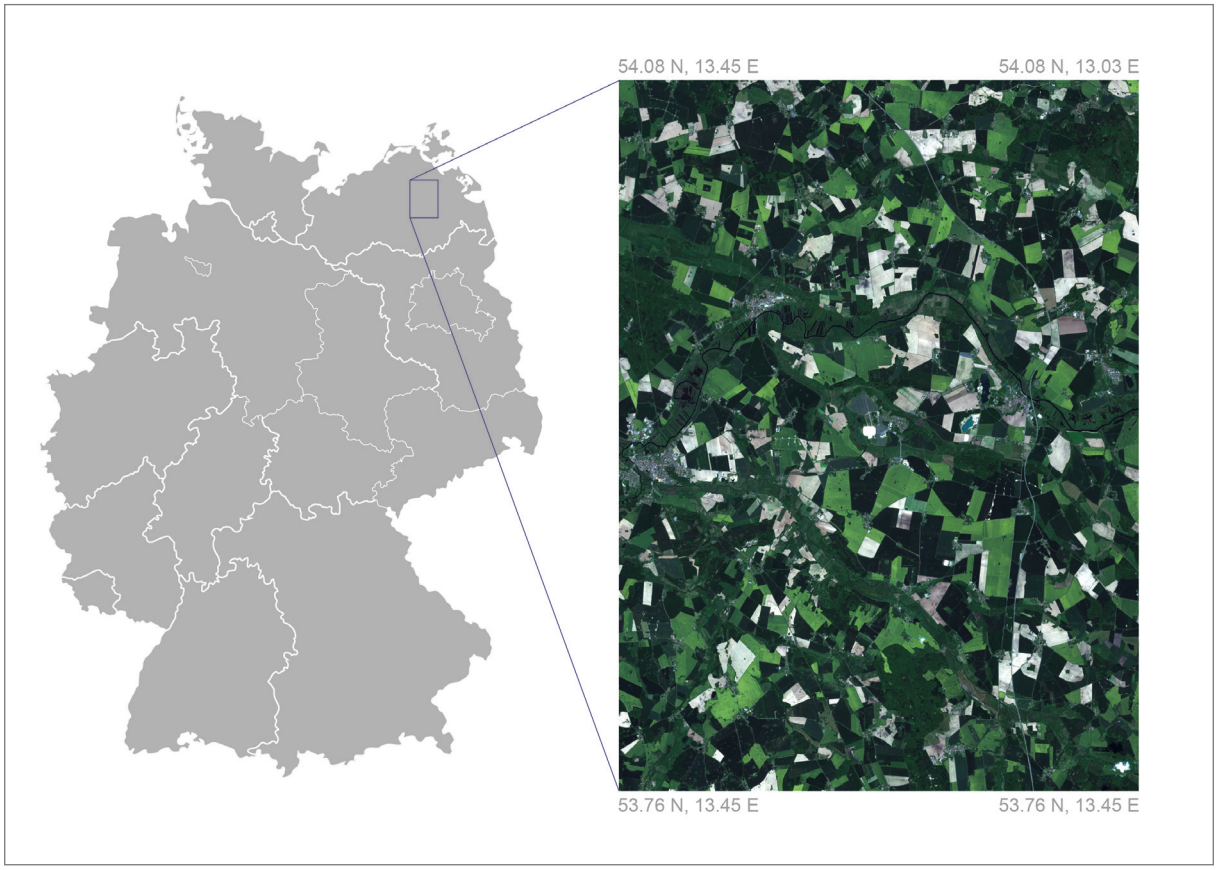

Fig. 4.1 Study area and location in Germany (left). Sentinel-2 satellite image, ESA (right).

characterized by repeated glacial processes during the last glaciation („Weichsel Ice Age") and transformed into a hilly ground moraine landscape with representative glacier characteristics. Flat, hilly and undulating ground moraines alternate with hilly terminal moraines, glacial valleys, lake basins, kettle holes and eskers (Bundesanstalt für Geowissenschaften und Rohstoffe 2006). Natural and artificial drainage systems influence the topography and thus the soil composition of the fields. All fields are characterized by young moraine soil types.

4.3 Data

4.3.1 Earth observation data

All available optical satellite images recorded by Landsat 5, Landsat 7, Landsat 8, RapidEye, Sentinel-2 and Planetscope covering our study area between 2006 and 2018 (*Fig. 4.2)* were obtained. At the beginning of the period only data from Landsat 5 and 7 are available, the number of sensors increases to five in 2017. For some years (e.g. 2013) only few data sets are available for the study area, among other things due to the mostly cloudy weather conditions. The different sensors have their specific characteristics such as spatial and spectral resolution (*Table 4.1*), which are examined in the study for their suitability with regard to yield prediction. The data were transmitted at different processing levels and further processed if necessary, to work with an atmospheric corrected and georeferenced data base (*Table 4.1*).

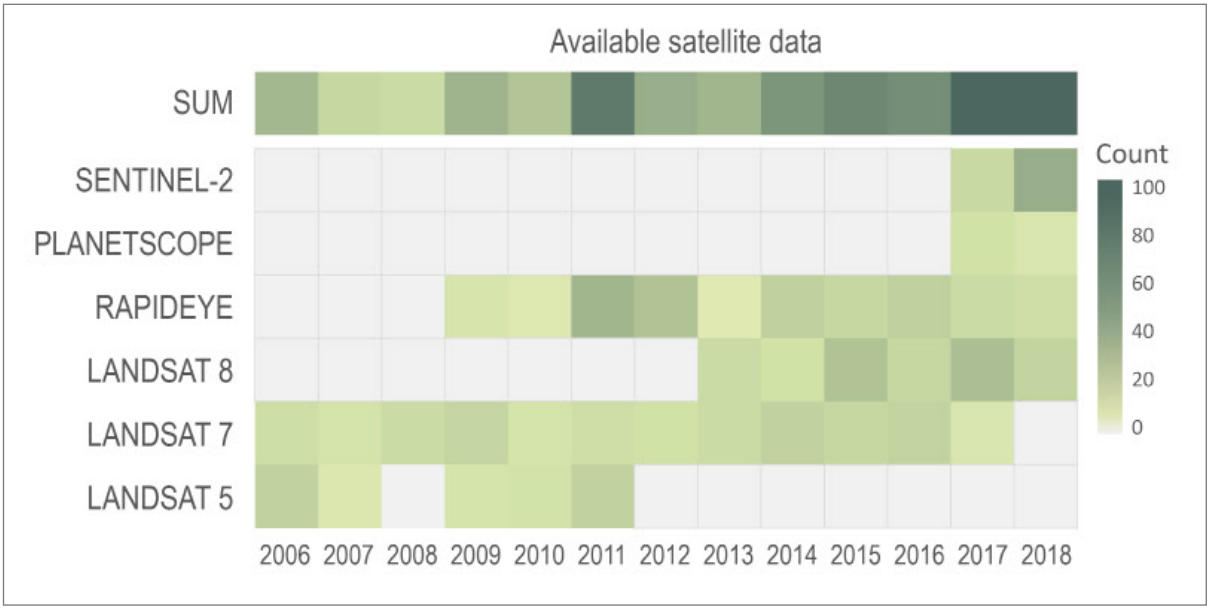

Fig. 4.2 Heatmap of satellite data availability for this study

Table 4.1 Overview of the availability and characteristics of the individual remote sensing sensors, as well as the processing steps performed. Not all recorded tiles are available for RapidEye at all times. Therefore, not every „No. of data sets" can always cover all yield data at the time of the recording.

Sensor	Years	No. of data sets	Spatial Resolution [1]	Spectral resolution used in study [2]	Processing	Literature
RapidEye Level 1B, 3A from RESA Archive	2009-2018	179	6.5 / 5 m	5 bands: blue, green, red, red edge, nir	Atmospheric Correction with ATCOR, Georeferencing with AROSICS	(Richter 2010; Borg,Daedelow and Johnson 2012; Scheffler et al. 2017)
Landsat 5	2006, 2007, 2009-2011	105	30 m	4 bands: blue, green, red, nir	Atmospheric Correction with ATCOR	(Richter 2010)
Landsat 7	2006-2017	280	30 m			
Landsat 8	2013-2018	127	30 m			
Planetscope Level 3A	2017-2018	21	3 m		Planetscope	(Planet Team 2017)
Sentinel-2	2017-2018	43	10 m	8 bands: blue, green, red, 3 red edge bands, nir	Atmospheric Correction and cloud masking with GTS2, Georeferencing with AROSICS	Scheffler et al., 2017; GFZ Potsdam)

1 *of used bands*

2 *Sensors offer more band choices*

4.3.2 Environmental data

Soil map (soiltype, BZ, AZ)

Soil information is based on the German "Bodenschätzung" (1:10.000) (BS) (Arbeitsgruppe Boden 2005), a soil map edited in the 1930s, which is kept updated, though not at the same spatial grid as the original data acquisition (50 x 50 m). The soil map contains soil polygons with information about parent material, integrated soil texture to a depth of 1 m and the soil development stage. Dobers, Ahl and Stuczyński (2010) elaborate on the development and characteristics of the BS. The parameters "Bodenzahl" (BZ) and "Ackerzahl" (AZ) are quantitative assessments of soil fertility and an indicator for potential agricultural productivity. They are given in integers in a range from 0 to 100, where 100 is the reference for the most fertile soil in Germany. The BZ is based on soil type and therefore productivity only, while the AZ takes other factors such as morphology and climatic characteristics into account.

Digital elevation model (TPI, TWI)

The digital elevation model (DEM) has a resolution of 5 m and is based on airborne LIDAR measurements (Amt für Geoinformation Vermessungs- und Katasterwesen 2011). The height data was used to calculate the Topographic Positioning Index (TPI) (Jenness 2006) with the GIS software SAGA (Conrad et al. 2015). The TPI has generally six classes describing land forms such as hilltop, upper slope, etc. and is sensitive to the scales used in the calculation and classification process. The shape of classes changes, if the outer radius of annulus in cells according to Jenness 2006 is changed. Therefore, two variations of the TPI were calculated: „TPI fine" with a radius of 25 meters and „TPI coarse" with a radius of 50 meters. The DEM was also used to calculate the Topographic Wetness Index (TWI) (Beven and Kirkby 1979), which is a steady state wetness index and is a function of slope and the upstream contribution area.

Map of Organic Carbon (C_{org})

Correlation analysis is also applied to a remote sensing product for mapping organic carbon. It is a distribution of organic carbon at the surface, developed by Blasch et al. 2015, using a multispectral RapidEye time series.

4.3.3 Farm and yield data

Yield data (Yield)

For this study, field boundary, crop cultivation and yield data for the test area were provided by two agricultural companies. The yield data was taken during harvest by a GPS controlled harvester. Yield measure was taken approximately every 1 meter (Farm 1) and approximately every 10 meters (Farm 2) within a tram line, if the sensor operated flawless, which is not always the case. In addition, Farm 1 operates Precision Farming over the entire time series with the aim of achieving homogeneous yields.

Farm 1 provided 315 yield records from 2006 to 2018 for this study, Farm 2 provided five large farm-wide records from 2012 and 2014 to 2017. The records were cropped to individual field-based yield data using field boundaries and resulted in 632 datasets of very various density. The data quality of the yield data is therefore different and is determined as much better for Farm 1.

After acquisition, false yield measurements were removed for the most part, by applying filters on tresher speed (discarding of values < 2% - treshold of all values and > 99% - threshold of all values), swath width (discarding of values < 4 m and > 9 m) and statistical outliers (e.g. grouping of point values and discarding of yield values with a difference of more than 2.5 times the standard deviation of the group). The Inverse Distance Weighted method was used to interpolate the point data into a 5-meter grid to visualize the yield data.

Electrical conductivity map (EM 38)

For Farm 1 maps of electrical conductivity from 2009 are available. These are measurements of a soil sensor, which vary depending on soil type and condition. Consequently, soil conditions can be derived from the measurements (Kühn et al. 2008). However, this parameter is highly variable, as it depends above all on the current soil moisture during the measurement. The data are available as point data. The data points were transferred to a grid. Due to the partly large point distance no interpolation was used, but a 25m buffer around the point values around the points was created.

Phenology data (BBCH)

Phenological data was provided by The German Meteorological Service (DWD) and by GFZ according to the BBCH-Codes (Hack et al. 1992), which is a decimal code system to identify phenological development stages of a plant and the standard phenology-scale in Germany. The records of the DWD are part of a long time series. For the years 2012 to 2018, field observations of BBCH collected by GFZ are available in the study area (Harfenmeister, Spengler and Weltzien 2019). Depending on the existence and the distance of the BBCH information to the respective field, the source (DWD or GFZ) for the phenological information was chosen in this study.

Weather data (Temperature, Precipitation)

Temperature and precipitation data for the entire observation period are provided by the climate stations in the DEMMIN area, which are operated by German Aerospace Center (DLR) (Borg et al. 2018) and GFZ (Itzerott et al. 2018). As reference values the median of the data of the 6 - 43 stations were determined.

Modeled soil moisture (moisture)

In order to supplement the weather data, the soil moisture was modeled for the interpretation of the results using the METVER model (Bach 2011). This is a complex 1D water balance model for calculating the evaporation of agricultural production areas. The values of the climate stations as well as soil information are used as input. The soil information around the station „Görmin“ (54.098 N, 13.408 E) was used. The soil characteristics are described by the parameters of the field capacity and the permanent wilt point.

In order for the model to produce a very good calculation of the soil water, the exact crop rotation with catch crops must be specified. As this was not completely known at the time of the study, the model was always calculated for one crop and may therefore deviate from the optimum.

4.4 Method

To understand the relationship between remote sensing and yield data, a large number of data sets from 13 years were analyzed. The data was obtained by extracting the satellite raster values or GIS raster values per yield point measurement. That is, if the area in question was not covered by clouds.

Table 4.2 Overview of the calculated vegetation indices, their formula, their origin and which sensor is available for the calculation. L5 = Landsat 5, L7 = Landsat 7, Landsat 8 = Landsat 8, RE = RapidEye, S2 = Sentinel 2, PS = Planetscope

Index	Name	Formula	Ref.	L 5	L 7	L 8	RE	S 2	PS
NDVI	Normalized Difference Vegetation Index	$NDVI = \frac{NIR - Red}{NIR + Red}$	Rouse et al. 1974	X	X	X	X	X	X
GNDVI	Green Normalized Difference Vegetation Index	$GNDVI = \frac{NIR - Green}{NIR + Green}$	Gitelson,Kaufman and Merzlyak 1996	X	X	X	X	X	X
SAVI	Soi Adjusted Vegetation Index	$SAVI = \frac{NIR - Red}{(NIR + Red) + 0.5} * (1 + 0.5)$	Huete 1988	X	X	X	X	X	X
NIR	Absolute reflectance values of the NIR band	NIR		X	X	X	X	X	X
SR	Simple Ratio	NIR / Red	Jordan 1969	X	X	X	X	X	X
IR/G	Ratio NIR and Green band (simple ratio)	NIR / Green	Jordan 1969	X	X	X	X	X	X
EVI	Enhanced Vegetation Index	$EVI = \frac{NIR - Red}{(NIR + 6 * Red - 7.5 * Blue) + 1}$	Huete,Justice and van Leeuwen 1999	X	X	X	X	X	X
CVI	Chlorophyll Vegetation Index	$CVI = NIR * \frac{Red}{Green^2}$	Vincini,Frazzi and D'Alessio 2008	X	X	X	X	X	X
GLI	Green Leaf Index	$GLI = \frac{2 * Green - Red - Blue}{2 * Green + Red + Blue}$	Viña et al. 2011	X	X	X	X	X	X
NDWI	Normalized Difference Water Index	$NDWI = \frac{Red - NIR}{Red + NIR}$	Gao 1996	X	X	X	X	X	X
MCARI	Modified Chlorophyll Absorption in Reflectance Index	$MCARI = ((NIR - Rededge) - 0.2 * (NIR - Green)) * (\frac{NIR}{Rededge})$	Daughtry et al. 2000				X	X	
NDRE	Rededge Normalized Difference Red-Edge	$NDRE = \frac{NIR - Rededge}{NIR + Rededge}$	BARNES et al. 2000				X	X	
NDRE / NDVI	Ratio of NDRE and NDVI	NDRE / NDVI	See above				X	X	
CCCI	Canopy Chlorophyll Content Index	$CCCI = \frac{\frac{NIR - Rededge}{NIR + Rededge}}{\frac{NIR - Red}{NIR + Red}}$	Barnes et al. 2000				X	X	
REIP	Red Edge Inflection Point	$REIP = 700 + 40 * (\frac{(\frac{Red + Rededge\ 3}{2}) - Rededge\ 11}{Rededge\ 2 - Rededge\ 1})$	Guyot 1990					X	

Therefore, a threshold for the blue band within the extent of each field was applied. If the standard deviation of such extent exceeded 150, cloud coverage was very likely and the data was therefore neglected. Depending on the spectral resolution, 15 indices were calculated from the satellite data, whereby 10 indices could commonly be calculated for all sensors (*Table 4.2*). In accordance with (Georgi et al. 2017; Vallentin et al. 2019), based on the same satellite and yield datasets the choice of indices was narrowed down to yield-relevant spectral indices as follows. Nonetheless, the collection does not claim exhaustiveness and could be extended in future studies.

4.4.1 Correlation calculation

These experiments were conducted:

A. by the direct correlation calculation between all grid points and yield points per field,

B. by the correlation calculation of the mean satellite grid values and mean yield values per field and year and

C. by the correlation calculation of all satellite grid values and all yield point values per year and per fruit, independent of the fields.

For each experiment and each data pair the Spearman correlation (Daniel 1990) was determined. Earlier studies (Georgi et al. 2017; Vallentin et al. 2019) showed a monotonous but non-linear correlation between satellite data and yield data, which would rules out correlation methods based on linear correlation assumptions. Often one reason for the non-linearity is the saturation of vegetation indices, which in high ranges do not correlate as strongly with the yield as in the lower and middle ranges.

It will be investigated how individual data sets correlate with yield data to find out which data sets are most suitable for potential yield modelling. Since each data set, be it satellite data or geodata, makes a different statement about the vitality of the crop and at least the satellite data are not mutually dependent, a bivariate analysis was chosen. In this way, the relevance of individual data sets can be highlighted and examined. The correlation values were therefore calculated into absolute values, to enable a ranking

They were then evaluated in terms of crop, phenology, yield level, choice of data source and indices, and weather conditions. In the following analysis of the results, the guideline for good correlations is the median of correlations in the respective group considered. Nevertheless, the outliers were also evaluated upwards in order to give an assessment of which parameters correlate most with each other. The correlation is given as Spearman Correlation Coefficient r also called “Spearman’s Rho” and this always refers to the correlation between the yield data and the data source to be analyzed.

The analysis and visualisation was done by using R (R Core Team no date) with the use of the packages ‘raster’ (Hijmans 2015), ‘rgdal’ (Bivand,Keitt and Rowlingson 2015), ‘stringr’ (Wickham 2012), ‘data.table’ (Dowle et al. 2014), ‘ggplot2’ (Wickham 2009), ‘gridExtra’ (Auguie 2012) and ‘automap’ (Hiemstra et al. 2008).

4.5 Results and Discussion

4.5.1 Experiment A: Direct correlation calculation between all grid points and yield points per field

4.5.1.1 Main results and observations

The correlation analysis based on the extraction of data source values per yield data point contains a broad spectrum of correlations. From no correlation up to correlation values of r=0.94. However, high correlation values above 0.75 are more outliers than standard and the median of all correlation values is 0.16, which also reflects unfavorable conditions. The results show however, that a positive correlation between yield and satellite data exists under certain conditions (*e.g. Fig. 4.10*). These conditions are influenced by the density and homogeneity of the crop, by the choice of satellite data, by the choice of index, the analyzed crop itself and by the acquisition date of a satellite image. Consequently, it is also possible to deduce yield characteristics from remote sensing data. The environmental GIS data have shown very low correlations in this study (*Fig. 4.16*). The certainty of a yield prediction is influenced by additional factors, such as level of average (expected) yield and phenology of the crop. A brief overview of the best performances in this study is summarized in

Table 4.3 Short summary of the results and indication of which vegetation index with which sensor has the highest correlations to which phenological phase.

CROP	TOP INDIZES	BEST BBCH	BEST SYSTEM	FIGURE
Rye	NDRE (RapidEye)	early: 31,33 late: 65, 61, 83	RapidEye	*Fig. 4.12* *Fig. 4.23 (Chapter 4 Appendix)*
	Red-NIR-Ratios: NDVI, EVI, SAVI, SR	early: 33	RapidEye	
		late: 65, 61, 51	Planetscope	
Wheat	NDRE (Rapideye)	early: 31 late: 76, 83, 51, 75	RapidEye	*Fig. 4.10, Fig. 4.12* *Fig. 4.22, Fig. 4.24 (Chapter 4 Appendix)*
	Red-NIR-Ratios: NDVI, EVI, SAVI, SR, GNDVI	early: 31	Planetscope, Sentinel-2	
		late: 83, 76, 75, 51	Planetscope, RapidEye	
Barley	Red-NIR-Ratios: NDVI, EVI, SAVI, SR, IR / G, NDWI	early: 31	Planetscope, RapidEye	*Fig. 4.12* *Fig. 4.25 (Chapter 4 Appendix)*
		late: 51 late: 75, 61	Planetscope, Sentinel-2, RapidEye	
Canola	NIR	early: 31	Sentinel-2	*Fig. 4.5, Fig. 4.13* *Fig. 4.21, Fig. 4.26 (Chapter 4 Appendix)*
	Red-NIR-Ratios: NDVI, EVI, SAVI, SR, GNDVI	late: 77, 71 late: 61	RapidEye, Planet, Sentinel-2	

Table 4.3.

As mentioned, environmental GIS data play a minor role in this study compared to satellite data for yield prediction, as they are almost always underperforming. This makes it all the more important to recognize that up-to-date data sets are needed to map the actual condition of the plants, although the growth of crop is undoubtedly directly dependent on the composition of the soil and

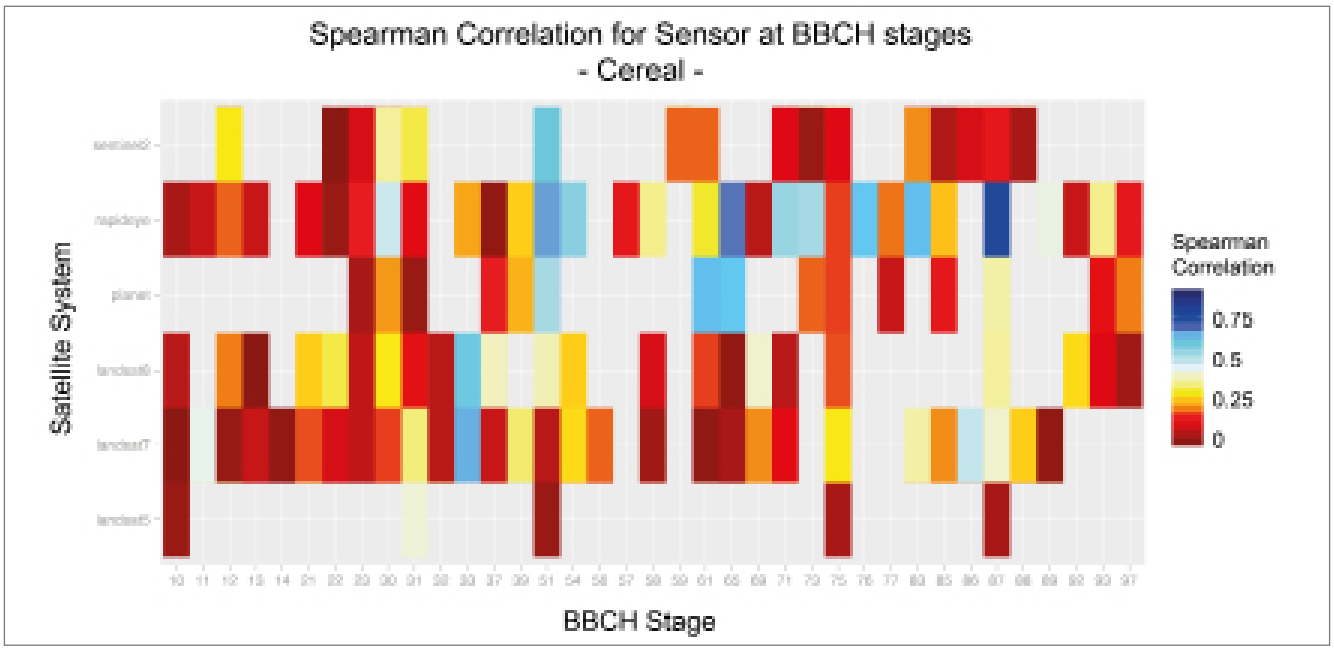

Fig. 4.3 Heatmap of all Spearman correlations calculated. Per sensor and BBCH stage for all cereal types.

topography.

In general, the correlation analysis shows certain tendencies, which data sets and which band combinations are favorable at which phenological stage to estimate the yield. *Figure 4.3* shows that when examining cereal, RapidEye data often show higher correlations than all other sensors. In this study

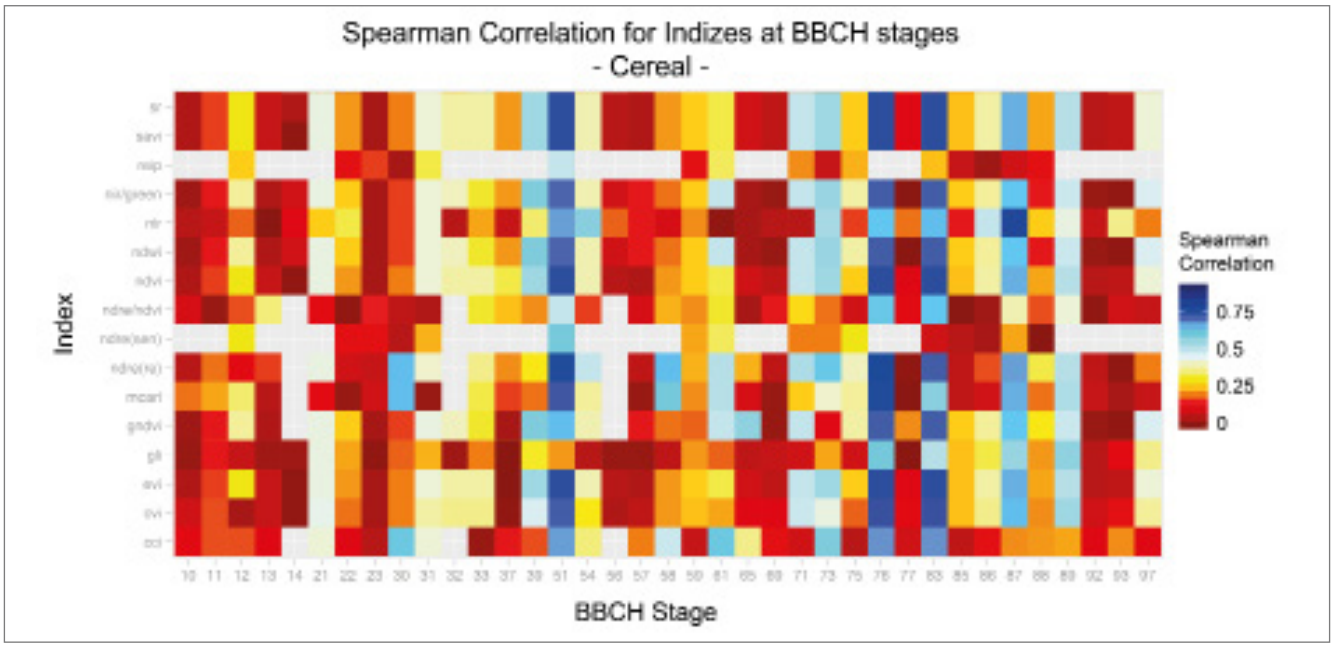

Fig. 4.4 Heatmap of all Spearman correlations calculated. Per index and BBCH stage for all cereal types.

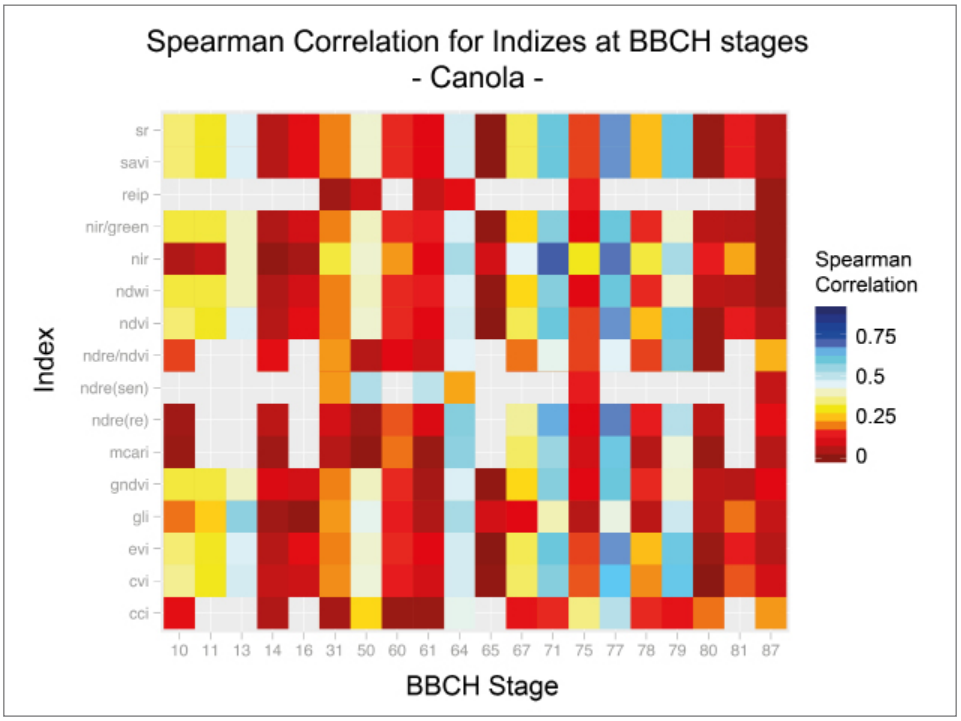

Fig. 4.5 Heatmap of all Spearman correlations calculated. Per vegetation index and BBCH stage for canola.

RapidEye belongs to the spatially high-resolution sensors and also has a band in the Red edge range. However, the availability of the data in this analysis is much higher than the data from Sentinel-2 and Planetscope. If this analysis is applied to canola, a similar pattern appears (*Fig. 4.21, Chapter Appendix*).

When considering which index, i.e. which combination of spectral bands, might be best suited to draw conclusions about the yield, certain patterns also emerge (*Fig. 4.4*). When looking at cereals, it can be observed that the correlations between satellite image and yield are almost consistently high in certain phenological phases, regardless of the index chosen. With the exception of the REIP. However, some indices perform well at certain BBCH stages, while others show much less correlation. This effect can be seen for example in BBCH stage 30 in *Figure 4.4*.

The fact that there is a stronger correlation in certain BBCH phases than in others can also be observed for canola (*Fig. 4.5*), but the appropriate indices here are partly different (*Table 4.3, Fig. 4.5*).

Overall, it can be observed that the correlations are highest for cereal crops wheat, barley and rye and less for canola. Factors to be considered when choosing satellite data for yield estimation and interpreting the results are:

I. Density of crop over field / Heterogeneity of field

II. Sensor resolution, spectral and spatial

III. Calculated vegetation index

IV. Phenological stage of crop

These factors are presented and discussed below. When interpreting the results, it should be noted that not only the type of data and yield levels have an influence on the correlation results, but also

farm management and the way the data are aggregated in the A-C experiments.

4.5.1.2 Impact of managing strategy and quality of yield data on the results

The evaluation of the data also revealed differences between the correlation strength of Farm 1 and Farm 2. The positive outliers are usually attributable to Farm 2, which often measured far less yield value points in the fields studied compared to Farm 1 (*Fig. 4.19, Chapter Appendix*). It cannot be excluded that the mass of yield measurement points of Farm 1 contains more uncertainties than the low number of Farm 2. The reliance on yield measurements as a basis for analysis can in itself be problematic, as the researchers rarely stand directly on the fields and check the accuracy of the thresher recording over time. The available data sets are very valuable due to their long time series and high spatial coverage but should not always be interpreted without skepticism.

However, the different correlation levels of Farm 1 and Farm 2 can be the consequence of the differing farming strategies. Farm 1 has been operating precision farming for more than ten years and seeks to homogenize the crop over the season until harvest. Farm 2, to the authors' knowledge, did not operate any precision farming during the period under review and may aim to exploit the high-yield areas in the field to the full. The yields of Farm 2 are on average higher than those of Farm 1, but the crop is spatially more heterogeneous. This can therefore also be seen in the satellite data and leads, for the reasons explained above, to a higher correlation.

4.5.1.3 Impact of decrease of resolution on the result

In the experiments B) and C) in this correlation analysis, in which the extracted data points are generalized in two different ways, much better correlations appear than in the experiment of A) mainly discussed in the following chapter. The generalization of the data and the associated reduction of the resolution of the points inevitably leads to a reduction of the information. However, the aim of this study is above all a correlation analysis within a field for the area of application of precision farming.

4.5.1.4 Factor i : Density of crop over field / Heterogeneity of field

In this case, the years 2015 to 2018 are selected in order to illustrate the influence of different yield levels per year on the correlation, as the data basis is also densest here. A comparison of the years 2015 to 2018 (*Fig. 4.6*) shows that the mean and maximum correlation values achieved for 2015 and 2017 are far below those for 2016 and 2018, although the data density is comparable and high-resolution satellite data are available throughout.

If the yield information is added, the picture is reversed. In those years in which the farmers achieved high yields, the correlations between yield and satellite imagery are lower than in those years with low yields. The reason for this is the proxy approach. The satellite sensors do not directly measure the grain yield as recorded during yield mapping. The vegetation indices are sensitive to variables such as biomass, vitality, LAI, density and chlorophyll content, which in turn are related to yield potential (Babar et al. 2006; Ren et al. 2008). If the crop is very vital and very dense, i.e. has a high LAI and a high biomass, even a sensor from space can only detect a few spatial patterns. In addition, saturation occurs in most indices above a certain threshold value, so that nuances in

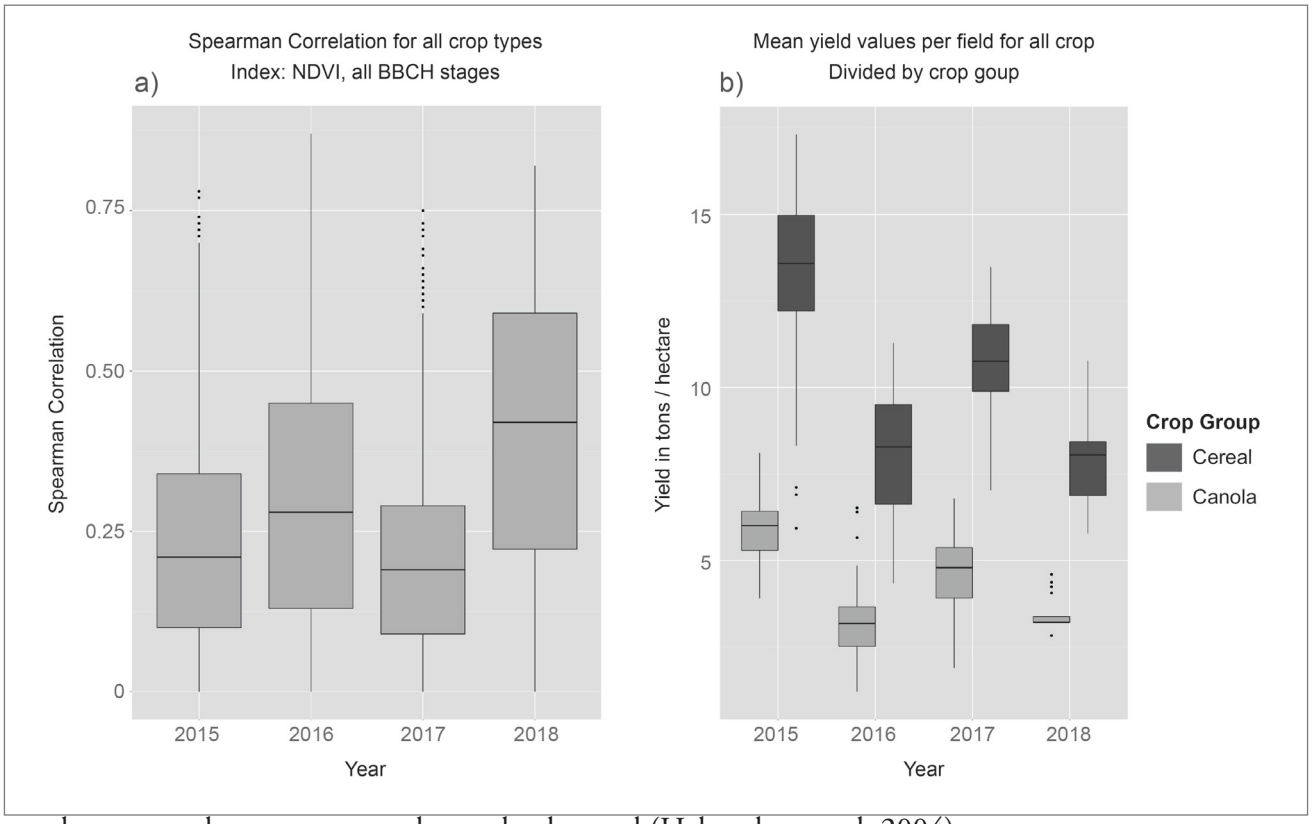

the upper value range can no longer be detected (Haboudane et al. 2004).

Fig. 4.6 Spearman Correlation per year, restricted to NDVI calculations, all BBCH stages (a). Mean yield level per field in tons per hectare per years 2015 – 2018 (b).

However, if the crop develops very heterogeneous because the soil and / or weather conditions are not in favor for growth and / or development, the probability of successfully recognizing yield patterns appears to increase according to these results. Especially for cereals, the maximum correlations per field can depend on the average yield of the field. In high-yield locations, i.e. fields whose biomass is in usually very high, the correlations between NDVI and the average yield of the field decrease (*Fig. 4.7*). Fields with low and average yield perform better in the correlation analysis.

These findings do not apply though, if the final yield is reduced by extreme weather events or damage caused by animals and diseases, which were all not by the satellite data or only occurred after the recording date may have reduced the yield.

Figure 4.3 and *Figure 4.4* show for the test area and the present large data set a correlation between the amount of yield and the correlations between yield and satellite data sets. This leads to the conclusion that in case of high homogeneity of the fields and high expected yield, the satellite data can be less reliable to make a reliable statement about the yield than in the other case. During the growing season, it is usually difficult to estimate the expected yield. For agronomists, however, the consideration of weather data and the availability of water close to the roots can provide information. The availability of water is a decisive factor in yield development. Water scarcity reduces stromatal conductance and photosynthesis in the leaves. This can - in theory - influence the metabolic capacity of the seed (Egli 2017). In water-intensive phases such as heading, low availability is particularly critical. Water stress in the 7-10 days after anthesis additionally causes a reduction of the final grain yield (Evans and Fisher 1999). In the grain filling phase, the temperature is also decisive.

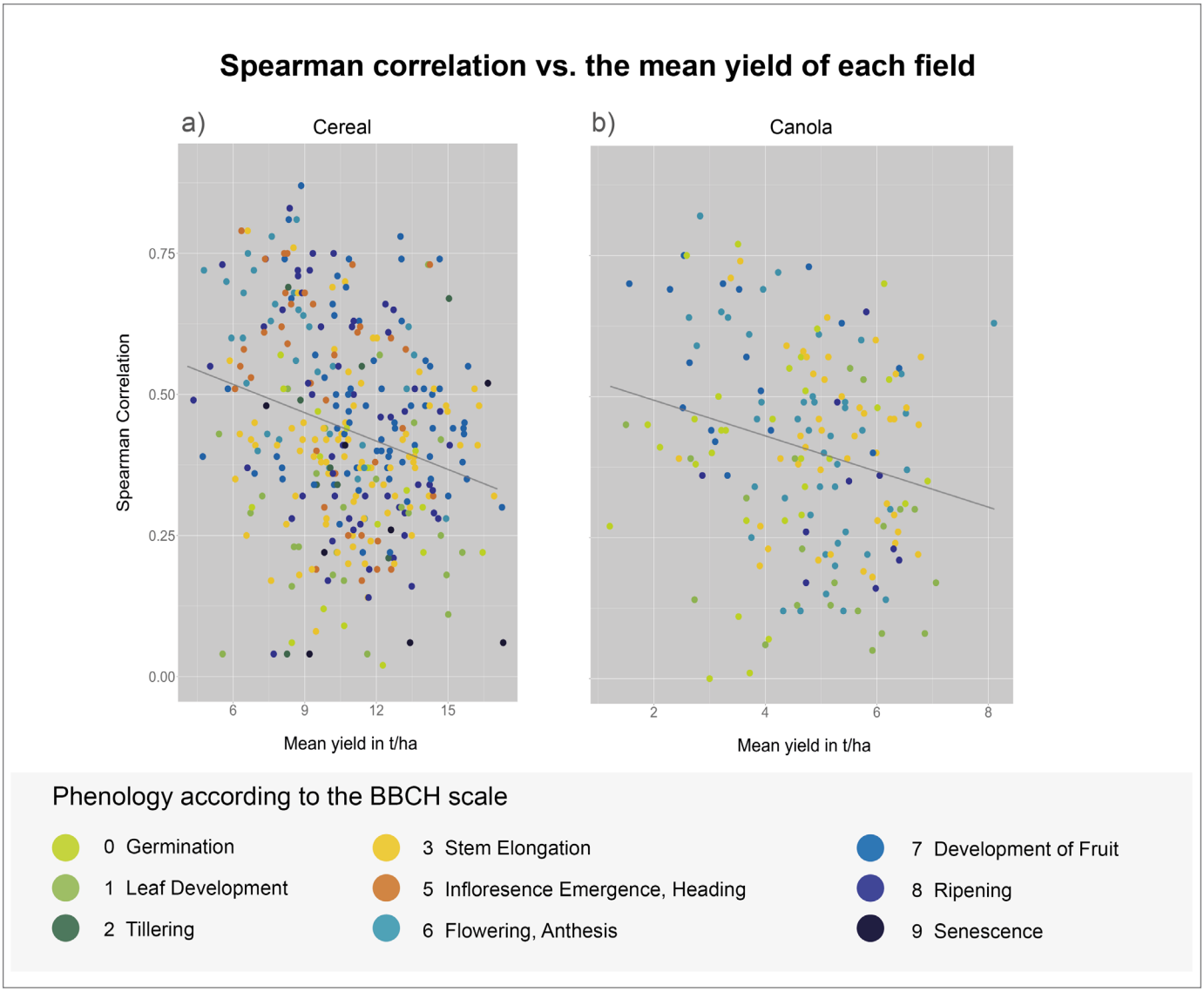

Fig. 4.7 Presentation of spearman (only index NDVI) correlation versus average yield per field to show the influence of high yields on the correlations. For cereal (a) and for canola (b).

High temperatures in this phase can significantly reduce the grain yield (Evans and Fisher 1999). Soil moisture modelling from 2016 and 2018 shows a rapid and steady drop in values already at the beginning of the phenological phase of wheat. In all relevant phenological phases, less and less water was available, which led to poorer yields (*Figure 4.8*). The precipitation and temperature data support this (*Fig. 4.8*). In 2017, on the other hand, precipitation was significantly increased and thus soil water and yields also increased.

If, therefore, the availability of water in the soil falls steadily from the beginning of the growing season - as in 2016 - or from an early phenological phase on - as in 2018 - this is an indication of poorer yields than in other years. This in turn is an indication of the greater reliability of satellite data in predicting yield estimates, at least in this study area. The same applies to the evaluation of data from previous years. The indicators on how reliable remote sensing prediction of yield is, can be drawn from yield data itself and from the presented meteorological data.

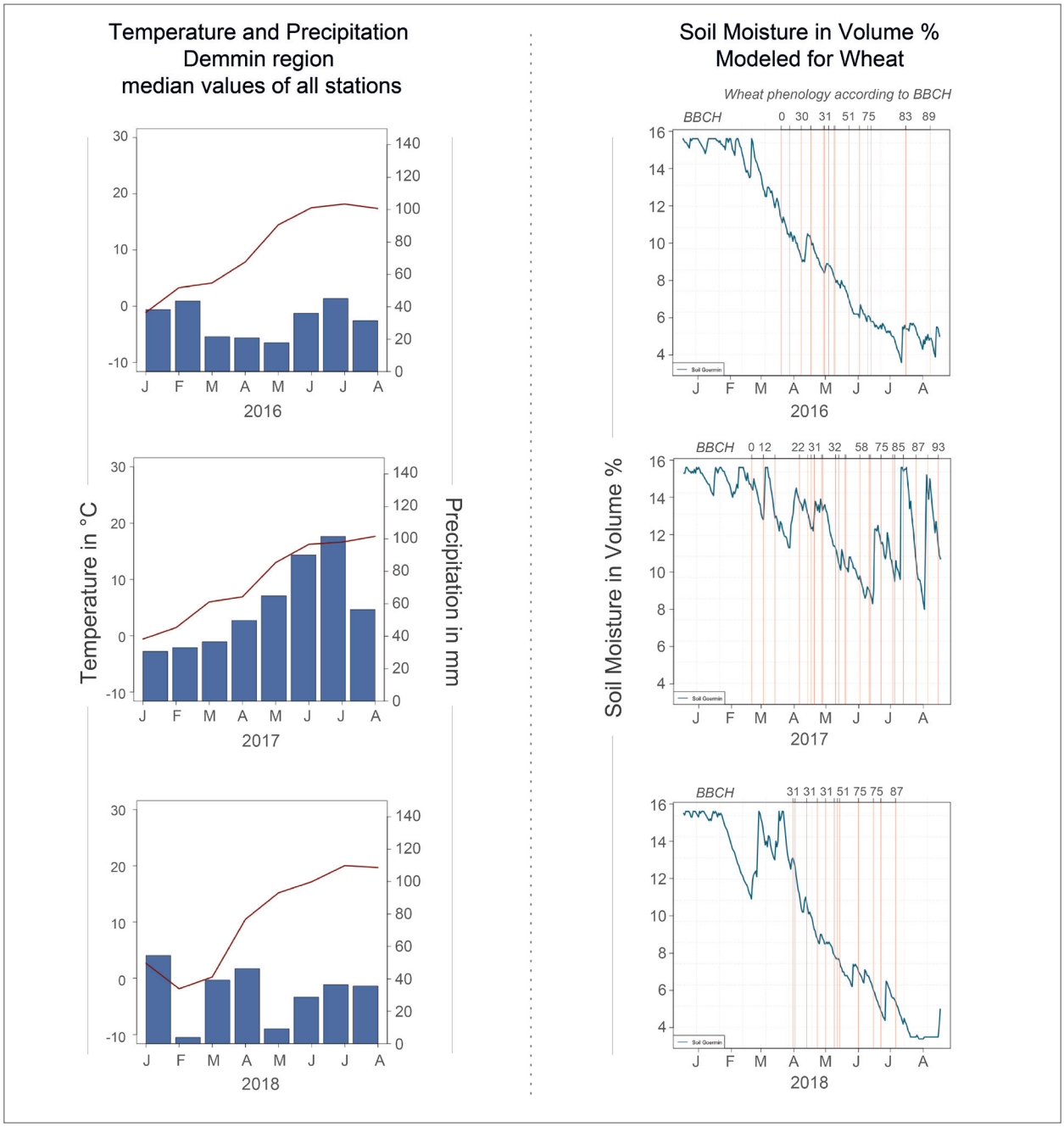

Fig. 4.8 Left column: Weather data from the Demmin area weather stations. Right column: Modeled soil moisture for Wheat in the area around farm 1 (blue line) and BBCH stages of wheat (red lines).

4.5.1.5 Visible homogeneity on satellite images and histogram

The overall result shows a large variation in correlations. With the ideal combination of satellite image at the right phenological time with the right sensor, high correlations are still not guaranteed. This is because it is possible that there are simply no patterns in a field and the crop is homogeneous (*Fig. 4.9 a*). Whether a field is too homogeneous to model yield can often be seen visually in the satellite image or by the histogram of vegetation index values of the entire field. If the spread is particularly small, especially in comparison to a field that is visually very heterogeneous (*Fig. 4.9 b*) or whose soil map shows strong differences (*Fig. 4.9 d*), homogeneity is indicated. The impact of this homogeneity can be assumed by the distinguished levels of median Spearman correlations in *Figure 4.9 g)*.

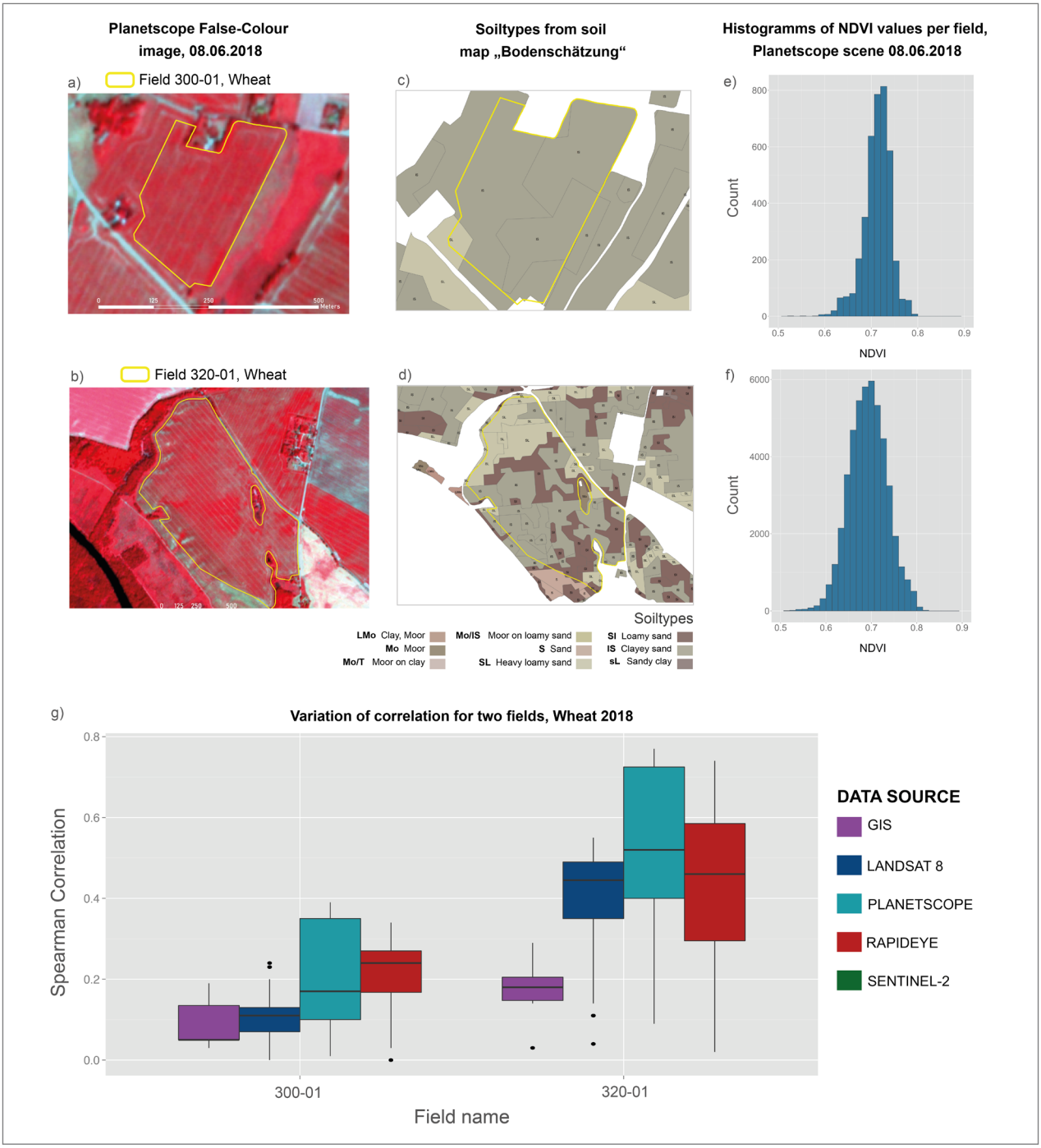

Fig. 4.9 Comparison of two fields 300-01(a,c,e) and 320-01 (b, d, f), belonging to farm 1. a) and b) False color image Planetscope, band combination NIR-Red-Green from 08.06.2018, wheat. c) and d) Soil types of the soil map. e) and f) Histograms of the NDVI values of the fields at the time of recording with different spread.) The variation of correlation values per field and data source, showing a clear difference between fields (g).

4.5.1.6 Factor II: Dependence on sensor resolutions, spatial and spectral

Spatial resolution

For these data in this study area, it can be observed that the spatial resolution of the different satellite sensors has different effects on the correlation strength. In the years in which the median correlations

are very high (e.g. 2018), the high-resolution sensors (Rapideye, Planetscope) perform much better than the poorly resolved sensors (Landsat series) and better than the 10m-resolved Sentinel-2 sensor (*Figure 4.10 b*). In years in which the correlation is poor and the yields very high (e.g. 2017), these differences are no longer as pronounced and the differences between the sensors almost disappears (*Figure 4.10 a*). Nevertheless, the better-resolved sensors perform generally a little better.
(e.g. 2017), these differences are no longer as pronounced and the differences between the sensors almost disappears (*Fig. 4.10 a*). Nevertheless, the better-resolved sensors perform generally a little better.

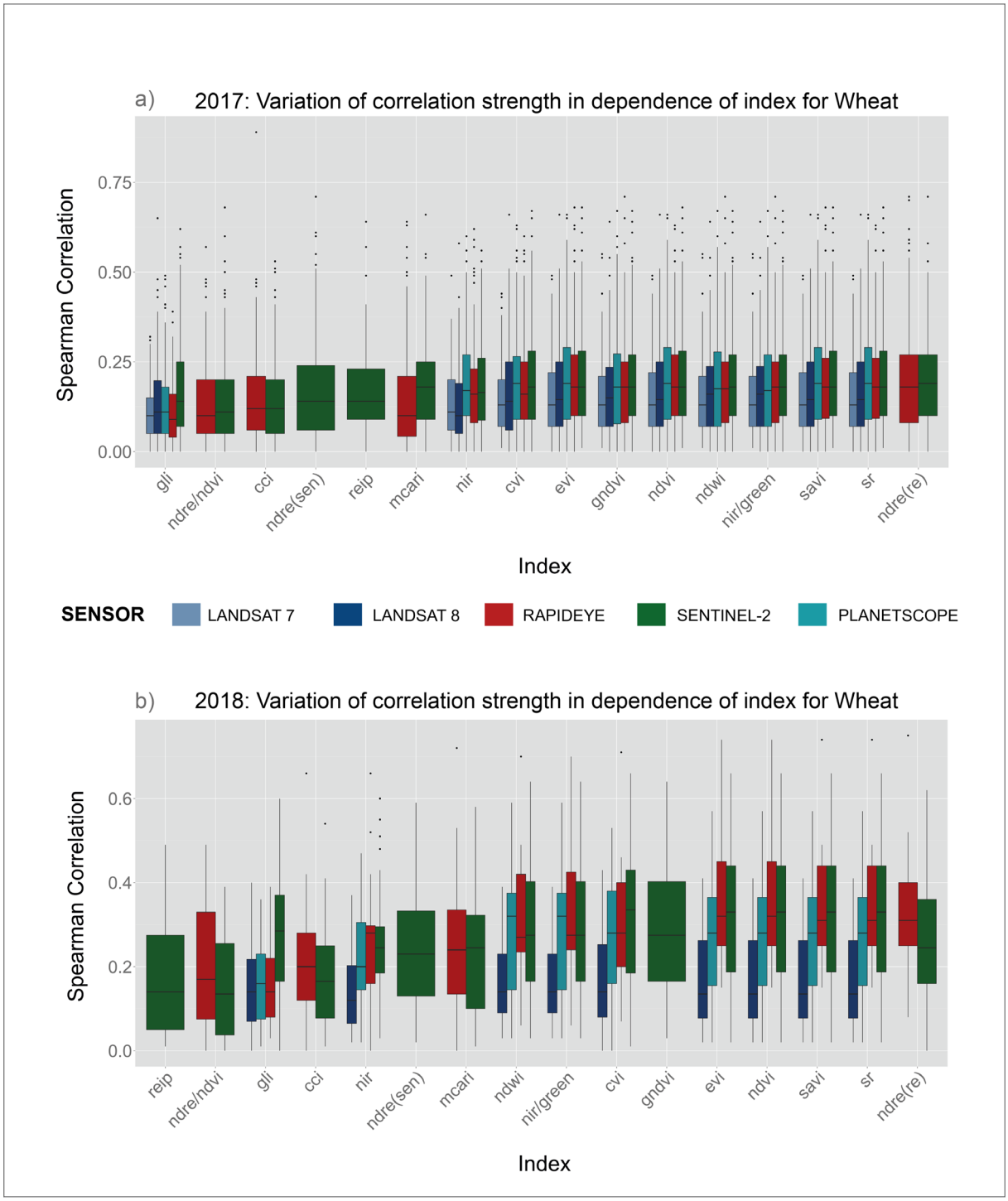

Fig. 4.10 Correlation per calculated index for Wheat in 2017 (a) and 2018 (b) and color-distinguished by remote sensing sensor.

It has to be considered, however, that the point yield data were directly compared with the pixel data of the satellite data in the analysis. The raster of the Landsat sensors therefore includes several yield points into one 30m pixel, whereby the same vegetation index is collected for each yield point. If the variance of the yield data in small areas is very high, this effect can lead to uncertainty. Averaging the yield values per grid cell would be possible but would also lead to data loss.
However, it cannot be ruled out that the differences in the performance of these sensors are also due to the different positions of the respective spectral bands (*Fig. 4.20, Chapter Appendix*)

Spectral resolution

As far as the yield parameter is concerned, vegetation indices from the red and NIR bands achieve the highest correlation in numerous cases (*Fig. 4.10 - 4.11*). Therefore, spectral resolution is not necessarily the decisive factor, if the red band and the NIR band are covered by the sensor. But this is only true if phenology is not taken into account. If the correlations are analyzed in a more differentiated way, as is done in the crop specific observations, indices with calculation of the red-edge channel at certain phenological points in time present themselves as more advantageous. Furthermore, if the nitrogen content or the pure biomass or leaf chlorophyll content is modelled, indices working with Red-Edge channels show very good results (Barmeier, Hofer and Schmidhalter 2017; Cui et al. 2019). This study cannot replicate this for the yield parameter generally, but for certain phenological stages.

The general suitability of a sensor depends additionally on the temporal resolution. The more often an image is available, the higher is the probability to meet the „appropriate“ phenological phases and to make a yield statement with low uncertainty.

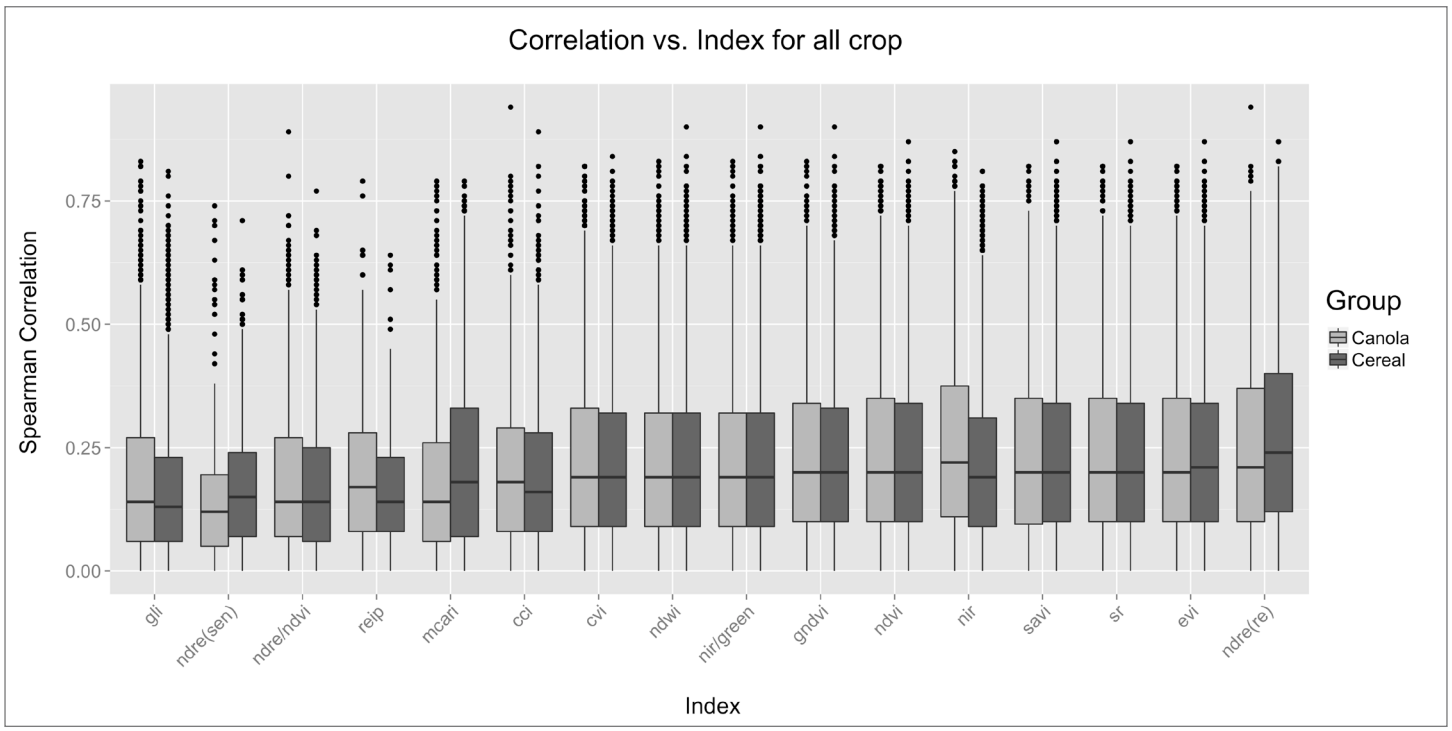

Fig. 4.11 Spearman correlations for all crop types in all years versus the vegetation index of remote sensing data, distinction between cereals and canola.

4.5.1.7 Factor III: Dependence on calculated vegetation index

Even if the correct index was selected for the correct BBCH stage, the correlation is not the same for every field. Here again the degree of heterogeneity of the crop is decisive. If, however, a field shows clear crop and therefore most likely yield patterns, then there is rarely a single best index, but several, with the same band combination. Some indices, especially the NDVI, tend to saturate at a certain LAI and are no longer sensitive in the high-density range. For cereals, the NDRE, which includes the Red-Edge channel, has the best performance, according to *Figure 4.11*. If compared to the REIP, which can be calculated with the Sentinel-2 bands and which is also used by online fertilization sensors in precision agriculture, the REIP underlies the NDRE by far in this study – concerning the correlation with yield.

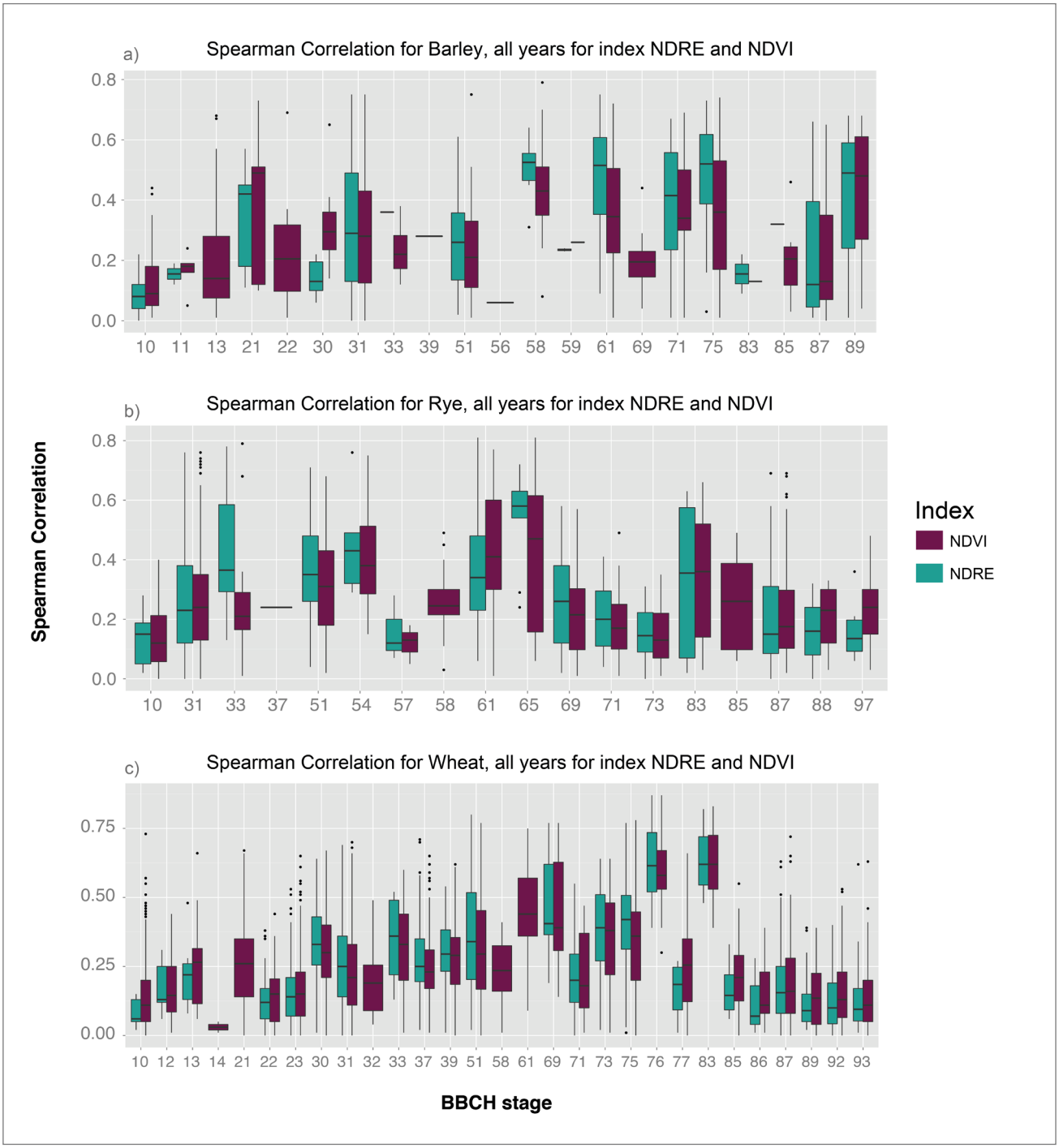

Fig. 4.12 Spearman correlation per BBCH stage for all cereal types, color-distinguished by NDVI and NDRE indices.

Performance of NDVI and red edge index NDRE for cereal

In the literature and in practice the NDVI already has a very high standing. However, if one compares the correlations between NDVI and yield and sets this against the correlations when using the NDRE, which includes the red edge band, the NDVI in this study predominantly performs less well for cereal (*Fig. 4.12*). However, the strength of the correlation depends on the cereal type and the respective BBCH stage and there are certainly times when the NDVI performs better. In the early BBCH stages of barley (11, 21) the NDVI performs better than the NDRE (*Fig. 4.12 a*). From BBCH 51 the image changes and the NDRE performs far better than the NDVI. Towards the end of the vegetation phase, the two indices are equal. This strong contrast is probably due to the structure of the barley spikes, which form long awns during the vegetation period. The spikes of barley lie down with increasing weight, so that the surface of a barley field has a completely different structure than, for example, a wheat field. Depending on the phenology, this structural difference can be easily detected with radar satellite data (Harfenmeister, Spengler and Weltzien 2019).

In the case of rye (*Fig. 4.12 b*), the NDRE almost always performs better than the NDVI, except in BBCH stage 61 and at the end of the vegetation phase.

Looking at the correlations in wheat, the NDVI performed better than the NDRE at the beginning of the vegetation phase and at the end. In the phenological phases in between, NDRE performs better, but the differences between NDVI and NDRE are not as strong as for rye and barley.

It can therefore be concluded that the correlation strength in the data available is influenced by multiple factors, which do not have the same effect on each other in every constellation. As shown in *Figure 4.4 - 4.5*, the phenological stage of the crop during which a satellite image is taken is a very important factor, whereas many indices perform equally well or similarly, if the optimal BBCH stages are met.

4.5.1.8 Factor IV: Phenological stage of crop

For all types of crops applies: not every phenological phase is suitable for yield prognosis. The phases in which no significant growth has taken place, in which the crop is fully dense or completely ripened, are not suitable (*Fig. 4.3 - 4.5, 4.12*). For remote sensing sensors to provide meaningful values, the crop must be present but not too homogeneous in appearance, specifically in spectral characteristics. In the context of this study, certain phenological phases for yield prediction have proven to be favorable for specific crop species (*Table 4.3*), which also coincides with existing literature (Marti et al. 2007; Knoblauch et al. 2017). A detailed discussion on the topic of phenology, which is crop group dependent, will follow in the results and discussion on crop specific observation – IV a) and IV b) .

Despite the reliable data basis of the phenological data, no weekly recordings of the BBCH stages were available for this study, neither cloud-free satellite images in this frequency. Therefore, this study presents the best correlations at the times and with the data available for this purpose and does not claim to be exhaustive.

Cereal

The cereal types wheat, rye and barley are basically very well suited for yield prediction, so the above factors of homogeneity and BBCH stage are given in the selection of satellite images and their acquisition date. This study identifies the best growing stages of cereal for the determination of final yield at the beginning of flowering, during the development of the fruit and at the very beginning of the ripening phase. Still, also good correlations were achieved during stem elongation and beginning of heading (*Fig. 4.13*).

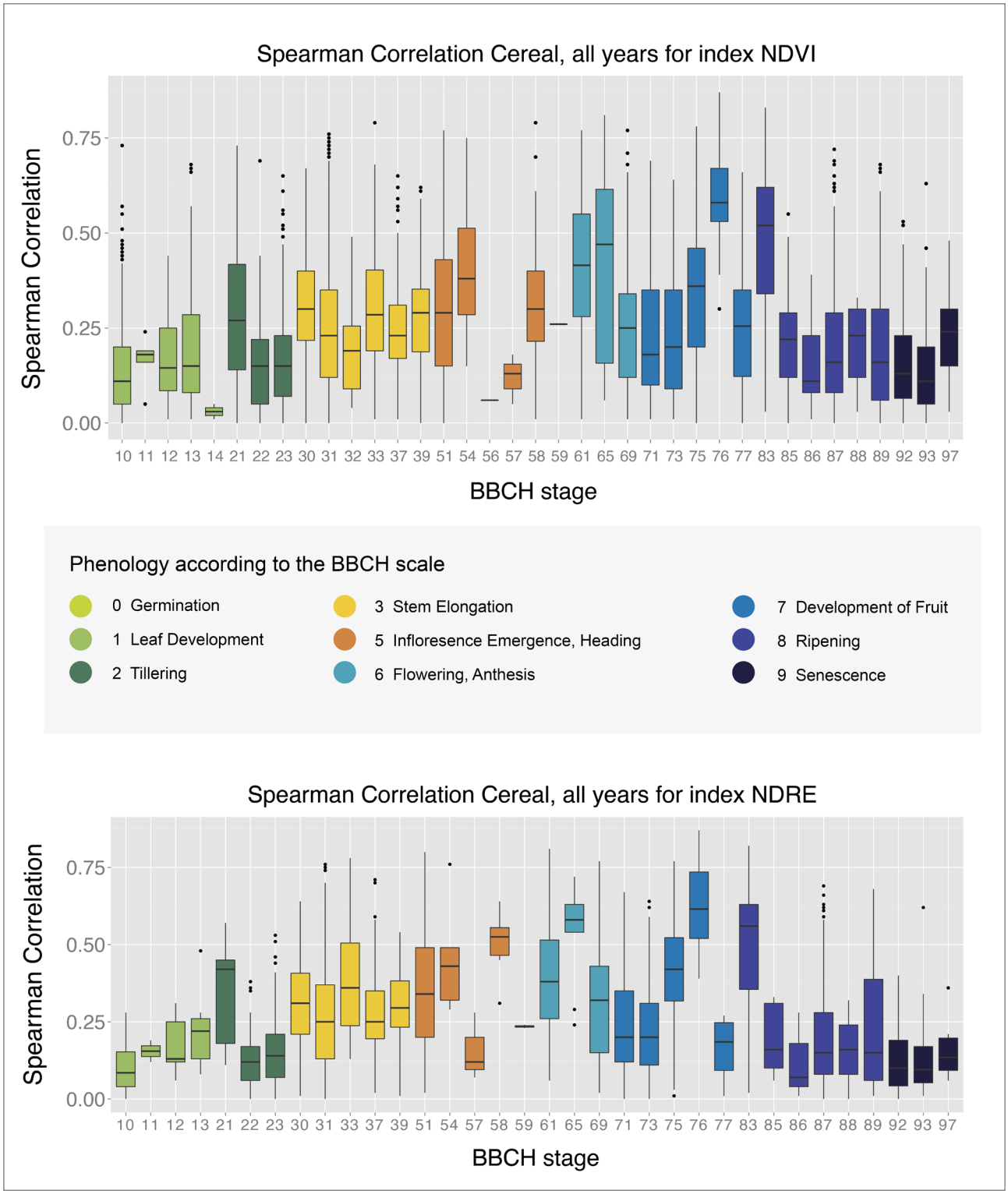

Fig. 4.13 Spearman correlations per phenological phases according to BBCH scale, wheat, all years, Index: NDVI and NDRE.

The grain yield cannot be measured directly with remote sensing. But the grain yield is closely related to the vegetative components of the cereal plant. The yield itself is produced during the grain filling phase. But the photosynthetically active plant parts such as stem, leaves and roots form the synthetic capacity to enrich the grains. It therefore makes sense that the correlation between vegetation index and final yield in the early stages of the grain filling phase shows a very high correlation (*Fig. 4.13*), as already discussed by Shanahan et al. 2001 and Marti et al. 2007.

The distribution of the relative biomass, which can be indicated by vegetation indices, can also be recorded before the ripening phase, which is why correlations between satellite image and yield are already present during tillering and more so stem elongation (*Fig. 4.13*). However, the uncertainty of a yield prediction depends on the further development of the plant under the given weather conditions and the management.

The comparison of *Figure 4.13 a* and *Figure 4.13 b* shows here also, that the NDRE performs better than or NDVI when the three cereals are taken together. Nevertheless, the NDVI correlations are also acceptably high in similar phenological phases (except 58 and 65).

Canola

The results concerning canola are much less straight forward than for cereals. The correlation analysis showed results with high uncertainty for canola. Among the fields of Farm 2 there were high correlation values (max r = 0.94, median r = 0.15) between vegetation indices and canola yield, but on Farm 1 the maximum correlations were much lower (max r = 0.71, median r = 0.16).

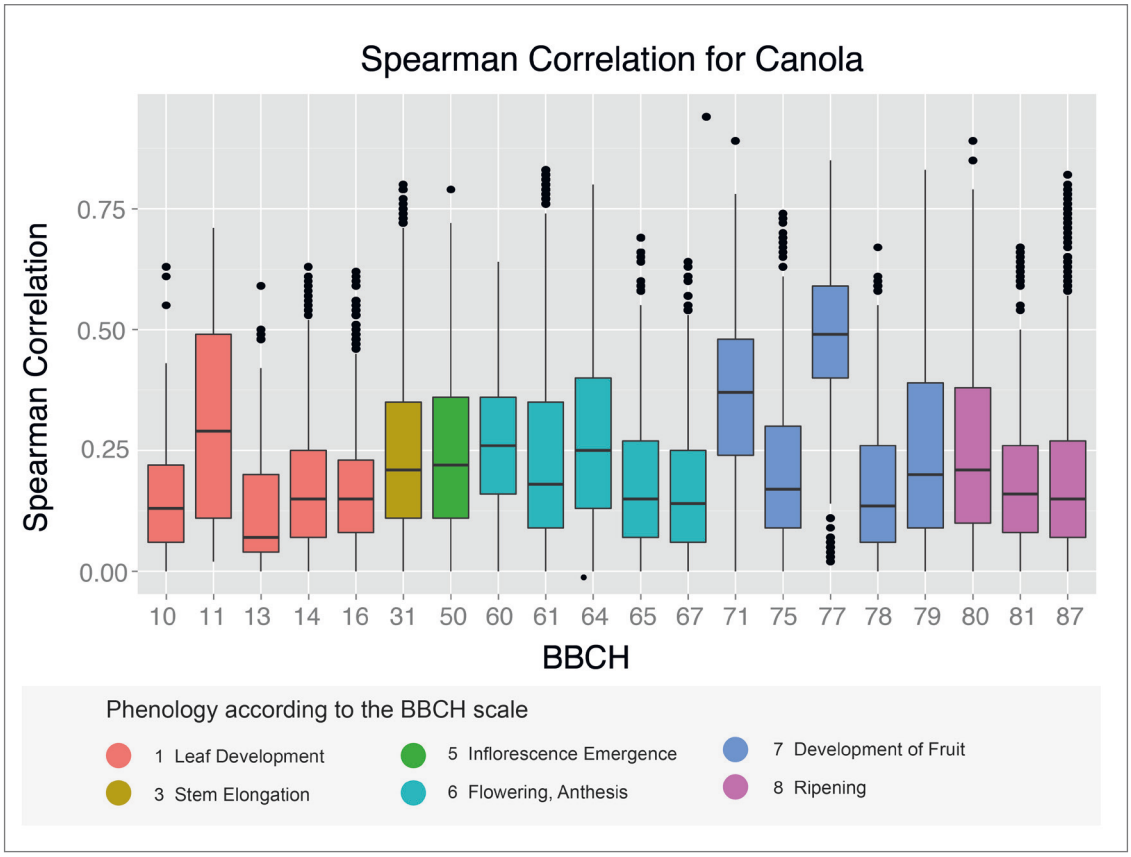

Fig. 4.14 Spearman correlations per phenological phases according to BBCH scale, canola, all years

A yield prognosis for canola is much more difficult than for cereals or maize, since the vegetative parts of the plant are less significant in the formation of the grain yield (Sulik and Long 2016). It is assumed that the number of flowers is a suitable proxy, but due to their spectral characteristics they are less sensitive to indices involving the red and infrared channels (Sulik and Long 2016). An important temporal finding is that the relationship between NDVI and yield decreases with flowering (Piekarczyk,Sulewska and Szymańska 2011). Holzapfel et al. 2009 found that the NDVI data obtained between the six-leaf stage (BBCH 16) and the beginning of flowering (BBCH 60) are correlated with the canola harvest. In this study the highest correlations were also more or less obtained in these stages, at BBCH 31 and BBCH 61 (*Fig. 4.14*). Even higher correlations were achieved at BBCH 71 and 77 during fruit development.

The „classic" vegetation indices are therefore less suitable for yield estimation or are associated with great uncertainty. Remote sensing indices such as NDVI record vegetative growth, for crops such as canola there is interest in the seed that belongs to reproductive growth. Indices such as NDVI are very useful in the analysis of crops such as wheat and maize that have inconspicuous flowers and simply „green-up" and then „green-down" after entering the reproductive growth phases. Numerous Brassica oilseeds have „green-up", then „yellow-up" with striking yellow flowers and an overlap of „yellow-down" and „green-down" during ripening (Sulik and Long 2016).

For those reasons and the lack of a clear – farm-independent – pattern in this analysis, the authors do not feel confident to make similar recommendations for the choice of the „right" satellite images, as in the case of cereals. The fact that there are far fewer studies on the correlation of spatial data to canola yield, compared to cereals, indicates caution in the interpretation of the results of the canola yield analysis and suggests further studies

Interestingly, if correlations between NDVI and NIR with yield data are analysed, the reflection in the NIR band correlates much better for BBCH stage 61 and later (*Fig. 4.15*). Whereas before that, the NDVI yields better results.

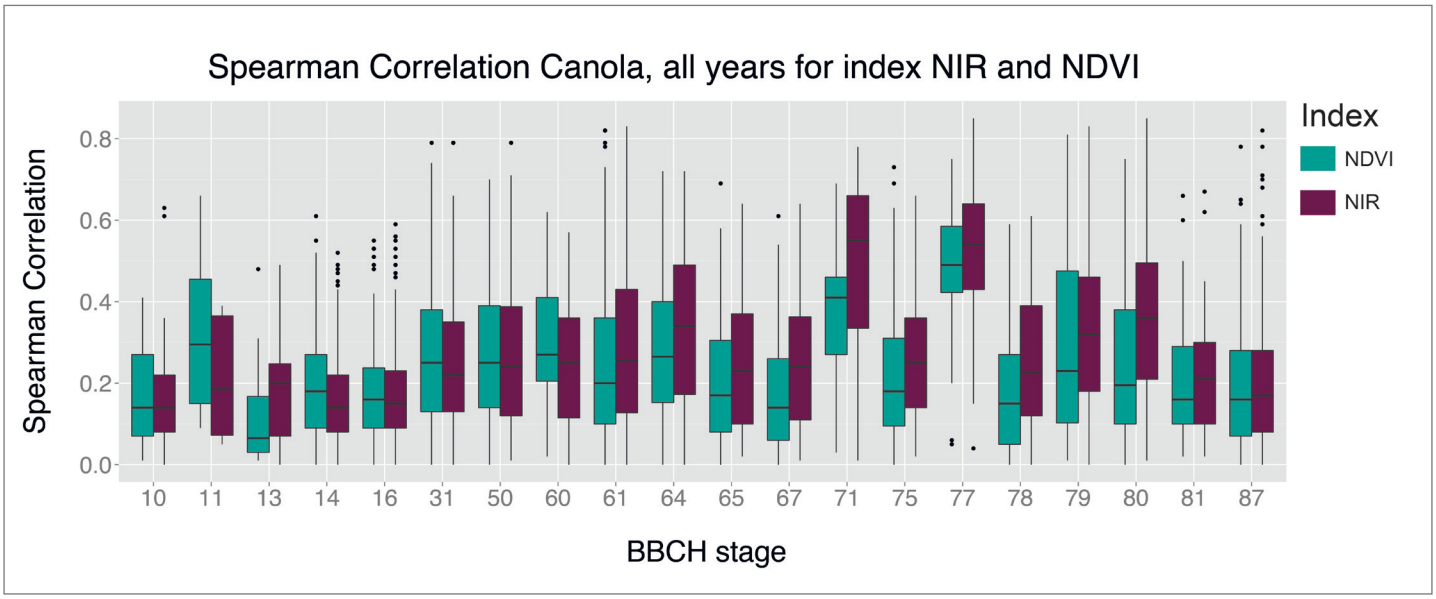

Fig. 4.15 Spearman correlation for canola from all years and by BBCH stage. Color distinction by NIR and NDVI index.

4.5.1.9 Relevance of environmental GIS data

The relevance of GIS data for yield modelling is considered negligible in this study. In most cases, the correlation values between GIS data set and yield are very low (mean r = 0.12, median r = 0.09, max r = 0.9). The performance of geodata and satellite data (*Fig. 4.16*) can be clearly distinguished. When analyzing the correlations for each crop individually, the inferior performance is also abundant (*Fig. 4.23 - 4.26, Chapter Appendix*). In the years in which the overall correlations are poor, this difference is also less pronounced.

The best performance is achieved by those „GIS" data that are a product of satellite data in this study, such as the map of the organic matter (mean r = 0.16, median r = 0.15, max r = 0.71). It cannot be denied that the crop growth system is very complex, and that soil and relief certainly influence the yield. Therefore, it makes sense to use these data in addition to the satellite images for an extended yield prognosis, possibly with a lower weighting, as they usually do not show the actual condition of the crop.

The fields in this study are mostly located in regions with flat topography and rather fertile soil compared with other regions. Furthermore, Farm 1 has been operating precision agriculture for more than a decade, aiming to homogenize the fields despite the heterogeneous inventory. These factors can also be reasons for the underperformance of environmental GIS data in this study.

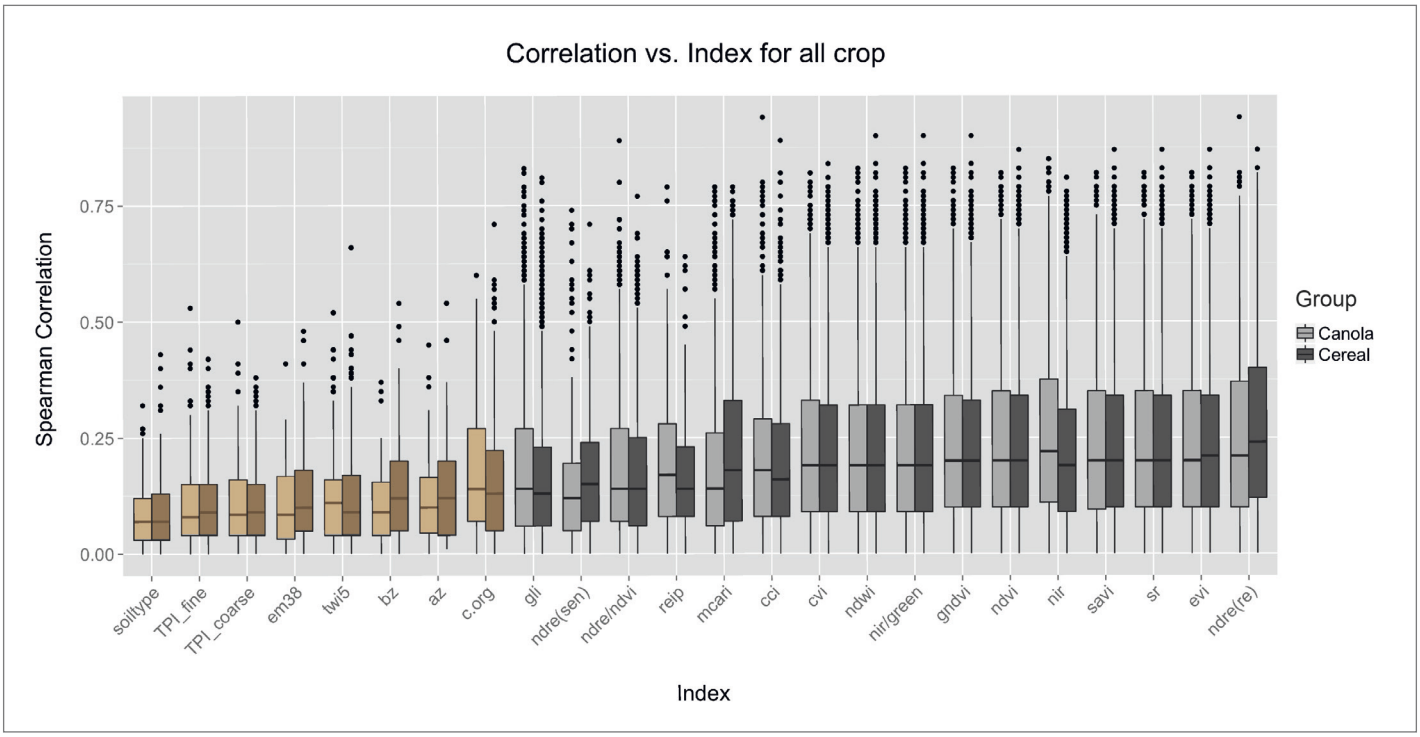

Fig. 4.16 Spearman correlations for all crop types in all years versus the vegetation index of remote sensing data and environmental GIS data, distinction between cereals and canola.

The comparison between the point yield data and often polygon-based geodata, which are thus much more coarsely resolved, is probably unfavorable as an analytical approach. It would be more advantageous to calculate an average yield per polygon and calculate the correlation. However, results from earlier studies (Vallentin et al. 2019) allow the conclusion that the satellite data are much more meaningful for the yield prognosis in the fields investigated here.

4.5.2 Experiment B and C: Correlation calculation of the mean satellite grid values and mean yield values per field and year (B) and correlation calculation of all satellite grid values and all yield point values per year and per crop, independent of the fields (C).

A field-internal yield estimate is not always required and mean values for a field or regional trend are sufficient. The results discussed so far are based on the correlations calculated A) per field. For a regional view one can also evaluate the correlation of B) the mean values of each individual field and C) the correlation of all extracted yield and reference data per crop and year, independent of the fields. The performance of these three methods is very different.

Method B) stands out particularly due to its high correlations (*Fig. 4.17*). If only the mean values formed per field are considered, a better yield modelling can be achieved. However, then no field-internal patterns are analyzed and there is uncertainty - depending on the size of the region - that the crops under consideration are not in the same phenological stage, which makes the selection of satellite images difficult. Nonetheless, a monotonous relationship can be observed when comparing the mean yield values with the mean NDRE values, for example for cereal in BBCH stage 76 (*Fig. 4.18*). Methods A) and C) perform similar, with C) usually performing a little better. Here, the pure mass of yield data compared with satellite data could compensate for individual noise within the fields. From these observations follows the hypothesis that yield modelling should not be carried out on a point or pixel basis, but on a partial field basis. Remote sensing yield modelling could be very promising per field zone, which is also in line with most PA methods.

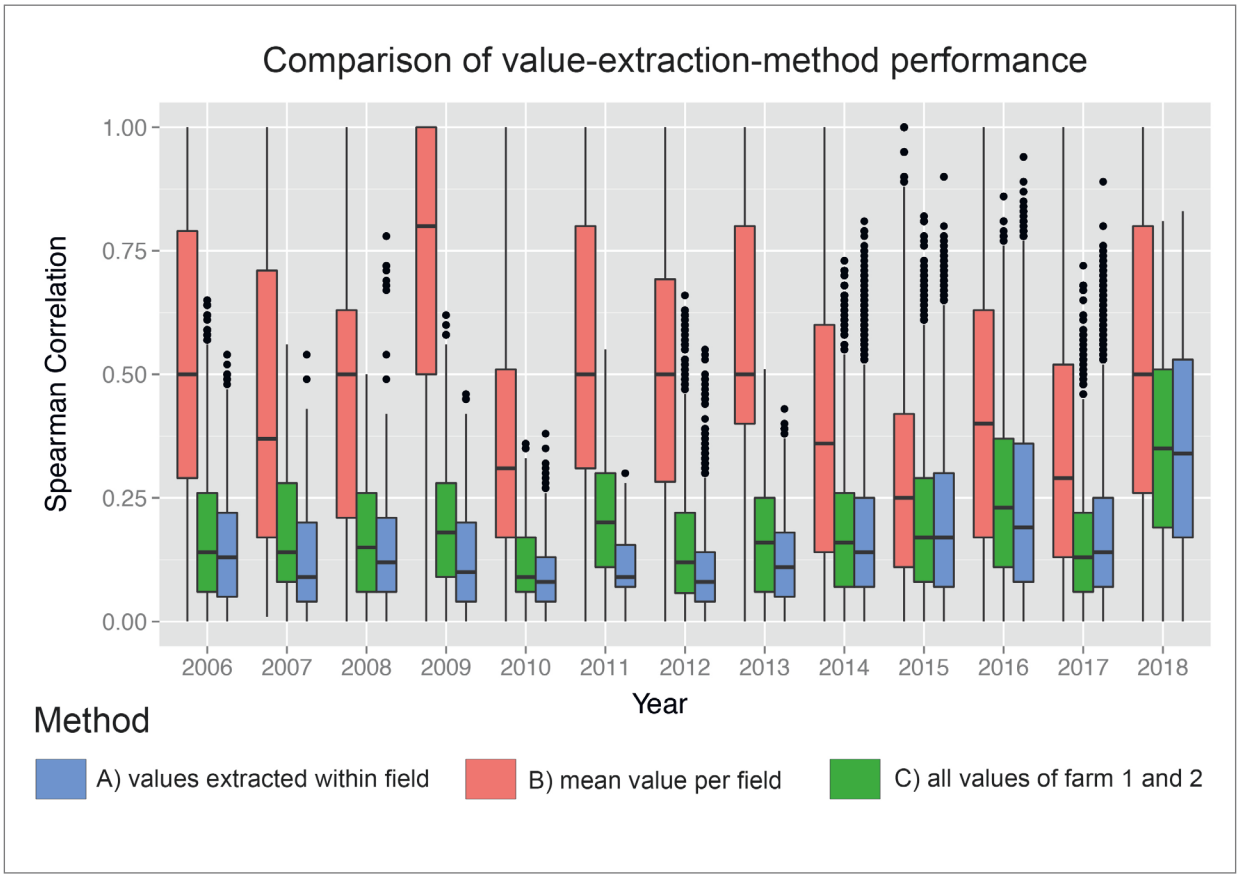

Fig. 4.17 Comparison of extraction methods as a basis for correlation analysis. A) extraction of yield and data values per field; B) extraction of mean values of each individual field; C) extraction of yield and data values for all points per fruit and year, independent of the fields.

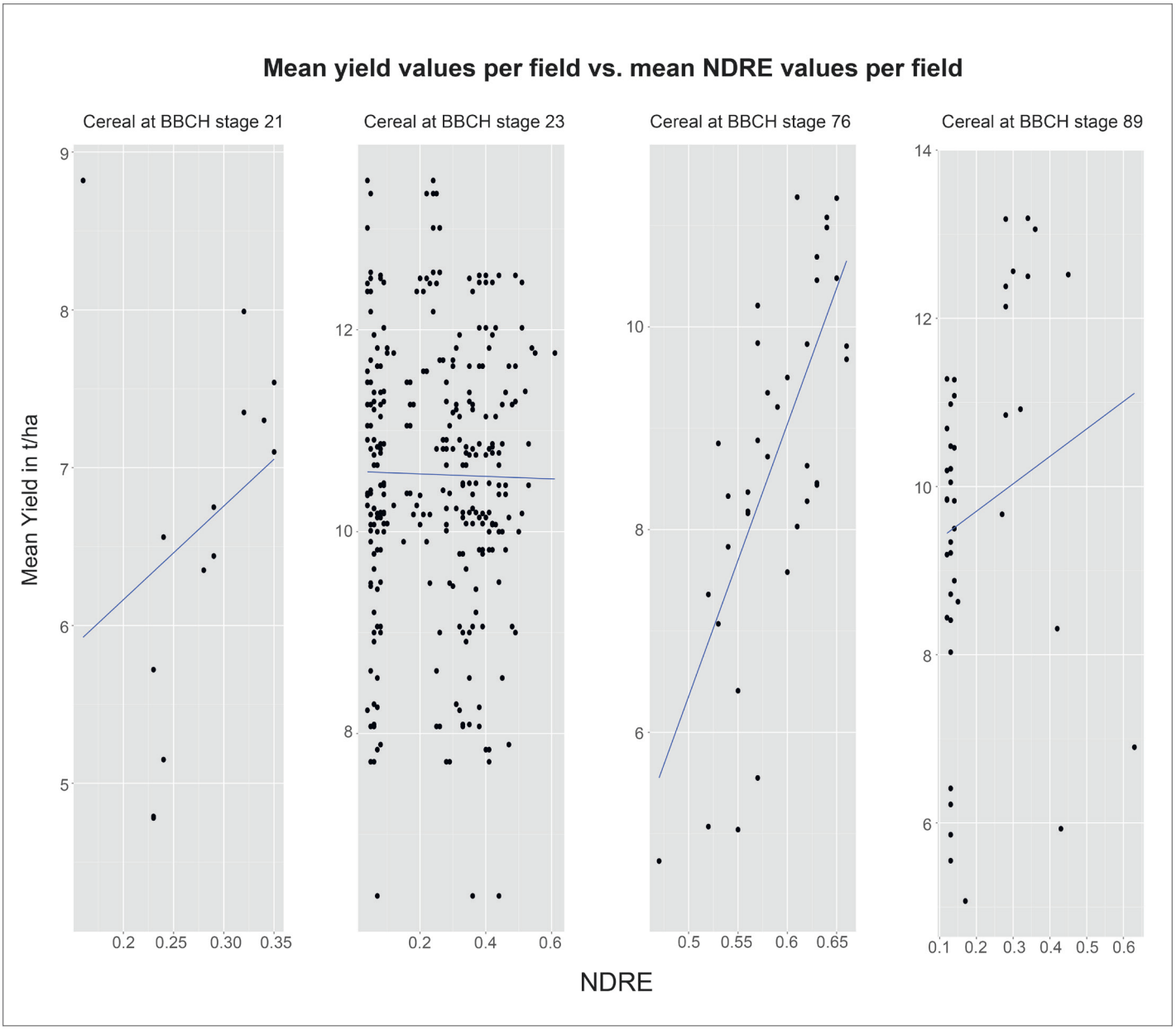

Fig. 4.18 Dependence of mean yield per field on mean NDRE per field for Cereal in phenological BBCH phases 21, 23 (tillering), 76 (medium milk / development of fruit), 89 (fully ripe).

4.6 Conclusions and Outlook

This study has shown that not every satellite image can be used for yield estimation or yield zoning. One must make a careful selection, depending on the type of crop, the phenology of the crop, the resolution of the sensor and the spectral bands considered in the index calculation. It can also be seen that a yield estimate for cereals promises much more success than for canola, which also reflects the distribution of scientific work to date. For the user, it is advisable to evaluate the heterogeneity on the satellite image visually and using the histogram, for example the NDVI values. If no patterns are recognizable and the crop is homogeneous, the uncertainty in the yield estimation is very high.

The data basis of this study is very large, but not complete. If the estimation of yield from satellite data is to be introduced as a standard procedure, a solid data basis for the validation and extension of the results presented here must be collected. Ideally, the exact phenology per field would have to be collected in large and multiple test areas, for example on the basis of remote sensing methods(Chu et al. 2016; Hufkens et al. 2019; Nasrallah et al. 2019). Working in Germany and in countries with similar average field sizes, the use of optical sensors with the spatial and spectral resolution of Sentinel-2, RapidEye and Planetscope satellites is recommended. Furthermore, it would have to be ensured that the yield data were recorded completely correctly and that random samples were taken if necessary. However, this approach is associated with high manpower and cooperation with farmers. When looking at canola in particular, further studies are useful because the correlations are not yet quite clear in the literature. An analysis of the same data in other regions and natural habitats would provide a valuable basis for the use of satellite data in agriculture. Such a correlation analysis should not only be a point-to-point comparison, but also the correlations per management zone of the field or per soil type area in the field.

Concerning the method of correlation analysis, future work should use not only a bivariate analysis, but also a multivariate one. The plant and soil system and the factors influencing yield are complex. For yield modelling, it is useful to combine several relevant remote sensing data sets in order to obtain the best possible result (Vallentin et al. 2019). The investigation of remote sensing data from the radar and hyperspectral range should be used in future analyses as well as UAV data. With increasing knowledge gained from this type of data analysis, yield modelling from satellite data and sustainable management in agriculture can be established. Satellite data will not be able to predict the direct grain yield, but with further research under different aspects in different natural areas and climate zones, the estimates will certainly become better and better.

4.7 Acknowledgements

The authors would like to thank Climate-KIC for project funding (Fellows Programme 13-1.1.1., Task ID ARED0004_2013-1.1-011_P024-09), Edgar Zabel and the cooperating farms for data and support. We thank the German Aerospace Centre (DLR) for providing the data from the RapidEye Science Archive (RESA 617 FKZ) and the weather stations, the DWD for providing the soilwater model METVER and Planet Labs Inc. for providing Planetscope data for student research purposes.

4.8 Author Contributions

Claudia Vallentin, Daniel Spengler and Sibylle Itzerott designed to overall approach. Claudia Vallentin did the the programming and the data analysis, as well as the manuscript. Birgit Kleinschmit and Christoper Conrad contributed to the discussion and general paper review.

4.9 Conflicts of Interest

The authors declare no conflict of interest.

4.10 Chapter 4 Appendix

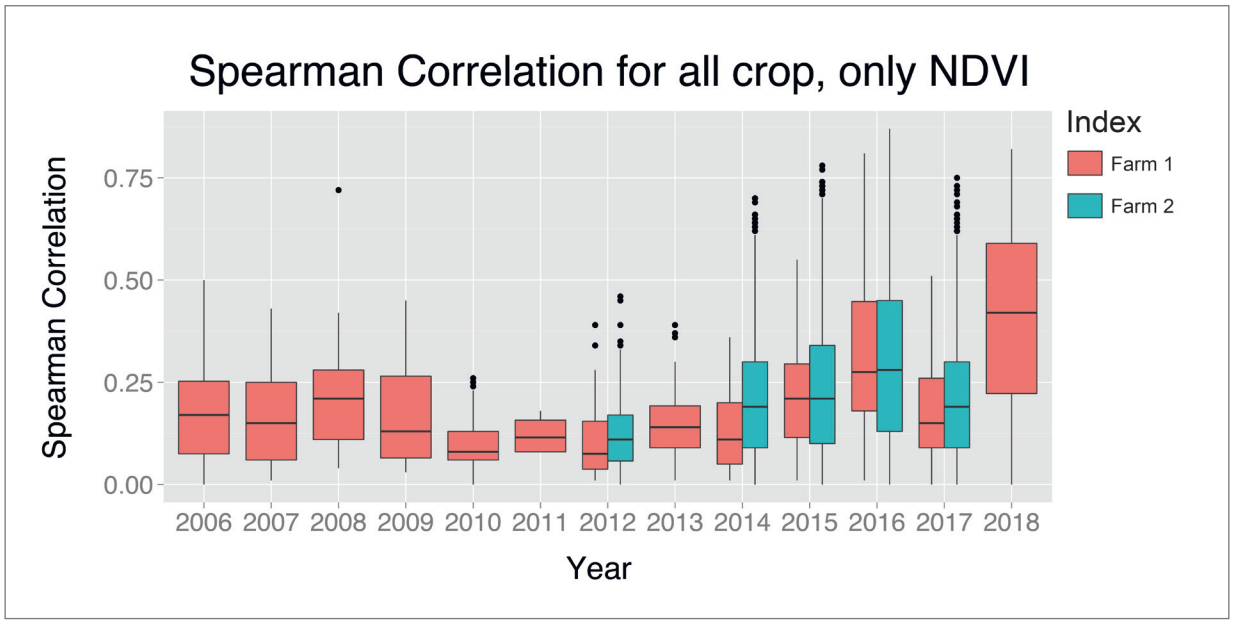

Fig. 4.19 Differentiation of the Spearman Correlations per year between Farm 1 and Farm 2

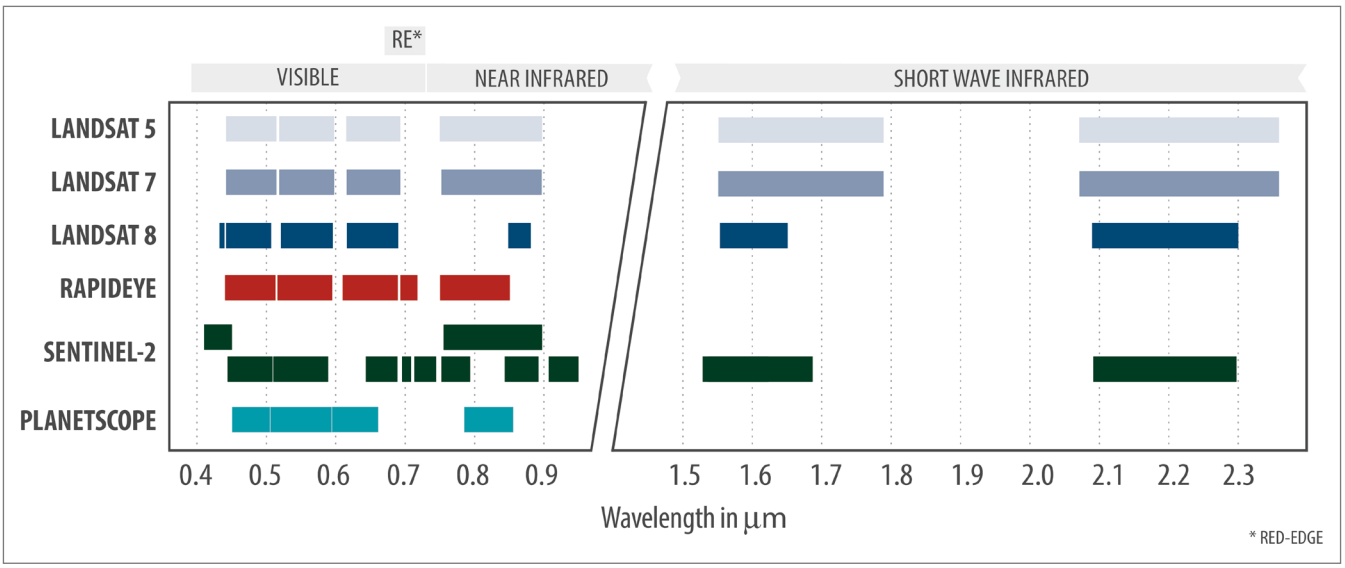

Fig. 4.20 Bands positions of sensors used in this study.

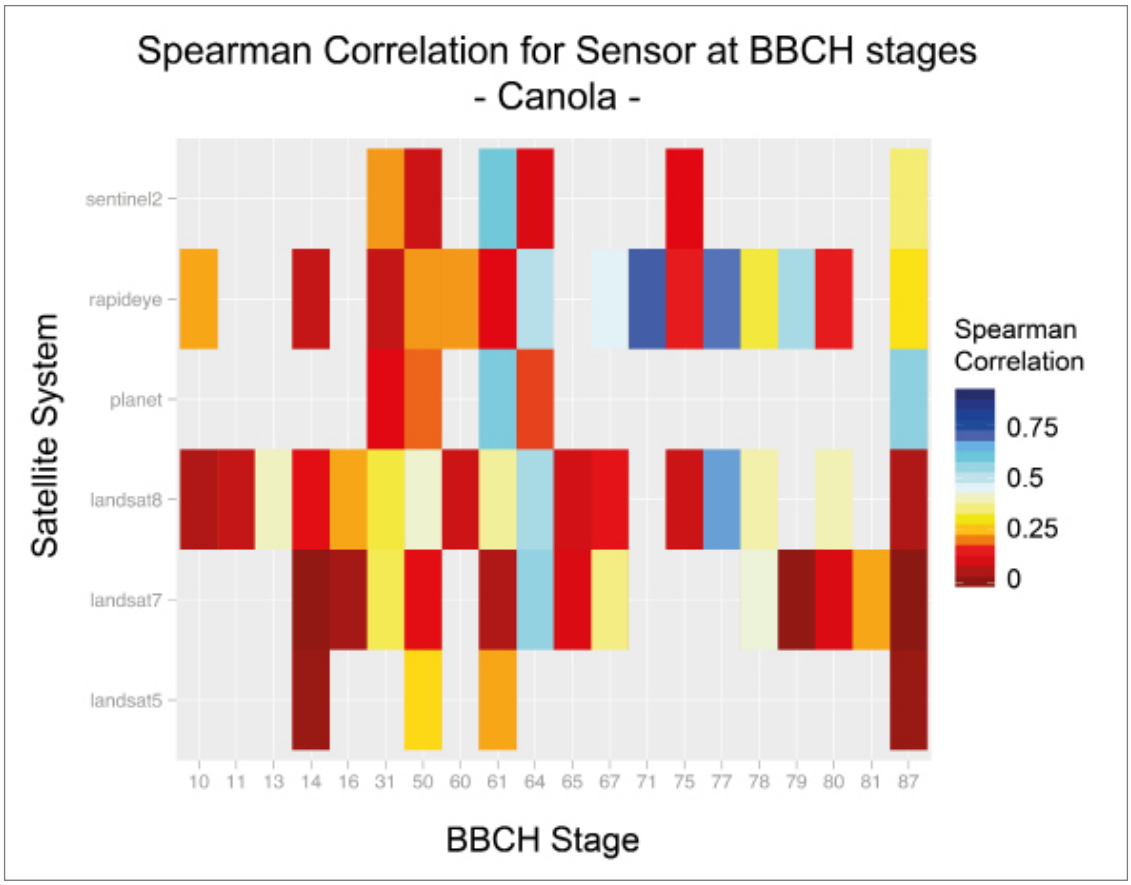

Fig. 4.21 Heatmap of all Spearman correlations, per satellite sensor and BBCH stage for Canola

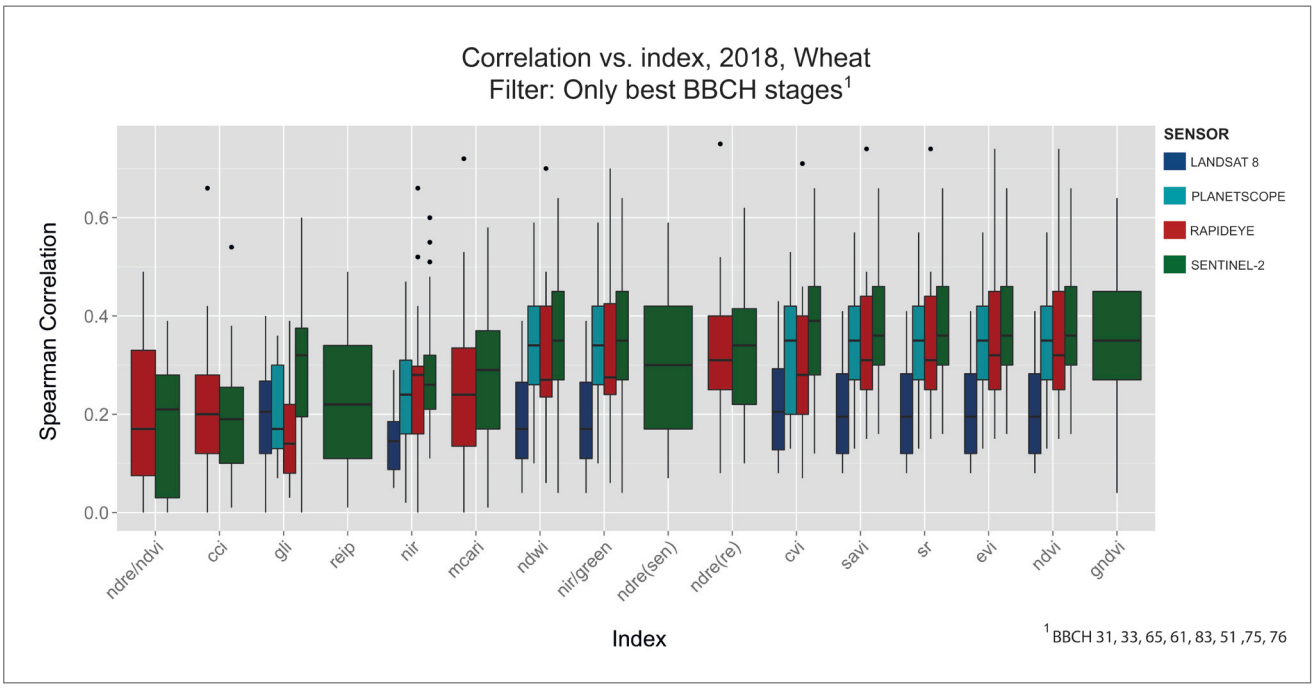

Fig. 4.22 Correlation by index in 2018 for wheat. Only the most suitable BBCH stages were selected. Color distinction by satellite sensor.

Additional figures for rye

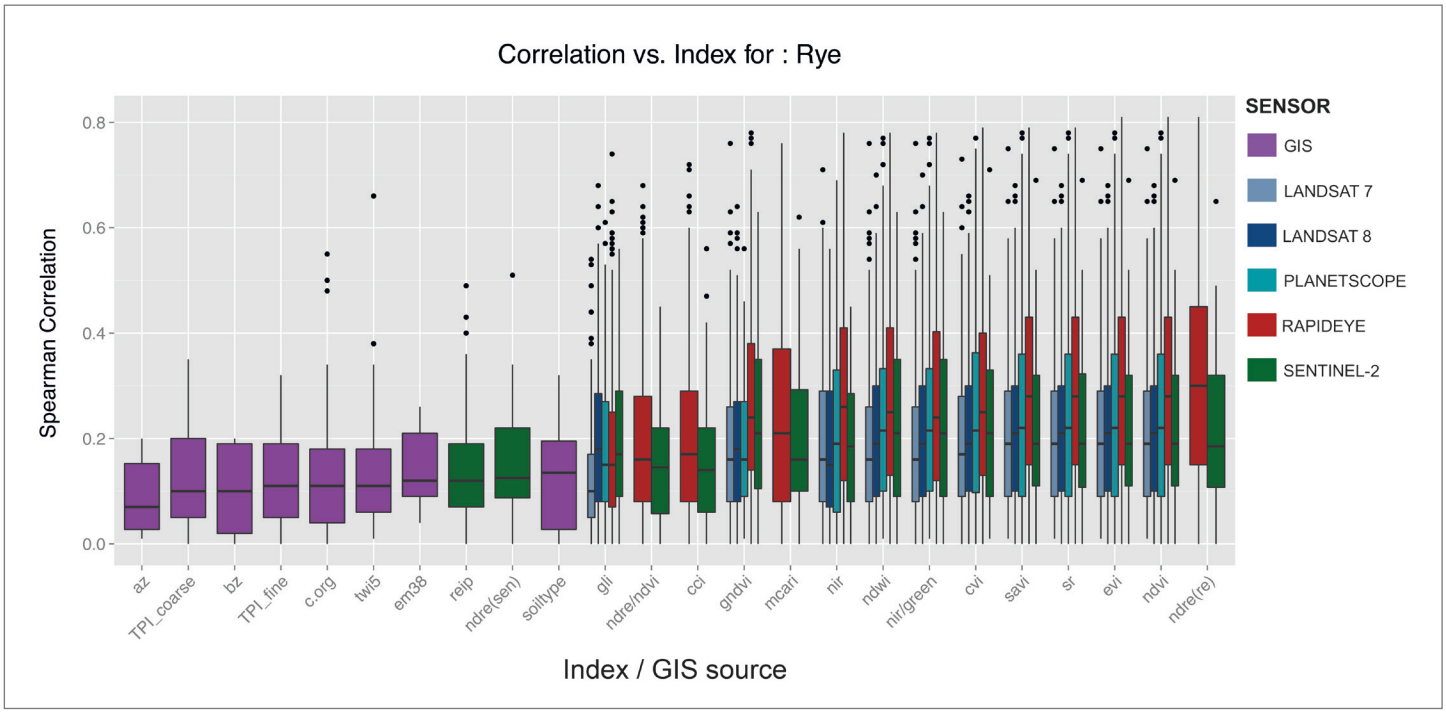

Fig. 4.23 Spearman correlation per index for rye, all years and all fields

Additional figures for wheat

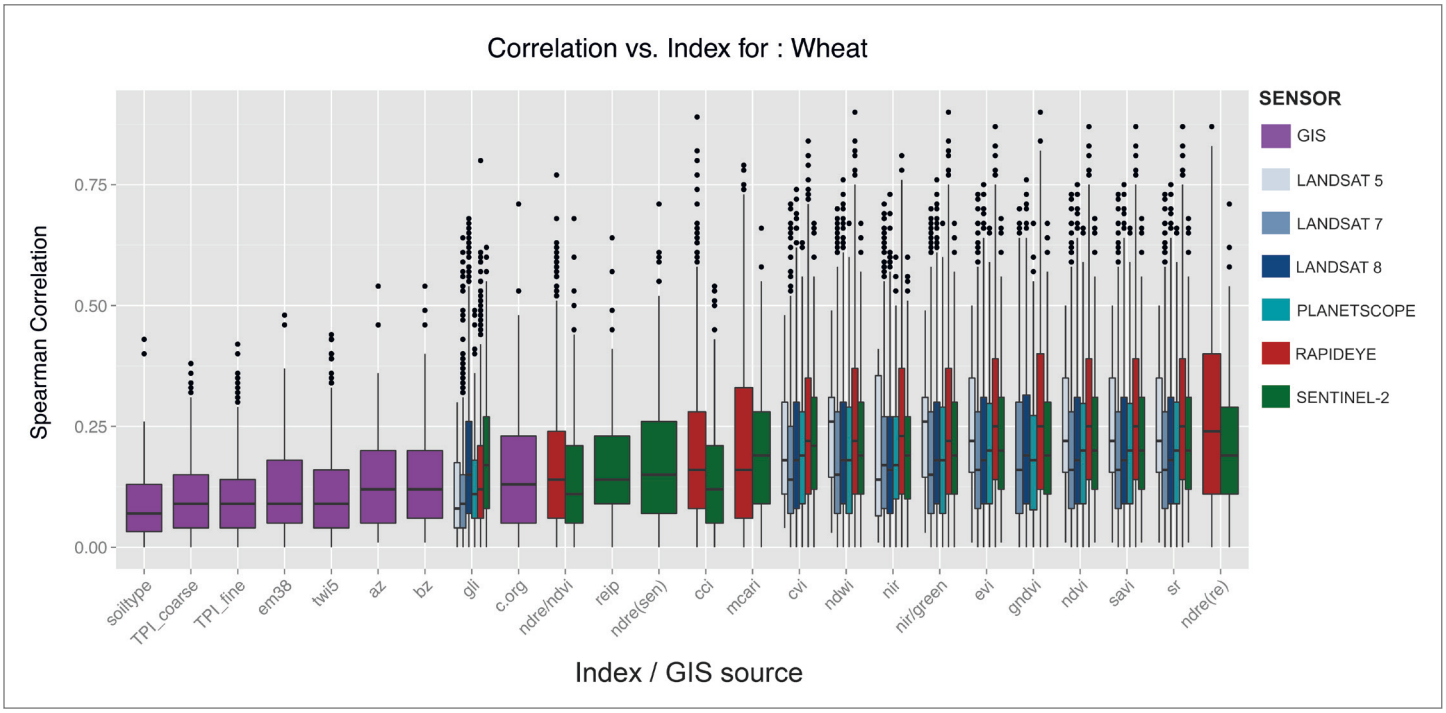

Fig. 4.24 Spearman correlation per index for wheat, all years and all fields

Additional figures for barley

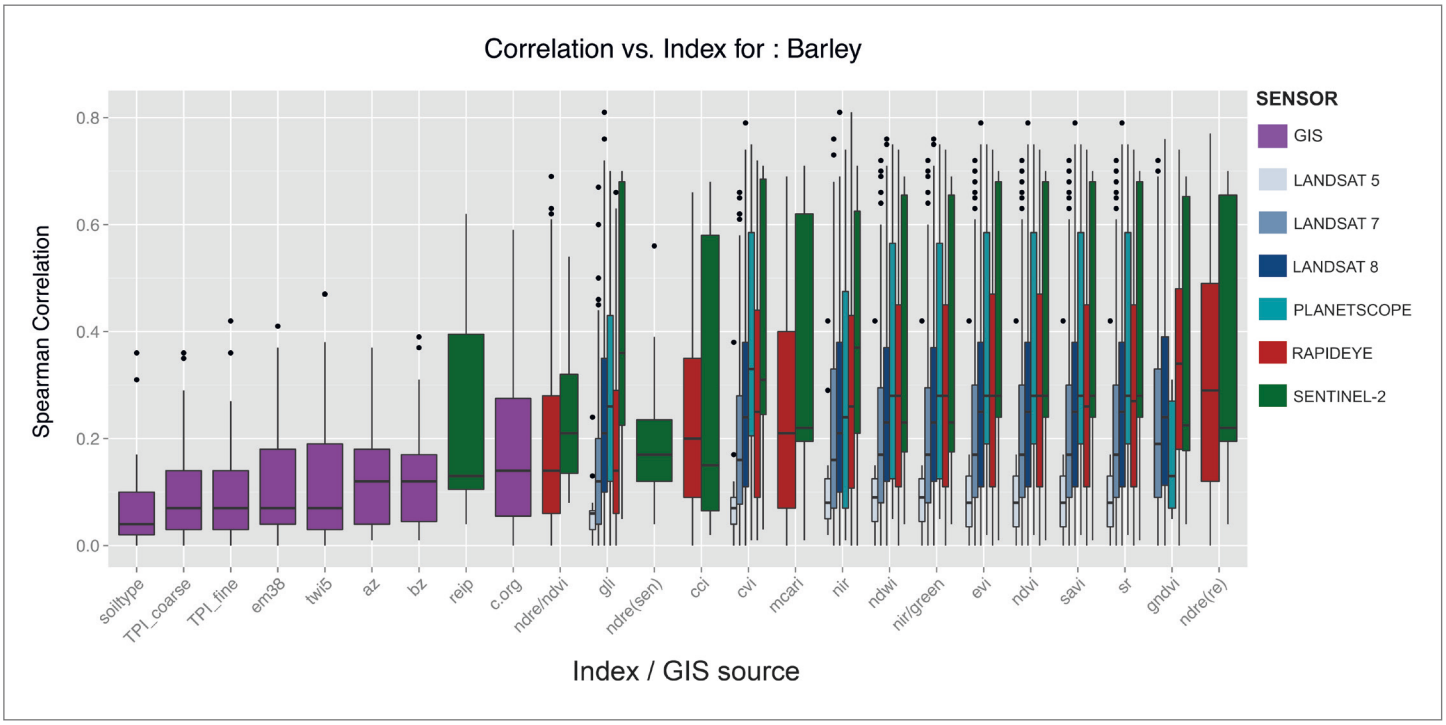

Fig. 4.25 Spearman correlation per index for barley, all years and all fields. TPI = Topographic Positioning Index, em38 = electrical conductivity measurement, twi5 = Topographic Wetness Index (5m), az = „Ackerzahl", bz = „Bodenzahl", c.org = Map of organic carbon.

Additional figures for canola

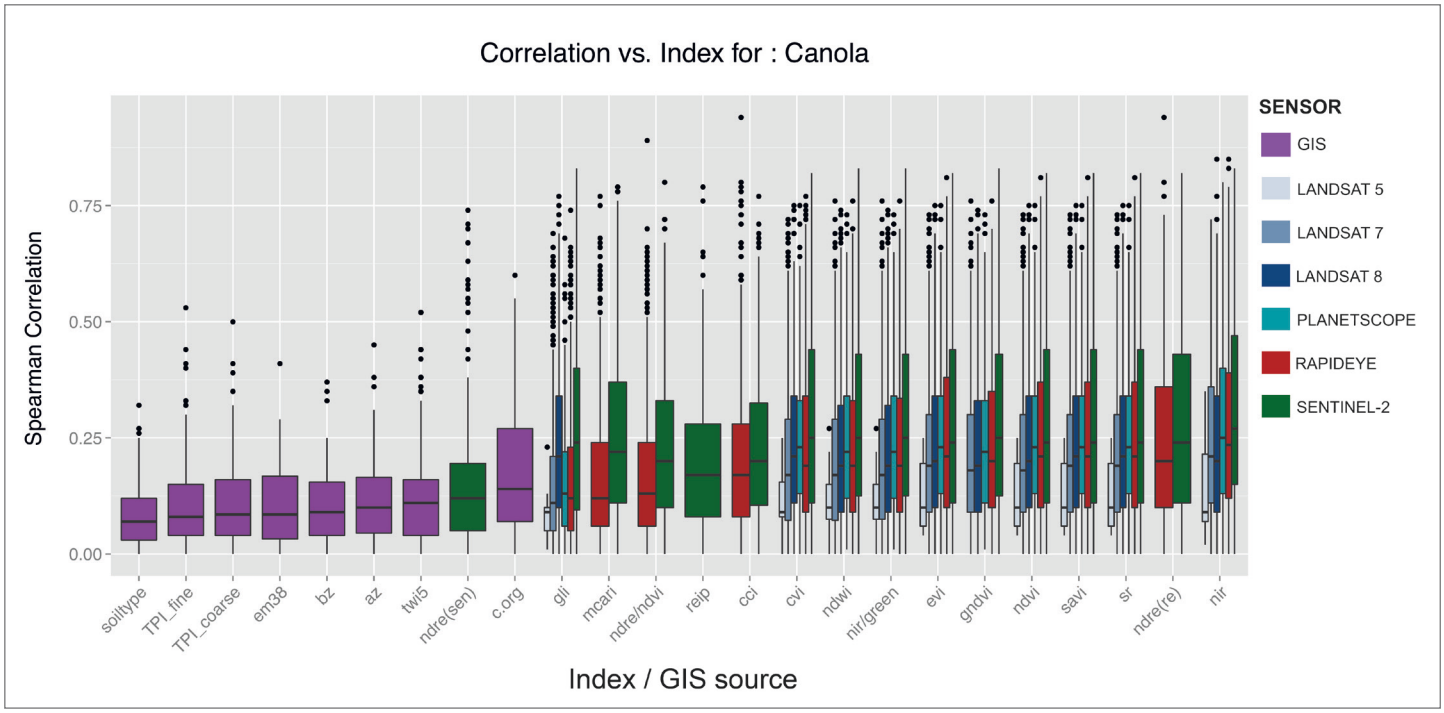

Fig. 4.26 Spearman correlation per index for canola, all years and all fields

5 Synthesis

5.1 Conclusions

The overall research objective of this thesis is to investigate the suitability of optical satellite data for precision agriculture applications. In this large topic area, this thesis investigates the relationship between different characteristics of satellite data and yield data of cereals and canola, as well as the possibility of dividing an agricultural field into management zones based on this relationship. This chapter discusses the results of this work in the context of the research objectives posed, as described in Section 1.3, and more generally the suitability of satellite data in PA applications.

5.1.1 General conclusions and evaluation of results

In the investigation of the relationships between optical satellite data and yield data, which links all three research manuscripts, the results show not only correlation between the two data types, but also the possibility to use this correlation for zoning within each field. There is also the consideration that the grain yield and the nitrogen content of the plant cannot be measured directly by remote sensing. Nevertheless, satellite data provide sufficient information to assess at least relatively the yield distribution and thus generate added value for agriculture. This added value in agriculture and especially in precision farming can lead to better, more efficient and above all more sustainable practices.

The importance of this is the awareness that the inference of yield and other agronomic parameters from satellite data is not done directly, but by means of a model. For models that are developed on a field basis, as in this thesis, their transferability must be tested before they are ready for the commercial market. If the results of the correlation analysis are used and the input of satellite data is limited to certain phenological periods, a transferability of the developed methods to other fields and regions can be regarded as positive. This is especially the case for cereals, since here the correlations between satellite image and yield are on average stronger and above all more comprehensible than, for example, for canola.

The zoning of the fields using the two methods developed is based on the assumption that patterns can be identified in a field and that the plants do not grow homogeneously. This results in a broad range of reflectance values in a satellite image tailored to the field. It is precisely on the basis of these values that the zoning is generated using quantile class boundaries and thus follows a simple and recurring principle. Exactly for this reason it should not matter if the methods are applied in another region, because it is only decisive that heterogeneity is given in a field. At this point, however, it would still be important to validate the successful transferability with the corresponding yield data and to adapt the methods accordingly.

A real consolidation of remote sensing in agriculture requires above all very robust and trustworthy models. The experience with farmers shows that there is a high demand to get really reliable information. If too much is promised that cannot be delivered, the disapproval of the new methods is all the more persistent. The methods developed here, as well as the correlation analysis, should therefore be extended to include and evaluate a wide range of other data. Such a process should not be underestimated, however, since the aggregation and evaluation of big data is very time-consuming.

The use of remote sensing in agriculture currently still requires a lot of expert knowledge and manual work. But the data of the COPERNICUS mission are freely available, very relevant for agriculture and for the methods presented here. The data from the Sentinel-2 satellite also show partly strong correlations to yield data. There are, however, factors that reduce the success of optical satellite data in agriculture. These include the strong dependence on a cloud-free or low-cloud scene. The interpretation of the patterns on a field is simply not possible if a cloud or a cloud shadow covers the area of interest. In particularly rainy years or rainy regions, the use of optical satellite data can only be made possible to a limited extent. In addition, the Sentinel-2 data are too coarse resolved for some applications at 10 or 20 meters in Germany.This is hardly sufficient for the detection of weeds or plant diseases. Drones can be a great help for these questions. Not only can they provide high-resolution remote sensing data, they can also be used flexibly and spontaneously. Meanwhile, they can carry all kinds of sensors. Multispectral cameras with NIR coverage are already common. In this case, the methods discussed here can also be used, because they are applicable independent of spatial resolution. The processing of UAV data, however, requires either a lot of time or a mostly commercial software.

In any case, remote sensing, as well as the contents of this thesis, can add value to agriculture and precision farming. The way of automation still has a long way to go, the automatic and semi-automatic zoning method presented here can bring the process a few steps forward.

5.1.2 Automatic delineation algorithm for site-specific management zones based on satellite remote sensing data

Research Objective R-01: Development of a fully automated method based on optical satellite data, which divides an agricultural field into long-term relative yield zones, which can be used as MZ

The core of the method is characterized by the value spectrum of reflections in different bands within the boundaries of a field. Both the automatic selection of the suitable satellite images, for example cloud clearance, plant growth, not maximum plant density, etc., as well as the division of the field into zones are based on this value range within the field. The results of the study show that a simple division of the field into zones can be successful and transferable to other fields of the same farm. In theory, the method should also be transferable to any other field, because the zoning works with relative thresholds, which always refer to the respective value range.

Any field on which green plants grow will reflect strongly in the near infrared range and show patterns by the spatial variation of this reflection. The transfer of the automatic selection process to another satellite sensor is not quite trivial, because the thresholds, which have been tested for the method, work for RapidEye data sets. Most likely, these thresholds have to be tested and adapted for data from other sensors, which in turn limits transferability.

The method makes a zoning on the basis of mean values over several years and therefore makes a statement about the yield potential of the past years rather than about the expected yield within a

current growth period. It functions independently of the knowledge about the type of crop, but this is exactly where there is a shortcoming in the method. If a user, for example a higher authority, does not know the crop rotation of a field, the presented method works, but is not as reliable as the crop rotation is known. This is due to the fact that the correlation between satellite data and yield data varies for different crops. This variation is evident in the analysis in Chapter 4.

If the automatic zoning method is only used for cereals or maize, much more reliable and better results can be obtained. The reliability of using the automatic zoning method on canola fields is rather low, as can be seen from the correlation analysis in Chapter 4 as well as from the literature cited. It is assumed that there is a correlation, which has not yet been understood exactly, because it is not straight-forward like the correlation between satellite data and cereal yield, where the biomass at certain stages of phenology has an impact. Naturally, the fertility of the soil is independent of the type of crop. In the same way, the topography, the water holding capacity and thus the water supply and nutrient content play a decisive role. However, these are also factors which are extremely difficult or even impossible to detect by remote sensing. If only the reflection properties of the above ground biomass are considered, a conclusion about the canola yield is uncertain. This does not imply that rape cannot be managed with PA. Variable sowing and variable fertiliser application are available in practice. But the support with satellite data cannot be defined clearly enough by the results of this thesis and the current publications.

The question remains as to whether crop patterns from other crops could also provide information about the yield, as many crops are grown in addition to cereals and canola. Single satellite images of the field 100-01 showed sugar beet in an early stage of development - with pronounced spatial crop patterns. These crop patterns were mainly characterized by soil, relief and nutrient differences of the field. An empirical relationship could not be established because no yield data were available for sugar beet. Neither could maize, which is often cultivated in the region, be included. However, scientific studies on the yield estimation of maize from remote sensing data are often available and predominantly from the American region (e.g. Shanahan et al. 2001; Jaynes et al. 2003; Jiang et al. 2009). The automatic delineation method could theoretically be transferred to all crop types, for which the final yield is assumed to correlate with the above-ground biomass and / or LAI within the growing period or at specific points in time.

5.1.3 Delineation of Management Zones with spatial data fusion and belief theory

Research Objectives R-02 a and b: Development of a method which, in addition to satellite data, also considers other map material, such as soil information, to generate relative yield zones using a data fusion model. Evaluation of a statistical model which is able to integrate the expert knowledge of a farmer into the data fusion in order to open the algorithm for human knowledge and thus improve the method.

The method of this scientific work combines a data fusion approach for spatial data and the integration of human knowledge into the fusion process. The method also aims to classify yield zones that can be used as MZs. Thus, all data sources used in the fusion process must also be interpreted

with regard to the parameter. For practical application it would therefore be realistic that there are not only one, but two experts whose knowledge is integrated. On the one hand there is the remote sensing expert, who interprets the satellite data in terms of yield expectations, and on the other hand there is the farmer, who, for example, interprets soil classes or relief units such as a hilltop or a depression in his own field in terms of yield expectations. The method can be individually adapted to each field and offers a high degree of individuality. It also gives the end user the possibility to influence the result of the zone modelling and adapt it to his individual experience. The method also takes into account the uncertainties that can arise both from the quality or reliability of the data sources and from the uncertainty that the expert has.

Modeling with beliefs is not widespread in agriculture, but has high potential precisely because of the possibility of user involvement. The „AgriFusion“ project (Spengler and Heupel 2017) funded by the Ministry of Food and Agriculture also uses the TBM for modelling yield potential and has been able to attract several companies from the geo- and agribusiness sector. Especially the calculation of the set parameters in the TBM with each other is comprehensible and therefore potentially more trustworthy for a large group of users in agriculture than a comparable „black box“ algorithm, which cannot explain the calculation path to the result.

The hurdle of the method is currently a complex set-up of the input parameters. Thus each data source must be classified in units in order to make an interpretation of the classes possible at all. A soil map is already available in units (soil type, „Bodenzahl“), but an elevation model must first be converted into a morphology describing format, such as the Topographic Positioning Index. The resulting classes (e.g. flat, hilltop, slope) depend on the respective threshold values that are set when calculating the TPI. An automated conversion of the elevation data into a TPI can therefore not take place, since the user of the TBM must first deal with the morphology of the respective field or also with the sub-region, in which the fields are located. The TPI must at least be compared visually with the elevation model to determine whether the calculated units make sense or whether they were mapped too coarsely or too finely. This preliminary classification is therefore a first source of uncertainties in the later result.

The same applies to the classification of the remote sensing data used in the TBM. If the interpretation of the data sources is done by a human expert, it is nearly impossible to interpret a continuous data set (e.g. a NDVI raster of a field) regarding the yield expectation or the MZ. In this case, a classification of the data set must also be carried out in advance. In the presented scientific work, the NDVI raster was divided into three classes, separated by two quantile thresholds, each determined by the respective value range of the raster. The type and the relative position of the threshold value were tested in several loops and those with the correlation of the resulting zones with the yield zones were tested. However, it cannot be ruled out that there is now a better method of classification which can reduce the uncertainty.
If all input data is classified in advance, the interpretations must be assigned to each class. Depending on the number of input data and the number of classes, this process can take a long time. This is especially the case when the expert‘s experience in different fields diverges and the set-up of the TBM for each field has to be strongly adapted. From a scientific point of view, this step also entails the risk of uncertainties and errors. From a practical point of view, this is a hurdle because the time-consuming process may not be supported by experts from agriculture. It would therefore be conceivable here if the advance classification and at least one interpretation on a proposal basis were automatically generated from learning algorithms.

As a result of the „AgriFusion“ project (Spengler and Heupel 2017), however, a web application has been developed in which farmers can contribute their knowledge in a user-friendly manner, so that yield potential can be calculated with the help of the TBM. So there are definitely marketable applications that address TBM and data fusion.

Input data from previous years as well as yield data and weather data could be used here for learning purposes. On the one hand, this would reduce the transparency of the method, since machine learning methods would be integrated. Nevertheless, this automated interpretation could be scrutinized or adapted by the expert if it does not correspond to the actual experience with the field.

The method presented in this thesis was introduced using a limited example: one field in one year for one type of crop. This is sufficient to explain the TBM fundamentally and to develop the method. Nevertheless, the method cannot be considered robust at this stage and must be tested and validated in other fields, with other crops, multi-temporally and with other data sources. Only this further development and development of robustness can increase the relevance of the method and make the chance of a transfer into practice possible.

5.1.4 Agricultural yield mapping with satellite time series and geodata - an evaluation of various data frames

Research Objective R-03: Analysis of the relationships between optical satellite data of different sensors at different times and the yield data of the corresponding years. Which satellite data are best suited for yield-relevant questions and at which point in time?

The work investigates the relationship between optical satellite data, environmental geodata and agricultural yield data. The method used is the determination of the Spearman correlation between the respective parameters, consequently a bivariate dependency analysis. This correlation analysis should answer the question whether the yield can be estimated with spatial image and geodata before the harvest and at what time. In a time series of 13 years, a wide range of yield and spatial data was evaluated. It shows that the range of correlations within this study is very large. These data sets are therefore suitable for predicting the yield within the season to a certain extent. This seems most likely to work for cereals and less for canola. However, there are also data sets that do not correlate at all with the yield. These include above all environmental GIS data and remote sensing data of recording dates irrelevant for yield estimation.

The study gives a very good overview of the direct bivariate dependencies and can therefore also be a guideline for other scientists and practitioners. The investigation of such a dense and long-term data set is not available in the representative region of Northern Germany. One reason for this is often either the non-existence of yield data or the fact that these data are not passed on to persons or institutions that evaluate them. The quality of yield data also varies greatly. If a field is harvested with several machines, then these yields must be calibrated. In the peripheral area of the field, incorrect measurements often occur (Blackmore and Marshall 1996; Doerge 1999; Dobers 2002), as well as when the speed and other parameters deviate greatly. So the question is how much one can trust these data. The quality of the yield data in this study certainly also varies between the two farms.

Nevertheless, the point density of Farm 1 is very high and the data goes back to 2006. Thus, not only is the data availability high, but it indicates, that the farmer himself has gained enough experience with the data to reduce possible faultiness and rise reliability of the data over the years. The alternative to these yield data would be manual yield measurements in the field. But such a dataset is not available for this period and this large area. Consequently, the accuracy of the yield data and the associated correlation results must not be evaluated completely quantitatively, but rather the correlation values relative to each other. The resulting picture is much clearer and gives room for further study of the interesting data sources. The analysis therefore provides at least which data sets are relatively best suited and thus also provides input for the application of the methods from Chapters 2 and 3.

The difficulty of evaluating the correlation analysis also lies in the choice of the presentation of the results. The selected figures explain individual dependencies, such as the phenological phase. However, they often illuminate partial aspects, since the complete database is not always represented in one illustration, but a subset that is subject to different filters. The evaluation of the analysis shows the most important aspects, the database without question holds further potential for the investigation of further questions.

Discussion of the correlation analysis

The approach of a simple correlation analysis with the background of the number of machine learning algorithms does not seem to cover the complex topic well enough. Nevertheless, the bivariate analysis shows the basic relationships and significance of individual data sources. These relationships must be understood in order to go one step further towards multivariate analysis and advanced algorithms. Also, to be able to question the results of these again.

For understanding the complexity of the crop growing system and the interrelations with remote sensing and GIS data, a correlation analysis under consideration of the combination of several data sources would be meaningful. The analysis presented here gives first indications for a preselection of the data sources. Thus, only clearly relevant data sources can be used in a constructive correlation analysis in order to reduce the calculation and information intensity.

5.2 Impact on Agriculture

Agriculture in Germany and around the world is becoming increasingly important in the debate about the drivers and consequences of climate change. Ecological demands are rising, as are the demands of a growing population that needs to be fed. Competition on the world market and competition between agricultural areas - the cultivation of food versus animal feed versus biomass for energy use - is increasing the pressure on agriculture. The German government is currently pursuing plans to optimize agriculture through digitization and precision farming within the framework of laws and regulations. Agriculture in Germany is partly restricted in its activities by the European Union, but also by the regulations of the federal governments. The demands that the current fertilizer regulation, which restricts the use of fertilizers on fields, are aggravated are increasing and becoming louder. As soon as this planned tightening occurs, solutions that lead to efficient, local

and demand-oriented fertilization will become even more important. These include methods that can divide the fields into yield zones and management zones, which are distributed according to the vitality of the plants and the yield potential of the crop.

In this respect, the scientifically developed methods of Chapters 2 and 3 can make a valuable contribution if they are put into practice. Both a cost-effective method (Chapter 2) could be implemented, and an even more precise one, which is partly controlled by the experiences of the farmer himself (Chapter 3). The MZs derived from the methods could be used either directly for planning soil sampling and seed sowing, or for variable fertilizer application. The MZs can also be used to support the measurements of online sensors, which measure during the fertilizer application in the field. In the so-called „Map Overlay" procedure, the addition of remotely sensed MZs can optimize the calculation of the fertilizer application.

Although the methods presented here require further development, validation and testing for transfer into practice, this thesis, especially Chapter 4, shows that there is definitely a connection between remote sensing and agricultural parameters. Although this is widely known in the scientific community, the analysis of a 13-year data series underpins this fact immensely. The analysis also reveals that not every type of satellite image makes the same statement about a parameter as the yield. The knowledge at which specific phenological time of the crop an indication for crop yield is possible is not widely spread in the literature, which is why this was investigated. It cannot be ruled out, of course, that companies specializing in yield modelling have already generated this knowledge. Still, for all stakeholders in agriculture, whether farmers, consultants or companies, such an analysis brings added value and knowledge.

5.3 Highlights

- Optical satellite data are suitable for applications in precision farming, if they provide information at least in the near infrared range, better in the red edge range
- There is an empirical correlation between grain yield and optical satellite data; to a certain extent this also applies to rapeseed
- High-resolution remote sensing data in significant phenological phases of the crop determine the reliability of a yield estimation
- Development of two practice-oriented methods suitable for precision farming
- The delineation of a field into relative yield zones, which can also be used as management zones, is made possible with these methods: automatically and semi-automatically by bringing in agronomic expert knowledge
- The automatic method requires only multispectral satellite data and the outline of the field, whereby the appropriate satellite data are automatically selected and the field is then classified into five relative yield zones

- The semi-automatic method uses the TBM model, i.e. belief structures, to achieve a data fusion of satellite images, relief and ground information. The user can contribute his knowledge to this process and make the classification of the three relative yield zones more precise and reliable

- Two novel zoning methods for precision farming and newly generated knowledge about the relationship between remote sensing and yield enrich the field of agronomic remote sensing

5.4 Future Research

5.4.1 Management Zones in PA

There is no doubt that the need for research in the field of smart agriculture is very high. National strategies for the digitization of agriculture, as proclaimed by the Federal Ministry of Food and Agriculture in Germany (BMEL 2018), support these research projects. The aim should be for every farmer to be able to obtain a map of the management zones of his farm‘s fields in order to adapt his measures such as fertilization, irrigation or sowing in a sustainable, resource-saving and environmentally friendly way. In order to provide such an information service, however, intensive research into crop pattern recognition using satellite data and classification into MZ is still required. An automated method as described in Chapter 2 can be applied here and further developed.

The method could be tested with different satellite data, especially the freely available COPERNICUS and Landsat data. The method can be improved by including additional crop types and developing MZ according those crops. It would therefore be necessary to investigate how different crops cultivated at least in Germany or Central Europe show crop patterns in satellite images, under which conditions and to what extent these patterns also correlate with yield or other parameters such as biomass or nitrogen content. In Germany, a broad network of phenological data is freely available through the Deutscher Wetterdienst (DWD). These data could also be included in such an analysis, as the work from Chapter 4 has shown that the time of taking a satellite image is decisive for a robust inference of data on yield. This will apply not only to the crop types canola and cereals studied, but also to many other arable crops.

With an automated method for the delineation of MZ, there is still great potential in the integration of methods of machine learning. It can be explored whether the provision of past data sets, especially remote sensing data and yield data, has a beneficial effect on the modelling of current MZ or yield - if these data are linked by machine learning. The problem here can be that this past data must be trusted because neither satellite data nor yield data can be re-recorded. If, however, trustworthy data is available, research into the automated generation of knowledge from archive data brings immense added value for further development.

A major advantage of future research over the research presented here is the constantly growing archive of remote sensing and in-situ data. While in the method of the second chapter RapidEye data from five years were combined, one could now consider up to nine years, or apply the method only to the same crops or groups as cereals, strengthened by the robustness of a multi-year data basis.
It could also be explored whether the success and the validation of the models differ depending on

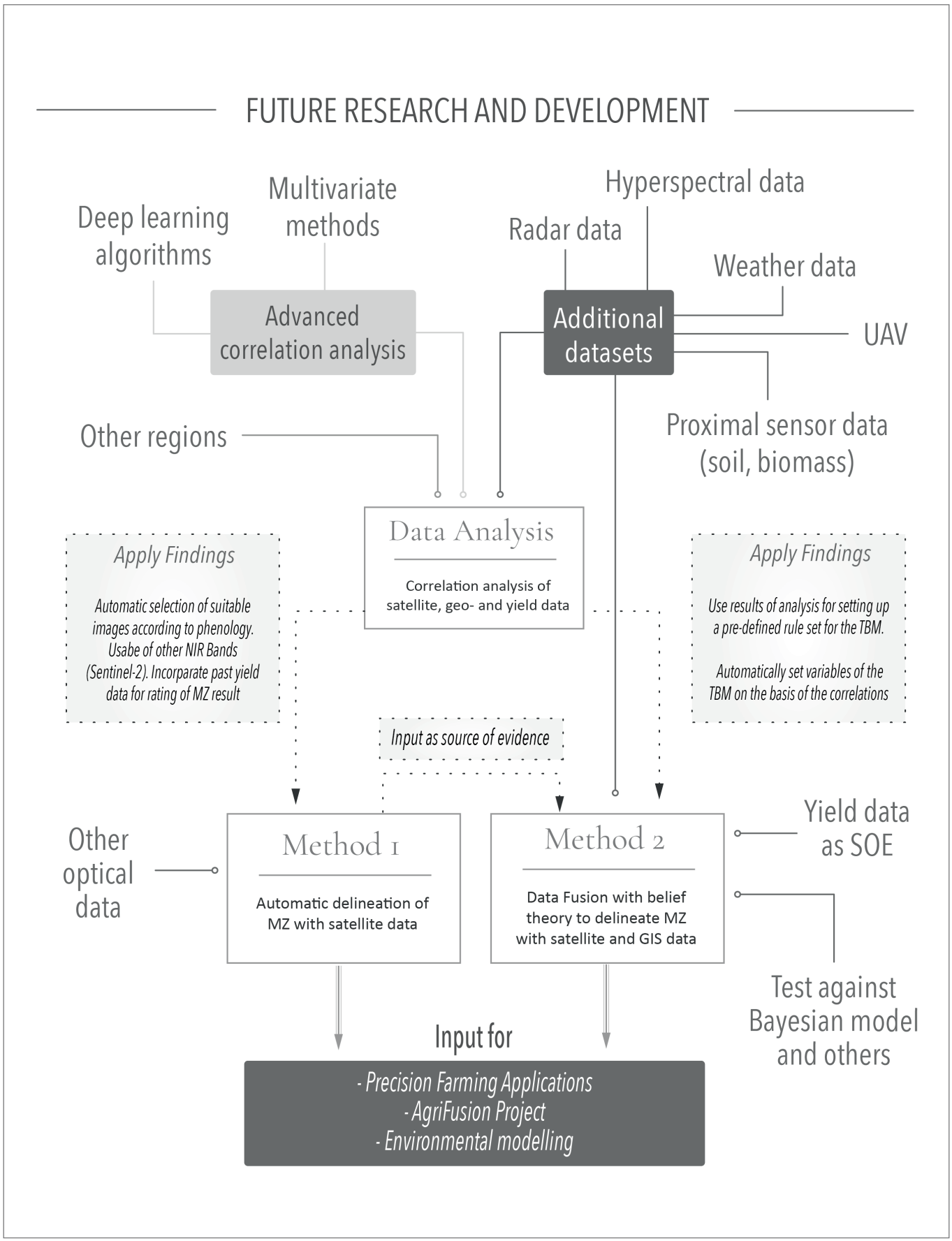

Fig 5.1 Context in which the individual works can be further developed individually and together within the framework of future research.

the meteorology of the years. In order to answer the question, if the delineation method perform better in rather dry years, where crop yields are down, as teh results of Chapter 4 indicate. With an increasing amount of satellite data, the influence of the growth-enhancing conditions of individual years on the final result could be investigated.

5.4.2 Data fusion in precision agriculture

In the field of data fusion in precision farming, there is currently still a great need for research, and the data fusion method presented in Chapter 3 also has great potential for further research. It could be explored how the validation of data fusion changes if other years are taken into consideration and how these results are compared. One question is whether the method works better in dry years with little rain or in wet years with a lot of rain. As a result, it can be investigated whether the method is particularly suitable for certain regions or climate zones, and whether the same applies to the automatic delineation method. Particularly in the case of questions dealing with data fusion, the research process is seldom completely completed because there is always more data that can be taken into account in the fusion.

Possible data sets that can be tested in further work: optical satellite data, radar satellite data, UAV images of various spectral characteristics, hyperspectral images, maps of electrical conductivity, nutrient maps of field sampling, past yield maps, biomass maps of the online sensor on the thresher, derived products from GIS and remote sensing data such as Topographic Wetness Index, evapotranspiration, but also the integration of point measurements and meteorological data. Such an analysis would be very time- and computation-intensive, but would advance the area of data fusion for the derivation of MZ and other agricultural parameters. Such an analysis can then also test which data is most important and relevant in relation to the final parameter - for example yield. Such quantification can then be reflected in the TBM variable „reliability“.

Further research may also focus on the evaluation of individual data sources for the TBM. The consideration of expert knowledge in the workflow of the method gives the potential user control. Nevertheless, this interpretation will be very subjective, which is also intended in principle. If a preset interpretation were to be made available, not only retrospective satellite data and the corresponding yield data could be analyzed, but also the individual interpretation of the individual data sources from a significant number of different farmers. It would be necessary to answer the question whether a farmer in region A provides a soil map with the same hypotheses and beliefs as a farmer in region B. Here it can be compared which physical characteristics of a field lead to which interpretation and to what extent these interpretations differ from each other. In the creation of preset interpretations by deep learning, this could be exactly what integrates humanity back into the system.

Further potential for research in this area is the comparison of different fusion methods. The choice of the TBM in this paper is well-founded and understandable. However, it was not tested how this system performs in the delineation of MZ in comparison to other fusion methods such as Bayes or support vector machine - using the same initial data. And to what extent can the user still contribute his own experience? Such an analysis would also be quite intensive in the preparation of the data and the programming of the individual method, tailored to the question and the creation of MZ. In general, there is no large comparative study that analyses and qualitatively compares the

current methods for delineation of MZ. This step is also rather difficult, since each author and each developer of a method has used different and sometimes not comparable data. But at least not the same yield data for the validation of the respective method. In such a comparative study there is a high research potential that can benefit science and the user.

5.4.3 Transferability of Methods / Research and Development

In the research area of PA, of which the derivation of MZ is a subarea, new methods for deriving agricultural parameters such as yield are constantly being developed as digitisation progresses and the availability of current data increases. The basic difficulty is that the system of crop cultivation with the many components from soil and water supply to the plant and the management measures is highly complex. This complexity is increased by comparing different regions with different conditions. Therefore, the question often arises as to whether models, which anyway represent only a part of these complex systems, are transferable at all. For future research, this would therefore be an absolutely important object for developing robust models. Unfortunately, transferability does not usually involve new methodological developments or groundbreaking research results and is therefore more likely to be found in „research and development“ departments of companies. Nevertheless, testing the methods presented here and other methods would be very important for the division of MZ and yield modelling. If this test of transferability is again put in connection with a comparison with other methods, a scientific gain can also be achieved here, which makes it worthwhile to publish a scientific paper on it. The fact that a method may not be transferable also leaves room for scientific discussion of the reasons for this and thus leads to a better understanding of the large system of plant cultivation.

5.4.4 Further Analysis of Big Data

In order to understand and investigate this complex system and to further develop the methods developed for it, a much more large-scale study to analyse the relationships between the data would be very valuable. In Chapter 4 of this thesis, this was done for a spatially limited region and a selection of data. Since the results here are very exciting and informative for the application of remote sensing in agriculture, the extension of such a study is scientifically very relevant. Based on the analysis presented here, a similar correlation analysis could be carried out in other regions. The same applies to other crops, if yield data are available for them. Also the consideration of further remote sensing data sets, such as hyperspectral, thermal or radar data, recorded in different scales, from UAV to satellite would be relevant. The relationship between these correlations and the meteorological data could also be investigated in such research. In the analysis in this thesis, the weather conditions during the season were mainly used to explain the results. The logical link in the analysis and a parameter derived from it, which describes under which meteorological conditions the correlation between spatial data set and yield is highest, is still to be developed.

An important parameter in the study is phenology, which is provided in Germany by the Deutscher Wetterdienst (DWD), the meteorological service, but in large meshed time periods. The use of phenology derived from satellite data (Chu et al. 2016; Hufkens et al. 2019; Nasrallah et al. 2019)

can increase the density of phenological information, create more knowledge and generate more robust statements.

The correlation results could be stored in a database or used directly as input for the interpretation steps in the TBM. However, this would require that the quality of the correlation results, which depend significantly on the quality and density of the yield data, be assigned to each correlation value. With such a gradation of the quality of the results, a real Big Data analysis can also be carried out and it would not be necessary to directly select in advance which data are worth analyzing.

Such a large-scale analysis of a large number of data sets would be extremely computationally intensive and would also require large storage capacities. When evaluating such a scientific project, it is therefore important to assess whether a) the mass of big data must be limited and only representative regions or data sets can be used, whether b) further correlation coefficients can be calculated or other parameters can be used to measure the correlation, and whether c) additional data mining algorithms of machine learning or artificial intelligence can be applied to obtain the best qualitative results. The latter also offers the possibility of further tasks in research dealing with the question which data mining algorithms are best suited for the exploration of remote sensing data.

5.4.5 Conclusions on future research and development

The future of precision farming should automatically integrate and process remote sensing data, as well as other agronomically relevant data, into processes and operational systems. This automation is necessary because the farmer himself has few resources available to evaluate the data manually. This degree of automation requires both knowledge, which is generated and constantly expanded, and methods that function robustly and generate products and recommendations on the basis from remote sensing data. The methods presented in this thesis provide an excellent basis to be integrate into such a system. Especially the TBM is able to generate the uncertainties per pixel and would provide the result with a quality index, which would be necessary for the broad integration in practice.

Especially the integration of the methods still needs to be worked on in practice, because the interfaces in the farm management software and the agricultural machinery are not well developed. Likewise, the transfer of technology from science to practice must be a focus of attention. With projects like „AgriFusion“ this is already being realised, but much more effort is needed to close the gap between science and established applications in agriculture.

The need for further research is therefore high and so is the transfer of knowledge about the connections between remote sensing and agriculture into the practice.

References

Adamchuk, V. (2011). On-the-go soil sensors - are we there yet? in The Second Global Workshop on Proximal Soil Sensing. Montreal.

Ahamed, T., Tian, L., Zhang, Y. and Ting, K. C. (2011). A review of remote sensing methods for biomass feedstock production. *Biomass and Bioenergy*, 35(7), 2455–2469. doi: 10.1016/j.biombioe.2011.02.028.

Ahn, C.-W., Baumgardner, M. F. and Biehl, L. L. (1999). Delineation of Soil Variability Using Geostatistics and Fuzzy Clustering Analyses of Hyperspectral Data. *Soil Science Society of America Journal*, 63(1), 142. doi: 10.2136/sssaj1999.03615995006300010021x.

van Alphen, B. J. and Stoorvogel, J. J. (1999). A Methodology to Define Management Units in Support of an Integrated, Model-Based Approach to Precision Agriculture. in Robert, P. C., Rust, R. H., and Larson, W. E. (eds), *Precision Agriculture*, 1267–1278. doi: 10.2134/1999.precisionagproc4.c30b.

Amt für Geoinformation Vermessungs- und Katasterwesen. (2011). DGM 5 - Digitales Geländemodell Gitterweite 5m - Mecklenburg-Vorpommern. Schwerin.

Andarzian, B., Bakhshandeh, A. M., Bannayan, M., Emam, Y., Fathi, G. and Alami Saeed, K. (2008). WheatPot: A simple model for spring wheat yield potential using monthly weather data. *Biosystems Engineering*, 99(4), 487–495. doi: 10.1016/j.biosystemseng.2007.12.008.

Atzberger, C. (2013). Advances in Remote Sensing of Agriculture: Context Description, Existing Operational Monitoring Systems and Major Information Needs. *Remote Sensing*, 5(2), 949–981. doi: 10.3390/rs5020949.

Auguie, B. (2012). gridExtra: functions in Grid graphics.

Babar, M. A., van Ginkel, M., Klatt, A. R., Prasad, B. and Reynolds, M. P. (2006). The Potential of Using Spectral Reflectance Indices to Estimate Yield in Wheat Grown Under Reduced Irrigation. *Euphytica*, 150(1–2), 155–172. doi: 10.1007/s10681-006-9104-9.

Bach, S. (2011). Anpassung des agrarmeteorologischen Wasserhaushaltsmodells METVER an aktuelle Erfordernisse vor dem Hintergrund sich wandelnder klimatischer Randbedingungen und pflanzenbaulicher Gegebenheiten. Universität Leipzig.

Baret, F., Houlès, V. and Guérif, M. (2007). Quantification of plant stress using remote sensing observations and crop models: the case of nitrogen management. *Journal of experimental botany*, 58(4), 869–80. doi: 10.1093/jxb/erl231.

Barmeier, G., Hofer, K. and Schmidhalter, U. (2017). Mid-season prediction of grain yield and protein content of spring barley cultivars using high-throughput spectral sensing. *European Journal of Agronomy*, 90, 108–116. doi: 10.1016/J.EJA.2017.07.005.

Barnes, E., Sudduth, K., Hummel, J., Lesch, S., Corwin, D., Yang, C., Daughtry, C. and Bausch, W. (2003). Remote- and ground-based sensor techniques to map soil properties. *Photogrammetric Engineering and Remote Sensing,* 69(6), 619–630.

Barnes, E. M., Clarke, T. R., Richards, S. E., Colaizzi, P. D., Haberland, J., Kostrzewski, M., Waller, P., Choi, C., Riley, E., Thomposn, T., Lascano, R. J., Li, H. and Moran, M. S. (2000). Coninncident Detection of Crop Water Stress, Nitrogen Status ans Canopy Density Using Ground-Based Multispectral Data. in *Proceedings of the 5th International Conference on Precision Agriculture and other resource management July 16-19, 2000, Bloomington, MN USA*.

Bartlett, M. S. (1935). The Effect of Non-Normality on the t Distribution. *Mathematical Proceedings of the Cambridge Philosophical Society*, 31(02), 223. doi: 10.1017/S0305004100013311.

Baruth, B., Royer, A., Klisch, A. and Genovese, G. (2008). The use of remote sensing within the MARS crop yield monitoring system of the European Commission. *Proceedings ISPR*S, 27, 935–940.

Basnyat, P., McConkey, B., Selles, F. and Meinert, L. (2005). Effectiveness of using vegetation index to delineate zones of different soil and crop grain production characteristics. *Canadian Journal of Soil Science*, 85(2), 319–328.

BBCH working group. (2001). Growth stages of mono-and dicotyledonous plants. Edited by U. Meier.

Behling, R., Roessner, S., Segl, K., Kleinschmit, B. and Kaufmann, H. (2014). Robust Automated Image Co-Registration of Optical Multi-Sensor Time Series Data: Database Generation for Multi-Temporal Landslide Detection. *Remote Sensing*, 6(3), 2572–2600. doi: 10.3390/rs6032572.

Benedetti, R. and Rossini, P. (1993). On the use of NDVI profiles as a tool for agricultural statistics: The case study of wheat yield estimate and forecast in Emilia Romagna. *Remote Sensing of Environment*, 45(3), 311–326. doi: 10.1016/0034-4257(93)90113-C.

De Benedetto, D., Castrignanò, A., Rinaldi, M., Ruggieri, S., Santoro, F., Figorito, B., Gualano, S., Diacono, M. and Tamborrino, R. (2013). An approach for delineating homogeneous zones by using multi-sensor data. *Geoderma*, 199, 117–127. doi: 10.1016/j.geoderma.2012.08.028.

Beven, K. J. and Kirkby, M. J. (1979). A physically based, variable contributing area model of basin hydrology. *Hydrological Sciences Bulletin*, 24(1), 43–69. doi: 10.1080/02626667909491834.

Bivand, R., Keitt, T. and Rowlingson, B. (2015). rgdal: Bindings for the Geospatial Data Abstraction Library.

Blackburn, G. A. (2007). Hyperspectral remote sensing of plant pigments. *Journal of experimental botany*, 58(4), 855–67. doi: 10.1093/jxb/erl123.

Blackmore, B. S. and Marshall, C. J. (1996). Yield Mapping; Errors and Algorithms. in P.C. Robert et al. (ed.) *Precision Agriculture: Proc. of the 3rd Intl. Conf. Minneapolis*, 403–416. doi: 10.2134/1996.precisionagproc3.c44.

Blasch, G., Spengler, D., Hohmann, C., Neumann, C., Itzerott, S. and Kaufmann, H. (2015). Multitemporal soil pattern analysis with multispectral remote sensing data at the field-scale. *Computers and Electronics in Agriculture*, 113, 1–13. doi: 10.1016/J.COMPAG.2015.01.012.
BMEL. (2018). Digitalisierung in der Landwirtschaft.

Boden, A. (2005). Bodenkundliche Kartieranleitung. 5th edn. Hannover: Schweizerbart'sche Verlagsbuchhandlung.

Bognár, P., Kern, A., Pásztor, S., Lichtenberger, J., Koronczay, D. and Ferencz, C. (2017). Yield estimation and forecasting for winter wheat in Hungary using time series of MODIS data. *International Journal of Remote Sensing*, 38(11), 3394–3414. doi: 10.1080/01431161.2017.1295482.

Borg, E., Maass, H., Renke, F., Jahncke, D., Stender, V., Hohmann, C., Berg, M., Itzerott, S., Spengler, D. and Conrad, C. (2018). TERENO (Northeast), Climate stations of the German Aerospace Center (DLR). V. 1.0. GFZ Data Services. doi: http://doi.org/10.5880/TERENO.DLR.CL.2018.AL.

Borg, E., Daedelow, H. and Johnson, R. (2012). RapidEye Science Archive (RESA) - Vom Algorithmus zum Produkt.

Boydell, B. and McBratney, A. B. (1999). Identifying Potential Within-Field Management Zones from Cotton-Yield Estimates. *Precision Agriculture*, 3(1), 9–23. doi: 10.1023/A:1013318002609.

Brock, A., Brouder, S. M., Blumhoff, G. and Hofmann, B. S. (2005). Defining Yield-Based Management Zones for Corn–Soybean Rotations. *Agronomy Journal*, 97(4), 1115. doi: 10.2134/agronj2004.0220.

Bundesanstalt für Geowissenschaften und Rohstoffe. (2006). Bodenübersichtskarte 1:200.000 (BÜK200) - CC2342 Stralsund. Hannover.

Cai, Y., Guan, K., Lobell, D., Potgieter, A. B., Wang, S., Peng, J., Xu, T., Asseng, S., Zhang, Y., You, L. and Peng, B. (2019). Integrating satellite and climate data to predict wheat yield in Australia using machine learning approaches. *Agricultural and Forest Meteorology*, 274, 144–159. doi: 10.1016/j.agrformet.2019.03.010.

Cambouris, A. N., Nolin, M. C., Zebarth, B. J. and Laverdiere, M. R. (2006). Soil management zones delineated by electrical conductivity to characterize spatial and temporal variations in potato yield and in soil properties. *American Journal of Potato Research*, 83(5), 381–395.

Cao, Z., Wang, Q. and Zheng, C. (2015). Best hyperspectral indices for tracing leaf water status as determined from leaf dehydration experiments. *Ecological Indicators*, 54, 96–107. doi: 10.1016/j.ecolind.2015.02.027.

Chu, L., Liu, Q., Huang, C. and Liu, G. (2016). Monitoring of winter wheat distribution and phenological phases based on MODIS time-series: A case study in the Yellow River Delta, China. *Journal of Integrative Agriculture*, 15(10), 2403–2416. doi: 10.1016/S2095-3119(15)61319-3.

Clevers, J. and Kooistra, L. (2012). Using Hyperspectral Remote Sensing Data for Retrieving Canopy Chlorophyll and Nitrogen Content. *Ieee Journal of Selected Topics in Applied Earth Observations and Remote Sensing*, 5(2), 574–583. doi: 10.1109/JSTARS.2011.2176468.

Cohen, S. and Levi, O. (2013). Combining spectral and spatial information from aerial hyperspectral images for delineating homogenous management zones. *Biosystems Engineering*, 114(4), 435–443. doi: 10.1016/j.biosystemseng.2012.09.003.

Colaço, A. F. and Bramley, R. G. V. (2018). Do crop sensors promote improved nitrogen management in grain crops? *Field Crops Research*, 218, 126–140. doi: 10.1016/j.fcr.2018.01.007.
Conrad, O., Bechtel, B., Bock, M., Dietrich, H., Fischer, E., Gerlitz, L., Wehberg, J., Wichmann, V. and Böhner, J. (2015). System for Automated Geoscientific Analyses (SAGA) v. 2.1.4. *Geoscientific Model Development*, 8(7), 1991–2007. doi: 10.5194/gmd-8-1991-2015.

Crnojevic, V., Lugonja, P., Brkljac, B. and Brunet, B. (2014). Classification of small agricultural fields using combined Landsat-8 and RapidEye imagery: case study of northern Serbia. *Journal of Applied Remote Sensing*, 8(1), 083512. doi: 10.1117/1.JRS.8.083512.

Cui, B., Zhao, Q., Huang, W., Song, X., Ye, H. and Zhou, X. (2019). Leaf chlorophyll content retrieval of wheat by simulated RapidEye, Sentinel-2 and EnMAP data. *Journal of Integrative Agriculture*, 18(6), 1230–1245. doi: 10.1016/S2095-3119(18)62093-3.

Dalla Marta, A., Grifoni, D., Mancini, M., Orlando, F., Guasconi, F. and Orlandini, S. (2013). Durum wheat in-field monitoring and early-yield prediction: assessment of potential use of high resolution satellite imagery in a hilly area of Tuscany, Central Italy. *The Journal of Agricultural Science*, 153(01), 68–77. doi: 10.1017/S0021859613000877.

Daniel, W. W. (1990). Applied nonparametric statistics. PWS-KENT Pub.

Daughtry, C. S. ., Walthall, C. ., Kim, M. ., de Colstoun, E. B. and McMurtrey, J. . (2000). Estimating Corn Leaf Chlorophyll Concentration from Leaf and Canopy Reflectance. *Remote Sensing of Environment*, 74(2), 229–239. doi: 10.1016/S0034-4257(00)00113-9.

DLG e.V. (2017). Landwirtschaft 2030 Signale erkennen. Weichen stellen. Vertrauen gewinnen. DLG-Verlag GmbH.

Dobers, E. S. (2002). Methoden der Standorterkundung als Grundlage des DGPS-gestützten Ackerbaus. Dissertation. Universität Göttingen.

Dobers, E. S. (2005). Verbesserung und Erweiterung digitaler Bodenkarten unter Verwendung des Transferable Belief Models. in DBG-Workshop: Methoden zur Datenaggregierung und –regionalisierung in der Bodenkunde, der Bodengeographie und in Nachbardisziplinen.

Dobers, E. S. (2008). Generation of new soil information by combination of data sources of different content and scale using GIS and belief structures. *Raporty PIB*, 12: 31-44.

Dobers, E. S., Ahl, C. and Stuczyński, T. (2010). Comparison of Polish and German maps of agricultural soil quality using GIS. *Journal of Plant Nutrition and Soil Science*, 173(2), 185–197. doi: 10.1002/jpln.200800317.

Doerge, T. (1999). Yield map interpretation. *Journal of Production Agriculture*, 12(1), 54–61.

Doraiswamy, P. C., Moulin, S., Cook, P. W. and Stern, A. (2003). Crop Yield Assessment from Remote Sensing. *Photogrammetric Engineering and Remote Sensing*, 69(6), 665–674.

Dowle, M., Short, T., Lianoglou, S., with contributions from R Saporta, A. S. and Antonyan, E. (2014). data.table: Extension of data.frame.

Egli, D. (2017). Seed biology and yield of grain crops. Plant and Soil Sciences Faculty Book Gallery. Edited by D. B. Egli. Wallingford: CABI. doi: 10.1079/9781780647708.0000.

Elsayed, S., Elhoweity, M., Ibrahim, H. H., Dewir, Y. H., Migdadi, H. M. and Schmidhalter, U. (2017). Thermal imaging and passive reflectance sensing to estimate the water status and grain yield of wheat under different irrigation regimes. *Agricultural Water Management*. 189, 98–110. doi: 10.1016/J.AGWAT.2017.05.001.

Evans, L. T. and Fisher, R. A. (1999). Yield potential: Its definition, measurement, and significance. *Crop Science*, 39(6), 1544–1551. doi: 10.2135/cropsci1999.3961544x.

Flowers, M., Weisz, R. and White, J. G. (2005). Yield-Based Management Zones and Grid Sampling Strategies. *Agronomy Journal*, 97(3), 968. doi: 10.2134/agronj2004.0224.

Foerster, S., Kaden, K., Foerster, M. and Itzerott, S. (2012). Crop type mapping using spectral–temporal profiles and phenological information. *Computers and Electronics in Agriculture*, 89, 30–40.

Franzen, D. W., Hopkins, D. H., Sweeney, M. D., Ulmer, M. K. M. K. and Halvorson, A. D. (2002). Evaluation of soil survey scale for zone development of site-specific nitrogen management. *Agronomy Journal*, 94(2), 381–389. doi: 10.2134/agronj2002.0381.

Fridgen, J., Kitchen, N., Sudduth, K., Drummond, S., Wiebold, W. and Fraisse, C. (2003). Management Zone Analyst (MZA): Software for subfield management zone delineation. *Agronomy Journal*, 96(1), 100–108.

Fu, Q., Wang, Z. and Jiang, Q. (2010). Delineating soil nutrient management zones based on fuzzy clustering optimized by PSO. *Mathematical and Computer Modelling*, 51(11), 1299–1305. doi: 10.1016/j.mcm.2009.10.034.

Gao, B. (1996). NDWI—A normalized difference water index for remote sensing of vegetation liquid water from space. *Remote Sensing of Environment*, 58(3), 257–266. doi: 10.1016/S0034-4257(96)00067-3.

Gaso, D. V., Berger, A. G. and Ciganda, V. S. (2019). Predicting wheat grain yield and spatial variability at field scale using a simple regression or a crop model in conjunction with Landsat images. *Computers and Electronics in Agriculture*, 159, 75–83. doi: 10.1016/j.compag.2019.02.026.

Gausman, H. W. (1973). Photomicrographic Record of Light Reflected at 850 Nanometers by Cellular Constituents of Zebrina Leaf Epidermis1. *Agronomy Journal*, 65(3), 504. doi: 10.2134/agronj1973.00021962006500030045x.

Gausman, H. W. (1977). Reflectance of leaf components. *Remote Sensing of Environment*, 6(1), 1–9. doi: 10.1016/0034-4257(77)90015-3.

Gavioli, A., de Souza, E. G., Bazzi, C. L., Guedes, L. P. C. and Schenatto, K. (2016). Optimization of management zone delineation by using spatial principal components. *Computers and Electronics in Agriculture*, 127, 302–310. doi: 10.1016/j.compag.2016.06.029.

Ge, Y., Thomasson, J. A. and Sui, R. (2011). Remote sensing of soil properties in precision agriculture: A review. *Frontiers of Earth Science*. doi: 10.1007/s11707-011-0175-0.

Geisler, G. (1988). Pflanzenbau. Berlin; Hamburg: Parey.

Georgi, C., Spengler, D., Itzerott, S. and Kleinschmit, B. (2017). Automatic delineation algorithm for site-specific management zones based on satellite remote sensing data. *Precision Agriculture*, 19(4), 684-707. doi: 10.1007/s11119-017-9549-y.
GFZ Potsdam. (no date). gts2 / gts2_client · GitLab.

Gili, A., Álvarez, C., Bagnato, R. and Noellemeyer, E. (2017). Comparison of three methods for delineating management zones for site-specific crop management. *Computers and Electronics in Agriculture*, 139, 213-223. doi: 10.1016/j.compag.2017.05.022.

Gitelson, A. A., Kaufman, Y. J. and Merzlyak, M. N. (1996). Use of a green channel in remote sensing of global vegetation from EOS-MODIS. *Remote Sensing of Environment*, 58(3), 289–298. doi: 10.1016/S0034-4257(96)00072-7.

Goswami, S. B. (2012). A Review : The application of Remote Sensing , GIS and GPS in Precision Agriculture. *International Journal of Advanced Technology & Engineering Research*, 2(1).

Graf, L., Kausch, I., Bach, H. and Hank, T. (2019). Using Harmonic Analysis Of Green LAI Time Series Obtained From Sentinel-2 Imagery For Daily Representation Of Crop Growth In A Hydro-Agroecological Model. in *Dreiländertagung der DGPF, der OVG und der SGPF*, Band 28.

Griffin, T. W., Shockley, J. M., Mark, T. B., Shannon, D. K., Clay, D. E. and Kitchen, N. R. (2018). Economics of Precision Farming. in Precision Agriculture Basics. American Society of Agronomy, Crop Science Society of America, and Soil Science Society of America, Inc., 221–230. doi: 10.2134/precisionagbasics.2016.0098.

Guo, C., Zhang, L., Zhou, X., Zhu, Y., Cao, W., Qiu, X., Cheng, T. and Tian, Y. (2018). Integrating remote sensing information with crop model to monitor wheat growth and yield based on simulation zone partitioning. *Precision Agriculture*, 19(1), 55–78. doi: 10.1007/s11119-017-9498-5.

Guyot, G. (1990). Optical properties of vegetation canopies. Optical properties of vegetation canopies. Butterworths, 19–43.

Haas, T. C. (1990). Kriging and automated variogram modeling within a moving window. *Atmospheric Environment*. Part A. General Topics, 24(7), 1759–1769. doi: 10.1016/0960-1686(90)90508-K.

Haboudane, D., Miller, J. R., Pattey, E., Zarco-Tejada, P. J. and Strachan, I. B. (2004). Hyperspectral vegetation indices and novel algorithms for predicting green LAI of crop canopies: Modeling and validation in the context of precision agriculture. *Remote Sensing of Environment*, 90(3), 337–352. doi: 10.1016/J.RSE.2003.12.013.

Hack, H., Bleiholder, H., Buhr, L., Meier, U., Schnock-Fricke, U., Weber, E. and Witzenberger, A. (1992). A uniform code for phenological growth stages of mono- and dicotyledonous plants - Extended BBCH scale, general -. *Nachrichtenblatt Deutscher Pflanzenschutzdienst*, 44(12), 265–270.

Hank, T., Bach, H. and Mauser, W. (2015). Using a Remote Sensing-Supported Hydro-Agroecological Model for Field-Scale Simulation of Heterogeneous Crop Growth and Yield: Application for Wheat in Central Europe. *Remote Sensing*, 7(4), 3934–3965. doi: 10.3390/rs70403934.

Hansen, P. M. and Schjoerring, J. K. (2003). Reflectance measurement of canopy biomass and nitrogen status in wheat crops using normalized difference vegetation indices and partial least squares regression. *Remote Sensing of Environment*, 86(4), 542–553. doi: 10.1016/S0034-4257(03)00131-7.

Harfenmeister, K., Spengler, D. and Weltzien, C. (2019). Analyzing Temporal and Spatial Characteristics of Crop Parameters Using Sentinel-1 Backscatter Data. *Remote Sensing*, 11(13), 1569. doi: 10.3390/rs11131569.

Hay, R. K. M. and Walker, A. J. (1989). An introduction to the physiology of crop yield. Longman Scientific & Technical.

He Ke-xun, Zaho Shu-he, Lai Jian-bin, Luo Yun-xiao and Qin Zhi-hao. (2013). Effects of Water Stress on Red-Edge Parameters and Yield in Wheat Cropping. *Spectroscopy and Spectral Analysis*, 33(8), 2143–2147. doi: 10.3964/j.issn.1000-0593(2013)08-2143-05.

Heinrich, I., Balanzategui, D., Bens, O., Blasch, G., Blume, T., Böttcher, F., Borg, E., Brademann, B., Brauer, A., Conrad, C., Dietze, E., Dräger, N., Fiener, P., Gerke, H. H., Güntner, A., Heine, I., Helle, G., Herbrich, M., Harfenmeister, K., Heußner, K.-U., Hohmann, C., Itzerott, S., Jurasinski, G., Kaiser, K., Kappler, C., Koebsch, F., Liebner, S., Lischeid, G., Merz, B., Missling, K. D., Morgner, M., Pinkerneil, S., Plessen, B., Raab, T., Ruhtz, T., Sachs, T., Sommer, M., Spengler, D., Stender, V., Stüve, P. and Wilken, F. (2018). Interdisciplinary Geo-ecological Research across Time Scales in the Northeast German Lowland Observatory (TERENO-NE). *Vadose Zone Journal*. John Wiley & Sons, Ltd, 17(1), 180116. doi: 10.2136/vzj2018.06.0116.

Le Hegarat-Mascle, S., Richard, D. and Ottle, C. (2002). Multi-scale data fusion using Dempster-Shafer evidence theory. in *IEEE International Geoscience and Remote Sensing Symposium*, 911–913. doi: 10.1109/IGARSS.2002.1025726.

Hiemstra, P. H., Pebesma, E. J., Twenh"ofel, C. J. W. and Heuvelink, G. B. M. (2008). Real-time automatic interpolation of ambient gamma dose rates from the Dutch Radioactivity Monitoring Network. *Computers & Geosciences*. doi: http://dx.doi.org/10.1016/j.cageo.2008.10.011.

Hijmans, R. J. (2015). raster: Geographic Data Analysis and Modeling.

Holzapfel, C. B., Lafond, G. P., Brandt, S. A., Bullock, P. R., Irvine, R. B., James, D. C., Morrison, M. J. and May, W. E. (2009). Optical sensors have potential for determining nitrogen fertilizer topdressing requirements of canola in Saskatchewan. *Canadian Journal of Plant Science*, 89(2), 411–425. doi: 10.4141/CJPS08127.

Hornung, A., Khosla, R., Reich, R., Inman, D. and Westfall, D. G. (2006). Comparison of Site-Specific Management Zones: Soil-Color-based and Yield-Based. *Agronomy Journal*, 98(2), 407. doi: 10.2134/agronj2005.0240.

Huete, A. . (1988). A soil-adjusted vegetation index (SAVI). *Remote Sensing of Environment*, 25(3), 295–309. doi: 10.1016/0034-4257(88)90106-X.

Huete, A., Justice, C. and van Leeuwen, W. (1999). MODIS Vegetation Index (MOD 13): Algorithm theoretical basis document.

Hufkens, K., Melaas, E. K., Mann, M. L., Foster, T., Ceballos, F., Robles, M. and Kramer, B. (2019). Monitoring crop phenology using a smartphone based near-surface remote sensing approach. *Agricultural and Forest Meteorology*, 265, 327–337. doi: 10.1016/J.AGRFORMET.2018.11.002.

Hurd-Karrer, A. M. and Taylor, J. W. (1929). The water content of wheat leaves at flowering time. *Plant physiology*, 4(3), 393–7.

Idso, S. B., Pinter, P. J., Jackson, R. D. and Reginato, R. J. (1980). Estimation of grain yields by remote sensing of crop senescence rates. *Remote Sensing of Environment*, 9(1), 87–91. doi: 10.1016/0034-4257(80)90049-8.

IPCC. (2014). Food Security and Food Production Systems. in Climate Change 2014: Impacts, Adaption and Vulnerability Part A: Global and Sectoral Aspects. Cambridge: Cambridge University Press, 485–533.

Itzerott, S., Hohmann, C., Stender, V., Maass, H., Borg, E., Renke, F., Jahncke, D., Berg, M., Conrad, C. and Spengler, D. (2018). TERENO (Northeast), Climate stations of the GFZ German Research Centre for Geoscienes (GFZ). V. 2.0. GFZ Data Services. . doi: http://doi.org/10.5880/TERENO.GFZ.CL.2018.ALL.

Itzerott, S. and Kaden, K. (2006). Ein neuer Algorithmus zur Klassifizierung landwirtschaftlicher Fruchtarten auf Basis spektraler Normkurven. *Photogrammetrie, Fernerkundung, Geoinformation: PFG*, 6, 509–518.

Jaynes, D. B., Kaspar, T. C., Colvin, T. S. and James, D. E. (2003). Cluster Analysis of Spatiotemporal Corn Yield Patterns in an Iowa Field. *Agronomy Journal*, 95(3), 574-586. doi:10.2134/agronj2003.5740

Jenness, J. (2006). Topographic Position Index (TPI), 42.

Jensen, J. R. (2007). Remote Sensing of the Environment: An Earth Resource Perspective. 2nd Edition.

Jiang, P., He, Z., Kitchen, N. R. and Sudduth, K. A. (2009). Bayesian analysis of within-field variability of corn yield using a spatial hierarchical model. *Precision Agriculture*, 10(2), 111–127. doi: 10.1007/s11119-008-9070-4.

Jones, H. G. and Vaughan, R. A. (2010). Remote sensing of vegetation. Oxford: Oxford University Press.

Jordan, C. F. (1969). Derivation of Leaf-Area Index from Quality of Light on the Forest Floor. *Ecology*, 50(4), 663–666.

Khanal, S., Fulton, J. and Shearer, S. (2017). An overview of current and potential applications of thermal remote sensing in precision agriculture. *Computers and Electronics in Agriculture*. doi: 10.1016/j.compag.2017.05.001.

Kitchen, N. R., Sudduth, K. A., Myers, D. B., Drummond, S. T. and Hong, S. Y. (2005). Delineating productivity zones on claypan soil fields using apparent soil electrical conductivity. *Computers and Electronics in Agriculture*, 46(1–3), 285–308. doi: 10.1016/j.compag.2004.11.012.

Knoblauch, C., Watson, C., Berendonk, C., Becker, R., Wrage-Mönnig, N. and Wichern, F. (2017). Relationship between Remote Sensing Data, Plant Biomass and Soil Nitrogen Dynamics in Intensively Managed Grasslands under Controlled Conditions. *Sensors*, 17(7), 1483. doi: 10.3390/s17071483.

Kühn, J., Brenning, A., Wehrhan, M., Koszinski, S. and Sommer, M. (2008). Interpretation of electrical conductivity patterns by soil properties and geological maps for precision agriculture. *Precision Agriculture*, 10(6), 490–507. doi: 10.1007/s11119-008-9103-z.

Länder, S. Ä. des B. und der. (2010). Agrarstrukturen in Deutschland Einheit in Vielfalt: Regionale Ergebnisse der Landwirtschaftszählung 2010.

Lark, R. M. (1998). Forming spatially coherent regions by classification of multi-variate data: an example from the analysis of maps of crop yield. *International Journal of Geographical Information Science*, 12(1), 83–98. doi: 10.1080/136588198242021.

Lark, R. M. and Stafford, J. V. (1997). Classification as a first step in the interpretation of temporal and spatial variation of crop yield. *Annals of Applied Biology*, 130(1), 111–121. doi: 10.1111/j.1744-7348.1997.tb05787.x.

Lillesand, T. M. and Kiefer, R. W. (1987). Remote Sensing and Image Interpretation. 2nd Editio. John Wiley and Sons.

Lobell, D. B., Thau, D., Seifert, C., Engle, E. and Little, B. (2015). A scalable satellite-based crop yield mapper. *Remote Sensing of Environment*, 164, 324–333. doi: 10.1016/j.rse.2015.04.021.

Lu, D. (2006). The potential and challenge of remote sensing-based biomass estimation. *International Journal of Remote Sensing*, 27(7), 1297–1328. doi: 10.1080/01431160500486732.

Lück, E., Gebbers, R., Ruehlmann, J. and Spangenberg, U. (2009). Electrical conductivity mapping for precision farming. *Near Surface Geophysics*, 7(32), 15–25. doi: 10.3997/1873-0604.2008031.

Macdonald, J. M., Korb, P. and Hoppe, R. A. (2013). Farm Size and the Organization of U.S. Crop Farming.

MacMillan, R. A., Pettapiece, W. W., Watson, L. D. and Goddard, T. W. (1999). A Landform Segmentation Model For Precision Farming. in *Precision Agriculture*. American Society of Agronomy, Crop Science Society of America, Soil Science Society of America (ACSESS publications), 1335–1346. doi: 10.2134/1999.precisionagproc4.c36b.

Mahlein, A.-K., Oerke, E.-C., Steiner, U. and Dehne, H.-W. (2012). Recent advances in sensing plant diseases for precision crop protection. *European Journal of Plant Pathology,* 133(1), 197–209. doi: 10.1007/s10658-011-9878-z.

Marti, J., Bort, J., Slafer, G. A. and Araus, J. L. (2007). Can wheat yield be assessed by early measurements of Normalized Difference Vegetation Index? *Annals of Applied Biology*, 150(2), 253–257. doi: 10.1111/j.1744-7348.2007.00126.x.

Mauser, W., Bach, H., Hank, T., Zabel, F. and Putzenlechner, B. (2012). How spectroscopy from space will support world agriculture. in *Geoscience and Remote Sensing Symposium (IGARSS), 2012 IEEE International*, 7321–7324. doi: 10.1109/IGARSS.2012.6351970.

Monteith, J. L. (1978). Reassessment of Maximum Growth Rates for C3 and C4 Crops. *Experimental Agriculture*, 14(1), 1–5. doi: 10.1017/S0014479700008255.

Moral, F. J., Terrón, J. M. and Silva, J. R. M. da. (2010). Delineation of management zones using mobile measurements of soil apparent electrical conductivity and multivariate geostatistical techniques. *Soil and Tillage Research*, 106(2), 335–343. doi: 10.1016/j.still.2009.12.002.

Moran, M. S., Inoue, Y. and Barnes, E. M. (1997). Opportunities and Limitations for image-based remote sensing in precision crop management. *Remote Sensing of Environment*, 61, 319–346.

Mulla, D. J. (2013). Twenty five years of remote sensing in precision agriculture: Key advances and remaining knowledge gaps. *Biosystems Engineering*, 114(4), 358–371. doi: 10.1016/j.biosystemseng.2012.08.009.

Müller, J. (1987). Verdunstung landwirtschaftlicher Produktionsgebiete in ausgewählten Vegetationsabschnitten und deren statistische, modellmäßige und kulturbezogene Bewertung. Martin-Luther-Univ. Halle-Wittenberg.

Nasrallah, A., Baghdadi, N., El Hajj, M., Darwish, T., Belhouchette, H., Faour, G., Darwich, S. and Mhawej, M. (2019). Sentinel-1 Data for Winter Wheat Phenology Monitoring and Mapping. *Remote Sensing*, 11(19), 2228. doi: 10.3390/rs11192228.

Navarro-Hellín, H., Martínez-del-Rincon, J., Domingo-Miguel, R., Soto-Valles, F. and Torres-Sánchez, R. (2016). A decision support system for managing irrigation in agriculture. *Computers and*

Electronics in Agriculture, 124, 121–131. doi: 10.1016/j.compag.2016.04.003.

Paloscia, S., Pettinato, S., Santi, E., Notarnicola, C., Pasolli, L. and Reppucci, A. (2013). Soil moisture mapping using Sentinel-1 images: Algorithm and preliminary validation. *Remote Sensing of Environment*, 134, 234–248. doi: 10.1016/j.rse.2013.02.027.

Park, S. and Im, J. (2016). Classification of croplands through fusion of optical and SAR time series data. *ISPRS - International Archives of the Photogrammetry, Remote Sensing and Spatial Information Sciences*, 703–704. doi: 10.5194/isprsarchives-XLI-B7-703-2016.
Pedroso, M., Taylor, J., Tisseyre, B., Charnomordic, B. and Guillaume, S. (2010). A segmentation algorithm for the delineation of agricultural management zones. *Computers and Electronics in Agricultur*e, 199–208. doi: 10.1016/j.compag.2009.10.007.

Peng, Y., Zhu, T., Li, Y., Dai, C., Fang, S., Gong, Y., Wu, X., Zhu, R. and Liu, K. (2019). Remote prediction of yield based on LAI estimation in oilseed rape under different planting methods and nitrogen fertilizer applications. *Agricultural and Forest Meteorology*, 271, 116–125. doi: 10.1016/j.agrformet.2019.02.032.

Piekarczyk, J., Sulewska, H. and Szymańska, G. (2011). Winter Oilseed-Rape Yield Estimates from Hyperspectral Radiometer Measurements. *Quaestiones Geographicae*. Sciendo, 30(1), 77–84.

Ping, J. and Dobermann, A. (2003). Creating spatially contiguous yield classes for site-specific management. *Agronomy Journal*, 95(5), 1121–1131.

Qui, H. (2006). Thermal Remote Sensing of Soil Moisture : Validation of Presumed Linear Relation between Surface Temperature Gradient and Soil Moisture Content. Melbourne.

R Core Team. (2012). R: A Language and Environment for Statistical Computing. Vienna, Austria: R Foundation for Statistical Computing, 2012 [Online]. Available: http://www.r-project.org/.

Ran, Y., Li, X., Lu, L. and Bai, Z. (2008). Land Cover Classification Information Decision Making Fusion Based on Dempster-Shafer Theory : Results and Uncertainty. *Proceedings of the 8th Symposium on Spatial Accuracy assessment in Natural Resources and Environmental Sciences*, 240–247.

Rees, W. G. (2001). Physical Principles of Remote Sensing. Cambridge University Press.

Ren, J., Li, S., Chen, Z., Zhou, Q. and Tang, H. (2007). Regional yield prediction for winter wheat based on crop biomass estimation using multi-source data. *IEEE International Geoscience And Remote Sensing Symposium*, 1–12(Sensing and understanding our planet), 805–808.

Ren, J., Chen, Z., Zhou, Q. and Tang, H. (2008). Regional yield estimation for winter wheat with MODIS-NDVI data in Shandong, China. I*nternational Journal of Applied Earth Observation and Geoinformation*, 10(4), 403–413. doi: 10.1016/J.JAG.2007.11.003.

Richter, R. (2010). Atmospheric/topographic correction for satellite imagery. ATCOR-2/3 users guide, version 7.1. ReSe Applications Schläpfer, Switzerland.

Robert, P. C., Rust, R. H., Larson, W. E., Snyder, C., Havlin, J., Kluitenberg, G. and Schroeder, T. (1999). Evaluating the Economics of Precision Agriculture. in Precision Agriculture. American Society of Agronomy, Crop Science Society of America, Soil Science Society of America, 1621–1632. doi: 10.2134/1999.precisionagproc4.c67b.

Rouse, J. W. J., Haas, R. H., Schell, J. A. and Deering, D. W. (1974). Monitoring vegetation systems in the Great Plains with ERTS. NASA. Goddard Space Flight Center 3d ERTS-1 Symp., 1, 309–317.

Sakamoto, T., Gitelson, A. A. and Arkebauer, T. J. (2013). MODIS-based corn grain yield estimation model incorporating crop phenology information. *Remote Sensing of Environment*, 131, 215–231. doi: 10.1016/j.rse.2012.12.017.

Scheffler, D., Hollstein, A., Diedrich, H., Segl, K., Hostert, P., Scheffler, D., Hollstein, A., Diedrich, H., Segl, K. and Hostert, P. (2017). AROSICS: An Automated and Robust Open-Source Image Co-Registration Software for Multi-Sensor Satellite Data. *Remote Sensing*, 9(7), 676. doi: 10.3390/rs9070676.

Schepers, A. R., Shanahan, J., Liebig, M. A., Schepers, J. S., Johnson, S., Jr, A., Aaron Schepers, A. R., Luchiari Jr, A., Shanahan, J. F., Johnson, S. H. and Luchiari, A. (2004). Appropriateness of Management Zones for Characterizing Spatial Variability of Soil Properties and Irrigated Corn Yields across Year. *Agronomy Journal*, 96, 195-203. doi:10.2134/agronj2004.1950

Schlemmer, M. R. and Major, D. J. (2001). Use of Remote-Sensing Imagery to Estimate Corn Grain Yield. *Agronomy Journal*, 93(3), 583. doi: 10.2134/agronj2001.933583x.

Šedina, J., Pavelka, K. and Raeva, P. (2017). UAV remote sensing capability for precision agriculture, forestry and small natural reservation monitoring. in Bannon, D. P. (ed.), 102130L. doi: 10.1117/12.2267858.

Seelan, S. K., Laguette, S., Casady, G. M. and Seielstad, G. a. (2003). Remote sensing applications for precision agriculture: A learning community approach. *Remote Sensing of Environment*, 88(1–2), 157–169. doi: 10.1016/j.rse.2003.04.007.

Serrano, L., Filella, I. and Pen, J. (2000). Remote Sensing of Biomass and Yield of Winter Wheat under Different Nitrogen Supplies. *Crop Science*, 40, 723–731. doi:10.2135/cropsci2000.403723x

Shaddad, S. M., Madrau, S., Castrignanò, A. and Mouazen, A. M. (2016). Data fusion techniques for delineation of site-specific management zones in a field in UK. *Precision Agriculture*, 17(2), 200–217. doi: 10.1007/s11119-015-9417-6.

Shafer, G. (1976). A mathematical theory of evidence. Princeton, N.J.: Princeton University Press.

Shafer, G. (2016). Dempster's rule of combination. *International Journal of Approximate Reasoning,* 79, 26–40. doi: 10.1016/J.IJAR.2015.12.009.

Shanahan, J. F., Schepers, J. S., Francis, D. D., Varvel, G. E., Wilhelm, W. W., Tringe, J. M.,

Schlemmer, M. R. and Major, D. J. (2001). Use of Remote-Sensing Imagery to Estimate Corn Grain Yield. *Agronomy Journal*, 93(3), 583. doi: 10.2134/agronj2001.933583x.

Sharma, L. and Bali, S. (2017). A Review of Methods to Improve Nitrogen Use Efficiency in Agriculture. *Sustainability*, 10(2), 51. doi: 10.3390/su10010051.

Simbahan, G., Dobermann, A. and Ping, J. (2004). Site-specific management - Screening yield monitor data improves grain yield maps. *Agronomy Journal*, 96(4), 1091–1102.

Smets, Ph. and Kennes, R. (1994). The Transferable Belief Model. *Artificial Intelligence*, 66, 191–243.

Smith, D. L. and Hamel, C. (2013). Crop Yield Physiology and Processes. Springer Berlin.

Song, X., Wang, J., Huang, W., Liu, L., Yan, G. and Pu, R. (2009). The delineation of agricultural management zones with high resolution remotely sensed data. *Precision Agriculture*, 10(6), 471–487. doi: 10.1007/s11119-009-9108-2.
Spengler, D. and Heupel, K. (2017). AgriFusion Project Website. Available at: https://www.gfz-potsdam.de/en/section/remote-sensing/projects/agrifusion/

Sulik, J. J. and Long, D. S. (2016). Spectral considerations for modeling yield of canola. *Remote Sensing of Environment*, 184, 161–174. doi: 10.1016/J.RSE.2016.06.016.

Swinton, S. M. and Lowenberg-DeBoer, J. (1998). Evaluating the Profitability of Site-Specific Farming. *American Society of Agronomy, Crop Science Society of America, Soil Science Society of America*, 11(4), 439. doi: 10.2134/jpa1998.0439.

T., Evans, L. and A. Fischer, R. (1999). Yield Potential: Its Definition, Measurement, and Significance. *Crop Science*, 39, 1544–1551.

Team, P. (2017). Planet Application Program Interface: In Space for Life on Earth. San Francisco,CA.

Teimouri, M., Mokhtarzade, M. and Valadan Zoej, M. J. (2016). Optimal fusion of optical and SAR high-resolution images for semiautomatic building detection. *GIScience & Remote Sensing*, 53(1), 45–62. doi: 10.1080/15481603.2015.1116140.

Thenkabail, P. S. (2003). Biophysical and yield information for precision farming from near-real-time and historical Landsat TM images. *International Journal of Remote Sensing*, 24(14), 2879–2904. doi: 10.1080/01431160710155974.

Tilling, A. K., Leary, G. O., Ferwerda, J. G., Jones, S. D., Fitzgerald, G. and Edge, R. (2006). Remote Sensing to Detect Nitrogen and Water Stress in Wheat. *in Proceedings of the 13th ASA Conference*, 1–9.

Tyc, G., Tulip, J., Schulten, D., Krischke, M. and Oxfort, M. (2005). The RapidEye mission design. *Acta Astronautica*, 56(1), 213–219. doi: 10.1016/j.actaastro.2004.09.029.

Ustin, S. (ed.). (2004). Manual of Remote Sensing, Volume 4, Remote Sensing for Natural Resource Management and Environmental Monitoring. 3rd Edition.

Vallentin, C., Dobers, E. S., Itzerott, S., Kleinschmit, B. and Spengler, D. (2019). Delineation of management zones with spatial data fusion and belief theory. *Precision Agriculture*, 1–29. doi: 10.1007/s11119-019-09696-0.

Viña, A., Gitelson, A. A., Nguy-Robertson, A. L. and Peng, Y. (2011). Comparison of different vegetation indices for the remote assessment of green leaf area index of crops. *Remote Sensing of Environment*, 115(12), 3468–3478. doi: 10.1016/J.RSE.2011.08.010.

Vincini, M., Frazzi, E. and D'Alessio, P. (2008). A broad-band leaf chlorophyll vegetation index at the canopy scale. *Precision Agriculture*, 9(5), 303–319. doi: 10.1007/s11119-008-9075-z.

Webster, R. and Oliver, M. A. (1990). Statistical Methods in Soil and Land Resource Survey. New York: Oxford University Press.

Whelan, B. M., McBratney, A. B. and Minasny, B. (1996). Spatial prediction for precision agriculture. in Proceedings of the 3rd international conference on precision agriculture. Minneapolis, Minessota, 331–342.

Wickham, H. (2009). ggplot2: elegant graphics for data analysis. Springer New York.

Wickham, H. (2012). stringr: Make it easier to work with strings.
Wu, H., Siegel, M., Stiefelhagen, R. and Yang, J. (2002). Sensor Fusion Using Dempster-Shafer Theory. IEEE Instrumentation and Measurement Technology Conference Anchorage, 21–23.

Xue, J., Leung, Y. and Fung, T. (2017). A Bayesian Data Fusion Approach to Spatio-Temporal Fusion of Remotely Sensed Images. *Remote Sensing*, 9(12), 1310. doi: 10.3390/rs9121310.

Yang, C., Everitt, J. H. and Bradford, J. M. (2006). Comparison of QuickBird Satellite Imagery and Airborne Imagery for Mapping Grain Sorghum Yield Patterns. *Precision Agriculture*, 7(1), 33–44. doi: 10.1007/s11119-005-6788-0.

Yao, R.-J., Yang, J.-S., Zhang, T.-J., Gao, P., Wang, X.-P., Hong, L.-Z. and Wang, M.-W. (2014). Determination of site-specific management zones using soil physico-chemical properties and crop yields in coastal reclaimed farmland. *Geoderma*, 232–234, 381–393. doi: 10.1016/j.geoderma.2014.06.006.

Zhang, Y., Chen, J. M., Miller, J. R. and Noland, T. L. (2008). Leaf chlorophyll content retrieval from airborne hyperspectral remote sensing imagery. *Remote Sensing of Environment*, 112(7), 3234–3247. doi: 10.1016/j.rse.2008.04.005.

Zheng, B. (2008). Using satellite hyperspectral imagery to map soil organic matter, total nitrogen and total phosphorus. Indiana University.